Theoretical study on reactivity of different sulfide collectors and their binding affinity toward Cu(II), Zn(II) and Pb(II) ions.

by

Manjeet Chowdhry

A thesis submitted in partial fulfillment of the requirements for the degree of

Doctor of Philosophy

in

Chemical Engineering

Department of Chemical and Materials Engineering
University of Alberta

Abstract

Collectors are one of the most important ingredients of froth flotation in mineral processing, as they selectively render the desired minerals more hydrophobic than others. Current crop of sulfide collectors interact with almost all sulfide minerals. This necessitates the use of complicated reagent schemes to ensure efficient processing of typical polymetallic sulfide ores. Given the routine variability in ore composition and other operational parameters, these schemes are often very difficult to implement. For efficient and economical processing of lean grade, finely disseminated, and mineralogical complex future ore bodies, new collectors exhibiting superior collecting power and enhanced mineral selectivity need to be developed. However, till now no definitive criterion has been developed to guide us in design of such reagents. Mineral selectivity of collectors is a function of their molecular structure and specifications of mineral surfaces. Thus, establishing a comprehensive framework to guide us in determining the structural requirements for a collector to be selective towards a particular mineral, or to be used in a given scenario, is the most logical way to go ahead. However, it is very hard to relate structural features of a collector to its reactivity and binding ability through use of experimentally based approaches. In comparison, computational chemistry methods, such as density functional theory, are much more suitable for this purpose. Majority of sulfide collectors adsorb on minerals via chemical reactions with metal ions on the mineral surface or in the bulk solutions. Therefore, modeling the interaction of collectors with metal ions instead of mineral surfaces as a first approximation is more appropriate, as it is relatively fast and computationally economic.

In this work, interactions of three important collector classes, namely, anionic thiol collectors, neutral collectors, and mercapto azole reagents, were modeled with three common heavy metal ions, namely, Cu, Pb and Zn. Reactivity of individual collector molecules is

expressed quantitatively as well as qualitatively through use of: (i) theoretically calculated parameters (partial charges, spatial distribution and hybridization of frontier molecular orbitals, and geometrical parameters), and (ii) well-established reactivity descriptors (chemical potential, hardness, and global electrophilicity). The predicted orders of reactivity are linked to differences in the structures of collector molecules. Interaction energies for metal-collector complexes were calculated to assess the binding ability of collectors. Azole reagents were predicted to be most reactive, followed by anionic thiols. All collectors showed higher preference for Cu followed by Pb. Anionic thiol collectors were found to bind metal atoms in a bidentate fashion. Their reactivity and binding ability follow the order: dithiocarbamate > xanthate > dithiocarboxylate > trithiocarbonate > dithiophosphate. Neutral collectors interact with metal ions mainly through S atom of the thio-carbonyl group. The order of reactivity and binding ability is: thiourea > thionocarbamate > monothiocarbonate > dithiocarbonate > trithiocarbonate. Among the mercapto azole reagents, collectors of imidazole series were predicted to be most reactive, followed by thiazole series. These reagents interact with metals through exocyclic S and endocyclic imine N atom, and form chelate rings at metal centers.

The predicted order of reactivity and binding abilities agree well with the experimental observations reported in the past. This study, thus, establishes that a relationship between structure of flotation collectors and their reactivity towards different minerals could be formulated by considering metal-reagent interactions. The results obtained for neutral collectors and heterocyclic aromatic reagents eliminate the existing ambiguity in literature regarding their binding mechanism. This study shows that computational studies are very helpful in clarifying some of the unexplainable observations in experimental flotation, such as a very weak flotation efficiency of trithiocarbonate reagent compared to xanthates and dithiocarbamate reagents.

Acknowledgements

First and foremost, I would like to thank my supervisors Professor Zhenghe Xu and Professor Qingxia Liu, and co-supervisor Professor Phillip Choi, for their guidance, outstanding supervision and most importantly for their unconditional support and encouragnement throughout my PhD studies. During last five years, I have learnt a lot from them in both academic and non-academic arenas. I have been truly inspired by the knowledge, dedication, hardwork and multi-tasking ability of Dr. Xu and Dr. Liu. Being honest with myself, I know I lack some of these qualities and would definitely work hard to develop them in myself in the immediate future.

Also, special thanks to Ms. Lisa Carreiro, Mr. Jim Skwarok, Ms. Patricia Siferd, Mr. Carl Corbett and Ms. Lily Laser for their administrative support. Many a times, one or more of you have amazed me with your efficiency and dedication to your work.

I would also like to thank my colleagues and friends Dr. Robel Teklebrhan, Dr. Triratna Muneshwar and Dr. Diwen Zhou for their time, thoughtful discussions and feedback on my work. I also thank all the fellow students of the Department of Chemical and Materials Engineering at University of Alberta for their support.

I am grateful to C^5MPT for the financial and material support. I am thankful to Westgrid, Compute Canada for providing the computational resources needed for my project.

Finally my deepest gratitude goes to my family and friends for their love, encouragement, patience and support throughout my academic journey. I dedicate this work to my late father, Anoop Singh Sindhu and uncle, Dr. Bhoop Singh Sindhu for instilling in me the value of hard work and education, and for their support throughout my life.

Table of Contents

List of Tables

List of Figures

Chapter – 1

Introduction

1.1. Background

Froth flotation is the single most commonly utilized separation process in the minerals industry to concentrate a wide variety of metal ores, industrial minerals, and coals (Rao, Kundu, & Parker, 2012; Urbina, 2003). Apart from its extensive use in extractive metallurgy, flotation has also found important applications in several other fields, including plastics separation, paper recycling, wastewater treatment, oil sands processing, contaminated soil clean-up, oily sewage treatment, fly-ash beneficiation, and food and chemical processing, etc. In mineral flotation, valuable minerals such as galena (PbS), sphalerite (ZnS), and chalcopyrite ($CuFeS_2$) are separated from gangue (siliceous matter and iron sulfides) by utilizing differences in their wetting properties (Fairthorne, Fornasiero, & Ralston, 1996). The success of flotation essentially lies in the efficient chemical and electrochemical control of the system, for which a variety of chemical reagents are employed, including collectors, frothers, depressants, and activators (Urbina, 2003; H. Yekeler & Yekeler, 2006).

The success of flotation depends on selectively making the desired mineral hydrophobic while keeping the remaining ore constituents hydrophilic. The hydrophobic solid particles then attach to the air or gas bubbles dispersed through the pulp and rise to the surface, from where they are removed with the froth to form the mineral concentrate (Rao et al., 2012). The choice of collector type to be used is of vital importance in flotation as these reagents induce differences in the hydrophobicity of the mineral surfaces, and hence facilitate the attachment of minerals to air

bubbles (Porento & Hirva, 2002; H. Yekeler & Yekeler, 2006). For this sole reason, collector design and development is undoubtedly the most important aspect of flotation research.

Numerous studies were carried out during the last century, and the flotation research was immense, particularly that relating to the interaction of collector reagents with sulfide, oxide, and silicate minerals (Bag, Das, & Mishra, 2011; Urbina, 2003). This has led to the discovery of thousands of new reagents. However, only a handful of them have made their way to commercialization or have been used in practice (Nagaraj, 1994; Nagaraj & Ravishankar, 2007). Despite of massive research, reagents' selectivity toward certain mineral surfaces is still clueless (Kitchener, 1984). Till date no theory has been developed that could guide us in selection of the functional group and molecular structure of a collector to achieve a desired separation efficiently (Rao et al., 2012). Currently, the reagent schemes for different ores are developed through trial and error approach and experimenting with different types of existing collector reagents and their modified forms.

Sulfide mineral flotation has been dominated by sulfhydryl collectors, which include xanthates, dithiophosphates, thionocarbamates, etc. In particular, xanthates and their derivatives have been very popular and account for over two-third of world's total collector consumption (Fairthorne et al., 1996; Jiwu, Longling, & Kuoxiong, 1984; Klimpel, 1988). Sulfhydryl collectors, including xanthates, are powerful reagents that interact with a majority of sulfide minerals. However, they suffer some practical disadvantages, including minimal selectivity between different sulfide minerals, weak response towards oxidized/tarnished or mixed sulfide-oxide ores, and ease of decomposition (Fairthorne et al., 1996; Montalti, Fornasiero, & Ralston, 1991; Nagaraj, Wang, & Frattaroli, 1986; Nagaraj, Lewellyn, Wang, Mingione, & Scanlon, 1988). This often accounts for an increase in plant operating costs as additional reagents are

employed to achieve the desired selectivity and recovery. Many researchers have indicated that chelating reagents have the advantage of offering better selectivity and metal specificity (Marabini & Rinelli, 1973; Marabini & Rinelli, 1982; Nagaraj, 1982). A large number of compounds, with numerous combinations of donor atoms, mainly sulphur- nitrogen and sulphur-oxygen combinations have been tested. Up to date, the status of flotation reagents in industry has been largely unchanged (Rao et al., 2012).

As high-grade and relatively easy to process mineral resources rapidly becoming a rare commodity; lean-grade, finely disseminated and mineralogical complex ores have increasingly become the source of our metals and raw materials needs (Marabini, Barbaro, & Alesse, 1991; Urbina, 2003). Effective and economical processing of these difficult-to-treat ore deposits demand an urgent need to design and develop new performance chemicals for flotation industry (Marabini et al., 1991; Urbina, 2003). In particular, the industry would like to see more powerful and tailor made collectors aimed for specific applications (Malhotra, 1994; Nagaraj, Day, & Gorken, 1999; Pradip & Rai, 2003). Design of such collectors is by no means an easy task, as there could be millions of molecules that could be designed, synthesized and tested. Conventional approaches of collector design mainly utilize empirical rules of thumb and past experience (Pradip et al., 2002; Pradip, 2012). These approaches are expensive in terms of both time and resource requirements, and significant achievement is not always guaranteed (Pradip, 2012). These approaches are likely to prove incapable and inadequate for design and development of efficient collectors for future processing needs. Therefore, there is an urgent need to develop a scientifically robust methodology that can pave the way for the design and development of novel flotation chemicals customized for specific applications (Pradip & Rai, 2003; Pradip, 2012).

Collector reagents generally comprise of two parts: head group and tail group. The function of the head group is to selectively attach or bind to the mineral surfaces and/or metal ions of interest, and the role of hydrocarbon tail is to impart hydrophobicity. Flotation performance and collector efficiency are commonly measured in terms of experimental parameters, such as flotation recovery, contact angle, and induction time. However, these parameters are not a direct representation of the ability of a collector reagent to bind or attach to a mineral surface or metal ion, as their measurement is also influenced by the hydrocarbon radical along with different operational parameters.

Several mechanisms have been proposed for the flotation of sulfide minerals with different collectors. However, the reactions between the collectors and the sulfides of transition base metals are not fully understood yet (Crozier, 1991; Persson & Malmensten, 1991; H. Yekeler & Yekeler, 2004). Nonetheless, it is now widely accepted that flotation of base metal sulfides with collectors mainly involves either one or more of these mechanisms: chemisorption, surface chemical reaction, surface precipitation, or physisorption (Nagaraj & Ravishankar, 2007). In chemisorption and surface chemical reaction mechanisms, collectors adsorb on sulfide minerals by forming a metal complex (Nagaraj & Ravishankar, 2007). In physisorption, collector molecules are held at mineral surfaces through weak van der Waals forces. In systems, where flotation is mainly induced by surface precipitation, collector molecules complex with metal ions in the bulk[1], and the metal-collector complexes precipitate on mineral surfaces induce the surface hydrophobicity. In most of the systems, collector molecules chemisorb and/or physisorb onto minerals' surface at mono or sub-monolayer coverage followed by deposition of metal-collector precipitates or oxidation product(s) of collectors (Fuerstenau & Han, 2002).

[1] Metal ions enter the bulk phase through dissolution of mineral surfaces.

Selectivity of flotation reagents is largely determined by the molecular recognition phenomena underlying their reaction with metal species at mineral/water interface or in bulk (Pradip, 1994). These molecular recognition mechanisms are essentially based on the structural/stereochemical compatibility between the molecular architecture of the collector with heavy metal ions present on mineral surface linked to the specific surface structure (the nature and the spatial arrangement of adsorption sites on the surface) of the mineral with which it is interacting (Pradip & Rai, 2003), and the stability of resulting metal-collector complex at mineral surface or in bulk. Therefore, to design a flotation reagent for a specific application, a logical approach would be to theoretically identify the specific molecular recognition mechanism to specific metal ions or mineral surfaces, and to design the molecular architecture of new collectors accordingly (Pradip, 1994; Pradip & Rai, 2003). A good understanding of the molecular recognition mechanisms can be achieved by establishing a structure-function relationship between the current existing reagents, and mineral surfaces or heavy metals, based on computational chemistry.

Over the past three decades, computational quantum chemistry has emerged as a viable and powerful approach to explain and predict chemical behavior at subatomic level. These computational methods are valuable tools for understanding the complex chemical systems and prediction of their physiochemical properties (H. Yekeler & Yekeler, 2004). Computational chemistry methods such as density functional theory (DFT) and molecular dynamics (MD) are powerful tools to compute the relative magnitude of different types of interactions between collectors and mineral (or metal) species. Modeling the interactions between existing collectors and heavy metal ions or mineral surfaces can be useful in establishing a quantitative relationship between theoretically calculated parameters based on collectors' chemical structure and flotation

performance. A number of possible options of collectors can then be designed and evaluated for a given separation task in a short time, based on the computed value(s) of selected parameter(s).

Several research groups are currently engaged in studying interactions between collector reagents and mineral (or metal) species using molecular modeling tools. The geometrical structure and vibrational modes of ethyl and heptyl xanthates in metal xanthate complexes were studied by Hellstrom et al. (2006) using Hartree–Fock and DFT methods. They reported that vibrational frequencies calculated using DFT are in good agreement with the experimental results. Hellstrom et al. (2007) studied the interaction between ethyl xanthate on clean and hydroxylated Ge (III) surfaces using DFT. They showed a bidentate bridging conformation on a clean Ge(III) surface and a monodentate binding when the surface is saturated by hydrogen atoms. Hung et al. (2003) studied the adsorption of xanthate on pyrite surfaces using DFT and showed that xanthate undergoes chemisorption at defect sites on real FeS_2 surfaces. More recently, Chen et al. (2013) utilized DFT methods to study the adsorption of xanthate, dithiophosphate, and dithiocarbamate collectors on galena and pyrite mineral surfaces, and reported better selectivity offered by dithiophosphate and dithiocarbamate in galena-pyrite separation compared to xanthate.

Yekeler et al. (2004) studied the reactivity and interaction of different thiol collectors with Ag(+1) ions in vacuum phase. Based on the calculated highest occupied molecular orbital (HOMO) and interaction energies, dithiocarbamate was predicted to possess the strongest collecting power, followed by xanthate, trithiocarbonate and dithiophosphate. Same authors used the concepts of HOMO localization and HOMO energy along with Mulliken charges and electrostatic potential to predict the reactivity of different 2-mercaptobenzothiazole (MBT) derivatives from DFT calculations at the B3LYP level (H. Yekeler & Yekeler, 2006). Same

methodology was used to predict the reactive behavior of 2-mercaptobenzoxazole (MBO) and its derivatives (M. Yekeler & Yekeler, 2006). Bag et al. (2011) studied the effect of structure and length of hydrocarbon chain in xanthate collector on its reactivity and interaction with Cu(I) ion. Pradip et al. studied interactions of alkyl hydroxamates and oleate molecules with calcium minerals (2002; 2008) and rare earth minerals (Pradip & Fuerstenau, 2013) by using semi empirical methods. Liu et al. (2008; 2010) studied the effect of nature of substituent group present on N-atom on the performance of thionocarbamates and thiourea collectors by DFT methods. Studies on activation of sphalerite through adsorption of Pb, Cu and Fe ions on the ZnS surface have also been reported (Stelle, Wright, & Hillier, 2003; Sun, Hu, & Qin, 2004).

Majority of the studies that aimed to establish the relative reactivity of different collector molecules didn't include their binding with metal or mineral species or considered a single metal ion at most. However, sulfide ore bodies typically contain more than one metal of interest. For example, Cu minerals generally occur in association with one or more minerals of Pb, Au, Zn, or Mo. Also, these studies predicted the reactivity based on theoretically calculated parameters but did not relate the value of these parameters to collectors' structures. Studies that dealt with adsorption of collector molecules on mineral surface have been limited to a very few reagent-mineral combinations. Most of these were aimed to understand a detailed mechanism of adsorption, rather than establishing relative reactivity and binding ability of different reagents. Furthermore, different studies used different molecular modeling methods. Results obtained by using different methods may not be comparable in most of the cases.

Therefore, modeling of interaction of these collectors with multiple metal ions or mineral surfaces within a single study would be desirable. If we want to develop a powerful and robust framework to guide us in the design of novel performance collectors aimed at specific

applications, we essentially need to catalogue interactions between as many collector types and mineral surfaces or metal ions, as possible. In this thesis, interaction of a variety of reagents, representing three important collector classes, namely, collectors based on CS_2^- head group (commonly referred as thiol type), thio-carbonyl head group (commonly referred as neutral type), and heterocyclic aromatic reagents, were modeled with three different heavy metal ions, namely Cu, Pb, and Zn. Density functional theory (DFT) methods were used to model all the molecules. For all the collector-metal combinations, formation of MX_2 type metal-collector complexes was considered. Fuerstenau et al. (1974; 2002) has discussed the vital role played by formation, and subsequent adsorption/deposition of these complexes, in the success of sulfide mineral flotation.

It is important to mention here that these reagents have equally important applications in other industries, including heavy metal bearing industries. Heavy metal bearing industries such as mining operations, electroplating facilities, and power generation centers leave behind large amount of heavy metals as waste product. These heavy metals need to be removed from wastewater streams before they can be released to the environment, since they have a very high tendency to enter food chain and to accumulate in living organisms. Accumulation of heavy metals, including Cu, Pb, Zn, Ni, Cd, As and Cr, beyond a certain limit (metal specific) may lead to detrimental effects on human physiology and other biological systems. The reagents are dissolved in aqueous bodies, where they complex heavy metals, and subsequently results in precipitation of metal-reagent complexes. As the environmental regulations are becoming increasingly stringent, design of powerful metal specific chemical precipitants or complexing agents is an urgent requirement for this industry too.

1.2. Project Scope

The ability of a collector reagent to bind particular metal specie in bulk or on mineral surfaces is mainly dependent on the molecular structure of collector's head functional group. Experimentally driven parameters, such as contact angle, flotation recovery, etc. are not very capable means for extracting this information. DFT, the most efficient and fairly accurate computational quantum chemistry method, is an appropriate tool to relate the structural characteristics of collector molecules to their reactivity and binding affinity towards different metals.

Flotation is the process of physical separation of one mineral from other(s). So modeling of adsorption of a variety of collector molecules on surfaces of different minerals appears to be a better approach than modeling interaction between collector molecules and metal ions. However, modeling of the adsorption process is time consuming and computationally intensive. Modeling the interaction of collector molecules with metal ions, on the other hand, could be achieved in a relatively short time. The formulation of a robust relationship between collector's structure and its reactivity toward different metal/minerals requires inclusion of a wide variety of complexing agents. Therefore, the latter approach is more suitable as large number of collectors with different molecular structures can be covered in a small time frame. Once the structural criteria for metal selective collectors are established, a few new promising collectors may be developed for each metal. Adsorption of these molecules can then be modeled on mineral surfaces containing that particular metal. The molecule(s) exhibiting best adsorption characteristics can then be synthesized and their collecting performance can be experimentally tested.

1.3. Objectives

The objectives of this study are:

(i) To investigate the interaction between three important collector classes (anionic thiol type reagents, neutral reagents based on thio-carbonyl head group, and heteroatomic aromatic chelating reagents) and bivalent ions of Pb, Zn, and Cu metals in solution, to gain an atomic level insight into the interactions encountered in flotation and heavy metal precipitation industry.

(ii) To predict the (relative) reactivity of different collectors in terms of theoretically calculated parameters and to relate the trend in values of calculated parameters with variations in molecular structures of collectors.

(iii) To predict the strength of metal-collector interaction via calculation of interaction energy for the modeled metal-collector complexes, and to compare the trend observed in calculated interaction energies with the trend observed in predicted molecular reactivity of different collectors.

(iv) To compare the predicted trends in molecular reactivity and interaction energy with observed flotation performance as reported in published literature.

(v) To examine the effect of different substituent functional groups on the reactivity and binding capability of different collector reagents.

(vi) To provide the guideline for the design of novel collectors for sulphide flotation.

As mentioned earlier in Section 1.1. and 1.2., the robust framework that could guide us in design and development of metal or mineral specific (or selective) collectors should be based on the study of interaction between as many collector and metal types as possible. The data obtained

and learnings from this study will be used in conjugation with data for other collector-metal combinations, to formulate the structural characteristics of collectors that are very selective towards a particular metal.

1.4. Organization of Thesis

The thesis is organized into seven chapters and the details of each chapter are described as follows:

Chapter 1 presents the general background of this study and introduces the objectives and scope of current work. Chapter 2 provides a general overview of froth flotation process. The fundamental concepts of flotation process and role of different type of reagents were briefly reviewed, followed by a concise discussion on different types of collectors used in sulfide flotation and their mechanisms of action. Chapter 3 focuses on the theoretical background of computational quantum chemistry methods and introduces the methodology adopted for this study. Chapter 4 details the computational results for reactivity and metal affinities of reagents based on thiol ($–CS_2^-$) head group. This chapter has been written in context of removal of heavy metals from industrial wastewater streams; however, the observations and findings are equally applicable to flotation industry. Chapters 5 and 6 discuss the results for heterocyclic aromatic reagents and reagents based on thiocarbonyl (C=S) head group, respectively. Finally, the conclusions and summary of the entire research project with possible directions for future work are presented in Chapter 7.

1.5. References

Bag, B., Das, B., & Mishra, B. K. (2011). Geometrical optimization of xanthate collectors with copper ions and their response to flotation. *Minerals Engineering, 24*(8), 760-765.

Chen, J., Lan, L., & Chen, L. (2013). Computational simulation of adsorption and thermodynamic study of xanthate, dithiophosphate and dithiocarbamate on galena and pyrite surfaces. *Minerals Enginneering, 46-47*, 136-143.

Crozier, R. D. (1991). Sulphide collector mineral bonding and the mechanism of flotation. *Minerals Engineering, 4*(7–11), 839-858.

Fairthorne, G., Fornasiero, D., & Ralston, J. (1996). Solution properties of thionocarbamate collectors. *International Journal of Mineral Processing, 46*(1–2), 137-153.

Fuerstenau, M. C., Clifford, K. L., & Kuhn, M. C. (1974). The role of zinc-xanthate precipitation in sphalerite flotation. *International Journal of Mineral Processing, 1*(4), 307-318.

Fuerstenau, M. C., & Han, K. N. (2002). Metal–Surfactant precipitation and adsorption in froth flotation. *Journal of Colloid and Interface Science, 256*(1), 175-182.

Hellstrom, P., Holmgren, A., & Oberg, S. (2007). An ab-initio study of ethyl xanthate adsorbed on Ge (111) surface. *Journal of Physical Chemistry, 111*(45), 16920-16926.

Hellstrom, P., Oblatt, S., Fredriksson, A., & Holmgren, A. (2006). A theoretical and experimental study of vibrational properties of alkyl xanthates. *Spetrochim. Acta, 65A*, 887-895.

Hung, A., Yarovsky, I., & Russo, S. (2003). Density-functional theory studies of xanthate adsorption on the pyrite FeS2 (110) and (111) surfaces. *Journal of Chemical Physics, 118*(13), 6022-6029.

Jiwu, M., Longling, Y., & Kuoxiong, S. (1984). Novel frother-collector for flotation of sulphide minerals - CEED. *Reagents in the Minerals Industry,* London. 287-290.

Kitchener, J. A. (1984). The froth flotation process: Past, present and future-in brief. in the scientific bases of flotation. In K. J. Ives (Ed.), *Scientific bases of flotation*. The Hague: Martinus Nijhoff Publishers.

Klimpel, R. R. (1988). The industrial practice of sulfide mineral collectors. Paper presented at the *Reagents in Mineral Technology,* New York. *, 27* 663-682.

Liu, G., Zhong, H., & Dai, T. (2008). Investigation of the selectivity of ethoxylcarbonyl thionocarbametes during the flotation of copper sulfides. *Minerals and Metallurgical Processing, 25*(1), 19-24.

Liu, G., Zhong, H., Xia, L., Wang, S., & Dai, T. (2010). Effect of N-substituents on performance of thiourea collectors by density functional theory calculations. *Transactions of Nonferrous Metals Society of China, 20*(4), 695-701.

Malhotra, D. (1994). Reagents in the mining industry: Commodities or speciality chemicals. *Reagents for better metallurgy* (pp. 75-80) SME-AIME.

Marabini, A. M., Barbaro, M., & Alesse, V. (1991). New reagents in sulphide mineral flotation. *International Journal of Mineral Processing, 33*(1–4), 291-306.

Marabini, A. M., & Rinelli, G. (1973). Flotation of pitchblend with a chelating agent and fuel oil. *Transactions of Institution of Mining and Metallurgy, 82*, C225-C228.

Marabini, A. M., & Rinelli, G. (1982). The development of a specific reagent for futile flotation. *AIME Annual Meeting,* Dallas.

Montalti, M., Fornasiero, D., & Ralston, J. (1991). Ultraviolet-visible spectroscopic study of the kinetics of adsorption of ethyl xanthate on pyrite. *Journal of Colloid and Interface Science, 143*(2), 440-450.

Nagaraj, D. R. (1982). Chelating agents in mineral processing. *III AIME Annual Meeting,* Dallas.

Nagaraj, D. R. (1994). A critical assessment of flotation agents. *Reagents for Better Metallurgy,* Littleton, CO. 81-90.

Nagaraj, D. R., Day, A., & Gorken, A. (1999). Nonsulphide minerals flotation: An overview. In B. K. Parekh, & J. D. Miller (Eds.), *Advances in flotation technology* (pp. 245-256). Littleton: SME.

Nagaraj, D. R., Lewellyn, M. E., Wang, S. S., Mingione, P. A., & Scanlon, M. J. (1988). New sulfide and precious metals collectors: For acid, neutral and mildly alkaline circuits. *Proceedings of XVIth International Mineral Processing Congress,* Stockholm. 1221-1232.

Nagaraj, D. R., & Ravishankar, S. A. (2007). Flotation reagents - A critical overview from an industry prospective. In M. C. Fuerstenau, G. Jameson & R. Yoon (Eds.), *Froth flotation: A century of innovation* . Littleton: SME.

Nagaraj, D. R., Wang, S. S., & Frattaroli, D. R. (1986). Flotation of copper sulfide minerals and pyrite with new and existing sulfur-containing collectors. *Proceedings of 13th CMMI Congress,* Singapore. 49-57.

Persson, P., & Malmensten, B. (1991). Interactions between sulfide minerals and alkylxanthate ions - 5. A vibration spectroscopic study of the interactions between chalcocite, synthetic copper(I) sulfide, acanthite and synthetic silver(I) sulfide, and ethylxanthate ions in aqueous and acetone solutions. *Colloids and Surfaces, 59*(0), 279-292.

Porento, M., & Hirva, P. (2002). Theoretical studies on the interaction of anionic collectors with Cu(+), Cu(2+), Zn(2+) and Pb(2+) ions. *Theoretical Chemistry Accounts, 107*(4), 200-205.

Pradip. (1994). Reagents design and molecular recognition at mineral surfaces. In P. Mulukutla (Ed.), *Reagents for better metallurgy* (pp. 245-252). Denver: SME-AIME.

Pradip. (2012). Rational design of selective industrial performance chemicals based on molecular modeling computations. (pp. 27-64) CRC Press.

Pradip, & Fuerstenau, D. W. (2013). Design and development of novel flotation reagents for the beneficiation of mountain pass rare-earth ore. *Minerals & Metallurgical Processing, 30*(1), 1-9.

Pradip, & Rai, B. (2003). Molecular modeling and rational design of flotation reagents. *International Journal of Mineral Processing, 72*(1–4), 95-110.

Pradip, Rai, B., Rao, T. K., Krishnamurthy, S., Vetrivel, R., Mielczarski, J., & Cases, J. M. (2002). Molecular modeling of interactions of alkyl hydroxamates with calcium minerals. *Journal of Colloid and Interface Science, 256*(1), 106-113.

Rai, B., & Pradip. (2008). Design of highly selective industrial performance chemicals: A molecular modeling approach. *Molecular Simulation, 34*, 1209-1214.

Rao, H. K., Kundu, T., & Parker, S. (2012). Molecular modeling of mineral surface reactions in flotation. *Molecular modeling for the design of novel performance chemicals and materials*

Stelle, H., Wright, K., & Hillier, I. (2003). A quantum-mechanical study of the (110) surface of sphalerite (ZnS) and its interaction with Pb(2+) species. *Physics and Chemistry of Minerals, 30*, 69-75.

Sun, W., Hu, Y., & Qin, Q. (2004). DFT research on activation of sphalerite. *Transactions of Nonferrous Metals Society of China, 14*(2), 376-382.

Urbina, R. H. (2003). Recent developments and advances in formulations and applications of chemical reagents used in froth flotation. *Mineral Processing and Extractive Metallurgy Review, 24*(2), 139-182.

Yekeler, M., & Yekeler, H. (2006). A density functional study on the efficiencies of 2-mercaptobenzoxazole and its derivatives as chelating agents in flotation processes. *Colloids and Surfaces A: Physicochemical and Engineering Aspects, 286*(1–3), 121-125.

Yekeler, H., & Yekeler, M. (2004). Reactivities of some thiol collectors and their interactions with Ag(+1) ion by molecular modeling. *Applied Surface Science, 236*(1–4), 435-443.

Yekeler, H., & Yekeler, M. (2006). Predicting the efficiencies of 2-mercaptobenzothiazole collectors used as chelating agents in flotation processes: A density-functional study. *Journal of Molecular Modeling, 12*(6), 763-768.

Chapter – 2

Froth Flotation and Collector Reagents

2.1. General Overview of Flotation Process

Froth flotation is considered as one of the most enabling technological inventions of the 20th century, and is the single most commonly utilized beneficiation method to separate valuable minerals from gangue constituents in mined ores. Apart from its extensive use in extractive metallurgy, flotation has also found important applications in several other fields, including plastics separation, paper recycling, wastewater treatment, oil sands processing, contaminated soil cleanup, oily sewage treatment, fly-ash beneficiation, and food and chemical processing, etc. Flotation is a highly selective process and therefore, it is often considered advantageous over other separation methods. As the selectivity of flotation process can be manipulated through modification in different (physical and chemical) operating conditions, it has been successfully applied to concentration of a variety of minerals, including sulfides, oxides, silicates, and coal, since its inception in early 1900s. Along with mechanized mining, flotation has permitted the economic recovery of valuable minerals from much lower grade and complex ore bodies which used to appear unattainable in past. Currently, an estimated 9 billion tonnes of ore is treated globally utilizing froth flotation process annually (Saracoglu, 2013).

Fundamentally, flotation may be defined as a physicochemical process through which components (valuable and gangue) of a mineral ore are separated by utilizing differences in their wetting properties (Pearse, 2006; Wills & Napier-Munn, 2006). The key to success of flotation lies in the natural or imposed (induced) hydrophobicity of a certain mineral(s) while the other ore

constituents remain hydrophilic or less hydrophobic. A simplified schematic diagram of the flotation process is shown in Figure 2.1. A flotation cell is typically a large rectangular or cylindrical tank comprising air (or gas) spargers to supply air to the tank, and an impeller to agitate the slurry/air mix and to keep the mineral particles suspended in liquid phase. The flotation cell is fed with ground mineral slurry where solid particles are typically in sub 100µm range. The mineral slurry is treated with a variety of flotation chemicals either prior to its introduction in the flotation cell or within the flotation cell, to balance the flotation environment and to enhance or subdue the hydrophobicity of specific minerals.

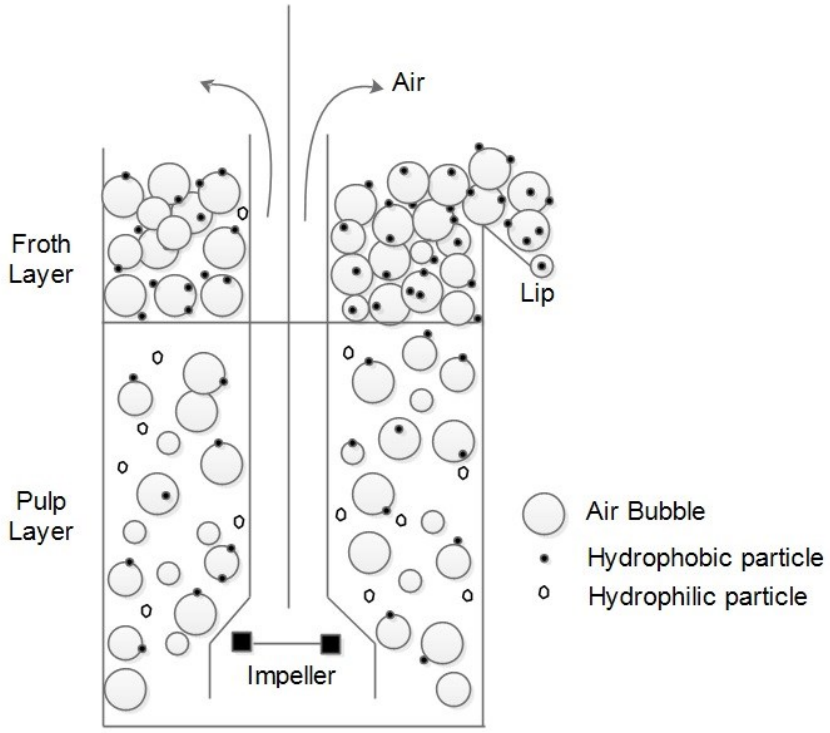

Figure 2.1. A schematic diagram representing the froth flotation process.

When air is introduced at the bottom of the cell, air bubbles rise through the agitated pulp and collide with suspended mineral particles. As certain mineral particles (to be separated) have

relatively higher surface hydrophobicity than remaining, they may get attached to the air bubbles at the event of collision. The particles attached to air bubbles are lifted to the top of pulp phase where a stable froth layer is formed, which is subsequently skimmed or migrates by itself over the lip (weir) of the flotation cell. Each bubble can potentially collide with many particles during its ascend, and therefore, it may carry several hydrophobic particles to the froth phase. The collected froth is further treated to form the mineral concentrate. The transport of hydrophobic particles to the froth phase via attachment to air bubbles is a highly selective process and termed as *true flotation*. During flotation, another small fraction of particles (both valuable and gangue) reports to the froth phase, either via *entrainment*, where the particles get lifted to froth phase due to upward motion of air bubbles and turbulence, and remain there suspended in the liquid channels separating the air bubbles, or via *physical entrapment,* where a particle may get trapped between two mineral laden bubble surfaces or between two hydrophobic particles attached to a bubble and transported to the froth phase. These particles may or may not report back to the pulp phase, depending on froth conditions and froth removal mechanism. Both these processes are unselective in nature and primarily responsible for a decrease in grade of the concentrated product. A schematic representation of true flotation and entrainment is shown in Figure 2.2. The hydrophilic particles, often termed as *gangue minerals*, remain suspended in the pulp phase and get flushed away as tailings.

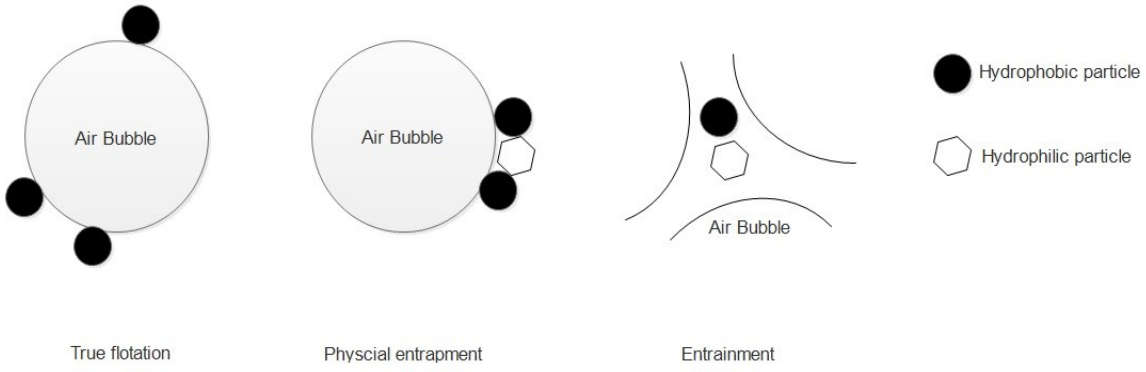

Figure 2.2. Different ways in which particles can report in froth phase: true flotation, physical entrapment, and entrainment of particles.

The process described above is commonly referred as *direct flotation* where valuable minerals form the hydrophobic fraction of the mineral slurry. Conversely, if gangue minerals are hydrophobic and tailings are collected in froth phase, leaving the valuable minerals back in pulp to form the mineral concentrate, the process is called *reverse flotation*. In an industrial setting, the flotation circuit typically comprises of a bank of flotation cells to allow multistage treatment of the slurry and to ensure minimum loss of valuable minerals to the final tailings.

2.2. Important Parameters in Flotation

Froth flotation is an intricate process that involves interplay of numerous factors, and makes flotation plants extremely difficult to optimize. Crozier (1992) listed over 25 parameters, which can influence flotation performance independently or in combination with other parameters. Klimpel (1984) classified the influencing parameters into three broad categories: (i) equipment/hydrodynamic components, (ii) operational components, and (iii) chemistry components. As illustrated in Figure 2.3, each of these parameters holds equal importance and an interactive relationship with other parameters. This means that change in one parameter will have

a compensating effect in (one or more) other parameters. Bradshaw (1997) pointed out that researchers should be extremely careful in experimental design and data analysis when isolating and studying the effect of a particular parameter on flotation performance.

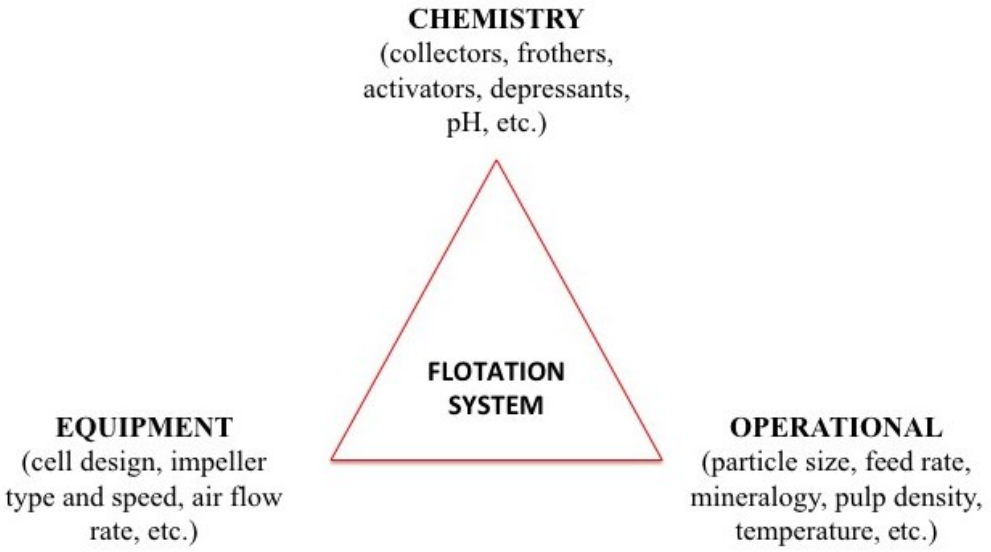

Figure 2.3. Summary of interrelated components of flotation process [adapted from (R. Klimpel, 1984)].

2.2.1. Equipment Parameters

Equipment parameters such as cell design, impeller tip velocity, impeller off-bottom clearance, and air inflow rate, etc. play an important role in determining hydrodynamic conditions in a flotation cell along with other factors such as particle size, feed rate, and frother type and concentration (Nasab, 2014; Newell & Grano, 2007). Hydrodynamic conditions in a flotation system are of vital importance as they control the particle-bubble interactions and thus effect overall flotation performance (Finch, Xiao, Hardie, & Gomez, 2000). The effect of equipment

parameters and hydrodynamics on flotation performance is however not the focus of this study, and therefore no further details are included here.

2.2.2. Operational Parameters

Operational parameters that influence flotation performance include ore mineralogy, particle size, pulp density, and feed rate (R. Klimpel, 1984). Mineralogical characteristics such as grain size, composition, association of different ore constituents, etc. are vital in understanding the flotation response of a mined ore as they play a significant role in determining how particles will be liberated during comminution stage and interact with different reagents or bubbles in flotation environment. Pulp density and feed rate are important in determining hydrodynamic conditions in flotation systems. Concentration of solids in flotation systems is also an important factor in determining froth stability as higher concentrations generally favour a more stable froth (Lovell, 1976).

The role of particle size in flotation has been massively studied and often considered very complex. It is generally observed that for a particular flotation system, there exists an inverted U shape flotation recovery (or flotation rate) versus particle size curve as shown in Figure 2.4 (Pearse, 2006; Rahman, Ata, & Jameson, 2012). Various studies on different ores have reported that there is an optimum size range, usually 10-100 μm, where high flotation efficiency is observed. Outside this range, recovery drops significantly for both fine and coarse particles (Anthony, Kelsall, & Trahar, 1975; Feng & Aldrich, 1999; Trahar, 1976). The reason behind poor recovery and slow flotation kinetics of coarse particles has been associated with poor liberation and high probability of detachment of particles from bubble surfaces (Gontijo, Forenasiero, & Ralston, 2007; Öteyaka & Soto, 1995; Tao, 2005). Fine particles on the other hand, show poor flotation response as they exhibit low collision efficiencies (with bubbles)

because they have small inertial force due to their lower masses (Tao, 2005; Yoon & Luttrell, 1989). Therefore, turbulent conditions in a flotation cell favor the recovery of fine particles over coarse particles (Schulze, 1984).

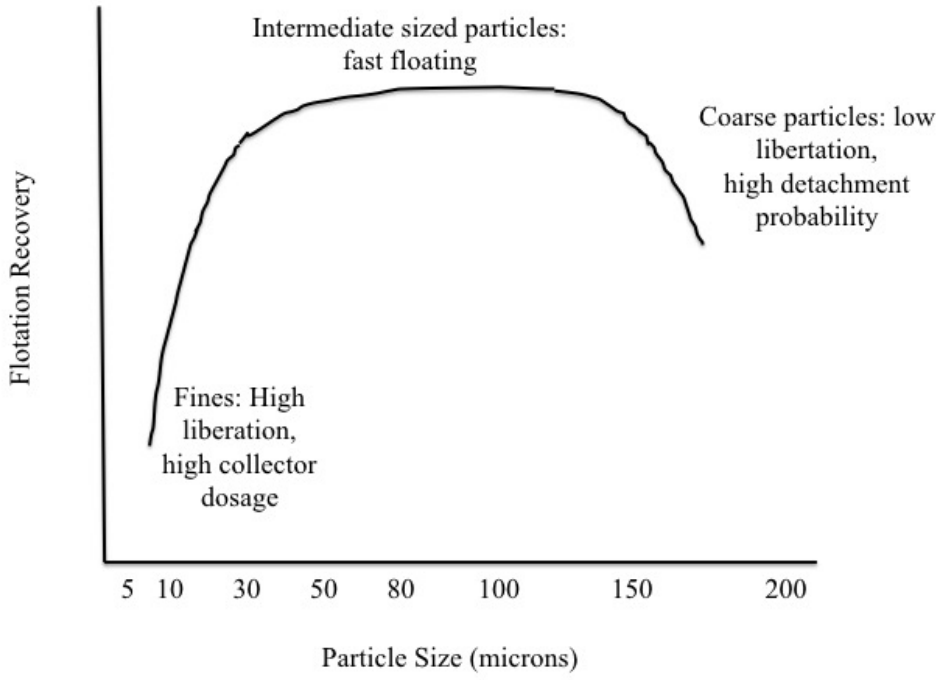

Figure 2.4. A typical inverted U shaped recovery versus particle size curve for flotation systems [adapted from (Pearse, 2006)].

However, it is noteworthy that relationship between flotation recovery and particle size not merely depends on physical effects (collision, attachment, and detachment) between particle and bubble but is also influenced by other interactive variables such as froth stability, reagents type and dosage, and particle size distribution. Schwarz (2004) suggested that particle size is an important factor in determining bubble coalescence and froth stability. Szatkowski and Freyburger (1985), in their study on fine hydrophilic particles reported that presence of fine particles in froth phase led to decreased bubble coalescence and thus promoted froth stability

which resulted in increased recovery of fine particles. Similarly, Livshits and Dudenkov(1965) suggested that coarse hydrophobic particles lead to higher froth stability as they act as a buffer between two bubbles. However, Moudgil (1992) in his study on flotation of coarse phosphate particles claimed that very large particles destabilize the froth due to their weight. Pease et al. (2006) reported that recovery of fine particles can be improved by narrowing the size distribution of hydrophobic particles in the flotation system. Moudgil et al. (1988) showed that presence of fine apatite particles (~ 100-500 μm) improves the recovery of coarse particles (500-1190 μm) without affecting the recovery of fine particles as long as fine and coarse particles are not conditioned together. They attributed higher recovery of coarse fraction to improved frothing efficiency in presence of fine particles. When fine and coarse particles are conditioned together, a decrease in recovery of coarse fraction was observed which was attributed to disproportionate adsorption of collector on fines and coarse fraction due to difference in specific surface areas (Moudgil et al., 1988; Vanangamudi, Kumar, & Rao, 1989).

2.2.3. Chemistry Parameters

As mentioned earlier the basis of froth flotation process is the difference in wettabilities of different minerals. The surface properties of raw minerals suspended in water are rarely suited for their separation through froth flotation. Therefore, chemical reagents are often needed to control the relative hydrophobicities of different ore constituents, and to maintain proper pulp and froth characteristics to facilitate mineral separation. In fact, reagents are generally considered as the most important aspect of the flotation process (S. M. Bulatovic, 2007a). According to Rao (2004), *"the process of flotation is fundamentally based on the judicious application of different classes of chemical agents performing specific functions"*.

Flotation reagents are generally classified into different categories based the function or purpose of a particular reagent. The selection of a set of reagents for a particular scenario depends on the specific mineral mixture being treated. The main classes of reagents used in flotation are collectors, frothers, depressants, activators, regulators, and flocculants. Since the inception of flotation process by minerals industry, thousands of chemicals were either tested or suggested as flotation reagents. However, only a small fraction of these reagents have been extensively used in actual practice (S. M. Bulatovic, 2007a).

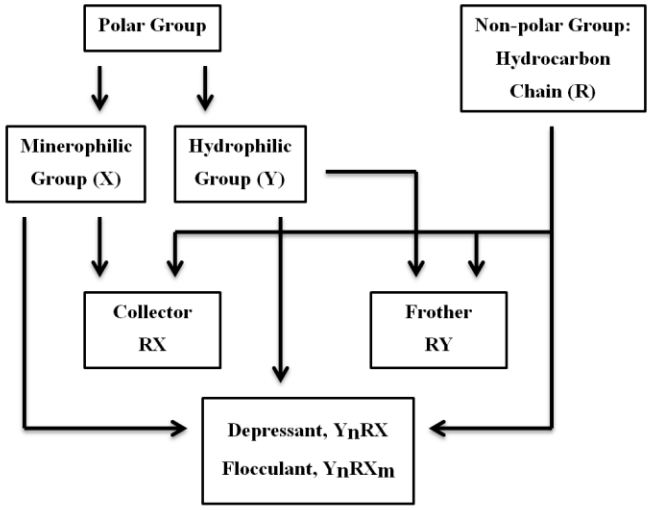

Figure 2.5. Basic structure of various flotation reagents [adapted from (Somasundaran & Wang, 2006a)].

Structure of flotation reagents comprises of polar and/or non-polar portions as shown in Figure 2.5 (Somasundaran & Wang, 2006a). The non-polar part is generally a hydrocarbon radical (liner, branched, or ring), has water repellent characteristics, and therefore is termed as hydrophobic group. As per Somasundaran and Wang (2006a), the polar part can be classified into two types: (i) hydrophilic groups that strongly interact with water, and (ii) minerophilic groups that interact with surfaces of polar minerals as well as water molecules. The non-polar

part may also act as a minerophilic group with non-polar minerals such as talc, mica, and coal via van der Waals forces. Through careful combination of these three basic groups a variety of flotation reagents can be designed. Therefore, the molecule structure of a flotation reagent can be divided into individual parts and their importance and effect on overall flotation performance may be analyzed.

2.2.3.1. Collectors

Collectors are reagents whose predominant function is to selectively induce hydrophobicity onto particles of a given mineral in the flotation pulp so as to facilitate their attachment onto air bubbles. The molecular structure of a collector reagent generally comprises of a minerophilic and a non-polar part. The non-polar portion of a collector reagent is a hydrocarbon radical (water repellant) whereas the minerophilic part interacts with the mineral surface by adsorption or chemical reactions. The action of collector molecules onto a mineral surface results in a configuration similar to as shown in Figure 2.6. As the non-polar group is oriented toward the water phase, the mineral surface is rendered hydrophobic due to the action of collector reagent.

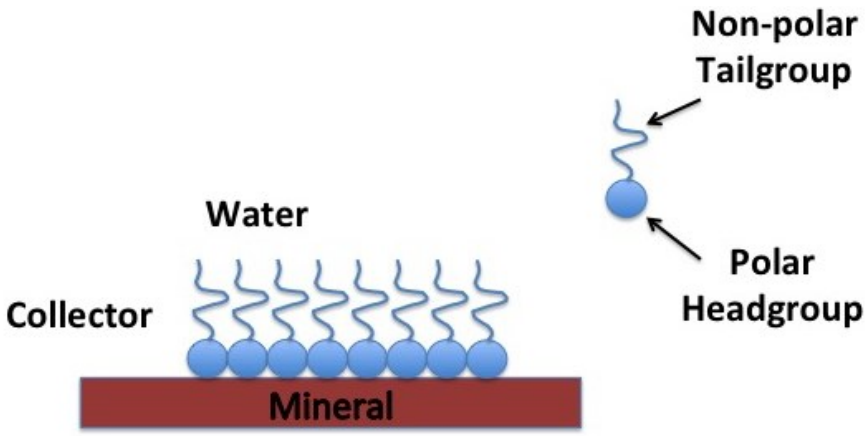

Figure 2.6. Adsorption of collector molecules onto the mineral surface.

The hydrophobic effect of the collector is directly associated to the length and structure of the hydrocarbon radical, whereas the effect of minerophilic part depends on the type and strength of its interaction with mineral surface and selectivity toward different mineral surfaces, both of which are determined by the composition and structure of the minerophilic group (S. M. Bulatovic, 2007a). On the basis of their dissociating properties in water, collectors can be divided into non-ionizing and ionizing reagents. Non-ionizing collectors are basically simple non-polar hydrocarbon compounds that render the selected minerals (generally non-polar) hydrophobic by forming a thin water-repellent layer on their surface. As these reagents lack a polar or minerophilic group, they do not form oriented adsorption layers on the mineral surface but stick to naturally hydrophobic minerals such as graphite and elemental sulphur via hydrophobic forces, thus enhancing the surface's hydrophobicity.

Ionizing collectors may be further divided into cationic and anionic reagents depending on which part of the dissociated reagent is minerophilic. Cationic collectors are generally based on positively charged amine group with one to four hydrocarbon radicals attached to N atom. Cationic collectors are mainly used in the flotation of minerals whose surfaces bear a natural negative charge in solution (at a particular pH). Cationic collectors are mainly utilized in recovery of silicate and oxide minerals (D. W. Fuerstenau & Urbina, 1990) and, for separation of sylvite (KCl) from halite (NaCl) (Pan, 2013).

Anionic collectors are organic reagents where the minerophilic group is either negatively charged or possess one or more atoms capable of donating electrons for bond formation with metals on mineral surfaces or in pulp phase. These reagents can be further divided into oxhydryl and sulfhydryl collectors based on the structure of the minerophilic group. Oxhydryl collectors are principally based on organic or sulfo acid anions, and the anionic part of the reagents

generally contains –X–O^- entity (where X: C, S, N, or P). Examples of common oxhydryl collectors are alkyl carboxylates, alkyl sulfates, hydroxamate, alkyl sulfonates, sulfosuccinate, phosphoric acid esters, etc. Oxhydryl collectors are generally powerful collectors with very low selectivity against gangue minerals. Their performance is highly dependent on chemistry of flotation pulp and the use of modifier reagents (S. M. Bulatovic, 2007a). Oxhydryl collectors are mainly used for flotation of silicate, sulfate, carbonate, and oxide minerals. Compared to sulfhydryl collectors, oxhydryl collectors have found limited applications in minerals industry, which has been attributed to lack of research on these reagents (S. M. Bulatovic, 2007a). More details on type, structure, and use of oxhydryl collectors can be found in some of the relevant books (S. M. Bulatovic, 2007a; D. W. Fuerstenau & Urbina, 1990).

The collectors containing sulfur atom as their principal electron-donating center (negative charge or unshared lone pair orbital) in combination with an organic radical are categorized as sulfhydryl reagents. In general, the electron donating sulfur atom is connected to carbon (thiols) or phosphorus atom. The C-S or P-S branch is linked to the hydrocarbon radical through a connecting element, which is generally carbon, oxygen, nitrogen, or sulfur atom. Sulfhydryl reagents are the most popular collectors in flotation industry and are used in flotation of a wide range of sulfide and oxide minerals. Sulfhydryl collectors can be anionic (e.g. xanthates, dithiophosphates, dithiocarbamate, etc.), or neutral (e.g. O,N-dialkylthionocarbamates, S,N-dialkyldithiocarbamates, xanthogenformates, N,N-dialkylthioureas, etc.).

When the minerophilic group of an oxhydryl or sulfhydryl collector also possesses an additional atom that can be coordinated by the metal at the same time, the reagent is (also) termed as a chelating reagent. This second atom is usually oxygen, nitrogen, sulfur, or phosphorus, and it generally coordinates with the metal via a dative bond. Following this

definition, a majority of commonly used sulfhydryl collectors such as xanthates, dithiocarbamates, and dithiophosphates are chelating type reagents. A large number of other chelating reagents have been evaluated for flotation applications and a few have also been found promising (Assis, Montenegro, & Peres, 1996; Barbaro, 2000; Lee, Archibald, McLean, & Reuter, 2009; Maier & Dobiáš, 1997; A. M. Marabini, Barbaro, & Alesse, 1991; A. M. Marabini, Ciriachi, Plescia, & Barbaro, 2007; Somasundaran & Nagaraj, 1984; Woods, Hope, & Watling, 2000). However, these new chelating type flotation reagents have not been applied to industrial scale flotation successfully apart from hydroxamate collector (S. M. Bulatovic, 2007a). Different types of sulfhydryl and chelating type collectors and their mode of action onto sulfide minerals is discussed in the following sections.

2.2.3.2. Frothers

Formation of stable froth is one of the most important aspects of froth flotation, wherein the valuable minerals are retained for further upgrading (Bezuidenhout, 2011). Generation of froth is generally achieved by addition of frothing agents, which are generally referred as frothers. Frother reagents are neutral molecules comprising a hydrocarbon chain (non-polar) and minerophilic group (polar). The hydrocarbon group can be straight, branched or cyclic whilst the polar group can be a hydroxyl, carbonyl, ester, carboxyl, amine, nitrile, phosphate or sulphate (Bezuidenhout, 2011). Frother molecules adsorb on the air-water interface such that the non-polar part is oriented in the air phase and polar part remains in water where it forms hydrogen bonds with water molecules (Laskowski, 1993). In addition to generation of a stable froth, frother reagents also play other important roles in flotation, which include:

(i) On adsorption of air-water interface, frother molecules form hydrogen bonds with neighbouring water molecules and form a stable water film around the bubble. Formation

of this capillary film leads to inhibition of bubble coalescence (Bezuidenhout, 2011; Pugh, 1996).

(ii) Adsorption of frothers on bubble surfaces creates favourable conditions for bubble-particle attachment by reducing the bubble rising velocity in the pulp phase (Finch, Nesset, & Acuña, 2008).

(iii) Use of frothers reduce bubble size and thus aid in the generation of fine bubbles (N. Ahmed & Jameson, 1985; Finch et al., 2008), which in turn enhances the flotation of finer fraction of particles.

(iv) Use of frother stabilise the bubble-particle aggregates by interaction with collectors (Bezuidenhout, 2011).

2.2.3.3. Regulators

In addition to collectors and frothers, a variety of other chemical reagents are used in flotation. These reagents are generally referred to as regulators. These reagents majorly govern the selectivity of flotation by modifying the action of collectors. In other words, they are added to flotation pulp to ensure that collector only adsorbs on the targeted minerals (S. M. Bulatovic, 2007a). There are three main types of regulator reagents: depressants, activators, and pH modifiers.

The function of a depressant is to inhibit flotation of selected minerals (generally these minerals are considered as part of gangue), by either adsorbing on their hydrophobic surfaces, thus rendering them hydrophilic, or preventing adsorption of collectors onto these minerals in case these minerals have affinity towards the collector in use. The primary requirements of depressants used in gangue depression are that they: (i) must have functional groups that adsorb preferential onto the gangue minerals, (ii) must have a strongly hydrophilic character, and (iii)

should not possess functional groups that compete with the collector for adsorption on the surface of the minerals that are meant to be floated (M. Fuerstenau, Chander, & Woods, 2007). Examples of commonly used depressants in sulfide flotation are cyanide (depresses sulfides of Zn, Cu, Fe, Ag, Cd, and Ni), lime, sodium sulphite (depresses sulfides of Zn and Fe), chromate (depresses lead sulfide), and polymeric molecules such as carboxymethyl cellulose (CMC) and gaurgum (depress talc and siliceous minerals) (Lovell, 1982).

Activators are reagents that directly interact with surfaces of selected minerals to improve or render conditions for the action of main collector onto this mineral. Examples of activators are copper sulphate (generally used to activate sulfide minerals of Zn, Fe, Sb, etc.) and sodium sulfide (used to activate oxidized or tarnished minerals) (Lovell, 1982).

For most of the sulfide ores, a particular mineral-collector combination works only in a certain pH range, as pH of the solution defines the surface conditions of mineral particles. This fact is majorly utilized in sequential flotation of different valuable minerals from a poly-metallic sulfide ore. Increase or decrease in solution pH to a certain level may also be necessary to depress some of the ore constituents which otherwise would be floated along the valuable mineral. The commonly used pH modifiers include lime ($Ca(OH)_2$), soda ash (Na_2CO_3), caustic soda (NaOH) and sulphuric acid (H_2SO_4).

2.3. Collector Reagents in Sulfide Flotation

2.3.1. Collector – Mineral Interaction

As mentioned earlier, selective adsorption of collector molecules on the surface of desired minerals is one of the most important aspects of flotation process. Adsorption of collector molecules on minerals in aqueous solutions is a complex process, as it depends on mineral

surface state as well as properties of solvent and reagent molecules. A reagent molecule adsorb on a mineral surface, only if the conditions are energetically favourable. The net driving force of adsorption is sum of a number of contributing forces including, electrostatic forces, covalent bonding, hydrophobic interactions, van der Waals forces, and hydrogen bonding. In addition, the lateral interaction (could be attractive or repulsive) between adsorbed species and desolvation of mineral surface and adsorbate molecules prior to adsorption may also contribute to the adsorption process. The net sum of all these forces/interactions determines whether the adsorption of reagent molecule on mineral surface is energetically favourable or not (Somasundaran & Wang, 2006b). For a detailed discussion on origin and nature of these forces, standard surface and interfacial science textbooks may be referred (Desjonqueres & Spanjaard, 1996; Somasundaran & Wang, 2006b).

In sulfide flotation, adsorption of collector molecules on mineral surfaces can be broadly classified into two categories: *physical adsorption* and *chemical adsorption*. In physical adsorption or physisorption, the adsorbent is typically held on adsorbate via weak van der Waals and electrostatic forces. During this phenomenon, the change in the electronic state of adsorbent and adsorbate is very minimal. Physisorption is generally characterized by high rate of adsorption, formation of multilayers of adsorbed species, and a decrease in adsorption rate with increasing temperature (Parfitt, 1983; Somasundaran & Wang, 2006b). Chemical adsorption or chemisorption mainly occurs when the adsorbent (collector molecule) is held by the adsorbate (mineral surface) through formation of a covalent bond. This adsorption normally involves an activation stage and is usually strong and irreversible. Chemisorption is characterized by higher energy changes, a lower rate of adsorption, and increase in adsorption rate with temperature.

Chemisorption is generally limited to sub-monolayer or monolayer coverage (Somasundaran & Wang, 2006b).[2]

2.3.2. Commonly Used Sulfide Collectors

As mentioned in section 2.3.3.1, collectors for sulfide minerals generally contain sulfur atom as their principal donating centre in combination with a hydrophobic organic ligand, and generally referred as thiol collectors. Majority of thiol collectors are derivatives of carbonic acid, carbamic acid, phosphoric acid, urea, and alcohols (Lovell, 1982). In this section, some of the commonly used collectors in sulfide minerals flotation are introduced.

2.3.2.1. Xanthate and its Derivatives

Xanthates

Xanthates are the most commonly used collectors for floating a wide variety of sulfide minerals and have been in use since as early as 1923 (Rao, 2004). In addition to sulfides, they have also been utilized in flotation of oxide minerals (e.g. oxide minerals of Pb, Cu, and Zn). The generic structure of xanthates is shown in Figure 2.7(a).

The hydrocarbon radical in xanthates generally consist of 2-6 carbon atoms as xanthates with longer hydrocarbon chains have very low solubility in water for most of the practical applications. Molecules with longer hydrocarbon chains are more powerful and less selective than molecules with shorter chains. Shorter chain xanthates (R = ethyl, propyl, iso-propyl) are generally utilized for the selective flotation of Cu-Zn, Pb-Zn, Cu-Pb-Zn sulfide ores. Whereas longer chain xanthates (R = amyl, hexyl) are generally utilized for bulk flotation of precious

[2] In some textbooks and published papers, chemical adsorption of collector is referred as chemisorption, whether it involves movement of metal atoms from their lattice sites on mineral or not.

metal sulfide ores (e.g. Au, Ag ores) and oxidized sulfide ores (these ores are sulfidized by using Na_2S or NaHS prior to addition of collector reagents).

In acidic conditions, xanthates readily decompose into carbon disulfide (CS_2) and alcohol (R-OH). The decomposition of xanthates increases with a reduction in solution pH and shortening of hydrocarbon chain length (S. M. Bulatovic, 2007a). These reagents are also susceptible to decomposition at very high pH conditions (S. M. Bulatovic, 2007a). The optimum pH range for application of xanthates varies from mineral to mineral and depends on mineral surface state. For example, pH range for effective flotation of galena (PbS), chalcocite (Cu_2S), chalcopyrite ($CuFeS_2$), and pyrite (Fe_2S_3) has been reported to be 3-11 (M. Fuerstenau et al., 2007), 0-11 (M. C. Fuerstenau, Huiatt, & and Kuhn, 1971; Kuhn, 1968), 2-12 (M. Fuerstenau et al., 2007), and 1-4 (1-9 at high concentration of reagent) (Elgiillani & Fuerstenau, 1968; M. C. Fuerstenau, Kuhn, & Elgiillani, 1968; Miller, 1970) , respectively. This difference in effective pH range is utilized to selectively float a particular mineral over other(s). For example, performing flotation of PbS and Cu_2S between pH 9 to 12 ensures partial selectivity against gangue iron sulfide minerals.

Dixanthogenates

Under oxidizing conditions (presence of O_2 or an oxidizing agent), xanthate molecules (X^-) may oxidize to form dixanthogenate (X_2, also referred as dixanthogen) (Figure 2.7(b)), which is the neutral dimer of xanthate,

$$2X^- \leftrightharpoons X_2 + 2e^- \tag{2.1}$$

Oxidation due to the mere presence of oxygen is thermodynamically favourable, however, very slow. Dixanthogen formation in this manner is generally assumed to be negligible in flotation systems. However, the electrochemical oxidation of xanthate is fast kinetically, on mineral

surfaces capable of undergoing reduction, such as pyrite and chalcopyrite surfaces (M. Fuerstenau et al., 2007). Complete oxidation of xanthate takes place between pH 2-4 for Fe^{3+} and 2-10 for Cu^{2+} (M. C. Fuerstenau et al., 1971; Kakovsky, 1957). Like xanthates, dixanthogenates (may) also adsorb on mineral surfaces and impart hydrophobicity; however, the mechanism of adsorption is different.

Mechanism of Adsorption

Though adsorption of xanthates (and other thiol collectors) on surfaces of different minerals have been extensively studied during the last century, there remain some unresolved aspects and unanswered questions with respect to mechanism of collector adsorption (S. Bulatovic, 2007). It is still ambiguous, which products of the reactions between xanthates and minerals are responsible for imparting hydrophobicity to mineral surfaces (Finkelstein & Allison, 1976). Also, role of oxygen in xanthate adsorption is still not very clear. Some researchers have stated that xanthate adsorption on sulfide minerals takes place only in the presence of oxygen, whereas others have reported that presence of oxygen have negative impacts on xanthate adsorption (Kitchener & Laskowski, 1968). A comprehensive review of all the studies relating to xanthate adsorption on sulfide minerals can be found elsewhere (Mendiratta, 2000).

Also, it is believed that because of the presence of a large number of xanthate species in any xanthate flotation system (xanthate ion, xanthic acid, carbon disulfide, dixanthogen, monothiocarbonate, etc.), coupled with possibility of presence of mineral particles with different surface states, xanthate adsorption on sulfide minerals could be very unlikely described by only a single mechanism (S. Bulatovic, 2007).

Nevertheless, it is now very well accepted that xanthate (and its derivatives) adsorb onto sulfide minerals through a mixed potential mechanism (Mendiratta, 2000). The cathodic reaction

in this mechanism involves reduction of oxygen (which may proceed through different steps depending on pulp conditions) (S. M. Ahmed, 1978; Damjanovic, 1969; Haung & Miller, 1978; Rand & Woods, 1984),

$$O_2 + 4H^+ + 4e^- \rightarrow 2H_2O \tag{2.2}$$

and the anodic reaction determines the mode of interaction between xanthate molecules and sulfide mineral surface, which may take place in one or more of these fashions (Mendiratta, 2000):

(a) Chemisorption, where xanthate ion (X^-) interact and complexes with the surface without movement of metal atoms (ions) from their lattice site. In chemisorption, adsorption is generally limited to a monolayer,

$$X^- \rightarrow X_{ads} + e^- \tag{2.3}$$

(b) Surface reaction, where xanthate molecules (ions) interact with the surface along with movement of metal atoms from their lattice sites. In this case, multilayers of reaction product may form,

$$MS + nX^- \rightarrow MX_n + S + ne^- \tag{2.4}$$

where n is the oxidation state of metal in sulfide mineral (MS). In very high oxidizing conditions, sulfate species may form instead of elemental sulfur.

(c) Formation and subsequent adsorption of dixanthogen on the mineral surface:

$$2X^- \rightarrow X_2 + 2e^- \tag{2.5}$$

In (a) and (b) the reagent is chemically bound to the surface, while dixanthogen (from (c)) is held on the surface through physisorption. In all three cases, the adsorption of collector render mineral surface hydrophobic.

In addition to the three mechanisms of collector adsorption described in previous paragraph, reagent molecules also interact with metal ions (from the mineral surface) away from the surface in the pulp. If the rate of dissolution and diffusion of metal atoms through the boundary layer is greater than rate of diffusion of collector molecule to the surface, bulk precipitation of metal-collector complex may occur. Bulk precipitated metal-collector complexes generally adsorb on the mineral surface through physisorption. The bulk precipitated metal-collector complexes may be adsorbed directly on the mineral surface or on top of the chemisorbed layer of xanthate ions or metal-xanthate complex.

Depending on the mineral, one or more of the above interaction mechanisms may be responsible for rendering the mineral hydrophobic. For example, adsorption of xanthate on PbS and Cu_2S proceeds through formation of a monolayer (or sub-monolayer) coverage of chemisorbed xanthate followed by physisorption of bulk precipitated lead xanthate and cuprous xanthate complexes (M. C. Fuerstenau, 1982; Houot & Duhamet, 1993). The species of xanthate that adsorbs on sphalerite (ZnS) surface has been reported as bulk precipitated zinc xanthate (M. C. Fuerstenau, Clifford, & Kuhn, 1974; M. C. Fuerstenau, Natalie, & Rowe, 1990; Yamasaki & Usiu, 1965). Similarly, xanthate adsorbs on pyrite surface in form of dixanthogen (Allison, Goold, Nicol, & Granville, 1972; M. C. Fuerstenau et al., 1968; Majima & Takeda, 1968), while both the presence of chemisorbed xanthate and dixanthogen has been reported for chalcopyrite surface (Allison et al., 1972; M. C. Fuerstenau, 1982; Kuhn, 1968).

Ackerman et al. (1987) linked the mechanism of interaction between anionic collectors and sulfide minerals, with the mineral semiconductor type. The principle hydrophobic species for interaction between xanthates and p-type semiconductor minerals, such as galena, chalcocite, covellite, and bornite, etc., is the chemisorbed metal thiolate (MX). Xanthate adsorption as

dixanthogen is more common in n-type semiconductor mineral, such as chalcopyrite and pyrite. n-type semiconductor minerals showed a continuous decline in flotation recovery and rate between pH 5-10.5, whereas flotation performance of p-type semiconductor minerals remain constant (high) between this pH range. It implies that flotation of n-type semiconductor minerals works best in acid circuits. Surfaces of poor conductor minerals such as sphalerite and stibnite undergo neither chemisorption nor surface reaction, instead are rendered hydrophobic due to bulk precipitation phenomenon.

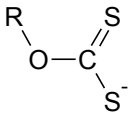

(a). Xanthate

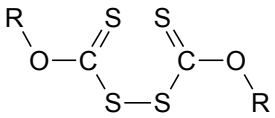

(b). Dixanthogenate

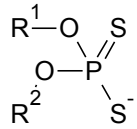

(c). Dialkyl dithiophosphate

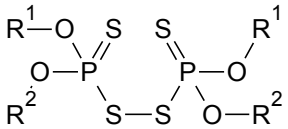

(d). Diphosphatogen

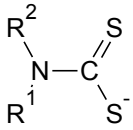

(e). Dialkyl dithiocarbamate

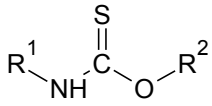

(f). Dialkyl thionocarbamate

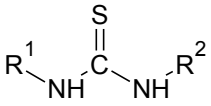

(g). Dialkyl thiourea

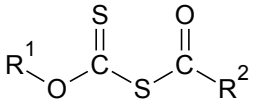

(h). Xanthogen formate

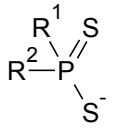

(i). Dialkyl dithiophosphinate

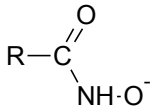

(j). Alkyl hydroxamate

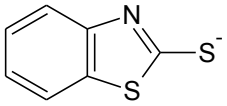

(k). Mercaptobenzothiazole (MBT)

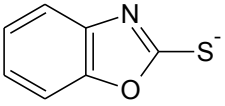

(l). Mercaptobenzoxazole (MBO)

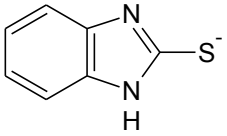

(m). Mercaptobenzoimidazole (MBI)

Figure 2.7. The generic molecular structure of commonly used sulfide collectors (R, R^1, R^2: hydrocarbon radicals).

2.3.2.2. Dithiophosphates and Diphosphatogens

The general structure of dithiophosphate collectors is given in Figure 2.7(c). These reagents are the most widely used collectors after xanthates. The dithiophosphates exhibit similar chemical and flotation properties as xanthates, and the corresponding dimer molecule for dithiophosphate collectors is diphosphatogen, $(DTP)_2$. The generic structure of $(DTP)_2$ is given in Figure 2.7(d). They are used alone or in combination with xanthates for almost all sulfides, precious metals and platinum group minerals (S. Bulatovic, 2007). Similar to xanthates, adsorption of $(DTP)_2$ on mineral surface has been reported for chalcopyrite (Finkelstein & Poling, 1977) and pyrite (M. C. Fuerstenau et al., 1971), both n type semiconductors. The adsorbed form in chalcocite, kovellite, and bornite, all p-type semiconductors, has been reported as metal-dithiophosphate (MDTP) (Finkelstein & Poling, 1977). Both n-type and p-type semiconductor minerals show similar trends for solution pH and flotation recovery for dithiophosphates as in the case of xanthates (Ackerman et al., 1987). The alkyl chain in commonly used dithiophosphate collectors contains 2-4 carbon atoms. Increasing the number of carbons in the alkyl chain increases the collecting power. Dithiophosphates with chain lengths greater than four carbons have been reported to exhibit frothing characteristics in addition to their collecting ability (Adkins & Pearse, 1992; S. Bulatovic, 2007). Dithiophosphates are weaker collectors than xanthates and have slower flotation kinetics in the recovery of bulk sulfides. However, they are more selective than xanthates, especially in preventing the iron sulfides from floating, particularly at high pH (R. R. Klimpel, 1999). Another significant advantage of dithiophosphates over xanthates is that they do not decompose in acid solutions.

2.3.2.3. Dithiocarbamates

As shown in Figure 2.7(e), dithiocarbamates (DTC) have similar generic structure as xanthates, wherein O atom is replaced by N atom. They also exhibit similar adsorption characteristics as xanthates and dithiophosphate; however, they have stronger collecting power due to greater mesomeric electron donating ability of N atom and presence of two hydrocarbon groups (in dialkyldithiocarbamate) (Lotter & Bradshaw, 2010; Raju & Forsling, 1991); Dithiocarbamate collectors are used in flotation of copper minerals as they possess enhanced selectivity for Cu. In addition to copper sulfides, they have been found more promising than xanthates for floating copper oxides, carbonates, and arsenopyrite. Adsorption of dithiocarbamate collectors has been studied mainly for copper minerals. Flotation of covellite proceeds through formation of $[Cu(DTC)]^+$ and $Cu(DTC)_2$ at the mineral surface, while for cuprite surface, species responsible for imparting hydrophobicity are Cu(I)DTC, $[Cu(DTC)]^+$, and $Cu(DTC)_2$ (Raju & Forsling, 1991). Similarly, for bornite, chalcopyrite, and chalcocite minerals, the species primarily responsible for hydrophobicity has been identified as $Cu(DTC)_2$, Cu(I)DTC, and $Cu(DTC)_2$ respectively (Goold, 1972; Hodgson & Agar, 1989; Raju & Forsling, 1991). The dithiocarbamate molecules chemically bound on the surface of copper minerals whereby the metal atoms are dislodged from their lattice sites. Despite of possessing better selectivity for Cu sulfides and oxide minerals, dithiocarbamates are not widely used in industry as they are much more expensive than xanthates and dithiophosphates (Rao, 2004). However, they are frequently used along with other collectors, including xanthates, dithiophosphates, and mercaptobenzothiazoles, for recovery of a wide variety of minerals, including galena, arsenopyrite, pyrite, and chalcopyrite (D. Bradshaw, 1997; D. J. Bradshaw & O'Connor, 1997; D. J. Bradshaw & O'Connor, 1994). The synergic effects of dithiocarbamates generally result

improved flotation rates, improved recovery of coarse particles, and reduction in amount of collector required compared to when only other collectors are used (Lotter & Bradshaw, 2010).

2.3.2.4. Thionocarbamates and Thioureas

Collectively, these collectors have become the third most utilized collector family after xanthates and dithiophosphates. The generic molecular structure of these reagents is shown in Figure 2.7(f) and 2.7(g). They have found extensive use in the flotation industry, especially for copper and copper activated zinc minerals. These collectors give excellent recovery for copper minerals (chalcopyrite > chalcocite > covellite > bornite), low recovery for lead minerals, and very low to negligible recovery for zinc and iron minerals (Ackerman et al., 1987; Fairthorne, Fornasiero, & Ralston, 1997b; Houot & Duhamet, 1993). The main functional group in these collectors is the thio-carbonyl group. There exists an ambiguity in literature regarding the way these collectors bind to the mineral surface. Some studies concluded that the reagents bind to metal atoms mainly through S atom (Brown, Hope, Schweinsberg, & Fredericks, 1995; Fairthorne et al., 1997b; Woods & Hope, 1999). Others proposed chelate formation at the metal centers through S and N (or O) atoms (Ackerman, Harris, Klimpel, & Aplan, 1984; Ackerman et al., 1987; A. M. Marabini et al., 1991). Thioureas are generally more powerful than thionocarbamates as thio-carbonyl group in thiourea is bound to two N atoms compared to one N and one O atom in thionocarbamate. Presence of two N atoms results in greater delocalization of lone pair electrons of N atoms over the thio-carbonyl center.

Flotation recovery with these collectors decreases with increasing pH and declines abruptly at $pH > pK_a$; best flotation results are generally obtained around pH 5 (Fairthorne et al., 1997b). At $pH < pK_a$, the collectors exist as neutral molecules in solution. The better performance of the neutral form has been attributed to its lower solubility compared to ionic form. Due to lower

solubility, the collector is more likely to adsorb on the mineral surface and thus, have a higher collecting ability (Finkelstein & Poling, 1977; Nagaraj & Somasundaran, 1981). The interaction of these collectors with copper minerals is a two-step process. First the neutral collector molecules chemisorb on the mineral surface at monolayer coverage. This is followed by multilayer adsorption (physisorption) of neutral collector molecules over the chemisorbed layer (Fairthorne et al., 1997b). The most significant advantages of these collectors, over more powerful xanthates and dithiophosphates are superior pyrite rejection, much better selectivity against lead and zinc minerals, and effectiveness at low pH. The major disadvantage is that they are generally more expensive than both xanthates and dithiophosphates (R. R. Klimpel, 1999).

More recently developed N-alkoxy carbonyl derivatives have been reported to form six membered rings with metal center through S and O atoms (carbonyl oxygen) (Fairthorne, Fornasiero, & Ralston, 1997a; Fairthorne et al., 1997b; Mielczarski & Yoon, 1989). Thus, these modified collectors form a more stable complex with the metal atoms than their parent reagents. However, lower flotation recovery with N-alkoxy-O-alkyl-thionocarbamate has been reported, and this has been attributed to decrease in collector's pK_a value (~ 8) upon introduction of the alkoxy group. The pKa for N-alkoxy-N-alkyl-thiourea still remain above 12, and give higher recovery than N,N-dialkyl-thiourea (Fairthorne et al., 1997b). Thiocarbanilide (diphenyl urea, $(C_6H_5–NH)_2–C=S$)) and diphenylthiocarbazide ($(C_6H_5–NH–NH)_2–C=S$) are two popular thiourea collectors where the N atoms have aryl substituent in place of alkyl groups. Thiocarbanilide (thiol tautomer) is a very effective and selective collector for galena, whereas diphenylthiocarbazide can be utilized for flotation of nickel and cobalt minerals after activation by Cu^{2+} ions (S. M. Bulatovic, 2007b).

2.3.2.5. Xanthogen Formates

The generic structure of xanthate formate molecule is given in Figure 2.7(h). These collectors were developed in 1960s, as reagents for flotation of copper minerals in acid pulp. These reagents mainly exist as neutral molecules in solution and bind to metal atoms with S of thio-carbonyl groups and O of carbonyl group, thus forming six-membered chelate rings with the metal centers (Ackerman et al., 1987; Ackerman, Harris, Klimpel, & Aplan, 2000). There are not many studies regarding their application and/or mechanism of adsorption on sulfide minerals expect for the mention that these collectors have been mainly utilized to recover copper in acid circuits (Ackerman, Harris, Klimpel, & Aplan, 1999; S. M. Bulatovic, 2007b).

2.3.2.6. Dithiophosphinates

Dithiophosphinates are relatively new collectors for sulfide ore flotation. The generic structure of dithiophosphinates is given in Figure 2.7(i). Compared to dithiophosphates where the two hydrocarbon radicals are linked to P atom through oxygen, in dithiophosphinates, the alkyl groups are directly attached to P atom. Due to removal of two highly electronegative oxygen atoms, the electron density at the PS_2^- center in dithiophosphinates is greater than dithiophosphates. This makes these reagents more powerful collectors compared to dithiophosphates (Liu et al., 2013). Dithiophosphinate collectors are generally considered very selective against pyrite. Therefore, they are used to float lead, copper, and precious metals from ores containing high content of pyrite (Avotins, Wang, & Nagaraj, 1994)

Not many studies have been conducted on flotation performance and adsorption mechanisms of these collectors. Pecina-Treviño et al. (2003) investigated interaction between sodium-diisobutyl dithiophosphinates, and galena and pyrite surfaces and concluded that the reagent adsorbs onto galena and pyrite by a chemisorption mechanism. For galena, recovery increases

with collector concentration and decreasing pH. For galena, high recovery was observed between pH 4-9 and at collector dosage $\geq 10^{-5}$ M, whereas pyrite floated effectively between pH 4-7 and at collector concentration $\geq 10^{-4}$. This implies reagent's selectivity towards lead minerals. It is also demonstrated that recovery of pyrite is higher in presence of Pb^{2+} ions, due to activating effect of Pb ions.

2.3.2.7. Chelating Reagents

Molecular structures of chelating reagents contain two or more atoms that are capable of bonding to the same metal center. In most of the cases, elements acting as donor sites are S, N, O, and P. Donor atoms may form part of a basic or an acidic functional group (D. W. Fuerstenau, Herrera-Urbina, & McGlashan, 2000). The donor atoms must be so located in the molecule that the formation of a ring structure including the metal atom is sterically possible (Somasundaran & Nagaraj, 1984). For a chelating agent to be effectively used as a flotation collector, presence of long hydrocarbon chain to provide hydrophobicity and water solubility are near-must conditions (Ackerman et al., 1987; A. Marabini, Cases, & Barbaro, 1989; Nagaraj, 1982). Metal specificity of a chelating reagent is decided by the relative stability of the various possible metal-ligand complexes. A large number of chelating reagents have been evaluated as potential flotation collectors, however, barring a selected few, industrial application of these reagents have not been successful so far,. The important chelating reagents in context of mineral flotation can be divided into three main categories: alkyl hydroxamates, oximes, and mercapto heterocyclic aromatic compounds. Details of majority of important oxime chelating reagents can be found in works of Fuerstenau et al. (2000) and Pradip (1988). Hydroxamates and mercapto heterocyclic aromatic compounds are discussed here, as these two classes of chelating reagents are considered the most important.

Hydroxamates

The generic structure of hydroxamates is shown in Figure 2.7(j). Hydroxamates are widely recognized for their strong chelating abilities with different metal ions, including transition metals such as Cu, Zn, Ni, Pb and Fe (Bodenant & Fages, 1995; Buglyó et al., 2007; Griffith et al., 2011; Šille, Šramko, Garaj, & Remko, 2009). A hydroxamate molecule has three coordination atoms (2Os and N), however complex formation mainly takes place through oxygen atoms (Buglyó et al., 2007; Griffith et al., 2011). Hydroxamate reagents are very powerful and selective collectors for a wide variety of flotation separation systems, especially for concentration of oxide copper minerals and native copper (D. W. Fuerstenau et al., 2000; Hope, Numprasanthai, Buckley, Parker, & Sheldon, 2012; Lee et al., 2009). Originally hydroxamates were introduced as collectors for both oxide and sulphide ores (Parker et al., 2012). However, ambiguity still exists on their applicability as a collector for sulphide minerals. Electrochemical studies have shown that chalcocite could be rendered hydrophobic using alkyl hydroxamate under high potential conditions when cupric ions are present on mineral surface due to oxidation (Hanson et al., 1987; Hanson & Fuerstenau, 1991). However, Fuerstenau et al. (2000) observed zero contact angles for hydroxamate treated chalcopyrite and covellite. In another study, chalcocite, bornite and chalcopyrite were rendered hydrophobic using n-octano hydroxamate due to formation of multilayered cupric hydroxamate on mineral surfaces (Parker et al., 2012).

Mercapto-benzoheterocyclic aromatic reagents

Mercaptobenzoazole compounds such as 2-mercapto-benzothiazole (MBT), 2-mercapto-benzoxazole (MBO), and 2-mercapto-benzimidazole (MBI) and their derivatives have emerged as powerful flotation collectors for Pb, Cu, and Zn ores (Maier & Dobiáš, 1997; A. M. Marabini et al., 1991; A. M. Marabini et al., 2007; Woods et al., 2000). The generic structures of these

reagents are given in Figures 2.7(k)-2.7(m). Previous studies have shown that these reagents bind to metal ions primarily through exocyclic S and imine N atoms. Marabini et al. (2007) showed that substituent groups attached to benzene ring in mercaptobenzoazole reagents have significant impact on their efficiency as flotation collectors. Maier and Dobias (1997) showed that at low dosage the collecting efficiency of MBT reagent for sulfide ores follows the order: chalcocite > galena > sphalerite. They also found that MBT has high affinity (and no selectivity) for mineral surfaces containing Pb or Cu and the selectivity towards galena over chalcocite can be improved by substituting pentyloxy group on the benzene ring. MBO and MBI were found weak collectors of galena due to their inability to chemisorb on mineral surface. However, reaction enthalpy during formation of $Pb(MBO)_2$ in bulk was found higher than $Pb(MBT)_2$ (Maier & Dobiáš, 1997). Foye and Lo (Foye & Lo, 1972) studied binding abilities of some mercaptobenzoazole reagents toward Cu^{2+}, Fe^{3+}, and Al^{3+} metal ions. They reported that binding ability of reagents for Cu^{2+} ion follows the order: 1-methyl-2-mercaptoimidazole > 2-mercaptobenzimidazole > 2-mercaptoimidazole, whereas for Fe^{3+} and Al^{3+} metal ions the order is: 1-methyl-2-mercaptoimidazole > 2-mercaptoimidazole > 2-mercaptobenzimidazole > 2-mercaptobenzothiazole.

2.3.2.8. Other Collectors

Apart from the collectors discussed in sections 2.4.2.1-2.4.2.8., there are numerous other collectors that have not been included here. Most of these collectors exhibit similar adsorption characteristics as one or more collectors already discussed in previous sections. These collectors include anionic ($R\text{-}S\text{-}CS_2^-$) and neutral (R-S-(C=S)-S-R') trithiocarbonates, monothiophosphate ($(RO)_2\text{-}(P{=}S)\text{-}O^-$), monothiophosphinate ($(R)_2\text{-}(P{=}S)\text{-}O^-$), organic sulfide collectors (R-S-R'),

and mercaptans (R-SH). There are a very few number of studies that have dealt with flotation performance and/or interaction mechanism of these collectors with sulfide minerals.

2.4. References

Ackerman, P. K., Harris, G. H., Klimpel, R. R., & Aplan, F. F. (1984). Effect of alkyl substituents on performance of thionocarbamates as copper sulphide and pyrite collectors. In M. J. Jones, & R. Oblatt (Eds.), *Reagents in mineral industry* (pp. 69-78). London: IMM.

Ackerman, P. K., Harris, G. H., Klimpel, R. R., & Aplan, F. F. (1987). Evaluation of flotation collectors for copper sulfides and pyrite, I. common sulfhydryl collectors. *International Journal of Mineral Processing, 21*(1–2), 105-127.

Ackerman, P. K., Harris, G. H., Klimpel, R. R., & Aplan, F. F. (1999). Use of chelating agents as collectors in the flotation of copper sulfides and pyrite. *Miner. Met. Process, 16*(1), 27-35.

Ackerman, P. K., Harris, G. H., Klimpel, R. R., & Aplan, F. F. (2000). Use of xanthogen formates as collectors in the flotation of copper sulfides and pyrite. *International Journal of Mineral Processing, 58*(1–4), 1-13.

Adkins, S. J., & Pearse, M. J. (1992). The influences of collector chemistry on kinetics and selectivity in base-metal sulphide flotation. *Minerals Engineering, 5*(3–5), 295-310.

Ahmed, N., & Jameson, G. J. (1985). The effect of bubble size on the rate of flotation of fine particles. *International Journal of Mineral Processing, 14*(3), 195-215.

Ahmed, S. M. (1978). Electrochemical studies of sulphides, II. measurement of the galvanic currents in galena and the general mechanism of oxygen reduction and xanthate adsorption on sulphides in relation to flotation. *International Journal of Mineral Processing, 5*(2), 175-182.

Allison, S. A., Goold, L. A., Nicol, M. J., & Granville, A. (1972). A determination of the products of reaction betweer various sulfide minerals and aqueous xanthate solution, and a correlation of the products with electrode rest potentials. *Metallurgical Transactions, 3*(10), 2613-2618.

Anthony, R. M., Kelsall, D. F., & Trahar, W. J. (1975). The effect of particle size on the activation and flotationof sphalerite. *Australian Institute of Mining and Metallurgy, 254* 47-58.

Assis, S. M., Montenegro, L. C. M., & Peres, A. E. C. (1996). Utilisation of hydroxamates in minerals froth flotation. *Minerals Engineering, 9*(1), 103-114.

Avotins, P. V., Wang, S. S., & Nagaraj, D. R. (1994). Recent advances in sulfide collector development. *Reagents for better metallurgy.* SME.

Barbaro, M. (2000). Lead and zinc ores: Flotation. In C. Poola, & M. Cooke (Eds.), *Encyclopedia of separation science* (III ed., pp. 3215-3218) Academic Press, Elsevier.

Bezuidenhout, J. (2011). *An investigation into the role of DTP as a co-collector in the flotation of a south african PGM ore.* (Unpublished MSc). University of Cape Town,

Bodenant, B., & Fages, F. (1995). Synthesis, metal binding, and fluorescence studies of a pyrene-tethered hydroxamic acid ligand. *Tetrahedron Letters, 36*(9), 1451-1454.

Bradshaw, D. (1997). *Synergism between thiol collectors.* (Unpublished PhD). University of Cape Town, Cape Town.

Bradshaw, D. J., & O'Connor, C. T. (1997). The synergism of thiol collectors in a mixture used for the flotation of pyrite. *XX Mineral Processing Conference,* Aachen. 343-354.

Bradshaw, D. J., & O'Connor, C. T. (1994). The flotation of pyrite using mixtures of dithiocarbamates and other thiol collectors. *Minerals Engineering, 7*(5–6), 681-690.

Brown, G. M., Hope, G. A., Schweinsberg, D. P., & Fredericks, P. M. (1995). SERS study of the interaction of thiourea with a copper electrode in sulphuric acid solution. *Journal of Electroanalytical Chemistry, 380*(1–2), 161-166.

Buglyó, P., Nagy, E. M., Farkas, E., Sóvágó, I., Sanna, D., & Micera, G. (2007). New insights into the metal ion-peptide hydroxamate interactions: Metal complexes of primary hydroxamic acid derivatives of common dipeptides in aqueous solution. *Polyhedron, 26*(8), 1625-1633.

Bulatovic, S. (2007). Adsorption mechanism of flotation collectors . *Handbook of flotation reagents: Chemistry, theory and practice. volume 1: Flotation of sulfide ores* (1st ed., pp. 125-152) Elsevier Science.

Bulatovic, S. M. (2007a). In Bulatovic S. M. (Ed.), *Handbook of flotation reagents: Chemistry, theory and practice*. Amsterdam: Elsevier.

Bulatovic, S. M. (2007b). Collectors. *Handbook of flotation reagents: Chemistry, theory and practice. volume 1: Flotation of sulfide ores* (1st ed., pp. 5-42) Elsevier Science.

Crozier, R. (1992). *Flotation: Theory, reagents and ore testing.* New York: Pergamon Press.

Damjanovic, A. (1969). In Bockris.J., Conway M. A. (Eds.), *Modern aspects of electrochemistry*

Desjonqueres, M. C., & Spanjaard, D. (1996). *Concepts in suface physics* (Second ed.) Springer.

Elgiillani, D. A., & Fuerstenau, M. C. (1968). Mechanisms involved in cyanide depression of pyrite. *Transactions AIME, 241*, 437.

Fairthorne, G., Fornasiero, D., & Ralston, J. (1997a). Formation of a copper-butyl ethoxycarbonyl thiourea complex. *Analytica Chimica Acta, 346*(2), 237-248.

Fairthorne, G., Fornasiero, D., & Ralston, J. (1997b). Interaction of thionocarbamate and thiourea collectors with sulphide minerals: A flotation and adsorption study. *International Journal of Mineral Processing, 50*(4), 227-242.

Feng, D., & Aldrich, C. (1999). Effect of particle size on flotation performance of complex sulphide ores. *Minerals Engineering, 12*(7), 721-731.

Finch, J. A., Xiao, J., Hardie, C., & Gomez, C. O. (2000). Gas dispersion properties: Bubble surface area flux and gas holdup. *Minerals Engineering, 13*(4), 365-372.

Finch, J. A., Nesset, J. E., & Acuña, C. (2008). Role of frother on bubble production and behaviour in flotation. *Minerals Engineering, 21*(12–14), 949-957.

Finkelstein, N. P., & Allison, S. A. (1976). Natural and induced hydrophobicity in sulphide mineral systems. *AICLHE Symposium Series, 71*(150), 165-175.

Finkelstein, N. P., & Poling, G. W. (1977). The role of dithiolates in the flotation of sulfide minerals. *Mineral Science and Engineering, 9*, 177.

Foye, W. O., & Lo, J. (1972). Metal-binding abilities of antibacterial heterocyclic thiones. *Journal of Pharmaceutical Sciences, 61*(8), 1209-1212.

Fuerstenau, M., Chander, S., & Woods, R. (2007). Sulphide mineral flotation. In M. Fuerstenau, G. Jameson & R. Yoon (Eds.), *Froth flotation – A century of innovation* (pp. 445-453). Littleton, Colorado: Society for Mining, Metallurgy and Exploration (SME).

Fuerstenau, M. C. (1982). Sulphide mineral flotation. In R. P. King (Ed.), *Principles of flotation* (pp. 159-182) South African Institute of Mining and Metallurgy.

Fuerstenau, M. C., Huiatt, J. L., & and Kuhn, M. C. (1971). Dithiophosphate vs xanthate flotation of chalcocite and pyrite. *Transactions AIME, 250*, 227.

Fuerstenau, M. C., Kuhn, M. C., & Elgiillani, D. A. (1968). The role of dixanthogen in xanthate flotation of pyrite. *Transactions AIME, 241*, 148.

Fuerstenau, D. W., Herrera-Urbina, R., & McGlashan, D. W. (2000). Studies on the applicability of chelating agents as universal collectors for copper minerals. *International Journal of Mineral Processing, 58*(1–4), 15-33.

Fuerstenau, D. W., & Urbina, R. H. (1990). Adsorption of cationic surfactants and the flotation of minerals. In D. N. Rubingh, & P. M. Holland (Eds.), *Cationic surfactants: Physical chemistry*. CRC Press.

Fuerstenau, M. C., Clifford, K. L., & Kuhn, M. C. (1974). The role of zinc-xanthate precipitation in sphalerite flotation. *International Journal of Mineral Processing, 1*(4), 307-318.

Fuerstenau, M. C., Natalie, C. A., & Rowe, R. M. (1990). Xanthate adsorption on selected sulfides in the virtual absence and presence of oxygen, part 1. *International Journal of Mineral Processing, 29*(1–2), 89-98.

Gontijo, C., Forenasiero, D., & Ralston, J. (2007). The limits of fine and coarse particle flotation . *Canadian Journal of Chemical Engineering, 85*, 739-747.

Goold, L. A. (1972). *The reaction of sulphide minerals with thiol compounds.* (No. 1439). Johannesburg, South Africa: National Institute of Metallurgy.

Griffith, D. M., Szocs, B., Keogh, T., Suponitsky, K. Y., Farkas, E., Buglyó, P., & Marmion, C. J. (2011). Suberoylanilide hydroxamic acid, a potent histone deacetylase inhibitor; its X-ray crystal structure and solid state and solution studies of its zn(II), ni(II), cu(II) and fe(III) complexes. *Journal of Inorganic Biochemistry, 105*(6), 763-769.

Hanson, J. S., & Fuerstenau, D. W. (1987). An electrochemical investigation of the adsorption of octyl hydroxamate on chalcocite. *Colloids and Surfaces, 26*(C), 133-140.

Hanson, J. S., & Fuerstenau, D. W. (1991). The electrochemical and flotation behavior of chalcocite and mixed oxide/sulfide ores. *International Journal of Mineral Processing, 33*(1-4), 33-47.

Haung, H. H., & Miller, J. D. (1978). Kinetics and thermochemistry of amyl xanthate adsorption by pyrite and marcasite. *International Journal of Mineral Processing, 5*(3), 241-266.

Hodgson, M., & Agar, G. E. (1989). Eilectrochemical investigations into the flotation chemistry of pentlandite and pyrrhotite: Process water and xanthate interactions. *Canadian Metallurgical Quarterly, 28*(3), 189-198.

Hope, G. A., Numprasanthai, A., Buckley, A. N., Parker, G. K., & Sheldon, G. (2012). Bench-scale flotation of chrysocolla with n-octanohydroxamate. *Minerals Engineering, 36–38*(0), 12-20.

Houot, R., & Duhamet, D. (1993). Floatability of chalcopyrite in the presence of dialkyl-thionocarbamate and sodium sulfite. *International Journal of Mineral Processing, 37*(3–4), 273-282.

Kakovsky, L. A. (1957). Physiochemical propreporties of some flotation reagents and their salts with ions of heavy iron-ferrous metals. *Int, Congry. Surface Activity,* London. *, 4* 225-237.

Kitchener, J. A., & Laskowski, J. S. (1968). The Hydrophylic–Hydrophobic transition on silica. *Journal of Colloid and Interface Science,* , 165-175.

Klimpel, R. (1984). Froth flotation: The kinetic approach. *Mintek 50,* Johannesburg, South Africa.

Klimpel, R. R. (1999). A review of sulfide mineral collector practice. In B. K. Parekh, & J. D. Miller (Eds.), *Advances in flotation technology* (pp. 115-128) Society for Mining, Metallurgy and Exploration, Inc.

Kuhn, M. C. (1968). (Unpublished PhD). Colorado School of Mines,

Laskowski, J. (1993). Frothers and flotation froth. *Mineral Processing and Extractive Metallurgy Review, 12*, 61-89.

Lee, K., Archibald, D., McLean, J., & Reuter, M. A. (2009). Flotation of mixed copper oxide and sulphide minerals with xanthate and hydroxamate collectors. *Minerals Engineering, 22*(4), 395-401.

Liu, G., Xiao, J., Zhou, D., Zhong, H., Choi, P., & Xu, Z. (2013). A DFT study on the structure-reactivity relationship of thiophosphorus acids as flotation collectors with sulfide minerals: Implication of surface adsorption. *Colloids and Surfaces A: Physicochemical and Engineering Aspects, 434*, 243-252.

Livshits, A. K., & Dudenkov, S. V. (1965). Some factors in froth stability. *Int. Min. Proc. Congr, 7*, 367-371.

Lotter, N. O., & Bradshaw, D. J. (2010). The formulation and use of mixed collectors in sulphide flotation. *Minerals Engineering, 23*(11–13), 945-951.

Lovell, V. M. (1976). Froth characterstics in phosphate flotation. In M. C. Fuerstenau (Ed.), *Flotation, A. M. gaudin memorial edition* (pp. 597-621). New York: Am. Inst. of Min. Metall and Pet. Engr.

Lovell, V. M. (1982). Industrial flotation reagents . In R. P. King (Ed.), *Principles of flotation* (pp. 73-91) South African Institute of Mining and Metallurgy.

Maier, G. S., & Dobiáš, B. (1997). 2-mercaptobenzothiazole and derivatives in the flotation of galena, chalcocite and sphalerite: A study of flotation, adsorption and microcalorimetry. *Minerals Engineering, 10*(12), 1375-1393.

Majima, H., & Takeda, M. (1968). Electrochemical studies of the xanthate-dixanthogen system on pyrite. *Transactions AIME, 241*, 431.

Marabini, A., Cases, J., & Barbaro, M. (1989). Chelating reagents as collectors and their absorption mechanism. In K. V. Sastry (Ed.), *Chellenges in mineral processing* (). Littleton, United States of America: AIME.

Marabini, A. M., Barbaro, M., & Alesse, V. (1991). New reagents in sulphide mineral flotation. *International Journal of Mineral Processing, 33*(1–4), 291-306.

Marabini, A. M., Ciriachi, M., Plescia, P., & Barbaro, M. (2007). Chelating reagents for flotation. *Minerals Engineering, 20*(10), 1014-1025.

Mendiratta, N. K. (2000). *Kinetic studies of sulfide mineral oxidation and xanthate adsorption.* (Unpublished PhD). Virginia Polytechnic Institute and State University, Virginia.

Mielczarski, J. A., & Yoon, R. H. (1989). Spectroscopic studies of the structure of the adsorption layer of thionocarbamate: I. on copper and activated zinc sulfide. *Journal of Colloid and Interface Science, 131*(2), 423-432.

Miller, J. D. (1970). *Pyrite depression by reductoon of sultion oxidation potential.* (No. 12010).Environmental Protectio Agency,.

Moudgil, B. M., Rogers, J. J., & Vasudevan, T. V. (1988). Effect of fines on the flotation recovery of coarse phosphate particles. *Int. Min. Proc. Congr.* Stockholm. *, 16*

Moudgil, B. M. (1992). *Enhanced recovery of coarse particles during phosphate flotation*. (No. 86-02-067). Gainesville, Florida:

Nagaraj, D. R., & Somasundaran, P. (1981). Chelating agents as collectors in flotation: Oximes 0 copper minerals systems. *Transactions AIME,* , 270-1351.

Nagaraj, D. R. (1982). Chelating agents in mineral processing. *III AIME Annual Meeting,* Dallas.

Nasab, M. E. l. D.,A. (2014). Investigation of the effects of hydrodynamic parameters on the flotation recovery of coal particles. *International Journal of Coal Preparation and Utilization, 34*(5), 260-275.

Newell, R., & Grano, S. (2007). Hydrodynamics and scale up in rushton turbine flotation cells: Part 1 - cell hydrodynamics. *International Journal of Mineral Processing, 81*(4), 224-236.

Öteyaka, B., & Soto, H. (1995). Modelling of negative bias column for coarse particles flotation. *Minerals Engineering, 8*(1–2), 91-100.

Pan, B. (2013). *Flotation of halite and sylvite from carnallite with dodecyl morpholine* . (Unpublished MSc). University of Utah,

Parfitt, G. D. (1983). In Parfitt G. D., Rochester C. H. (Eds.), *Adsorption from solution at the solid/liquid interface* (. ed.) Academic Press.

Parker, G. K., Buckley, A. N., Woods, R., & Hope, G. A. (2012). The interaction of the flotation reagent, n-octanohydroxamate, with sulfide minerals. *Minerals Engineering, 36–38*(0), 81-90.

Pearse, M. (2006). An overview of the use of chemial reagents in mineral processing. *Minerals Engineeering, 18*, 139-149.

Pease, J. D., Curry, D. C., & Young, M. F. (2006). Designing flotation circuits for high fines recovery. *Minerals Engineering, 19*(6–8), 831-840.

Pecina-Treviño, E. T., Uribe-Salas, A., Nava-Alonso, F., & Pérez-Garibay, R. (2003). On the sodium-diisobutyl dithiophosphinate (aerophine 3418A) interaction with activated and unactivated galena and pyrite. *International Journal of Mineral Processing, 71*(1–4), 201-217.

Pradip. (1988). Applications of chelates in mineral processing. *Minerals and Met. Proc, 5*

Pugh, R. J. (1996). Foaming, foam films, antifoaming and defoaming. *Advances in Colloid and Interface Science, 64*, 67-142.

Rahman, R. M., Ata, S., & Jameson, G. J. (2012). The effect of flotation variables on the recovery of different particle size fractions in the froth and the pulp. *International Journal of Mineral Processing, 106–109*, 70-77.

Raju, G. B., & Forsling, W. (1991). Adsorption mechanism of diethyldithiocarbamate on covellite, cuprite and tenorite. *Colloids and Surfaces, 60*, 53-69.

Rand, D. A. J., & Woods, R. (1984). Eh measurements in sulphide mineral slurries. *International Journal of Mineral Processing, 13*(1), 29-42.

Rao, S. R. (2004). *Surface chemistry of froth flotation* Springer US. doi:10.1007/978-1-4757-4302-9

Saracoglu, M. (2013). *Froth flotation performance enhancement by feed cavitation and magnetic particle addition* (PhD).

Schulze, H. (1984). *Physicochemical elementary processes in flotation. Elsevier Publishing.* Amsterdam: Elsevier Publishing.

Schwarz, S. (2004). *The relationship between froth recovery and froth structure.* (Unpublished PhD). Ian Wark Institute, Austrralia.

Šille, J., Šramko, M., Garaj, V., & Remko, M. (2009). Gas phase and solution state stability of complexes L...M, where M = Cu2+, Ni2+, or Zn2+ and L = R-C({double bond, long}O)NHOH (R = H, NH2, CH3, CF3, or phenyl). *Journal of Molecular Structure: THEOCHEM, 911*(1-3), 137-143.

Somasundaran, P., & Nagaraj, D. R. (1984). Chemistry and applications of chelating reagents in flotation and flocculation. In M. Jones, & R. Oblatt (Eds.), *Reagents in mineral industry* (pp. 209-219). London: Institution of Mining and Metallurgy.

Somasundaran, P., & Wang, D. (2006a). Application of flotation agents and their structure–property . *Solution chemistry: Minerals and reagents* (1st ed.,) Elsevier Science.

Somasundaran, P., & Wang, D. (2006b). Chapter 4 mineral–flotation reagent equilibria. *Developments in Mineral Processing, 17*, 73-141.

Szatkowski, M., & Freyburger, W. (1985). Kinetics of flotation with fine bubble. *Transactions of the Institute of Mining and Metallurgy (Section C), 94*, 61-70.

Tao, D. (2005). Role of bubble size in flotation of coarse and fine particles - A review. *Separation Science and Technology, 39*(4)

Trahar, W. J. (1976). The selective flotation of galena from sphalerite with special reference to the effects of particle size. *International Journal of Mineral Processing, 3*(2), 151-166.

Vanangamudi, M., Kumar, S. S., & Rao, T. C. (1989). Effect of fines content on the froth flotation of coal. *Powder Technology, 58*(2), 99-105.

Wills, B., & Napier-Munn, T. (2006). *Will's mineral processing technology* (7th ed.). Oxford, UK: Butterworth-Heinemann.

Woods, R., Hope, G. A., & Watling, K. (2000). A SERS spectroelectrochemical investigation of the interaction of 2-mercaptobenzothiazole with copper, silver and gold surfaces. *Journal of Applied Electrochemistry, 30*(11), 1209-1222.

Woods, R., & Hope, G. A. (1999). A SERS spectroelectrochemical investigation of the interaction of O-isopropyl-N-ethylthionocarbamate with copper surfaces. *Colloids and Surfaces A: Physicochemical and Engineering Aspects, 146*(1–3), 63-74.

Yamasaki, T., & Usiu, S. (1965). Infrared spectroscopic studies of xanthate adsorbed on zinc sulfide. *Transactions AIME, 232*, 36.

Yoon, R., & Luttrell, G. H. (1989). The effect of bubble size on fine particle flotation. *Mineral Processing and Extractive Metallurgy Review: An International Journal, 5*(1-4), 101-122.

Chapter – 3

Introduction to Computational Methods

The key to the scientific and technological advancement to meet the ever-changing needs in many physical sciences and engineering fields, such as design of improved performance chemicals for minerals flotation industry, is the understanding and controlling of the properties of matter at microscopic level such as individual atoms and molecules (Rai, 2012; Sholl & Steckel, 2009). During the last three to four decades, computational chemistry methods have emerged as powerful tools to study and explore the behavior and properties of matter at sub-atomic level, and have played an important role in design and development of novel materials. With the continuous development of new techniques, theories, computers, and algorithms, computational chemistry methods are well placed to investigate the complex relationship between molecular architecture of collector molecules and their resultant reactivity or selectivity toward different minerals or metal species in flotation environment.

Electronic structure theory, which is based on the principles of quantum mechanics, is the most accurate method to calculate various properties of a molecule or a set of molecules (Rai, 2012). This chapter presents a brief overview of the fundamentals of computational techniques based on quantum mechanics and then introduces the methodology adopted for this work.

3.1. Quantum Mechanics and Schrödinger Equation

The postulates, theorems, and laws of quantum mechanics were developed in the early 20th century as classical physics failed to explain the nature/behaviour of microscopic systems. The

inability of classical physics to describe microscopic systems, such as electrons and protons, is best understood in terms of Heisenberg's uncertainty principle (Heisenburg, 1927), which states that there exists a fundamental limit to the precision with which both position and momentum of a particle can be determined simultaneously. Mathematically, the Heisenberg's uncertainty principle can be expressed as,

$$\Delta x.\Delta p_x = h/4 \tag{3.1}$$

where Δx and Δp_x are the position and momentum of the particle respectively and h is the Planck's constant.

The dual wave/particle nature of particles, first proposed by De Broglie at the beginning of the 20th century, forms the basis of quantum mechanics. In this theory, all particles that have momentum (p) can exhibit wave-like properties associated to a wavelength (λ), and waves can similarly have particle-like properties. The de Broglie hypothesis of dual nature can be expressed mathematically as,

$$\lambda = h/p \tag{3.2}$$

Quantum mechanics assumes that microscopic systems are described by wave functions (ψ) that completely define all the physical and chemical properties of a system (Rai, 2012). Unlike classical mechanics where variables can be directly linked to physical measureable properties or observables, in quantum mechanics there exist quantum mechanical operators corresponding to each physical observable of a system, which when act upon a wave function provides the value (or range of values) of that physical property. For a system comprised of M particles and represented by many-body wave function ψ, the Hamilton operator (Hamiltonian, $\hat{H}$) provides

the eigenvalues of total energy E of the system using the time independent Schrödinger equation which can be expressed as,

$$\hat{\mathrm{H}}\psi = E\psi \tag{3.3}$$

The time independent wave function describing an atomic system comprising N electrons (e) and M nuclei (n) at positions $\vec{r}_i$ and $\vec{R}_A$, respectively, can be expressed as,

$$\psi = \psi(r, R) \tag{3.4}$$

and the Hamiltonian for such a system is given by,

$$\hat{\mathrm{H}} = \hat{T}_e + \hat{T}_n + V_{ne} + V_{ee} + V_{nn} \tag{3.5}$$

In atomic units ($m_e = e^2/(4\pi\epsilon_o) = 1$), $\hat{\mathrm{H}}$ can be expressed as[3],

$$\hat{\mathrm{H}} = -\sum_{i=1}^{N}\frac{1}{2}\nabla_i^2 - \sum_{A=1}^{M}\frac{1}{2M_A}\nabla_A^2 - \sum_{i=1}^{N}\sum_{A=1}^{M}\frac{Z_A}{|\vec{r}_{iA}|} + \sum_{i=1}^{N}\sum_{j>i}^{N}\frac{1}{|\vec{r}_{ij}|} + \sum_{A=1}^{M}\sum_{B>A}^{M}\frac{Z_A Z_B}{|\vec{R}_{AB}|} \tag{3.6}$$

The first two terms in Equations (3.5) and (3.6) are the kinetic energy operators of the electrons and nuclei, respectively. The third, fourth, and fifth terms are potential energy operators representing the electron-nuclei, electron-electron, and nuclei-nuclei interactions, respectively.

Equation (3.6) for Hamiltonian takes into account all interactions between different particles of the system. As the M nuclei can be placed anywhere, Equation (3.3) has 3M degrees of freedom, and therefore is very complex and difficult to solve analytically for all but the simplest

[3] Z_A is the atomic number and M_A is the mass of nucleus A.

systems (hydrogen atom, harmonic oscillator, etc.) and several approximations have to be made to arrive at a solution.

3.2. The Born-Oppenheimer Approximation

The Born-Oppenheimer or adiabatic approximation (Born & Oppenheimer, 1927) focuses on the expression of the Hamiltonian of a many-nuclei many-electron system. The momentum of electrons and nuclei are of the same order of magnitude, however, there is a huge difference in their masses ($M_A/m_e \geq 10^4$). This implies that electrons, which are way lighter, move much faster compared to nuclei. Thus, it can be assumed that for any nuclear movement in an atomic system, the electrons will instantly rearrange themselves into the lowest energy configuration. Thus, we can regard the nuclei as fixed with respect to the electrons, and the system under consideration can be described by a wave function of electrons moving under the influence of fixed nuclei.

In order to use the above approximation, we have to assume that Hamiltonian operator and time independent wave function can be separated into electron and nucleus dependent parts as (Hellstrom, 2007),

$$\hat{\mathrm{H}} = \hat{\mathrm{H}}_{\mathrm{e}}(\mathrm{r}) + \hat{\mathrm{H}}_{\mathrm{n}}(\mathrm{R}) \tag{3.7}$$

$$\psi(\mathrm{r},\mathrm{R}) = \psi_{\mathrm{e}}(\mathrm{r})\psi_{\mathrm{n}}(\mathrm{R}) \tag{3.8}$$

where $\psi_e(r)$ and $\psi_n(R)$ are the eigenfunction of $\hat{\mathrm{H}}_e$ and $\hat{\mathrm{H}}_n$ with eigenvalues E_e and E_n, respectively. Then, we have,

$$\hat{\mathrm{H}}\,\psi(\mathrm{r},\mathrm{R}) = (\hat{\mathrm{H}}_{\mathrm{e}} + \hat{\mathrm{H}}_{\mathrm{n}})\psi_{\mathrm{e}}(\mathrm{r})\psi_{\mathrm{n}}(\mathrm{R}) = (\mathrm{E}_{\mathrm{e}} + \mathrm{E}_{\mathrm{n}})\psi_{\mathrm{e}}(\mathrm{r})\psi_{\mathrm{n}}(\mathrm{R}) = \mathrm{E}\psi(\mathrm{r},\mathrm{R}) \tag{3.9}$$

Hence, the eigenfunctions of $\hat{H}$ are the product of the eigen functions of $\hat{H}_e$ and $\hat{H}_n$, and their eigenvalues are the corresponding sum. Considering that the third term in Equation (3.6) is dependent on R parametrically, we can rewrite Equation (3.8) as,

$$\psi(r, R) = \psi_e(r; R)\psi_n(R) \tag{3.10}$$

By neglecting the nuclei specific terms of Hamiltonian operator in Equation (3.5), i.e. $\hat{T}_n$ and V_{nn}, we get the electronic Hamiltonian operator which describes the state of N electrons in a potential field of fixed nuclei and is expressed as,

$$\hat{H}_{elec} = \hat{T}_n(r) + V_{ee}(r) + V_{ne}(R, r) \tag{3.11}$$

It is noteworthy that only the $\hat{T}_n$ term is negligible (i.e. kinetic energy of the nuclei). The V_{nn} term (nuclei-nuclei repulsion) is important and is constant. Therefore, it causes a constant shift in eigenvalues and has no effect on the eigen functions. The Schrödinger equation after implementation of this approximation thus becomes,

$$\hat{H}_{elec}\psi_e(r; R) = E_{elec}\psi_e(r; R) \tag{3.12}$$

where E_{elec} is the electronic energy of the system. Both E_{elec} and the eigen functions of Equation (3.12) depend explicitly on the electronic coordinates, and parametrically on the nuclear coordinates. Thus, for different sets of nuclear coordinates, the eigen function is a different function of electronic coordinates. Thus, using the Born-Oppenheimer approximation, the time independent Schrödinger equation for the electronic wave function can be solved separately from the Schrödinger equation for the nuclei.

3.3. Potential Energy Surfaces

As mentioned in previous section, the electronic energy, E_{elec}, doesn't represent the total energy (E_{tot}) of a system. As kinetic energy of nuclei is negligible,

$$\mathrm{E_{tot}} \cong \mathrm{E_{elec}} + \mathrm{V_{nn}} \tag{3.13}$$

Both E_{elec} and V_{nn}, change with any modification in nuclear coordinates. A potential energy surface (PES) describes the energy of system (E_{tot}) as a function of its nuclei coordinates. A PES can be obtained varying the nuclear coordinates and calculating the electronic energy corresponding to each configuration. PES of a system can be used to find equilibrium bond lengths and stable geometry conformations (reactants and products), which are found at energy minima as well as transition states, which are found at saddle points.

3.4. The Variational Principle

The variational principle provides an approximation of the ground-state energy, which is the lowest eigenvalue given by the Hamiltonian for a system (Fox, 2012). It states that any arbitrarily chosen wave function Φ, that satisfies the same boundary conditions as the wave function ψ, will always yield an energy E greater or equal to the exact ground state energy E_o. Mathematically, this can be expressed as,

$$\mathrm{E} = \langle \Phi | \hat{\mathrm{H}} | \Phi \rangle \geq E_o \tag{3.14}$$

This fact can be utilized to achieve the convergence toward E_o by minimizing $\langle \Phi | \hat{\mathrm{H}} | \Phi \rangle$ by varying the parameters of the normalized function Φ.

3.5. Orbitals and Quantum Numbers

The electronic wave function, $\psi_e(r)$ is related to the probability of finding electrons at certain energy levels with in an atomic system. The wave function that describes the properties of an electron in an atom is called an atomic orbital. To describe the movement and pathway of electrons in an atom containing more than one electron, four quantum numbers are used. The principal quantum number, *n*, specifies the energy of an electron and the most probable distance of the electron from the nucleus or the size of the orbital. It divides the entire space around the nucleus into shells. The angular momentum quantum number, *l*, divides the shell into smaller groups of orbitals called subshells and specifies the shape of each subshell (sharp, principlal, diffuse, fundamental, etc.) with a particular principle quantum number. The magnetic quantum number, m_l, specifies the number of orbitals and their spatial orientation with in a subshell of given energy and shape. It divides each subshell into $2l+1$ individual orbitals, which hold the electrons. The spin quantum number, m_s, designates the direction of the electron spin and may have values of only +1/2 (upward spin) or -1/2 (downward spin). According to Pauli Exclusion Principle, no two electrons in an atom can have the same set of all four quantum numbers. Thus, every atomic orbital is at most doubly occupied and the spins of two electrons occupying any particular atomic orbital must be opposite. Similarly, the mathematical wave function describing the behavior of an electron in a molecule is called molecular orbital. In quantum chemistry methods, a molecular orbital is generally expressed as a linear combination of individual atomic orbitals,

$$\phi_i = c_{1i}\chi_1 + c_{2i}\chi_2 + \cdots + c_{ni}\chi_n \tag{3.15}$$

where ϕ_i is a molecular orbital, χ_r (r =1, 2,.., n) are atomic orbitals, and c_{ri} is the coefficient which determines the weight of contribution of an atomic orbital (χ_r) in the molecular orbital.

3.6. Basis Sets

To obtain a numerical solution for Equations (3.3) or (3.12) within any approximation(s), first the eigen functions or molecular orbitals must be described through a set of known mathematical functions. This set is often termed as a basis set, and the individual functions are called basis functions. To describe a molecular system perfectly, the basis set has to be consisted of an infinite number of basis functions. However, computational effort of quantum chemistry techniques scales to the third power of number of basis functions used to describe the eigen function. So it is desirable to use a basis set that consists of as few basis functions as possible. Therefore, basis functions that make a significant contribution are preferred over those that do not. The choice of basis set is very crucial for the quality of results along with the choice of method used to solve Equations (3.3) and (3.12). Majority of the basis sets used in computational chemistry techniques are constructed using the following three functions:

(i) Slater-type orbitals (STOs)
(ii) Gaussian-type orbitals (GTOs)
(iii) Plane wave functions (PWs)

Slater-type orbitals (Davidson & Felle, 1986) are derived from the wave functions of hydrogen atom. STOs form a cusp at the nucleus due to the singularity of the potential on the nucleus, and exhibit an exponential decay at long range. STOs have the form,

$$\chi^{STO}(r) = P(r)e^{-\zeta r}Y_{lm}(\theta, \phi) \tag{3.16}$$

To implement STOs, two electron multi-centered integrals need to be computed numerically which is computationally very intensive (Fox, 2012). This drawback limits the use of STOs to small systems only.

To overcome the drawback associated with STOs, Gaussian-type orbitals were introduced, which have the form,

$$\chi^{GTO}(r) = P(r)e^{-\alpha r^2}Y_{lm}(\theta, \phi) \tag{3.17}$$

GTOs are not as good as STOs in describing the electron density. They do not show the correct behavior (cusp) at the nucleus and decay rapidly as they move away from the nucleus. However, the integrals of GTOs are much simpler compared to STOs and involve much less computational cost. The before mentioned shortcoming of GTOs can be compensated by using contracted Gaussian functions which are a linear combination of several GTOs and have the form,

$$c_1 e^{-b_1 r^2} + c_2 e^{-b_2 r^2} + c_3 e^{-b_3 r^2} + \cdots \tag{3.18}$$

The values of b and c are kept constant during the calculations and can be determined in several ways which are discussed elsewhere (Leach, 2001). The contracted Gaussian functions have approximately the same form as STOs (Cramer, 2004).

Plane wave functions are used to describe periodic systems, such as crystals, surfaces, etc. and have been originated from solid-state physics. These functions are not discussed here as the present study deals with molecular systems only. For details on plane wave functions, any standard textbook of computational quantum chemistry can be referred (Veszpremi & Feher, 1999).

3.6.1. Type of Basis Sets

3.6.1.1. Minimal Basis Set

Minimal basis sets are constructed by using only one basis function for each atom. The most commonly used minimal basis sets are STO-nG type, where n is the number of GTOs that are combined linearly to represent the corresponding STO.

3.6.1.2. Split-Valence Basis Sets

As it is the valence electrons that principally describe the chemical or physical behaviour of atoms or molecules under given conditions, in split-valence basis sets, valence atomic orbitals are described by more than one basis function while there is still only one basis function corresponding to each of core atomic orbitals. These basis sets are generally denoted in the form A-XYg. Here, A represents number of GTOs comprising each core atomic orbital basis function of core orbitals is constructed. X and Y denote that the valence atomic orbitals are composed of two basis functions each and that the first of these functions is a linear combination of X GTOs while the second basis function is a linear combination of Y GTOs. Two numbers after the hyphen (-) mean that the basis set is a double-zeta basis set. Similarly, split-valence basis sets where valence orbitals are composed of three or four basis functions are denoted as A-XYZg and A-XYZWg, respectively and termed as split-valence triple- and quadruple-zeta basis sets. Some examples of split-valence sets include 6-21G, 3-21G, and 6-311G.

3.6.1.3. Polarized Basis Sets

In polarized basis sets, basis functions corresponding to higher angular momentum quantum number than those required for the isolated atom are added to the valence orbitals. For example, if the basis set of an isolated atom is composed of only s- and p-orbitals, addition of basis

functions corresponding to d-orbital will result in polarization of the original basis set. Addition of these higher angular momentum functions to a split-valence basis set results in improved accuracy, especially for calculation of molecular geometries (Hellstrom, 2007). Addition of polarization functions also allows for non-uniform displacement of a charge away from the atomic nuclei, thereby improving descriptions of chemical bonding (Rai, 2012). Polarized basis sets are generally denoted as A-XYg(d) or A-XYZ(d, p). For example, the 6-31G(d) basis set is constructed by adding six d-type GTOs to the split-valence 6-31G basis set for each non-hydrogen atom, and 6-31G(d, p) basis set includes six d-type Gaussian primitives for all non-hydrogen atoms and a set of Gaussian p-type functions for hydrogen and helium atoms.

3.6.1.4. Diffuse Basis Sets

Species in which electron density is more spread out such as anions, lone pairs, and excited states cannot be described adequately by use of regular basis sets and require a set of diffuse (i.e. more spread out) basis functions to account for the outermost weakly bound electrons. The addition of diffuse functions to a split-valence basis set is denoted by a plus sign, as in 6-31+G or 6-31+G(d,p). Two plus signs signify addition of two sets of diffuse functions.

3.6.1.5. Contracted Basis Sets

In contracted basis sets, inner core electrons are represented by a constant, and valence electrons are represented by basis sets in a regular way. These basis sets require much less computational effort as the basis set is composed of much smaller number of basis functions. However, use of this type of basis sets always overestimates the system energy, as there is less variational freedom (Hellstrom, 2007).

3.6.1.6. High Angular Momentum Basis Sets

High Angular Momentum Basis Sets are the most complete basis sets available and include addition of multiple polarization functions, e.g 6-31G(2d), wherein two d-functions are added to heavy atoms, and 6-311G(2df, pd), wherein two d-functions and one f-function are added to heavy atoms, and p- and d-functions are added to hydrogen. The results obtained by using high angular momentum basis sets are generally more accurate compared to results obtained using basis sets described earlier.

3.6.2. Effective Core Potentials or Pseudopotentials

The number of basis functions that is required to describe the atomic orbitals of a system (or atomic orbitals of an atom) becomes very large when heavy atoms are present. However, as the core electrons do not have significant effect on chemical and physical properties, such as bonding, van der Walls interactions, etc., analytical functions can be used to represent the potential of nucleus and core electrons together, to the remaining valence electrons. These analytical functions are called pseudopotentials (Phillips, 1958). A major advantage of using pseudopotential functions in a basis set is that they can be made to include the relativistic effects of the core electrons, which become important in very heavy elements where core electrons move at speeds close to the speed of light (Fox, 2012).

The number of electrons that form the core and get represented by pseudopotential is an important factor to consider. A large-core pseudopotential includes all but the valence electrons, while a small-core pseudopotential only uses up to penultimate shell. In heavier metals, polarization of sub-valence shells can be chemically important and it is often worth the extra computational effort to explicitly include these shells (Fox, 2012).

An effective pseudopotential should fulfill the following criteria (Karhanek, 2010):

(i) Use of pseudopotential to represent nucleus and core electrons should not alter the valence wave function outside the core region (beyond r_c boundary).

(ii) The pseudo wave function should match the all electron wave function at the boundary.

$$\emptyset^{PS}(r) = \emptyset^{AE}(r), \qquad (\text{at } r = r_c \text{ in Figure 3.1}) \tag{3.19}$$

(iii) Both, the pseudo wave function, and its first derivative must be continuous at the boundary,

$$\frac{\partial \emptyset^{PS}}{\partial r}(r) = \frac{\partial \emptyset^{AE}}{\partial r}(r), \qquad (\text{at } r = r_c \text{ in Figure 3.1}) \tag{3.20}$$

(iv) In the core region, the pseudo wave function should be nodeless.

The graphical comparison between pseudo wave function (and potential) with all electron wave function (and potential) is shown in Figure 3.1 (Karhanek, 2010).

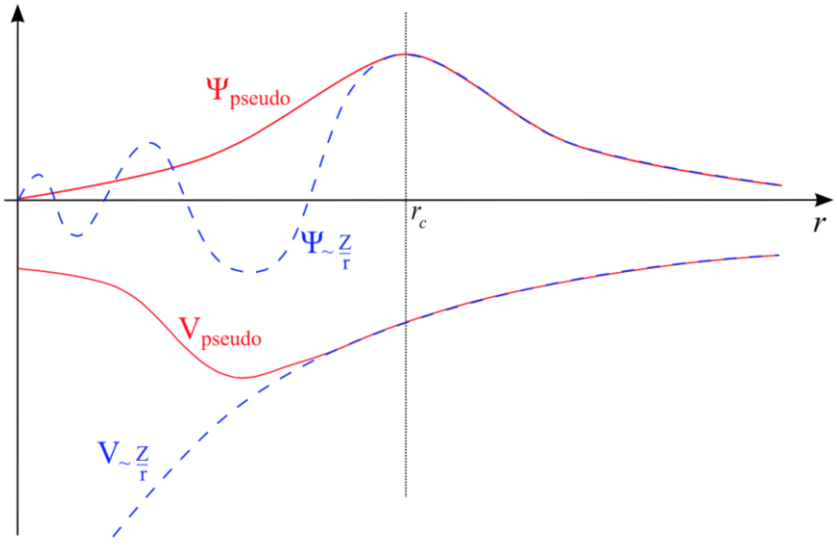

Figure 3.1. Comparison of a pseudo wave function (and potential) to all electron wave function (and potential). Core radius = r_c. [taken from (Karhanek, 2010)]

3.7. Approaches to Solve Schrodinger Equations

In quantum computational chemistry, there are different approaches that are used to solve the electronic Schrödinger equation (Equation 3.12) under different assumptions and approximations. Some of these approaches are described here.

3.7.1. Hartree-Fock Methods (HF)

The Hartree-Fock (HF) method is an approximate method for solving the molecular electronic Schrödinger equation (Equation 3.12). It breaks up the many-electron problem into a series of single electron problems. The wave function in Hartree-Fock theory follows the mean field approximation and is expressed as an anti-symmetric product of N (number of electrons) orthonormal spin orbitals (χ(x)), known as a Slater determinant. A spin orbital is a product of a spatial orbital ($\psi(r_1)$) and a spin function (either $\alpha(s)$ or $\beta(s)$). The spin orbitals χ_1 and χ_2 of two electrons residing in an orbital with spatial position r_1 can be expressed as,

$$\chi_1(r_1) = \psi(r_1).\alpha(s) \tag{3.21}$$

and

$$\chi_{12}(r_1) = \psi(r_1).\beta(s) \tag{3.22}$$

The combined wave function of two electrons residing in spin orbitals at spatial position r_1 and r_2, thus can be written as,

$$\phi_{12}(r_1, r_2) = \chi_1(r_1).\chi_2(r_2) \tag{3.23}$$

Following the Pauli principle,

$$\phi_{12}(r_1, r_2) = -\phi_{21}(r_2, r_1) = -\chi_1(r_2).\chi_2(r_1) \tag{3.24}$$

Therefore, the overall wave function having anti-symmetric characteristics can be expressed as a linear combination of $\phi_{12}(r_1, r_2)$ and $\phi_{21}(r_2, r_1)$,

$$\psi(r_1, r_2) = 2^{-\frac{1}{2}} (\chi_1(r_1).\chi_2(r_2) - \chi_1(r_2).\chi_2(r_1)) \tag{3.25}$$

where $2^{-\frac{1}{2}}$ is a normalization factor. The anti-symmetric wave function of Equation (3.25) can also be written in form of a determinant as,

$$\psi(r_1, r_2) = \begin{vmatrix} \chi_1(r_1) & \chi_2(r_1) \\ \chi_1(r_2) & \chi_2(r_2) \end{vmatrix} \tag{3.26}$$

and is called a Slater determinant. This approach can be extended to represent a molecular system comprising N electrons, where the Slater determinant becomes,

$$\psi(r_1, r_2, \ldots., r_N) = (N!)^{-1/2} \begin{vmatrix} \chi_1(r_1) & \chi_2(r_1) & \cdots & \chi_k(r_1) \\ \chi_1(r_2) & \chi_2(r_2) & \cdots & \chi_k(r_2) \\ \vdots & \vdots & \vdots & \vdots \\ \chi_1(r_N) & \chi_2(r_N) & \cdots & \chi_k(r_N) \end{vmatrix} = |\chi_1\chi_2 \ldots.\chi_k\rangle \tag{3.27}$$

Each row of the slater determinant represents one electron and the interchange of two rows represents interchange of state of two electrons. The Slater determinant captures the essential anti-symmetric behavior according to the Pauli principle and the exclusion principle and thus a suitable way of describing the overall wave function. However, the single-determinant approximation does not take into account the Coulomb correlation, which represent the coulombic repulsion between two electrons of opposite spins.

The single electron problem, with electron-electron interactions, is expressed using the Fock operator as,

$$f_i = -\frac{1}{2} \nabla_i^2 - \sum_{A=1}^{M} \frac{Z_A}{|\vec{r}_{iA}|} + V_{HF,i} = h_i + V_{HF,i} \tag{3.28}$$

where $V_{HF,i}$ is the average potential felt by electron i due to the other electrons and commonly referred as Hartree potential. The Hartree-Fock potential can be expressed in terms of coulomb and exchange operators and the resultant energy is expressed as a sum of Coulomb integrals,

$$\mathrm{J_{ij}} = \iint \chi_i^*(\mathrm{x_1})\chi_j^*(\mathrm{x_2})_1 \mathrm{r_{ij}^{-1}} \chi_i(\mathrm{x_1})\chi_j(\mathrm{x_2})\mathrm{d(x_1)d(x_2)} \tag{3.29}$$

and exchange integrals,

$$\mathrm{K_{ij}} = \iint \chi_i^*(\mathrm{x_1})\chi_j^*(\mathrm{x_2})_1 \mathrm{r_{ij}^{-1}} \chi_j(\mathrm{x_1})\chi_i(\mathrm{x_2})\mathrm{d(x_1)d(x_2)} \tag{3.30}$$

In Hartree-Fock approximation, the total electronic energy (E) of the system is expressed as,

$$\mathrm{E} = 2\sum_i^{N/2} \int \psi_i^*(\mathrm{r_i})\mathrm{h}\psi_i(\mathrm{r_i})\mathrm{dr_i} + \mathrm{J_{ij}} + \mathrm{K_{ij}} \tag{3.31}$$

Energy of the system is then minimized iteratively using the variational principle (Equation 3.14) to get E_{HF}, the Hatree-Fock energy. Calculation of the two electron integrals is the most computational intensive part of a Hartree-Fock calculation. As mentioned before, this method completely neglects the relativistic effects and correlation between electrons of same spins. The results obtained using this method are not very accurate as the method overestimates the electronic energy.

3.7.1.1. Correlation Energy

The difference between the exact ground state energy (E_O) and the HF energy (E_{HF}) is known as the missing electron correlation energy and is defined as (Lowdin, 1955),

$$E_{Corr} = E_O - E_{HF} \tag{3.32}$$

The missing correlation energy is typically a very small fraction of the total energy (typically less than 1%) (Whitfield, 2011). However it can be a very important contribution to many systems of physical and chemical interest (Li, 2009). Also, it is worth mentioning the value of

E_{Corr} also depends on basis set used to converge the energy. Therefore, the magnitude of E_{Corr} using a more sophisticated basis set with Hartree-Fock method will be less compared to when a smaller basis set is used.

Types of Correlation Energy

Generally, there are two types of correlation energy - dynamical correlation and non-dynamical correlation energy. Dynamical correlation error comes from the fact that in mean-field approximation electrons are not explicitly correlated. It means that, though ideally the electrons should be correlated such that they avoid one another due to the Coulomb interaction, however, in mean-field approximation an electron only see an averaged N − 1 electron cloud instead of N − 1 individual electron clouds. The dynamic correlation is specifically important in case of two electrons having opposite spin as depicted by pair correlation function in Figure 3.2 (Whitfield, 2011). The black line shows the pair correlation function for two electrons with opposite spins under Hartree-Fock approximation while the red line shows the instantaneous Coulomb repulsion between electrons. The red cusp is due to the instantaneous Coulomb repulsion between electrons.

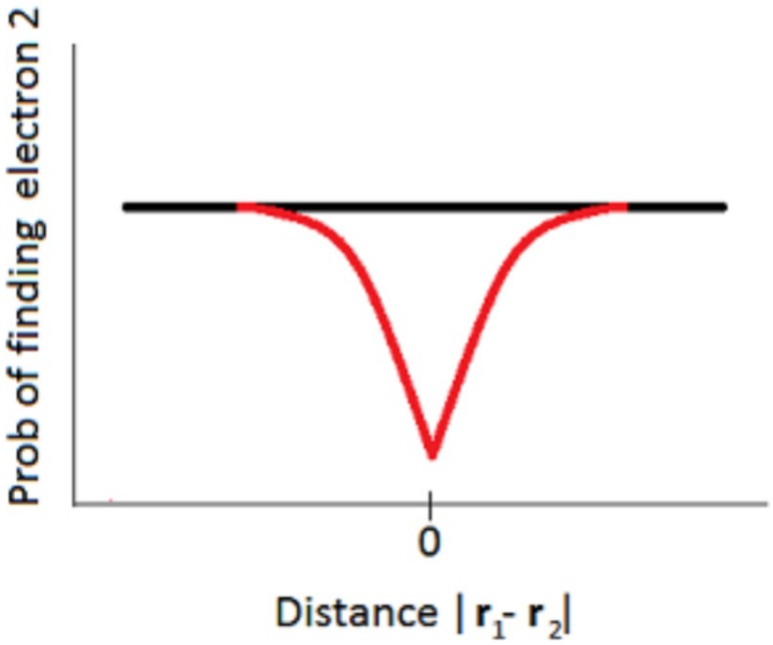

Figure 3.2. The pair correlation function of two opposite spin electrons at positions r_1 and r_2. In black is the Hartree-Fock pair correlation function, and, in red is the actual pair correlation function due to the Coulomb repulsion between charged particles. Taken from (Whitfield, 2011).

The non-inclusion of the explicit Coulomb interaction also results in the dynamic correlation error in pair correlation function of electrons possessing the same spin. However, this error is very small since anti-symmetry is strictly enforced by the use of Slater determinants.

Non-dynamical correlation occurs when the problem is not well described by a single configuration. When multiple configurations are degenerate or near-degenerate, the Hartree-Fock solution will give an error due to the single configuration assumption. Examples of such situations include bond breaking, excited state studies, and transition metal chemistry (Whitfield, 2011).

3.7.2. Post Hartree-Fock Methods

There are many approaches that aim to improve on Hartree-Fock method by taking account of some of the missing correlation energy. Collectively, all these approaches are termed as Post-HF methods. Examples of such methods are coupled cluster (CC), configuration interaction (CI), and Møller-Plesset perturbation theory (MP2, MP4), multi-configuration self-consistent field (MCSCF) and complete Active Space SCF (CASSCF) method. Authoritative and comprehensive discussions of these methods can be found in a range of excellent textbooks (Magnasco, 2013; Veszpremi & Feher, 1999).

3.7.3. Semi-Empirical Methods

Semi-empirical quantum chemistry methods are based on Hartree-Fock formalism, but make many further approximations, e.g. considering only valence electrons, or approximating or completely omitting some calculation steps, to increase computational speed. In most of the semi-empirical methods, the two-electron repulsion integrals are either approximated or not considered, which alone may decreases the scaling of integrals from N^4 to N^2 (where N is the number of orbitals). Consequently, results obtained with these methods are not accurate and need parameterization or fitting against experimental data. Depending on the way in which the differential overlap of the two center integrals involved in the wave functions is handled, they are categorized as complete neglect of differential overlap (CNDO) and neglect of diatomic differential overlap (NDDO) (Murrell & Harget, 1972; Pople & Segal, 1965; Pople, Santry, & Sehgal, 1965; Pople & Beveridge, 1970), intermediate neglect of differential overlap (INDO) (Clark, 1985), and modified neglect of differential overlap (MNDO) (Clark, 1985). Some of the recently developed semi-empirical methods include MOZYME (Stewart & Stewart, 1999), the

divide-and-conquer method (Dixon & Merz, 1996), and the self-consistent charge density functional based tight binding (SCC-DFTB) method (Frauenheim et al., 2000). In MOZYME methods, direct calculation of electron density and energy is performed without diagonalizing the semi-empirical self-consistent field (SCF) matrix. The divide-and-conquer method divides a large molecule into smaller segments and performs semi-empirical SCF calculations for individual segments. Summation of the electron densities of individual segments yields the electron density of the entire molecule, which is used to calculate the energy of the entire system. The SCC-DFTB method takes into account self-consistent redistribution of charges and accomplishes a substantial improvement in energies. Though these methods are quick and inexpensive, their use is limited to modeling of very large biological molecules, for which the more sophisticated *ab-initio* methods are not suitable (Dewar, Zoebisch, & Healy, 1985; Stewart, 1989; Theil, 1996).

3.7.4. Density Functional Theory (DFT)

In the previous sections, several different ways to approximately solve the electronic Schrödinger equation including the Hartree-Fock method, Møller-Plesset perturbation theory, and coupled cluster methods were introduced. These methods rely on the many body wave function as a central quantity. Once the wave function is known, the Schrödinger equation is solved within some approximations, and the energy of the system and all related properties are determined. The wave function of a N electron system is a function of 3N spatial variables together with spin variable. The multi dimensionality of the wave function limits the size of the systems that can be treated with these methods. In addition, large basis sets are beyond reach for most practical studies with wave function methods.

Density functional theory (DFT) based methods utilize electron density ($\rho(r)$) as the central quantity in place of the wave function. The electron density of a system is always a three-dimensional functional irrespective of the system size. However, it contains the same information as the 3N dimensional wave function. Consequently, DFT methods can handle much larger systems and basis sets. It is mainly because of this reason that DFT has become the most widely used approach in the computation chemistry world. DFT methods and applications have grown at an exponential rate due to their speed and reasonable accuracy. This section presents a brief introduction to DFT based methods. A comprehensive discussion of DFT can be found in a range of excellent textbooks (Engel & Dreizler, 2011; Lowdin, 1998).

DFT is primarily based on three important theorems. The first two theorems provide the basis for DFT and the third theorem introduces a practical way of its implementation. The foundation of DFT was laid by Hohenberg and Kohn in 1964, through their landmark paper (Hohenberg & Kohn, 1964). The two key findings of the paper are generally referred to first and second Hohenberg-Kohn theorems, which are described in the following sections.

3.7.4.1. First Hohenberg-Kohn Theorem

The first Hohenberg-Kohn theorem states that there exists a one to one mapping between the external potential and the ground state probability density. The proof of this theorem, which is discussed here, is for non-degenerate ground states and the proof for degenerate state can be found elsewhere (Levy, 1982). Suppose there is an electronic system (of N electrons) influenced by an external potential $V_{en}^{1}(r)$ and the electron density of this system is ρ(r). Now, if there exist another potential $V_{en}^{2}(r)$, which also corresponds to the same electron density ρ(r), then there are two Hamiltonians H_1 and H_2 for which ground state electron density is the same but the

normalized wave function ψ_1 and ψ_2 are different. If E_{01} and E_{02} are the ground state energies for H_1 and H_2, respectively, then we have

$$E_{01} = \langle\psi_1|H_1|\psi_1\rangle = \langle\psi_1|T + V_{ee}|\psi_1\rangle + \int \rho(r)V_{en}^1(r)dr \tag{3.33}$$

$$E_{02} = \langle\psi_2|H_2|\psi_2\rangle = \langle\psi_2|T + V_{ee}|\psi_2\rangle + \int \rho(r)V_{en}^2(r)dr \tag{3.34}$$

Following the variational principle and assuming that H_1 has unique ground state energy,

$$E_{01} < E'_{01} = \langle\psi_2|T + V_{ee}|\psi_2\rangle + \int \rho(r)V_{en}^1(r)dr$$

$$= E_{02} + \int \rho(r)\left(V_{en}^1(r) - V_{en}^2(r)\right)dr \tag{3.35}$$

Similarly,

$$E_{02} < E'_{02} = E_{01} + \int \rho(r)\left(V_{en}^2(r) - V_{en}^1(r)\right)dr \tag{3.36}$$

Thus, adding Equations (3.35) and (3.36) we get

$$E_{01} + E_{02} < E_{01} + E_{02} \tag{3.37}$$

However, this cannot be true. Hence, there cannot be two different potentials that can give same electron density. Also, as the difference in the potentials appears in both Equations (3.35) and (3.36), potentials that differ by a constant shift are equivalent. In other words, there exists a one-to-one mapping between density and external potential i.e. ρ(r) uniquely determines $V_{en}(r)$.

As a corollary of the theorem, there is also a one-to-one mapping between density and all properties of the system including the ground state energy, excited states energy, electric and magnetic properties, and any other property of the system (Li, 2009). This means that all the properties of a system are functions of its electron density, which in turn is a function of the positions of electrons.

Thus, energy E of a system can be expressed in form of electronic Schrödinger equation as,

$$E[\rho] = T[\rho] + T_{ne}[\rho] + V_{ee}[\rho] \tag{3.38}$$

where T is the kinetic energy functional, V_{ee} is the electron-electron coulombic interaction and T_{ne} contains the electron-nuclear potentials.

In Equation (3.38), $T[\rho]$ and $V_{ee}[\rho]$ terms are only dependent on ρ (and independent from any external potential) where as the term $T_{ne}[\rho]$ depends on the nuclear configuration, which changes from system to system. Therefore, Equation (3.38) can be written as,

$$E[\rho] = F[\rho] + \int \rho(r)V(r)\, dr \tag{3.39}$$

where V(r) is the external potential felt by electrons (having density $\rho(r)$) due to nucleus, and $F[\rho]$ (or $F[\rho(r)]$) is a universal functional of $\rho(r)$ and expressed as,

$$F[\rho] = T[\rho] + V_{ee}[\rho] \tag{3.40}$$

3.7.4.2. Second Hohenberg-Kohn Theorem

The second Hohenberg-Kohn theorem demonstrates that the ground state energy of a system can be obtained by the variational principle and the density that minimizes the total energy is corresponds to the ground state density. Following the variational principle,

$$E_0[\rho_0] \leq E_v[\rho] \tag{3.41}$$

where E_0 and ρ_0 are the ground state energy and density, respectively and $E_v[\rho]$ is the energy functional of Equation (3.39). Following the first theorem, ρ_0 uniquely defines the external potential V(r). Therefore, for an arbitrary wave function ψ' and corresponding electron density ρ',

$$\langle \psi'|H|\psi'\rangle = \int \rho'(r)V(r)dr + F[\rho'] = E[\rho'] \geq E_0[\rho_0] \tag{3.42}$$

As per Equation (3.42), the energy of the system will reach minimum only when the density is the ground state density. Thus, the ground state energy of a system can be obtained by minimizing the energy functional shown in Equation (3.39). However, it is still unknown how to obtain ρ(r) and $F[\rho(r)]$ for a given system.

3.7.4.3. The Kohn-Sham Theorem

The Kohn-Sham theorem (Kohn & Sham, 1965) introduces the methodologies of DFT and a practical method to implement those. It states that, for any electronic system, there exists a non-interacting system (i.e. $V_{ee} = 0$) that reproduces the same density. The first Hohenberg-Kohn theorem guarantees the uniqueness and existence of V^{KS} potential with $V_{ee} = 0$.

The external potential associated with this non-interacting system can be assumed as V^{KS}. Under Kohn-Sham formalization, one-electron Schrödinger equation takes the form,

$$\left(-\frac{1}{2}\nabla^2 + V^{KS}[\rho](r)\right)\phi_j(r) = \in_j \phi_j(r) \tag{3.43}$$

Here ϕ are the Kohn-Sham orbitals and the electron density is expressed as,

$$\rho(r) = \sum_i^N |\phi_i|^2 \tag{3.44}$$

3.7.4.4. Implementation of Kohn-Sham Theorem

The universal functional $F[\rho]$ for a non-interacting Kohn-Shan system can be expressed as,

$$F[\rho] = (T_{NI} + J)[\rho] + E_{xc}[\rho] \tag{3.45}$$

The first term T_{NI} is the kinetic energy operator for a non-interacting system. The kinetic energy of such as system is given by

$$T_{NI}[\rho] = -\frac{1}{2}\sum_j \langle\phi_j|\nabla^2|\phi_j\rangle \tag{3.46}$$

The kinetic energy of a non-interacting system captures majority of the kinetic energy of the system, however, this term is always less than or equal to the kinetic energy of the interacting system. The second term in Equation (3.45) represents classical coulomb-coulomb repulsion between the electrons. In Hartree-Fock theory, the potential associated with this energy is expresses as Hartree potential,

$$V_{HF}[\rho](r) = \int \frac{\rho\prime(r)}{|r-r''|} dr' \tag{3.47}$$

The final term $E_{xc}[\rho]$ in Equation (4.45), is called the exchange-correlation functional and includes all non-classical aspects of the electron-electron interactions, e.g. the exchange term in HF theory, any missing kinetic energy, and self interaction of electrons[3] (insert footnote), etc. The exact form of the exchange-correlation functional is not known and it is necessary to make some approximations, which are discussed in the next section. The potential associated with the exchange-correlation functional is called exchange-correlation potential, V_{XC}.

An effective potential (V_{eff}) can now be defined as,

$$V_{eff} = V_{HF}[\rho](r) + V_{XC}[\rho](r) + V_{ext}[\rho](r) \tag{3.48}$$

Equation (3.48) is generally referred as the Kohn-Sham equation. The Hartree-Fock type single particle equation now becomes

$$\left(-\frac{1}{2}\nabla^2 + V_{HF}[\rho](r) + V_{XC}[\rho](r) + V_{ext}[\rho](r)\right)\phi_j(r) = \in_j \phi_j(r) \tag{3.49}$$

Finally, the total energy of the N electron system can be expressed as,

$$E = \sum_i^N \varepsilon_i - \frac{1}{2}\iint \frac{\rho(r)\rho(r')}{|r-r'|} dr dr' + E_{XC}[\rho] - \int V_{XC}(r)\rho(r) dr \tag{3.50}$$

As V_{eff} depends only on $\rho(r)$, Equation (3.48) must be solved self-consistently or iteratively. The general procedure is to begin with an initial guess of the electron density, calculate V_{eff} from Equation (3.48), and then get the Kohn-sham orbitals. Using these orbitals, a new density is obtained from Equation (3.44) and the process is repeated until the potential and density converge to self-consistency. Finally, the total energy is calculated from Equation (3.50) with the final (or converged) electron density. Just as in the Hartree-Fock methods, the Kohn-Shan system is usually solved using basis sets.

3.7.4.5. Exchange-Correlation Functionals

To use the Kohn-Sham equation and to implement DFT methods, the form of the exchange-correlation functional must be known. However, like mentioned before, the exact form of E_{XC} is not known and generally some sort of approximation for E_{XC} is used. Currently, there are over 200 approximations to this functional in the open literature. In this section, some of the most common types of exchange-correlation functionals in widespread use are discussed.

The local-density approximation

The earliest and simplest approximation is the Local Density Approximation (LDA), which can be expressed as,

$$E_{XC}^{LDA}[\rho(r)] = \int \rho(r)\varepsilon_{XC}^{unif}\big(\rho(r)\big)d(r) \tag{3.51}$$

where ε_{XC}^{unif} is the exchange-correlation energy per particle of the homogenous electron gas of density $\rho(r)$, i.e. the exchange-correlation functional from the uniform electron gas is applied to other systems. In LDA functionals, the exchange-correlation energy is decomposed into exchange and correlation terms linearly as,

$$E^{XC} = E_X + E_C \tag{3.52}$$

so that separate expressions for E_X and E_C is sought. The exchange energy of uniform electron gas is known exactly and the correlation energy is generally obtained by fitting to the many-body free electron gas data of Gell-Mann and Brueckner and Ceperly and Alder (Ceperley & Alder, 1980; Gell-Mann & Brueckner, 1957). All the modern LDA functionals are almost similar, and differ only in how their correlation contribution have been fitted to the many-body electron gas data. The commonly used LDA functionals include the Perdew-Zunger (PZ)(Perdew & Zunger, 1981), Vosko-Wilk-Nusair (VWN)(Vosko, Wilk, & Nusair, 1980), and Perdew-Wang (PW)(Perdew & Wang, 1992). Strictly, LDA functionals work well for systems with slowly varying densities. The LDA functionals work very well for solid state physics applications including metal and semiconductor surfaces as these systems can be reasonably approximated by unform electron gas. However, these approximations are not very popular in molecular physics and chemistry, as molecules do not have nearly uniform electron densities [both online thesis].

The generalised gradient approximation

The shortcomings of the LDA functional for molecular physics led to the introduction of functionals that depend on the local density as well as its first gradient ($\nabla\rho(r)$). The generalised gradient approximation (GGA) is generally expressed as,

$$E_{XC}^{GGA}[\rho(r)] = \int \rho(r)\varepsilon_{XC}^{unif}\big(\rho(r)\big)\nabla\rho(r)d(r) \tag{3.53}$$

For many molecular properties, including geometries, ground state energies, vibrational analysis, etc. GGA functionals generally yield superior results compared to LDA functionals. For solid-state physics application too, the results obtained through GGA functionals are either superior or equivalent to LDA functionals. The most popular GGA functionals include PW91

(Perdew, Burke, & Wang, 1996) and PBE (Perdew, Burke, & Ernzerhof, 1997). A number of functionals with slight modifications to the PBE functional are also popular. These functionals include RPBE (Hammer, Hansen, & Nørskov, 1999), PBE-WC (Wu & Cohen, 2006), and PBEsol (Perdew et al., 2008), and they generally yield slightly better results for solids and their surfaces. Another popular GGA functional is AM05 (Armiento & Mattsson, 2005), which was specifically designed to include the surface effect and offers a much-improved performance for bulk properties, such as lattice constant and bulk modulus.

The meta-GGA functionals

Prompted by the success of GGAs, new functionals were introduced where potential is a functional of the density, its first and second ($\nabla^2\rho(r)$) gradients and/or the non-interacting kinetic energy functional ($1/2\sum_i|\nabla\phi_i|^2$). These functionals are commonly referred as meta-GGA functionals. Due to inclusion of additional degrees of freedom these functionals have a more complicated implementation methodologies and have not yet been exploited to a great extent except for some benchmarking studies of bulk materials and surfaces. Among, meta-GGA functionals, TPSS (Tao, Perdew, Staroverov, & Scuseria, 2003) has been used for both molecules and solids and have been shown to offer improved performance over LDAs and GGAs.

The hybrid functionals

These are the most popular and widely used functionals. Hybrid functionals utilize linear combinations of GGAs and add the exact exchange contribution derived from Hartree-Fock (Equation 3.30). Some of the most popular hybrid functionals include B3LYP (Becke, 1988; Becke, 1993a; Lee, Yang, & Parr, 1988), B3PW91 (Becke, 1988; Becke, 1993a; Perdew, 1991),

PBE0 (Adamo, Cossi, & Barone, 1999; Perdew et al., 1996), BH&HLYP (Becke, 1993b), etc. The B3LYP functional is linear combination of the LDA (VWN (Vosko et al., 1980)), the exact exchange functional, the B88 functional (Becke, 1988), and the LYP functional (Lee et al., 1988),

$$B_{XC}^{B3LYP} = (1-a)E_x^{LSD} + aE_x^{HF} + b\Delta E_x^B + (1-c)E_c^{LSD} + cE_c^{LYP} \tag{3.54}$$

The three fitting parameters, a, b, and c, which control the mixing of the HF exchange and density functional exchange and correlation were determined through fitting to well characterized experimental data using a training set of 50 small molecules (G2 reference set).

Similarly, the PBE0 functional (Adamo & , 1999; Perdew, Ernzerhof, & Burke, 1996)] combine linearly the PBE exchange energy and HF exchange energy and PBE correlation energy. PBE0 functional can be expressed as

$$\mathrm{E}_{XC}^{PBE0} = \frac{1}{4}\mathrm{E}_X^{HF} + \mathrm{E}_X^{PBE} + \mathrm{E}_C^{PBE} \tag{3.55}$$

Hybrid functionals have been shown to offer significant improved performance over LDA and GGA functionals for both molecules and solids. An important difference between hybrid functionals, and LSDs and GGAs is that LSDs and GGAs utilize the exact exchange of the electron gas and approximate just the correlation aspects, whereas hybrid functionals, such as B3LYP uses a mix of exact exchange (from LSD or GGA functionals) and approximate exchange (from HF) for the exchange part. It has been found that using a mix of exact and approximate exchange, often errors in correlation (always approximated) can be cancelled by errors in the exchange approximation, thus improving the overall accuracy of the results.

3.8. Selection of Method

To choose between various available approaches to solve the approximated Schrodinger equation for a system, structure of potassium-isopropyl-xanthate and lead-ethyl-xanthate molecules were optimized using HF and eighteen DFT methods. For lighter atoms, 6-31+G(d,p) basis set was used and for Pb atom LanL2DZ pseudopotential was used. The mean error in bond lengths and bond angles using different approaches are given in Table 3.1 along with the relative CPU time taken to complete the calculation. It should be noted that the actual time is not important as it is hardware dependent. The optimized geometrical parameters obtained by using CCSD method and 6-311+G(3df,3pd) basis set are used as reference. CCSD method is generally considered to produce highly accurate geometries. A large basis set is used with CCSD so that geometry of reference molecules is a close representation of the real system.

As evident from the data, DFT is not the fastest method, HF is. However, HF doesn't include any type of correlation. Consequently, the mean error in calculated bond lengths and bond angles is highest for HF. Among the DFT methods, surprisingly a significant difference in job completion time was not observed, except for methods with meta-GGA formalism. Hybrid meta-GGA functionals, especially B3LYP, X3LYP, O3LYP, and B3P86 yielded results with reasonable accuracy in much less time as compared to post-HF methods. The results obtained with B3LYP functional are most accurate among the hybrid functional DFT methods.

Table 3.1. Relative execution time and mean error in optimized geometries of potassium-isopropylxanthate and lead-ethylxanthate molecules for different ab-initio computational chemistry methods. Basis set: 6-31+G(d,p) for lighter atoms, LanL2DZ for Pb atom. Reference geometries optimized at CCSD/6-311+G(3df,3pd) level of theory.

Method	Type of method	Mean error in bond lengths (Å)	Mean error in bond angles (°)	Relative CPU time
CCSD	post-HF	Ref.	Ref.	19.67
HF		0.275	9.744	0.53
SVWN5	LSDA	0.209	5.548	0.78
BLYP	GGA	0.124	7.064	0.99
OLYP	GGA	0.169	3.837	1.12
PW91PW91	GGA	0.043	5.472	0.92
VSXC	meta-GGA	0.077	7.137	2.32
B3LYP	hybrid-GGA	0.011	0.604	1
O3LYP	hybrid-GGA	0.009	2.493	1.06
X3LYP	hybrid-GGA	0.019	1.96	1.03
B97-1	hybrid-GGA	0.141	2.844	1.12
B97-2	hybrid-GGA	0.166	2.879	1.06
B3P86	hybrid-GGA	0.023	3.923	1.08
PBE1PBE	hybrid-GGA	0.048	2.137	1.04
BHandHLYP	hybrid-GGA	0.093	3.749	1.14
PBeh1PBE	hybrid-GGA	0.041	4.841	1.04
B3PW91	hybrid-GGA	0.027	6.485	1.24
tHCTHhyb	hybrid-GGA	0.059	2.052	1.94
M06	hybrid meta -GGA	0.074	6.281	2.05
TPSSh	hybrid meta -GGA	0.053	5.954	1.84

3.8.1. Basis Set

3.8.1.1. Basis Set for Lighter Atoms

As mentioned in section 3.6, a basis set (collection of mathematical functions) is required for any ab-initio calculation for expanding the molecular orbitals or electron density of a system. In other words, basis set describes the wave function. The use of a good quality basis set is of critical importance as the accuracy of results is highly dependent on how closely the theoretical system represents the real system. Typically, it would require a basis set with infinite basis functions to describe the molecular system perfectly. However, the computational effort scales to third power of number of basis functions used in the calculations. So, practically a basis set should contain as minimum basis functions as possible. To select the basis function of optimum size to be used for the calculations involving interaction between collector ligands and metals, geometries of potassium salts and ionic forms of ethyl xanthate and 2-mercaptobenzothiazole were optimized in both neutral and anionic forms using B3LYP functional and different basis sets. The optimized geometrical parameters thus obtained, were compared with the values obtained by using the CCSD method and 6-311+G(3df,3pd) basis set. Results obtained from CCSD/6-311+G(3df,3pd) were used as reference as experimental geometrical parameters for anionic molecules cannot be obtained. CCSD method is generally considered to produce highly accurate geometries. A large basis set is used with CCSD so that geometry of reference molecules is a close representation of the real system. The mean error in optimized geometrical parameters and relative execution time for different basis sets are given in Table 3.2.

Table 3.2. Relative execution time and mean error in optimized geometries of potassium-ethyl-xanthate, ethyl xanthate ion, potassium-2-mercapto-benzothiazole and 2-mercapto-benzothiazole ion for different basis sets and B3LYP functional. Reference geometries optimized at CCSD/6-311+G(3df,3pd) level of theory.

Basis Set	Mean error in bond lengths (Å)	Mean error in bond angles (°)	Relative CPU time
STO-3G	0.216	14.280	0.15
STO-6G	0.211	11.227	0.27
3-21G	0.156	9.680	0.19
6-31G	0.139	9.570	0.27
6-31G(d)	0.087	2.302	0.52
6-31G(d,p)	0.086	2.290	0.60
6-31G +(d)	0.011	0.897	1
6-31G ++(d)	0.008	0.798	1.16
6-311++G(3df,3pd)	0.003	0.186	3.40

As evident from the data, minimal (STO-3G, STO-6G) and split-valance basis sets without added polarization and diffuse functions (3-21G, 6-31G) produced very inaccurate geometries. This is as per expected as these basis sets generally do not give good results for molecules containing charge or lone pair orbitals. Addition of polarization functions (6-31G(d) and 6-31(d,p) basis sets) increased the accuracy of calculations; however, still the error in bond lengths and bond angles is significantly high. Geometries obtained from basis sets with added polarization and diffuse functions are comparable to reference geometries. Also, evident is that geometries obtained with B3LYP/6-311++G(3df,3pd) combination are very close to geometries obtained with CCSD/6-311++G(3df,3pd).

3.8.1.2. Pseudopotential Basis Set for Pb, Cu and Zn

As described in section 3.6.2., , it is often desired to use an effective potential to describe the nucleus and core electrons of heavy metals rather than through the use of basis functions. To

select the most appropriate pseudopotential formalization for Cu, Zn an Pb atoms, geometry of lead-ethylxanthate and Cu(II)-diethyldithiocarbamate complexes were modeled using different pseudopotential functions. B3LYP functional was used to model these complexes and 6-311++G(3df,3pd) basis set was used for all other atoms. The optimized geometrical parameters were compared to their experimental values. The mean error in bond lengths and bond angles using different pseudopotential functions along with their execution time is given in Table 3.3.

Table 3.3. Relative execution time and mean error in optimized geometries of lead-ethylxanthate and Cu(II)-diethyldithiocarbamate complexes for different pseudopotential functions. Complexes were modeled using B3LYP functional. 6-311+G(3df,3pd) basis set was used for all the atoms except Cu and Pb.

Basis Set	Mean Error in Bond Lengths (Å)	Mean Error in Bond Angles (°)	Relative CPU Time
CEP-4G	0.019	1.164	1
CEP-31G	0.014	0.873	1.494
CEP-121G	0.003	0.83	1.672
LanL2MB	0.005	0.99	1.279
LanL2DZ	0.003	0.76	2.108
SDDAll	0.003	0.80	1.562

As evident from the data, all pseudopotential produced geometries within reasonable accuracy. The computational time for CEP-4G function is the least among the pseudopotentials considered; however, the mean errors for this function are highest. Based on computational time and accuracy SDD pseudopotentials appear to be most suitable.

Based on the results and discussion presented in Sections 3.8.1 and 3.8.2, the following combination is selected and has been used to obtain all the results presented and discussed in Chapters 4-7:

(i) DFT Method: B3LYP

(ii) Basis set for lighter elements: 6-311++G(3df,3pd)

(iii) Pseudopotential for Pb, Cu, and Zn: SDD

3.9. Modeling Systems in Solution

Typically, a DFT calculation is implemented in vacuum phase when it is reasonable to neglect any inter-molecular interactions. However, the reactions between flotation reagents and heavy metal ions or mineral surfaces take place in aqueous environment. The properties of molecules can differ considerably between the vacuum and solution phase. Therefore, it is desired to incorporate the effect of solvent molecules when determining reactivity and binding abilities of the collectors with metal ions. From a theoretical point of view, two extreme strategies are generally applied to implement solvation of molecules in computational chemistry studies, which are discussed in following sections.

3.9.1. Explicit Solvation

In explicit solvation models, presence of individual solvent molecules is considered. These methods treat the solvent as a large ensemble of molecules, and the properties of these ensembles are calculated by running molecular dynamics or Monte Carlo simulations following the laws of statistical mechanics (Maginn & Elliott, 2010; Reichardt, 2005; Snor, 2009). In explicit solvation, the electronic structure of solvent or solute molecules is not considered and inter-molecular interactions are treated using molecular mechanics force fields or intermolecular potentials (Struebing, 2011). Different atomic and molecular properties of the system such as geometry, bond strengths, atomic charges, etc. are described in terms of parameters derived from experimental data or higher level quantum mechanics techniques (Jensen, 1998). The accuracy of explicit solvation calculations depends on the accuracy of the force field or intermolecular

potentials utilized to model the solvation effect as well as on the accuracy of various fitted parameters. In general, explicit solvation in molecular mechanics or Monte Carlo formalism is considered a poor way to model the solvation effects (Snor, 2009). The accuracy of explicit solvation models can be greatly improved by considering laws of quantum mechanics to calculate various atomic and molecular properties and to model intermolecular interactions. However, the explicit treatment of the solvent molecules introduces a large number of degrees of freedom making such calculations highly complicated and computationally extensive. Thus, explicit solvation modeling through quantum chemical approach is generally limited to a few solvent molecules. However, this approach does not represent a whole picture as the precise estimation of solvation free-energies and other effects require consideration of a sufficiently large number of solvent molecules around the solute.

3.9.2. Implicit Solvation

Another common approach to model solution effects is the self-consistent reaction field (SCRF) method in which the presence of solvent molecules around a solute molecule is described as a polarizable continuum of uniform dielectric constant ε (Struebing, 2011). In SCRF methodology, the solute molecule is placed into a cavity within the solvent continuum. Solvation models based on SCRF methodology are also called implicit solvation methods. Implicit solvation models consider thermally averaged systems and generally require only a small number of parameters (e.g. dielectric constant, surface tension, density, etc.) to represent the solvent properties within reasonable accuracy (Cramer & Truhlar, 1999). These methods have been optimized to make nearly accurate predictions of free energies of solvation (Ho, Coote, & Truhlar, 1999). The solute molecule encapsulated in the cavity experiences a reaction field exerted by surrounding dielectric continuum, which causes a change in solute's polarization. Similarly, the reaction field of the

electron density of the solute, results in a change in the polarization of the surrounding medium. This recursive reaction potential is iterated computationally to achieve self- consistency which represents the equilibrium state.

Different implicit solvation methods define the cavity and the reaction field in different ways. In the **Onsager reaction field method** (Onsager, 1936), a solute molecule is considered as a polarizable dipole with dipole moment μ and polarizability α, and placed at the centre of a spherical (or ellipsoidal) cavity of radius a_o, as shown in Figure 3.3(A). The solute dipole induces a reaction field (or dipole) in the surrounding medium which in turn induces an electric field in the cavity which interacts with the solute dipole. It is noteworthy to mention here that this model typically generates very poor results for non-spherical molecules or molecules where the electron distribution cannot be effectively described in terms of dipole moment.

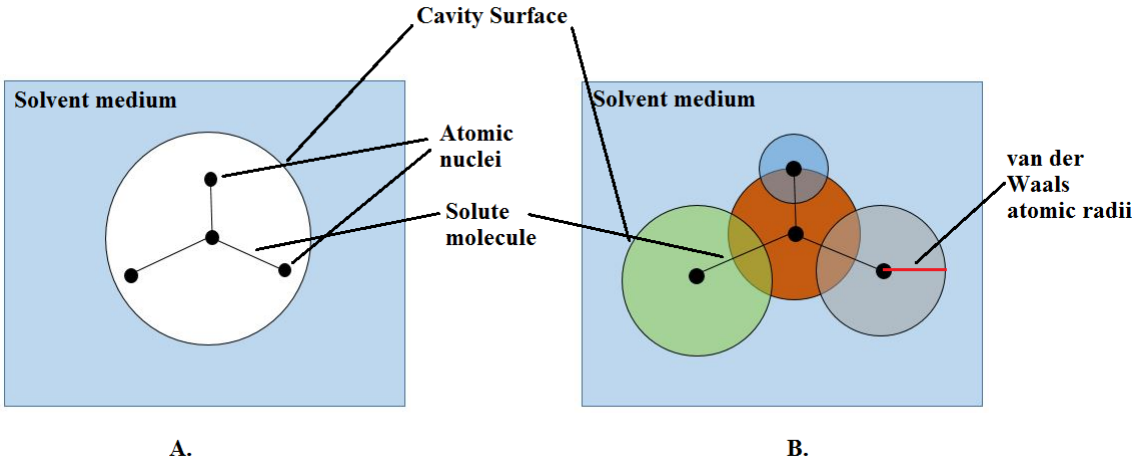

Figure 3.3. Schematic representation of a solute molecule placed in a cavity in, (A) Onsager reaction field method and (B) Polarizable Continuum Model (PCM) of implicit solvation.

Polarizable Continuum Model (PCM) (Miertus, Scrocco, & Tomasi, 1981) is a far more sophisticated method and presents a significant improvement in describing the solute-solvent interactions. In PCM, the cavity is defined as the union of a series of overlapping spheres

representing different atoms within a molecule as shown in Figure 3.3(B). Generally, van der Waals radii (or scaled van der Waals radii) of individual atoms are used to describe different spheres that constitute the cavity. During the computational procedure, the surface of the cavity is divided into a number of small surface elements or tesserae, each of surface area ΔS_i with a charge q_i placed at its centre. The charge q_i represents a combined effect of solute's and other tesseraes' electric fields at the i^{th} surface element. The initial surface charge density σ^o is derived from the electric field generated by unperturbed solute charge distribution ρ^o, and initial set of charges q_i^o are calculated according the following equation (Szarecka, Rychlewski, & Rychlewska, 1998):

$$q_i^o = \sigma(s_i)\Delta S_i \tag{3.56}$$

Now, these charges also contribute to the electric field and result in a new surface charge density σ which gives a new set of surface charges q_i. These steps are repeated until self-consistency is achieved and final set of surface charges q_i^f is obtained (Szarecka et al., 1998). The charges q_i^f generates a reaction field potential V_f, which is added to the unperturbed solute Hamiltonian (Equation 3.39) and the ground state energy of the system in solvated state is obtained by minimizing the energy functional shown in Equation 3.57 by following the methodologies described in section 3.7.

$$E[\rho] = F[\rho] + \int \rho(r)V(r)\,dr + \int \rho(r)V_f(r)\,dr \tag{3.57}$$

In PCM, the contribution of solvation to molecular free energy is considered as the sum over five different terms (Verdolino, 2009):

$$G^S = G_{cav} + G_{elec} + G_{rep} + G_{dis} + G_{thermal} \tag{3.58}$$

The first term G_{cav} accounts for the energy required to create a cavity of suitable size and shape in the solvent against the cohesive liquid forces, and can be computed by using several available methods (Maeder-Vigne & Claverie, 1987; Pierotti, 1976; Ulig, 1937)**.** The calculation of cavity energy G_{cav} generally uses the surface defined by the van der Waals spheres (VWS) as shown in Figure 3.4. In a typical PCM implementation, this term is calculated separately from the other four and is not included in the molecular Hamiltonian (Equation 3.57) as it doesn't change for a fixed geometry and a given temperature and solvent density (Verdolino, 2009).

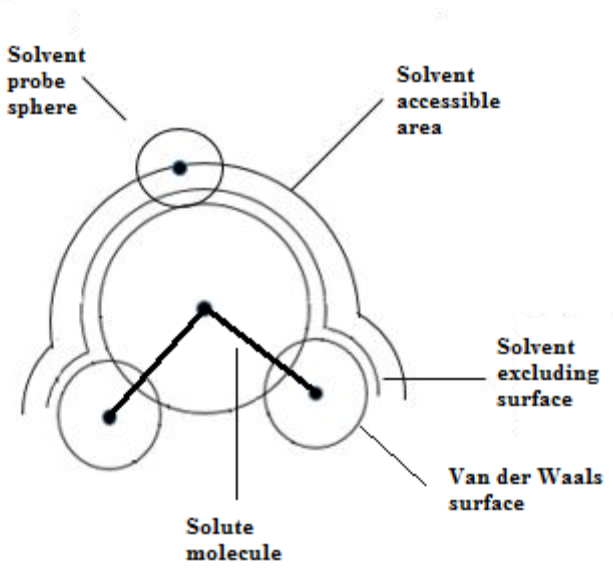

Figure 3.4. A schematic representation of solvent accessible area and cavity surface (union of van der Waals spheres for atoms constituting the solute molecule) in the PCM methodology of implicit solvation.

The G_{elec} term represents the electrostatic interactions between polarized solute molecule and solvent medium. G_{rep} and G_{dis} terms represent the free energy contribution due to the quantum mechanical exchange repulsion and dispersion. These three terms are evaluated by integrating their values for the individual tesserae or surface elements over the cavity surface and their

evaluation forms a part of the solution of Schrodinger equation shown in Equation 3.57. In other words, the reaction field potential V_f (in Equation 3.57) due to the solute ensemble in solvent cavity can be expressed as (Tomasi, Mennucci, & Cancès, 1999):

$$V_f = V_{elec} + V_{rep} + V_{dis} \tag{3.59}$$

The V_{elec}, V_{rep} and V_{dis} terms in Equation 3.59 represents the electrostatic, exchange repulsion and dispersion part of the reaction field potential V_f due to the charges q_i^f on the surface of the cavity . Generally, the solvent-accessible surface (SAS), (B. Lee & Richards, 1971) which is generally described by a rolling spherical probe on the VWS as shown in Figure 3.4, is utilized in the calculation of potentials shown in Equation 3.59. The dimension of the spherical probe depends on the nature and molecular properties of the solvent. The $G_{thermal}$ term accounts free energy contribution from thermal motion of various system constituents (nuclei and electrons) and its value is related to a reference state represented by unperturbed solvent and non-interacting electrons and nuclei of solute molecules. The difference between the free energy computed by using Equation 3.57 which includes PCM contribution to the Hamilton (plus G_{cav} and $G_{thermal}$) and the same quantistic level energy computed in vacuum using Equation 3.39 gives an estimation of ΔG_{sol} of the solute molecule. Detailed discussions of mathematical formulation for individual terms in Equation 3.58 and the quantum mechanics formulation of the PCM methodology can be found elsewhere (Cramer & Truhlar, 1999; Mennucci & Cammi, 2007; Verdolino, 2009). The PCM methogology produces fairly accurate results where electrostatic effects are prominent; however, it has some limitations in systems where non-electrostatic effects dominate the solute-solvent interactions (Mennucci et al., 2002).

Other popular implicit solvation models include **Isodensity PCM (IPCM)** and **Self-consistent Isodensity Polarized Continuum Model (SCI-PCM)**. In IPCM the cavity is defined

as an isodensity surface of the molecule. The initial isodensity is determined by an iterative process following a SCF convergence cycle. The wavefunction thus obtained is used to compute an updated isodensity surface, and the steps are repeated till the cavity shape converges upon the completion of the SCF. An isodensity surface describes the reactive shape of the molecule in a better manner compared to pre-defined shapes such as a sphere in Onsager model or a set of overlapping spheres in PCM. One of the major drawbacks of IPCM is that it neglects the terms corresponding to coupling of isodensity surface and the electron density of the solute molecule. SCI-PCM methodology considers full coupling between the cavity and the electron density of solute molecule and thus include the coupling terms neglected in IPCM. In this method the solvation effects are included in the iterative SCF computation rather than their calculation through an extra step afterwards as implemented in other implicit solvation methodologies. A detailed discussion and description of these methods can be found in review articles (Dupuis & King, 1978; Dupuis & King, 1977; R. G. Parr & Yang, 1989; Seeger & Pople, 1977; Takada, Dupuis, & King, 1981).

Apart from methods described in previous paragraphs Solvation Model based on Density (SMD) and Solvation Models (SMx, where x is alphanumeric label representing the version of this model) have also found applications in computational studies (Ho et al., 1999). These methods have been found to be more accurate than the models described previously especially for neutral molecules of smaller size.

It is noteworthy to mention that there is no one best method to incorporate solvation effects. The choice of method to be used depends on the size and nature of the solute molecule (e.g. neutral molecule or ion), type and nature of solvent, type of solvent effects being examined, and the desired accuracy of results (Snor, 2009). The accuracy of implicit solvation models can be

improved by considering an ensemble of a layer of implicit solvent molecules around the solute molecule inside the cavity which is surrounded by a continuum of polarizable solvent (Snor, 2009). However, this approach is very complex and computationally intensive as one has to try numerous configurations (number, position and orientation) of explicit solvent molecules around the solute in order to obtain a statistical average and optimum ensemble of solute and solvent molecules. Such a methodology should be limited to studies involving very small solute systems such as diatomic molecules or atomic ions or when a very accurate evaluation of solvation free energy of a solute molecule is desired.

Considering the size and number of molecules to be modeled in the present study, PCM methodology is used to model the solvation effects. It is assumed that associated errors in solvation energies of different molecules are comparable and doesn't influence the observed trends in molecular reactivity of collector reagents or interaction energies of metal-collector complexes.

3.10. Details of Methodology

In this study, all calculations were carried out using Gaussian 09 (Frisch et al., 2009) software package in the framework of density functional theory (DFT).

3.10.1. Geometry Optimization

Optimization of molecular geometry is the most important step in a computational chemistry study, as the calculated parameters are dependent on the resultant geometry. Different conformations and configurations were used as the starting guess of geometry for the molecules of both the collector ions and metal-collector complexes. The starting geometries of a particular collector molecule differed in bond lengths, bond angles, and dihedral angles. The variations

considered in starting geometries of metal-collector complexes varied in terms of metal-ligand bond lengths, bond angles subtended by ligands at the metal centre and dihedral angles with metal atom at the centre. For each molecule, approximately seven to eight starting geometries were considered. Among various optimized structures of a given molecule, the one with the lowest energy was selected for further evaluation. Rotational, translational and vibrational frequencies were computed at the same level of theory for the geometrically optimized molecules. It was observed that a tight convergence criterion using ultrafine grid was necessary to keep the rotational and translational modes within the desired (±10 cm^{-1}) range for some of the structures. This selection was applied to all molecules for consistency in calculations. Absence of any imaginary frequencies in the vibrational spectra confirmed that the optimized molecules correspond to the global minimum on their corresponding potential energy surfaces.

3.10.2. Molecular Properties

3.10.2.1. Atomic Charges

To obtain an initial guess of the potential reactive centres within a molecule, partial atomic charges were calculated by using Mulliken Population Analysis (MPA) scheme (Mulliken, 1955). In MPA, the overlap electronic population is equally divided among the two interacting atoms A and B. The summation of these densities over a particular atom k determines the net number of electrons (Nk) or electron density belonging to that atom. Partial atomic charge on atom k is then calculated as:

$$q_k = Z_k - N_k \tag{3.60}$$

where Z_k is the atomic number of atom k. Apart from not accounting the differences in electronegativity of atoms during partitioning the electron density, the most significant

disadvantage of MPA scheme is that the results are strongly dependent on the choice basis set and level of theory. However, all the calculations in the present study were done at the same level of theory and using the same basis sets.

3.10.2.2. Molecular Reactivity Descriptors

To elucidate detailed information about reactivity of individual collector molecules towards different metal ions in water, popular concepts of chemical reactivity indices, namely dipole moment (D), electronic chemical potential (μ) (R. Parr, Donnelly, Levy, & Palke, 1978; R. G. Parr & Pearson, 1983) absolute chemical hardness (η) (R. G. Parr & Pearson, 1983; Pearson, 1992) and global electrophilicity index (ω) (R. G. Parr, Szentpaly, & Liu, 1999) were used.

Dipole moment is a useful indicator of initial interaction between two chemical species in a reaction medium. Collector molecules with large dipole moment interact strongly with metal ions or mineral surfaces in aqueous solutions via strong van der Waals interactions (Liu et al., 2012). Electronic chemical potential and absolute chemical hardness are global reactivity descriptors defined as first and second order partial derivative of the energy, E, with respect to the number of electrons, N, at constant external potential, $v(\vec{r})$, due to the nuclei plus any external potential (Pearson, 1988; Pearson, 1992),

$$\mu = \left(\frac{\partial E}{\partial N}\right)_{v(\vec{r})} \tag{3.61}$$

$$\eta = \frac{1}{2}\left(\frac{\partial \mu}{\partial N}\right)_{v(\vec{r})} \tag{3.62}$$

Physically, μ describes the escaping tendency of electrons from an equilibrium system (Chattaraj & Maiti, 2003; Mebi, 2011), while η measures the resistance of a molecule to undergo any change in the electron distribution or charge transfer (Mebi, 2011; R. G. Parr & Pearson,

1983). Following the Koopmans' approximation (Koopmans, 1934), in the density functional theory formalism, μ and η can be expressed in terms of frontier orbital energies as,

$$\mu = \frac{(E_{HOMO}+E_{LUMO})}{2} \tag{3.63}$$

$$\eta = \frac{(E_{LUMO}-E_{HOMO})}{2} \tag{3.64}$$

where E_{HOMO} and E_{LUMO} are the orbital energies of highest occupied molecular orbital (HOMO) and lowest unoccupied molecular orbital (LUMO) of the n electron system (Kulkarni, Tanwar, & Pal, 2007). E_{HOMO} and E_{LUMO} are taken directly from the Gaussian output. μ and η are key indicators of the stability and overall reactivity of a chemical system, and are the most fundamental descriptors of charge transfer between two (or more) chemical systems during a chemical reaction (Islam & Ghosh, 2012). Two chemical systems when interact with each other, work towards equalization of chemical potential through electron transfer from system of higher chemical potential to that of lower chemical potential (Pearson, 1988). The difference in chemical potentials drives this transfer, and individual hardness parameters act as a resistance (Pearson, 1988).

Chemical potential is a useful indicator of whether a chemical species has electrophile or nucleophile nature. However, μ alone cannot be used as a measure of its electrophilicity or nucleophilicity. As Ayers *et al*. (2008a; 2008b) pointed out, a molecule with low chemical potential though a good electrophile, could still have bad electrophilicity owing to large value of its chemical hardness. Thus, a measure of molecular electrophilicity or nucleophilicity should incorporate both the chemical potential and the chemical hardness (Islam & Ghosh, 2012).

Parr *et al*. (1999) introduced a new global reactivity descriptor for chemical species that depends on both the electronic chemical potential and chemical hardness, and termed it as global

electrophilicity index (ω) (equation 3.65). The electrophilicity index is a measure of the stabilization in energy when a chemical system acquires an additional electronic charge ΔN from the environment (Islam & Ghosh, 2012). Thus, ω physically signifies the propensity or capacity of a chemical species to accept electrons. It allows a quantitative classification of the global electrophilic or nucleophilic nature of a molecule on a relative scale (Udhayakala, Samuel, Rajendiran, & Gunasekaran, 2013),

$$\omega = \frac{\mu^2}{2\eta} \tag{3.64}$$

Therefore, we have used μ, η and ω, which are useful quantitative descriptors for the stability, chemical reactivity and electrophilicity/nucleophilicity of atoms or molecules as a whole to evaluate the relative reactivity of different collector ions under consideration.

3.10.2.3. Gibbs Free Energy

The electronic structure calculations does not consider the effects of temperature and pressure, i.e. all the physical quantities derived from such computations are strictly valid at T = 0 K and p = 0 atm (where T and p are the temperature and pressure of the system). The effect of temperature and pressure on the atomic positions can be obtained by evaluating the total energy as a function of nuclear coordinates on the Born-Oppenheimer potential energy surface. Various thermodynamic functions can then be evaluated over the whole temperature and pressure range.

For a system at temperature T and pressure p the Gibbs free energy G is defined as:

$$G(T,p) = U + pV - TS, \text{ or} \tag{3.65}$$

$$G(T,p) = H - TS \tag{3.66}$$

where U is the internal energy, V is volume, S is the entropy, and H is the enthalpy of the system. At 0 K, the system doesn't experience any translational, vibrational and rotational motion. The

entropy of such a system is zero (third law of thermodynamics) and its internal energy is equal to the electronic energy. In a typical DFT formulation, the Gibbs free energy G of a system at temperature T and pressure p is expressed as:

$$G(T,p) = E_o + G_{corr} \tag{3.67}$$

where $E_o$is the total electronic energy at 0 K and G_{corr} is the free energy associated with system's enthalpy and entropy changes corresponding to temperature and pressure effects. G_{corr} can be expressed as:

$$G_{corr} = H_{corr} - TS_{tot} \tag{3.68}$$

where H_{corr} represents the change in enthalpy and S_{tot} represents the change in entropy of the system corresponding to temperature and pressure effects. S_{tot} and H_{corr} terms in Equation 3.68 can be expressed as:

$$S_{tot} = S_t + S_r + S_e + S_v \tag{3.69}$$

$$H_{corr} = \epsilon_{tot} + k_B T \tag{3.70}$$

$$\epsilon_{tot} = \epsilon_t + \epsilon_r + \epsilon_e + \epsilon_v \tag{3.71}$$

where S_t, S_r, S_e, and S_v represents the contribution to entropy from translation, rotational, electronic, and vibrational motions respectively, and ϵ_t, ϵ_r, ϵ_e, and ϵ_v represents the contribution to internal energy from translation, rotational, electronic, and vibrational motions respectively. The $k_B T$ (k_B = Boltzmann constant) term in Equation 3.70 corresponds to the pV term in Equation 3.65.

In thermodynamics, the statistical properties of a system in thermodynamic equilibrium are described by partition functions. The thermodynamic variables of the system, such as total

energy, entropy, enthalpy, and pressure, can be expressed in terms of the molecular partition function $\tilde{Q}$. If it is assumed that there exists only one conformation for the molecule and negligible coupling between electronic excitation, vibrations, and rotations, the molecular partition function can be expressed as a product of partition functions corresponding to the translational, rotational, vibrational, and electronic motions (Ho et al., 1999):

$$\tilde{Q} = q_t q_e q_e q_v \tag{3.72}$$

The partition functions corresponding to a particular component (i.e. translational, rotational, vibrational, or electronic motion) can be used to determine the entropy contribution from that component using the relation:

$$S = R\left(\ln(q_t q_e q_e q_v e) + T\left(\frac{\partial ln\tilde{Q}}{\partial T}\right)_V\right) \tag{3.73}$$

Similarly, the internal thermal energy contribution from a component can be obtained by using the relation:

$$\epsilon = N k_B T^2 \left(\frac{\partial ln\tilde{Q}}{\partial T}\right)_V \tag{3.74}$$

In thermodynamics, S_t, S_r, S_e, S_v, ϵ_t, ϵ_r, ϵ_e, and ϵ_v terms in Equations 3.69 and 3.71 are calculated using the Equations 3.73 and 3.74. Once the values of these terms are known, the Gibbs free energy of the system can be calculated by using Equations 3.66 – 3.71. A detailed discussion on thermodynamic partition functions and calculation of thermodynamic properties by using the partition functions can be found in the “Molecular Thermodynamics" textbook by McQuarrie and Simon (1999).

3.10.2.4. Interaction Energy of Metal-Collector Complex

The interaction energy between collector reagents and metal ions during the formation of metal-collector complexes is described in terms of the change in Gibbs free energy during the reaction as:

$$\Delta G_r = G(T,p)_{products} - G(T,p)_{reactants} \tag{3.70}$$

with T =298 K and p = 1 atm. The Gibbs free energy of individual molecules is calculated by the methodology described in Section 3.10.2.3.

3.11. References

Adamo, C., & Barone,V. (1999). Toward reliable density functional methods without adjustable parameters: The PBE0 model. *The Journal of Chemical Physics, 110(13),* 6158-6170.

Adamo, C., Cossi, M., & Barone, V. (1999). An accurate density functional method for the study of magnetic properties: The PBE0 model. *Journal of Molecular Structure: THEOCHEM, 493*(1–3), 145-157.

Armiento, R., & Mattsson, A. E. (2005). Functional designed to include surface effects in self-consistent density functional theory. *Phys. Rev. B, 72(8),* 0851081-0851085.

Ayers, P., & Parr, R. (2008a). Beyond electronegativity and local hardness: Higher-order equilization criteria for determination of a ground-state electron density. *Journal of Chemical Physics, 129*(5), 054111-054117.

Ayers, P., & Parr, R. (2008b). Local hardness equilization: Exploiting the embiguity. *Journal of Chemical Physics, 128*(18), 184108-184115.

Becke, A. D. (1988). Density-functional exchange-energy approximation with correct asymptotic behavior. *Physical Review A, 38*(6), 3098-3100.

Becke, A. D. (1993a). Density-functional thermochemistry. III. the role of exact exchange. *The Journal of Chemical Physics, 98*(7), 5648-5652.

Becke, A. D. (1993b). A new mixing of Hartree–Fock and local density-functional theories. *J. Chem. Phys, 98(2),*1372-1377.

Born, M., & Oppenheimer, R. (1927). Zur quantentheorie der molekeln. *Annalen Der Physik, 389*, 457-464.

Ceperley, D. M., & Alder, B. J. (1980). Ground state of the electron gas by a stochastic method. *Phys. Rev. Lett, 45(7),* 566-569.

Chattaraj, P. K., & Maiti, B. (2003). HSAB principle applied to the time evolution of chemical reactions. *Journal of the American Chemical Society, 125*(9), 2705-2710.

Clark, T. (1985). *A handbook of computational chemistry*. New York: John Wiley & Sons.

Cramer, C. J. (2004). *Essentials of computational chemistry* (2nd ed.) Wiley.

Cramer, C. J., & Truhlar, D. (1999). ChemInformAbstract:ImplicitSolvation models:Equilibria,structure,spectra,and dynamics. *Chemical Reviews, 99*, 2161-2200.

Davidson, E. R., & Felle, D. (1986). Basis set selection for molecular calculations. *Chem. Rev, 86*(4), 681-696.

Dewar, M. J. S., Zoebisch, E. G., & Healy, E. F. (1985). Development and use of quantum mechanical molecular models. AM1: A new general purpose quantum mechanical molecular model. *J. Am. Chem. Soc., 107*, 3902.

Dixon, S. L., & Merz, K. M. (1996). Semiempirical molecular orbital calculations with linear system size scaling. *J. Chem. Phys, 104*, 6643.

Dupuis, M., & King, H. F. (1978). Molecular symmetry. II. gradient of electronic energy with respect to nuclear coordinates. *Journal of Chemical Physics, 68*, 3998.

Dupuis, M., & King, H. F. (1977). Molecular symmetry and closed-shell SCF calculations. I. *International Journal of Quantum Chemistry, 11*(4), 613-625.

Engel, E., & Dreizler, R. M. (2011). *Density functional theory* Springer.

Fox, S. J. (2012). *Protein-ligand binding affinities from large-scale quantum mechanical simulations.* (Unpublished PhD). University of Southampton, Southampton.

Frauenheim, T., Seifert, G., Estner, M., Hajnal, Z., Jungnickel, G., & Porezag, D. (2000). *Phys. Stat. Sol (B), 217*, 41.

Frisch, M. J., Trucks, G. W., Schlegel, H. B., Scuseria, G. E., Robb, M. A., Cheeseman, J. R., . . . Fox, D. J. (2009). *Gaussian 09, revision A.1*. Wallingford CT: Gaussian, Inc.

Gell-Mann, M., & Brueckner, K. A. (1957). Correlation energy of an electron gas at high density. *Phys. Rev., 106(2),* 364-368.

Hammer, B., Hansen, L. B., & Nørskov, J. K. (1999). Improved adsorption energetics within density-functional theory using revised perdew-burke-ernzerhof functionals. *Phys. Rev. B, 59(11),* 7413-7421.

Heisenburg, W. (1927). Uber den anschaulichen inhalt der quantentheoretischen kinematik und mechanik. *Zeitschrift Fur Physik, 43*, 172-198.

Hellstrom, P. (2007). *Ab initio modelling of xanthates adsorbed on Ge and ZnS surfaces.* (Unpublished PhD). Luleå University of Technology, Sweden.

Ho, J., Coote, M. L., & Truhlar, D. G. (1999). Theoretical calculation of reduction potentials. In O. Hammerich, & B. Speiser (Eds.), *Organic electrochemistry* (5th ed., pp. 229-262). Florida: CRC Press.

Hohenberg, P., & Kohn, W. (1964). Inhomogeneous electron gas. *Phys. Rev., 136(3B),*B864-B871.

Islam, N., & Ghosh, D. C. (2012). On the electrophilic character of molecules through its relation with electronegativity and chemical hardness. *International Journal of Molecular Sciences, 13*(2), 2160-2175.

Jensen, F. (Ed.). (1998). *Introduction to computational chemistry*. Chichester, UK: John Wiley and Sons Ltd.

Karhanek, D. (2010). *Self-assembled monolayers studied by density functional theory.* (Unpublished PhD). University of Vienna, Vienna, Austria.

Kohn, W., & Sham, L. J. (1965). Self-consistent equations including exchange and correlation effects. *Phys. Rev., 140(4A),* A1133-A1138.

Koopmans, T. (1934). Uber die zuordnung von wellenfunk-tionen und eigenwerten zu den einzelnen elektronen eines atoms. *Physica, 1*, 104.

Kulkarni, B. S., Tanwar, A., & Pal, S. (2007). Reactivity descriptors and electron density analysis for ligand chemistry: A case study of 2,2'-bipyridine and its analogues. *Journal of Chemical Sciences, 119*(5), 489-499.

Leach, A. R. (2001). *Molecular modelling* (2nd ed.) Prentice Hall.

Lee, B., & Richards, F. M. (1971). The interpretation of protein structures: Estimation of static accessibility. *Journal of Molecular Biology, 55*(3), 379-IN4.

Lee, C., Yang, W., & Parr, Y. G. (1988). Development of the colle-salvetti conelation energy formula into a functional of the electron density. *Phys. Rev. B, 37(2),*785-789.

Levy, M. (1982). Electron densities in search of hamiltonians. *Physical Review A, 26*, 1200-1208.

Li, B. (2009). *Density-functional theory and quantum chemistry studies on "dry" and "wet" NaCl(001).* (Unpublished PhD). TU Berlin, Berlin.

Liu, G., Zeng, H., Lu, Q., Zhong, H., Choi, P., & Xu, Z. (2012). Adsorption of mercaptobenzoheterocyclic compounds on sulfide mineral surfaces: A density functional theory study of structure–reactivity relations. *Colloids and Surfaces A: Physicochemical and Engineering Aspects, 409*, 1-9.

Lowdin, P. O. (1998). In Lowdin P. O. (Ed.), *Advances in density functional theory* Elsevier.

Lowdin, P. O. (1955). Quantum theory of many-particle systems. I. physical interpretations by means of density matrices, natural spin-orbitals, and convergence problems in the method of configurational interaction. *Phys. Rev., 97*, 1474-1479.

Maeder-Vigne, F., & Claverie, P. (1987). Theoretical conformational study of carotenoporphyrins related to photophysical properties. *Journal of American Chemical Society, 109*(1), 24-28.

Maginn, E. J., & Elliott, J. R. (2010). Historical perspective and current outlook for molecular dynamics as a chemical engineering tool. *Industrial & Engineering Chemistry Research, 49*, 3059-3078.

Magnasco, V. (2013). *Elementary molecular quantum mechanics: Mathematical methods and applications* (2nd ed.). USA: Elsevier.

McQuarrie, D. A., & Simon, J. D. (1999). *Molecular thermodynamics* University Science Books.

Mebi, C. A. (2011). DFT study on structure, electronic properties, and reactivity of cis-isomers of $[(NC_5H_4\text{-}S)_2Fe(CO)_2]$. *Journal of Chemical Sciences, 123*(5), 727-731.

Mennucci, B., & Cammi, R. (Eds.). (2007). *Continuum solvation models in chemical physics: From theory to applications* Wiley.

Mennucci, B., Tomasi, J., Cammi, R., Cheeseman, J. R., Frisch, M. J., Devlin, F. J., . . . Stehpens, P. J. (2002). Polarizable continuum model (PCM) calculations of solvent effects

on optical rotations of chiral molecules. *The Journal of Physical Chemistry, 106*(25), 6102-6113.

Miertus, S., Scrocco, E., & Tomasi, J. (1981). Electrostatic interaction of a solute with a continuum. A direct utilization of ab initio molecular potentials for the prevision of solvent effects. *Chemical Physics, 55*(1), 117-129.

Mulliken, R. S. (1955). Electronic population analysis on LCAO-MO molecular wave function - I. *The Journal of Chemical Physics, 23*(10), 1833-1840.

Murrell, R. S., & Harget, A. J. (1972). *Semi-empirical self-consistent-field molecular orbital theory of molecules*. London: Wiely-Interscience.

Onsager, L. (1936). Electric moments of molecules in liquids. *Journal of American Chemical Society, 58*, 1486-1493.

Parr, R., Donnelly, R., Levy, M., & Palke, W. (1978). Electronegativity-the density functional viewpoint. *Journal of Chemical Physics, 68*, 3801-3807.

Parr, R. G., & Pearson, R. G. (1983). Absolute hardness: Companion parameter to absolute electronegativity. *Journal of the American Chemical Society, 105*(26), 7512-7516.

Parr, R. G., Szentpaly, L. V., & Liu, S. (1999). Electrophilicity index. *Journal of the American Chemical Society, 121*(9), 1922-1924.

Parr, R. G., & Yang, W. (Eds.). (1989). *Density-functional theory of atoms and molecules,*. New York: Oxford University Press.

Pearson, R. G. (1988). Absolute electronegativity and hardness: Application to inorganic chemistry. *Inorganic Chemistry, 27*, 734-740.

Pearson, R. G. (1992). The electronic chemical potential and chemical hardness. *Molecular Structure (Theochem), 255*, 261-270.

Perdew, J. P. (1991). In P. Ziesche, & H. Eschig (Eds.), *Electronic structure of solids* (pp. 11). Berlin: Akademie Verlag.

Perdew, J. P., Burke, K., & Ernzerhof, M. (1997). Generalized gradient approximation made simple. *Phys. Rev. Lett, 77(18),* 3865-3868.

Perdew, J. P., Ernzerhof, M., & Burke, K. (1996). Rationale for mixing exact exchange with density functional approximations. *The Journal of Chemical Physics, 105(22),* 9982-9985.

Perdew, J. P., Ruzsinszky, A., Csonka, I. G., Vydrov, O. A., Scuseria, G. E., Constantin, L. A., . . . Burke, K. (2008). Restoring the density-gradient expansion for exchange in solids and surfaces. *Phys. Rev. Lett, 100(13),* 1364061-1364064.

Perdew, J. P., & Wang, Y. (1992). Accurate and simple analytic representation of the electron-gas correlation energy. *Physical Review B, 45(23),* 13244-13249.

Perdew, J. P., & Zunger, A. (1981). Self-interaction correction to density-functional approximations for many-electron systems. *Physical Review B, 23,* 5048-5079.

Perdew, J. P., Burke, K., & Wang, Y. (1996). Generalized gradient approximation for the exchange-correlation hole of a many-electron system. *Phys. Rev. B, 54(23),* 16533-16539

Phillips, J. C. (1958). Energy-band interpolation scheme based on a pseudopotential. *Phys. Rev., 112*(3), 685-695.

Pierotti, R. A. (1976). A scaled particle theory of aqueous and nonaqueous solutions. *Chem. Rev,* (76), 717-726.

Pople, J. A., & Beveridge, D. L. (1970). *Approximate molecular orbital theory*. New York: McGraw-Hill.

Pople, J. A., Santry, D. P., & Sehgal, G. A. (1965). Appximate self-consistent molecular orbital theory: Invariant procedures. *J. Chem. Phys, 43,* S129

Pople, J. A., & Segal, G. A. (1965). Approximate self-consistent molecular orbital theory. II. calculations with complete neglect of differential overlap. *J. Chem. Phys, 43,* S136

Rai, B. (2012). Basic concepts in molecular modeling. In B. Rai (Ed.), *Molecular modeling for the design of novel performance chemicals and materials* (pp. 1-26) CRC Press.

Reichardt, C. (Ed.). (2005). *Solvents and solvent effects in organic chemistry* (3rd ed.). Germany: Wiley-VCH.

Seeger, R., & Pople, J. A. (1977). Self-consistent molecular orbital methods. XVIII. constraints and stability in Hartree–Fock theory. *The Journal of Chemical Physics, 66(7)*, 3045-3050.

Sholl, D. S., & Steckel, J. A. (2009). *Density functional theory: A practical introduction* Wiley-Interscience.

Snor, W. (2009). *Molecular modelling on cyclodextrin inclusion complexes.* (Unpublished PhD). University of Vienna, Vienna.

Stewart, J. J. P. (1989). Optimization of parameters for semi-empirical methods I - method. *J. Comput. Chem., 10(2)*, 209-220.

Stewart, J. J. P., & Stewart, A. C. (1999). Developing a semiempirical method. *Crystal engineering: The design and applicatiion of functional solids*. NATO ASI Ser.

Struebing, H. (2011). *Identifying optimal solvents for reactions using quantum mechanics and computer-aided molecular design.* (Unpublished PhD). Imperial College, London.

Szarecka, A., Rychlewski, J., & Rychlewska, U. (1998). Theoretical solvation models: Ab initio study of molecular aggregation. *Computation Methods in Science and Technology, 4*(1), 25-33.

Takada, T., Dupuis, M., & King, H. F. (1981). Molecular symmetry. III. second derivatives of electronic energy with respect to nuclear coordinates. *The Journal of Chemical Physics, 75(1)*, 332-336.

Tao, J., Perdew, J. P., Staroverov, V. N., & Scuseria, G. E. (2003). Climbing the density functional ladder: Non-empirical meta-generalized gradient approximation designed for molecules and solids, *Phys. Rev. Lett, 91(14),* 1464011-1464014.

Theil, W. (1996). Perspectives on semiempirical molecular orbital theory. *Adv. Chem. Phys., 93*, 703-757.

Tomasi, J., Mennucci, B., & Cancès, E. (1999). The IEF version of the PCM solvation method: An overview of a new method addressed to study molecular solutes at the QM ab initio level. *Journal of Molecular Structure: THEOCHEM, 464*(1–3), 211-226.

Udhayakala, P., Samuel, A. M., Rajendiran, T., & Gunasekaran, S. (2013). Theoretical assessment of corrosion inhibition performance of some pyridazine derivatives on mild steel. *Journal of Chemical and Pharmaceutical Research, 5*(8), 142-153.

Ulig, H. H. (1937). The solubilities of gases and surface tension. *Journal of Physical Chemistry, 41*(9), 1215-1226.

Verdolino, V. (2009). *New computational methods and developments for molecular response properties in condensed matter.* (Unpublished PhD). University of Parma, Parma, Italy.

Veszpremi, T., & Feher, M. (1999). *Quantum chemistry* Springer US.

Vosko, S. H., Wilk, L., & Nusair, M. (1980). Accurate spin-dependent electron liquid correlation energies for local spin density calculations: A critical analysis. *Canadian Journal of Physics, 58(8),* 1200-1211.

Whitfield, J. D. (2011). *At the intersection of quantum computing and quantum chemistry.* (Unpublished PhD). Harvard University, Cambridge, Massacchsetss.

Wu, Z., & Cohen, R. E. (2006). More accurate generalized gradient approximation for solids. *Phys. Rev., 73,* 2351161-2351166.

Chapter – 4

Reactivity and Binding Ability of Thiol Reagents[4]

4.1. Introduction

Rapid development of heavy metal bearing industries such as mining operations, electroplating facilities, power generation centres, electronic device manufacturing units, and tanneries has led to an increasingly significant discharge of heavy metals into the environment (Boddu, Abburi, Talbott, & Smith, 2003). Owing to their high solubility and non-biodegradable nature, heavy metals enter the food chain and tend to accumulate in living organisms (Barakat, 2011; Fu & Wang, 2011; Xu, Xie, & Xue, 2011). Many heavy metals including Cu, Pb, Zn, Ni, Cd, As and Cr are toxic and/or carcinogenic, leading to detrimental effect(s) on human physiology and other biological systems if ingested beyond the tolerance limit(s) (Babel & Kurniawan, 2004; Kurniawan, 2002). Therefore, heavy metal pollution is a great environmental concern, which is well reflected in increasingly stringent environmental regulations worldwide (Matlock, Henke, & Atwood, 2002).

Many remediation techniques have been used over the past few decades to deal with heavy metal contaminated wastewater, which include chemical precipitation (Charerntanyarak, 1999; Matlock et al., 2002; Ying & Fang, 2006), flotation (Medina, Torem, & de Mesquita, 2005; Waters, 1990; Yuan, Meng, Zeng, Fang, & Shi, 2008), ion exchange (Doula, 2009; S. Kang, Lee, Moon, & Kim, 2004), adsorption (K. C. Kang, Kim, Choi, & Kwon, 2008; Y. Li et al., 2010;

[4] This chapter has been prepared in context of use of chemical precipitating reagents to remove heavy metals from industrial wastewater streams. However, observations and findings are equally applicable to the flotation systems, all these reagents are important flotation collectors.

Wang, Zhou, Peng, Yu, & Yang, 2007), membrane separation (Landaburu-Aguirre, García, Pongrácz, & Keiski, 2009; Samper, Rodríguez, De la Rubia, & Prats, 2009), electrodialysis (Cifuentes, García, Arriagada, & Casas, 2009; Nataraj, Hosamani, & Aminabhavi, 2007), and electrochemical treatment (Valero & Ortiz, 2010). These methods along with their applicability, inherent advantages and limitations have been discussed in recent review articles (Barakat, 2011; Fu & Wang, 2011). Among these techniques, chemical precipitation is an effective and by far the most widely used process in the industry owing to its simplicity and lower capital costs (Fu & Wang, 2011; Ku & Jung, 2001).

Hydroxide and sulfide precipitation are the two most widely used chemical precipitation techniques (Marchioretto, Bruning, & Rulkens, 2002). Sulfide precipitation is generally more efficient than the hydroxide scheme as metal sulfides typically have lower solubility. Sulfide precipitation process is also far less pH sensitive as sulfide precipitates are not amphoteric, in contrast to the metal hydroxides (Fu & Wang, 2011). Moreover, sulfide precipitation is less influenced by the presence of complexing and/or chelating agents. The metal-sulfide sludge often exhibits better thickening and dewatering characteristics (Whang, Young, & Pressman, 1982). However, sulfide precipitation could lead to formation of toxic hydrogen sulfide gas if it is carried out under acidic conditions. The potential formation of toxic H_2S gas is the major limitation associated with this process along with concerns on the toxicity of sulfide due to reagent overdose, which often calls for post-treatment.

Constrained by limitations of conventional chemical precipitation processes and stringent environmental regulations, the industry has moved to chemicals that act to chelate heavy metals in aqueous systems and precipitate them as metal chelates (Fu & Wang, 2011; Matlock et al., 2002). Numerous studies have evaluated the application and performance of commonly available

chelating reagents as heavy metal precipitants. Among these, dithiocarbamate and its derivatives are the most popular and have been the focus of many investigations. Simple dithiocarbamate compounds such as dialkyl dithiocarbamate containing single chelating site (Fu, Chen, & Xiong, 2007; Matlock et al., 2002; Wing & Rayford, 1982) as well as super molecular precipitants such as sodium 1,3,5-hexahydrotriazinedithiocarbamate (HTDC) (Fu et al., 2007) and N,N-bis-(dithiocarboxy)piperazine (BDP) (Fu et al., 2007) offering multiple chelating centres have been tested, and found to be very effective for heavy metal removal from waste waters. Many researchers have also developed dithiocarbamate anchored polymer composites, and have reported excellent removal efficiency with enhanced settling characteristics of the resultant precipitates (Roy, Rawat, Chaoudhary, & Rai, 2004; Say, Birlik, Denizli, & Ersöz, 2006). Similarly, precipitants based on xanthate functional group have been found effective for removing heavy metals from contaminated water streams (Q. Chang & Wang, 2007; Y. Chang, Chang, & Chiang, 2003; Liang, Guo, Feng, & Tian, 2010; Tare & Chaudhari, 1987; Wing, Doane, & Russell, 1975; Zhu, Hu, & Wang, 2012).

Apart from xanthate and dithiocarbamate derivatives, many other compounds, mainly containing sulfur, nitrogen, and/or oxygen atoms at the binding sites have also been tested. Ying and Fang (2006) employed dipropyl-dithiophosphate to remove Pb, Cd, Cu, and Hg up to 99.9% at pH 3-6. In a separate investigation, butyl dithiophosphate was reported to remove Cu, Pb and Cd up to over 99% at a similar pH range (Xu et al., 2011). Matlock et al. (2002) demonstrated that the two commonly used commercial reagents, trimercaptotriazine (TMT) and sodium thiocarbonate (STC) fail to remove Cd, Cu, Fe, Pb, and Hg below the minimum required concentrations. Additionally, the precipitates formed were unstable and decomposed overtime to produce toxic substances. Same research group designed and developed DTPY (a pyridine-based

thiol compound) and $BDET^{2-}$ (1,3-benzenediamidoethanethiol), two thiol based multi-dentate ligands and found them to be very effective for removal of Cu/Cd and Hg/Pb, respectively (Blue, Jana, & Atwood, 2010; Matlock, Howerton, Henke, & Atwood, 2001; Matlock, Howerton, & Atwood, 2001).

Majority of the chelating ligands used in the industry, however, were not designed specifically for wastewater treatment. They made their way as they were effective in other fields demanding similar characteristics. For example, xanthate and dithiocarbamate reagents were first used to float sulfide mineral ores in the mineral processing industry. These reagents offer very limited metal selectivity, and very often lack the necessary binding sites capable of meeting the stringent requirements (Fu & Wang, 2011; Matlock et al., 2002). As a consequence, these reagents require very high dosages and may release toxic by-products during the decomposition process of the treated water (Fu & Wang, 2011; Henke, 1998; Matlock et al., 2002). Fu and Wang (2011) in their recent review article have emphasized the need of developing new reagents offering better metal selectivity and enhanced chelating capability. Binding capability and selectivity of such reagents are determined largely by the structural/stereochemical compatibility between the reagent molecules and heavy metal ions. Therefore, better reagents can be designed by framing structural criteria to make them metal selective. These criteria can be developed, by establishing a structure-function relationship between the existing reagents and different metal ions. Computational chemistry is a perfect tool for such tasks.

Computational chemistry methods are valuable tools for understanding the complex chemical systems and prediction of their physiochemical properties (H. Yekeler & Yekeler, 2004). The density functional theory (DFT) and molecular dynamics (MD) simulation are among the powerful techniques to model the interactions between two or more chemical species. Modeling

the interactions between existing reagents and heavy metal ions can be useful in establishing a relationship between molecular structure of reagent and its reactivity and binding capability with different metal ions. Based on these relationships structural criteria for metal selective reagents could be framed. A number of possible choices of reagents can then be designed and evaluated for a given metal in a short time.

In light of the above discussion, this study represents an attempt to understand the influence of structure of some simple anionic chelating reagents on their reactivity and their interactions with divalent cations such as Cu, Pb and Zn. Starting with a simple compound viz. an alkyl carboxylate, the head group and substituent group were gradually modified to cover important reagent classes, such as dithiocarboxylates, dithiocarbonates (xanthates), trithiocarbonates, dithiocarbamates and dithiophosphates. In the past, Porento and Hirva (2002) reported a similar study. However, they considered the formation of metal-reagent complexes of MX type (M: metal, X: reagent ligand) in vacuum, while the relevant precipitation reactions occur in the aqueous phase. In the current work MX_2 type binding in the aqueous solution phase is considered, addressing the formation of MX_2 type metal-reagent complexes reported in a number of experimental investigations (M. C. Fuerstenau, Clifford, & Kuhn, 1974; M. C. Fuerstenau & Han, 2002; Hellstrom, Oblatt, Fredriksson, & Holmgren, 2006).

4.2. Methodology

4.2.1. Computational Methods

All calculations were carried out using Gaussian 09 software package (Frisch et al., 2009). We used a three-parameter hybrid functional (B3LYP), originally devised by Becke (1993a) and later modified by Stephens *et al* (1994). The B3LYP functional combines the Becke's gradient-

corrected exchange functional (Becke, 1988) and Lee-Yang-Parr (Lee, Yang, & Parr, 1988a) and Vosko-Wilk-Nusair (Vosko, Wilk, & Nusair, 1980a) correlation functionals. The 6-311++G (3df,3pd) basis set was employed for all elements except Pb, Cu and Zn for which Stuggart-Dresden triple zeta effective core potentials (SDD) (Andrae, Haeussermann, Dolg, Stoll, & Preuss, 1990; Dolg, Wedig, Stoll, & Preuss, 1987) were used. The selection basis for this functional and basis set(s) combinations has been already discussed in section 3.8. Furthermore, the B3LYP functional has been used in many studies relating to transition metal complexes (Billes, Holmgren, & Mikosch, 2010; Rulisek & Havlas, 2000). Importance of solvent-mediated chemical reaction was realized by modeling the interactions in a self-consistent reaction field using Polarizable continuum model (PCM) (Miertus, Scrocco, & Tomasi, 1981), which has already been discussed in section 3.8 (solvent: water, dielectric constant = 78.36, T = 298 K).

4.2.2. Geometry Optimization and Vibrational Analysis

Optimization of molecular geometry is the most important step in a computational chemistry study, as the calculated parameters are dependent on the resultant geometry. Various conformations and configurations of different reagent ions and their resulting complexes with Pb(II), Cu(II) and Zn(II) metal ions were fully optimized to obtain their final geometries. Among various possible structures of a given molecule, the one with the lowest energy was selected for further evaluation. Rotational, translational, and vibrational frequencies were computed at the same level of theory for the geometrically optimized molecules. It was observed that a tight convergence criterion using ultrafine grid was necessary to keep the rotational and translational modes within the desired range (±10 cm^{-1}) for some of the structures. Absence of any imaginary frequencies in the vibrational spectra confirmed that the optimized molecules correspond to the global minimum on their corresponding potential energy surfaces. To validate the modeled

complexes, calculated vibrational spectra of the molecules were compared with the experimental spectra reported in open literature.

4.2.3. Chemical Reactivity

In order to elucidate detailed information about reactivity of individual reagent molecules towards different metal ions in water, popular chemical reactivity indices, including dipole moment (D), electronic chemical potential (μ) (R. Parr, Donnelly, Levy, & Palke, 1978; R. G. Parr & Pearson, 1983) , absolute chemical hardness (η) (R. G. Parr & Pearson, 1983; Pearson, 1992), and global electrophilicity index (ω) (R. G. Parr, Szentpaly, & Liu, 1999) were used.

Dipole moment is a useful indicator of interactions between two chemical species in a reaction medium. Reagent molecules with large dipole moment interact strongly with metal ions in aqueous solutions via strong van der Waals interactions (Liu et al., 2012). Electronic chemical potential and absolute chemical hardness are global reactivity descriptors defined as the first and second order partial derivative of the energy, E', with respect to the number of electrons, N, at constant external potential, $v(\vec{r})$ (Pearson, 1988; Pearson, 1992):

$$\mu = \left(\frac{\partial E\prime}{\partial N}\right)_{v(\vec{r})}, \eta = \frac{1}{2}\left(\frac{\partial \mu}{\partial N}\right)_{v(\vec{r})} \qquad (4.1, 4.2)$$

Physically, μ describes the escaping tendency of electrons from an equilibrium system, while η measures the resistance of a molecule to undergo any change in the electron distribution or charge transfer. Following the Koopmans' approximation (Koopmans, 1934), μ and η can be expressed in terms of frontier orbital energies as,

$$\mu = \frac{(E_{HOMO}+E_{LUMO})}{2}, \eta = \frac{(E_{LUMO}-E_{HOMO})}{2} \qquad (4.3, 4.4)$$

where E_{HOMO} and E_{LUMO} are the orbital energies of the highest occupied molecular orbital (HOMO) and lowest unoccupied molecular orbital (LUMO) of the N electron system. μ and η are key indicators of the stability and overall reactivity of a chemical system. They are the most fundamental descriptors of charge transfer between two (or more) chemical systems during a chemical reaction. Two chemical systems when interact with each other, work towards equalization of chemical potential through electron transfer from the system of higher chemical potential to that of lower chemical potential (Pearson, 1988). The difference in chemical potentials drives this transfer while individual hardness parameters act as a resistance (Pearson, 1988).

Chemical potential is a useful indicator of whether a chemical species has electrophile or nucleophile nature. However, μ alone cannot be used as a measure of its electrophilicity or nucleophilicity. As Ayers and Parr (2008a; 2008b) pointed out, a molecule with low chemical potential, though a good electrophile could still have bad electrophilicity if it has a large value of chemical hardness. Thus, a measure of molecular electrophilicity or nucleophilicity should incorporate both the chemical potential and the chemical hardness.

Parr *et al*. (1999) introduced a new global reactivity descriptor, global electrophilicity index (ω), for chemical species that depends on both μ and η. The electrophilicity index is a measure of the stabilization in energy when a chemical system acquires an additional electronic charge ΔN from the environment. Thus, ω physically signifies the propensity or capacity of a chemical species to accept electrons. It allows a quantitative classification of the global electrophilic or nucleophilic nature of a molecule on a relative scale. ω is defined as:

$$\omega = \frac{\mu^2}{2\eta} \tag{4.5}$$

μ, η, and ω, useful quantitative descriptors for the stability, chemical reactivity and electrophilicity/nucleophilicity of atoms or molecules as a whole, were used in this study to evaluate the relative reactivity of different reagent ions under consideration.

4.2.4. Ligands and Metal Species

In this study, reactivity of eight different organic reagents, including carboxylate (E-CO_2^-), monothiocarboxylate (E-COS^-), dithiocarboxylate (E-CS_2^-), xanthate (EO-CS_2^-), trithiocarbonate (ES-CS_2^-), alkyldithiocarbamate (EHN-CS_2^-), dialkyldithiocarbamate (E_2N-CS_2^-), and alkyldithiophosphate (EHO_2-PS_2^-), was explored using theoretical methods. In addition, their complexes with three heavy metal ions (Cu^{2+}, Zn^{2+}, and Pb^{2+}) was modeled and interaction energy for these complexes was calculated to explore the trend in metal affinities. The length of hydrocarbon tail was kept fixed as ethyl for all the organic reagents.

4.2.5. Binding Strength of Metal-Ligand Complexes

The interaction energy of different metal-ligand complexes was calculated as change in Gibbs free energies during the complex formation using Equation 4,

$$I.E = \Delta G_r\,(298K) = \sum(E_0 + G_{corr})_{products} - \sum(E_0 + G_{corr})_{reactants} \qquad (4.6)$$

where $I.E$ is the binding energy of the resultant complex, E_0 and G_{corr} are the electronic energy and the thermal correction to Gibbs free energy of the molecule, respectively.

4.3. Results and Discussion

4.3.1. Geometries

4.3.1.1. Reagents Ions

Sodium and potassium salts of thiol type reagents ionize in aqueous solutions owing to their ionic character (Boddu et al., 2003; Fu & Wang, 2011). Selected optimized geometrical parameters for negatively charged ligand ions are listed in Table 4.1. As seen from the data, bond lengths of two C-Y (or P-Y) bonds in $E–CS_2^-$, $E_2N–CS_2^-$, and $EHO_2–PS_2^-$ are similar while those of the other ligand ions are not. Authors of a previous study reported two equivalent P-S bonds in $(MeO)_2PS_2^-$ (Shaoyi et al., 1996). Calculated values for xanthate and dithiocarbamates anions are in good agreement with their reported experimental values (Coucouvanis, 1970; Tiekink & Winter, 2011). For example, experimental values for ∠S-C-S = 124°, r(C-O) = 1.35 Å, r(C-S) = 1.67 and 1.70 Å match closely with the calculated values 125.732°, 1.3477, 1.6959 and 1.7054 Å respectively. Nearly equal values for two C-Y or P-Y bonds (except in $E–COS^-$) suggest strong electron delocalization over the CS_2^- (or PS_2^- or CO_2^-) head group, and indicate toward bi-dentate bonding with metal ions. This is further supported by the observation that the calculated values for various C-S bonds lie between the standard single and double r(C-S) bond lengths of 1.82 and 1.60 Å respectively. Similarly, P-S and C-O bond lengths (in PS_2^- or CO_2^- head groups) are close to their standard double bond lengths of 1.94 and 1.21 Å respectively, thus indicating strong presence of double bond character. In $E–COS^-$, a shorter C-O bond length (more double bond character) and longer C-S bond length (more single bond character) than in $E–CO_2^-$ and $E–CS_2^-$ suggest that O competes more effectively than S for π-bond strength due to its higher

electronegativity. This results in less electron delocalization over $–COS^-$ head group, and thus indicates the preference towards mono-dentate binding through S atom.

Table 4.1. Selected optimized geometrical parameters for different anionic ligands: bond lengths (r) in angstrom (Å) and bond angles (∠) in degree (°)

Ligand ion	r(C-Y1) or r(P-Y1)[a]	r(C-Y2) or r(P-Y2)[a]	r(C-X)[b] or r(P-O)	∠O-C-O or ∠O-C-S or ∠S-C-S or ∠S-P-S
$E–CO_2^-$	1.2565	1.2608	1.5447	125.808
$E–COS^-$	1.2305[c]	1.7497[c]	1.5331	124.187
$E–CS_2^-$	1.6944	1.6945	1.5218	125.135
$EO–CS_2^-$	1.6959	1.7054	1.3477	125.732
$ES–CS_2^-$	1.6856	1.7024	1.7702	126.536
$ENH–CS_2^-$	1.7166	1.7301	1.3470	123.464
$E_2N–CS_2^-$	1.7317	1.7317	1.3561	120.149
$EHO_2–PS_2^-$	1.9912	1.9913	1.6173, 1.6285	117.493

[a] Y=O or S atom

[b] X: heteroatom bonded to $–CS_2^-$ (C, O, S or N)

[c] r(C-O) = 1.2305 Å and r(C-S) = 1.7497 Å

For dithiocarbamates, calculated values of C-N bond lengths (1.3470, 1.3561 Å) are much closer to the standard C-N double bond (1.38 Å) than to C-N single bond (1.47 Å), which indicate presence of strong double bond character and participation of C-N bond in electron delocalization with $-CS_2^-$ head group. All the bonds at the N center lie in the same plane as $-CS_2^-$ group. NBO analysis shows that the three σ-binding orbitals of N atom in dithiocarbamates are sp^2 hybridized and the lone pair has 100% p-character. Consistent with a previous study (Fu & Wang, 2011), C-N bond length is shorter in $ENH–CS_2^-$ than in $E_2N–CS_2^-$ as N atom in $E_2NH–CS_2^-$ has more negative charge. Hybridization of O atom in xanthate is also close to sp^2; the two σ-binding orbitals are $sp^{2.24}$ and $sp^{2.26}$ hybridized, and one lone pair has $sp^{1.60}$ hybridization. The second lone pair has 100% p-character and lies perpendicular to molecular plane. This suggests

presence of similar type of conjugative effects in xanthate as observed for dithiocarbamates. Evidently, C-O bond length (1.3477 Å) in xanthate lies between standard single and double C-O bond lengths of 1.43 and 1.21 Å respectively. Less double bond character of C-O bond compared to C-N bond can be explained in terms of higher electronegativity of O atom. The electronegativity of S heteroatom in trithiocarbonate is least among the three (O, N and S), so superior conjugation effects are expected. However, the C-S bond length (1.7702 Å) in trithiocarbonates (where S is the heteroatom) is very close to the standard single C-S bond (1.82 Å), suggesting weak conjugation. NBO analysis shows that the two lone pair orbitals of S atom in trithiocarbonate have ~ $sp^{1.5}$ and ~sp^{8} hybridization and two σ-binding orbitals are ~ $sp^{4.5}$ hybridized. Absence of a 100% p-character lone pair (and, thus a lone pair not perpendicular to the molecular plane) and difference in size of the overlapping orbitals (3p for sulfur and 2p for carbon atom) explain the weaker conjugative effects. The P-O bonds in dithiophosphate do not participate in conjugation as the $-PS_2$ and $-PO_2$ groups lie in different planes. This observation is well reflected in the calculated P-O bond lengths (1.6173, 1.6285 Å) which are very close to the standard single P-O bond length of 1.63 Å. The extent of conjugation between the lone pair orbital of the heteroatom and $-CS_2^-$ ($-PS_2^-$) head group is also reflected in trend observed for C-Y bond lengths.

4.3.1.2. Metal-ligand Complexes

The optimized geometrical structures for different metal-ligand complexes are shown in Figure 4.1. For a given metal, complexes of dithiocarboxylate, xanthate, trithiocarbonate, alkyldithiocarbamate, and dialkyldithiocarbamate have similar structures. Therefore, only alkyldithiocarbamate complexes are shown to represent these complexes collectively. Selected

optimized geometrical parameters for different metal-ligand complexes are tabulated in Table 4.2.

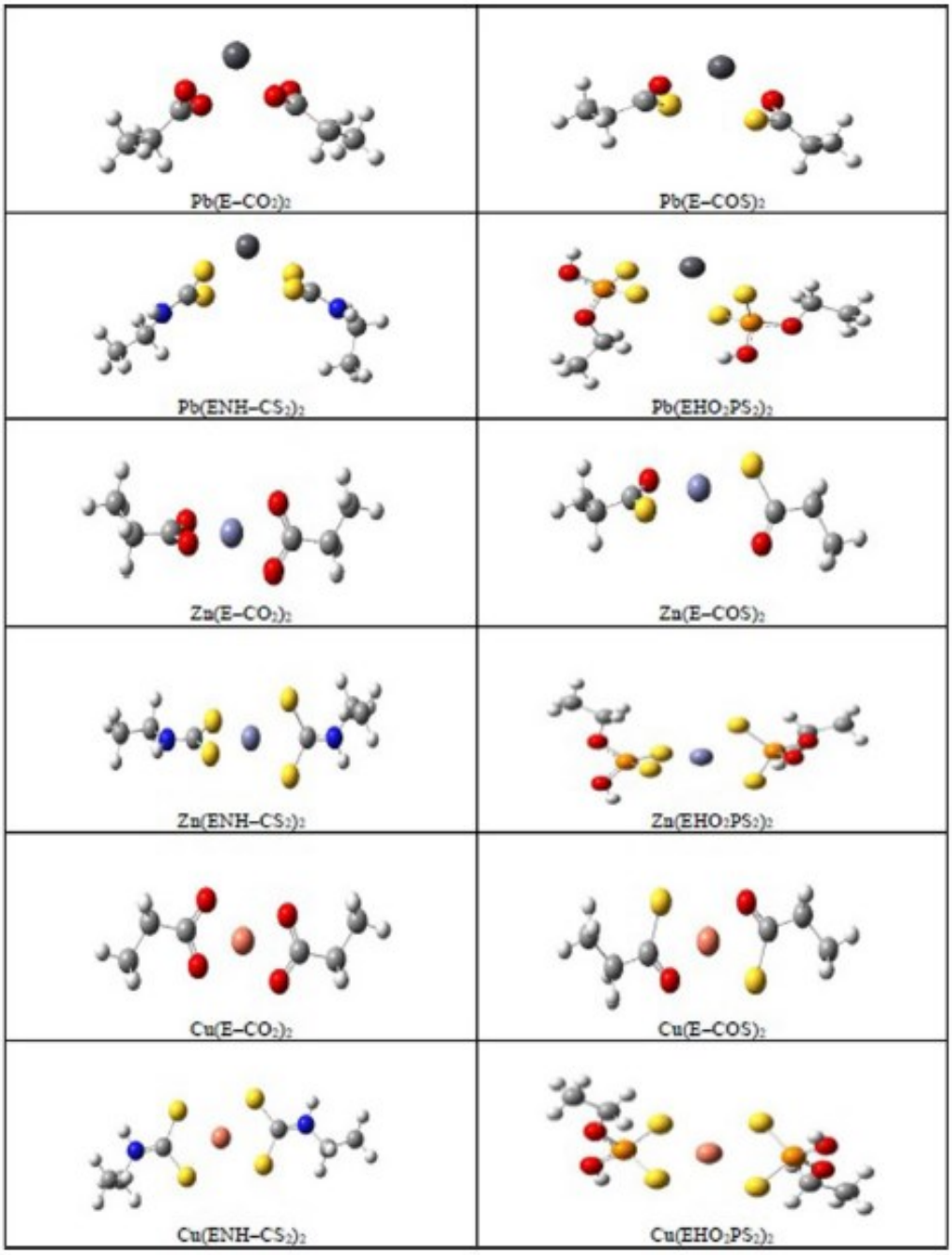

Figure 4.1. Optimized geometries of selected metal-ligand complexes in water. Water was modeled using the polarizable continuum model. E: ethyl. Color code: Red = O, Yellow = S, Blue = N, Grey = C, White = H, Black = Pb, Light blue = Zn, Pink = Cu).

All Pb complexes have a hemidirected or distorted square pyramid structure around the Pb atom. Each of the complexes is of non-planar asymmetric, although each coordinating sub branch is almost planar except alkyldithiophosphate, owing to tetrahedral geometry at P atom. The two complexing ligands in each of the complexes are symmetrically placed across the Pb atom except in $Pb(ENH–CS_2)_2$ and $Pb(EHO_2–PS_2^-)_2$ which bind to the Pb atom in a bidentate fashion, with two different M-Y bond lengths which differ by ~0.15-0.20 Å. Four M-Y bond lengths in $Pb(ENH–CS_2)_2$ and $Pb(EHO_2–PS_2^-)_2$ are all different from each other. However, they form two pairs with a difference of ~0.20 Å, where the shorter and longer bond lengths within each pair differ by only ~ 0.01 Å which could be treated negligible. Data reported for $Pb(EO–CS_2)_2$ and $Pb(E_2N–CS_2)_2$ complexes correlates well with previous theoretical investigations on the same compounds (Coucouvanis, 1970; Ghosh, Bagchi, & Das, 2011). Computational studies on structures of remaining Pb complexes were not found in the literature.

In all Zn complexes except $Zn(E–COS)_2$, the ligands bind to Zn atom in a bidentate manner such that two Y_2M planes are perpendicular to each other, thus forming a tetrahedral or slightly distorted tetrahedral structure around the Zn atom. Tetrahedral geometry of these ligands around the Zn center has been reported in various experimental and theoretical investigations, e.g., xanthate (Ikeda & Hagihara, 1966), dialkyldithiocarbamate (Costa Jr., Ondar et al., 2013), and dialkyldithiophosphate (Billes et al., 2010). The geometrical parameters calculated in this study match closely with those of the past investigations (Billes et al., 2010; Costa Jr. et al., 2013). In the case of $Zn(E–COS)_2$, S atoms lie in the same plane as Zn and one of the O atom, while the second O atom lies outside this plane, thus distorting the tetrahedral symmetry around the Zn center.

Table 4.2. Selected optimized geometrical parameters for different metal-ligand complexes: bond lengths (r) in angstrom (Å) and bond angles (∠) in degree (°).

Metal complex	r(M-Y)[1]	r(C-Y) or r(P-Y)[1]	r(C-X)[2] or r(P-O)	∠Y-Pb-Y	∠Y-C-Y or ∠Y-P-Y
$Pb(E–CO_2)_2$	2.3811, 2.5334	1.2777, 1.2568	1.5130	53.148	120.705
$Pb(E–COS)_2$	2.6048[3], 2.7657[4]	1.2391[3] , 1.7450[4]	1.5124	57.930	120.634
$Pb(E–CS_2)_2$	2.7816, 2.9972	1.7032, 1.6805	1.5096	61.690	122.671
$Pb(EO–CS_2)_2$	2.7869, 2.9868	1.7158, 1.6977	1.3193	62.607	123.341
$Pb(ES–CS_2)_2$	2.7960, 2.9909	1.7062, 1.6972	1.7355	62.160	123.077
$Pb(ENH–CS_2)_2$	2.7814, 2.9823, 2.7775, 2.9782	1.7303, 1.7203, 1.7328, 1.7206	1.3289, 1.3297	62.938, 62.915	121.710, 121.197
$Pb(E_2N–CS_2)_2$	2.7667, 2.9674	1.7456, 1.7244	1.3361	62.670	118.807
$Pb(EHO_2PS_2)_2$	2.8007, 3.0349, 2.8020, 3.0401	2.0278, 1.9929	1.6035, 1.5899	70.133, 70.015	113.276, 113.218
$Zn(E–CO_2)_2$	2.079, 2.0913, 2.0631, 2.113	1.2713, 1.2659, 1.2704, 1.2665	1.5085	63.146, 63.223	119.119, 119.001
$Zn(E–COS)_2$	3.1335[3], 2.2542[4]	1.7897[3], 1.2116[4]	1.5204	56.476, 56.433	123.941
$Zn(E–CS_2)_2$	2.423, 2.5059, 2.4611, 2.4363	1.6906, 1.698, 1.7003, 1.687	1.5087, 1.5095	73.597, 73.051	119.935, 120.057
$Zn(EO–CS_2)_2$	2.4128, 2.4756	1.7152, 1.704	1.3125	74.952	120.913
$Zn(ES–CS_2)_2$	2.4291, 2.4777	1.7126, 1.6964	1.7278	74.203	120.533
$Zn(ENH–CS_2)_2$	2.4255, 2.4319, 2.4255, 2.4363	1.7266, 1.7325, 1.7233, 1.7323	1.3246, 1.3252	75.644, 75.570	118.798, 119.09
$Zn(E_2N–CS_2)_2$	2.4089, 2.4345	1.7401, 1.7363	1.3302	75.375	116.811
$Zn(EHO_2PS_2)_2$	2.4486, 2.4768, 2.435, 2.4685	2.0194, 2.0134, 2.0139, 2.0171	1.5868, 1.5999	84.283, 84.745	110.141, 110.066
$Cu(E–CO_2)_2$	1.9974, 1.9968	1.2702, 1.2706	1.4994	65.915	116.804
$Cu(E–COS)_2$	2.0078[3], 2.3506[4]	1.26[3], 1.7194[4]	1.5011	70.794	116.122
$Cu(E–CS_2)_2$	2.3733, 2.3733	1.6905, 1.6905	1.4986	74.622	116.638
$Cu(EO–CS_2)_2$	2.3521, 2.3524	1.7057, 1.7056	1.3056	76.222	117.475
$Cu(ES–CS_2)_2$	2.3662, 2.3669	1.6988, 1.6985	1.7171	75.569	116.625
$Cu(ENH–CS_2)_2$	2.3569, 2.3550, 2.3567, 2.3585	1.7262, 1.7218, 1.7262, 1.7191	1.3203, 1.3205	76.253	115.056, 115.3
$Cu(E_2N–CS_2)_2$	2.3484, 2.3487	1.7321, 1.7317	1.3249	76.104	113.399
$Cu(EHO_2PS_2)_2$	2.3745, 2.3749, 2.3749, 2.3743	2.0108, 2.0106	1.5827, 1.5963	85.319	106.318

[1] Y=O or S atom

[2] X: heteroatom bonded to $–CS_2^-$ (C, O, S or N)

[3,4] Bond lengths involve O and S atoms, respectively

All copper complexes investigated in this study have square planar geometry around the Cu center. The ligands bind to the Cu atom with two Y-M bonds which are almost equal in length expect in $Cu(E–COS)_2$ where two Y atoms are different. Square planar geometry of the basic $–CS_4–$ moiety has been reported in past for Copper (II) dialkyldithiocarbamates (Ngo, Banger, DelaRosa, Toscano, & Welch, 2003)and Copper (II) xanthates (Ivanov, Bredyuk, Antzutkin, & Forsling, 2004).

The reason for the structural differences in these complexes essentially lies in the difference in the electronic structures of three metal ions. Complexes of Cu are square planar with predominant localization of the unpaired d-electron in Cu^{2+} ion ($Ar3d^9$), thus resulting in dsp^2 hybridization (Ivanov et al., 2004). The Zn^{2+} ion ($Ar3d^{10}$) receives two electrons from each of the four Y atoms (where Y= S or O) which are accommodated by the sp^3 hybrid orbitals at the Zn center (Billes et al., 2010). This sp^3 hybridization results in tetrahedral geometry. The hemidirected structures of Pb(II) complexes with anionic ligands and low coordination numbers (2-5) are well documented in literature. The origin of hemidirected geometry has been explained through Pb lone pair–ligands repulsion (Shimoni-Livny, Glusker, & Bock, 1998) or through mutual interactions between less-symmetric ligands which are further augmented by the influence of Pb lone pair electrons on Pb–Ligand bond orbital hybridization (Breza, Bučinský, Šoralová, & Biskupič, 2010).

In Pb and Zn complexes, the two C-Y or P-Y bonds (where Y = S or O) in each of the individual ligand are also different in length by 0.01-0.02 Å, where the longer bond corresponds to the Y atom closer to the metal atom. In Cu complexes, these bonds are almost equal as expected. In monothiocarboxylate complexes, the C-O bond length is shorter than their carboxylate counterpart, while C-S bond length is larger than dithiocarboxylate. This finding

indicates the preference of metal atom to bind strongly to S atom over O atom, owing to smaller difference in sizes, and suggests unidentate binding. This difference is largest in $Zn(E–COS)_2$, followed by $Pb(E–COS)_2$ and $Cu(E–COS)_2$. The C-O bond length in $Zn(E–COS)_2$ is very close to standard double C-O bond of 1.21 Å, while the C-S bond length is close to standard single C-S bond length, which strongly indicates unidentate binding mode. This proposed coordination is further supported by a large distance between Zn and O atoms. In this study, a decrease in different C-X (or P-O) bond lengths is noticed when the anionic ligands formed chelates with metal ions. In a previous experimental study, shortening in C-O bond length was observed when xanthate ions formed complexes with metals (Leppinen, 1990). A decrease in C-X bond length during complexation was also documented in previous theoretical investigations (Porento & Hirva, 2002; Tossell & Vaughan, 1993).

4.3.2. Reactivity of Reagent Molecules and their Binding with Metal Ions

For the simplicity of presentation and better understanding, this section is divided into two sub-sections. First we discuss the influence of the substitution of oxygen atom(s) by sulphur atom(s) in the carboxylate head group on its reactivity and binding ability with different metal ions. Followed by that the effect of different substituent groups attached to dithiocarboxylate head group on its reactivity and binding capacity is discussed.

4.3.2.1. Effect of Thio-substitution in Carboxylate Head Group

Keeping the alkyl (ethyl) group fixed, O atom(s) in carboxylate head group was (were) substituted by S atom(s) to explore the reactivity and binding ability of carboxylate ($ECOO^-$), monothiocarboxylate ($ECOS^-$) and dithiocarboxylate ($ECSS^-$) type organic reagents.

Computed values of different global reactivity descriptors (μ, η and ω) for these reagents are given in Table 4.3, along with their dipole moments and HOMO and LUMO energies. Dipole moments of these organic molecules are determined by the partial charges, bond lengths and bond angles between atoms comprising the head group. As expected, dipole moment of dithiocarboxylate is smaller than the carboxylate reagent as the sulphur atoms have low partial charges due to their lower electronegativity as compared to oxygen atoms. In the case of monothiocarboxylate ions, the effect of decreasing partial charges is counterbalanced by a longer C-S bond length, thus resulting in the highest dipole moment value among the three.

Table 4.3. Dipole moment, energy of frontier molecular orbitals and global chemical reactivity indices for carboxylate, monothiocarboxylate and dithiocarboxylate organic reagents.

Ligand ion	D (Debye)	HOMO (a.u[a])	LUMO (a.u)	μ (a.u)	η (a.u)	ω (a.u)
Ethylcarboxylate ($ECOO^-$)	7.51	-0.2233	-0.0014	-0.1123	0.1109	0.0568
Ethylmonothiocarboxylate ($ECOS^-$)	7.69	-0.1994	-0.0036	-0.1015	0.0979	0.0526
Ethyldithiocarboxylate ($ECSS^-$)	6.30	-0.1936	-0.0532	-0.1234	0.0702	0.1084

[a]1 atomic unit (a.u) = 627.509 $kcal.mol^{-1}$

The computed η values of $ECOO^-$> $ECOS^-$> $ECSS^-$ suggest that the reactivity of the head group increases with the replacement of oxygen atom(s) by sulphur. The decreasing μ values ($ECOS^-$ > $ECOO^-$ > $ECSS^-$) and increasing ω values ($ECOS^-$ < $ECOO^-$ < $ECSS^-$) indicate that the monothiocarboxylate reagents are the strongest nucleophiles, followed by carboxylate reagents. It is interesting to note that the reactivity order is the same as the order of the dipole moment ($ECOS^-$ > $ECOO^-$ > $ECSS^-$). However, it is noteworthy to mention that the most commonly utilized reagents in heavy metal chemical precipitation as well as collectors in sulfide flotation are based on dithiocarboxylate head groups and not on monothiocarboxylates or carboxylates.

In order to further explore the effect of thio substitution on the reactivity and binding ability of the carboxylate head groups towards heavy metal ions in solution, metal-complexes of these three reagents with Pb^{2+}, Cu^{2+} and Zn^{2+} ions were modeled. Binding of ligand ions to base metal ions in heavy metal laden waste water is usually affected by a number of other factors, including the presence of other metal species in the solution (Coetzer, du Preez, & Bredenhann, 2003; Ikumapayi, Makitalo, Johansson, & Rao, 2012). These metal ions enter the system through different sources such as the addition of the reagents, recycle of process water, and dissolution of minerals. To represent such species and to investigate the reasons behind the use of dithiocarboxylate based reagents in heavy metal extraction and sulphide mineral flotation practice, non-toxic metal species, Mg and Ca ions were also included in this part of the analysis. Interaction energies of different complexes were calculated using Equation 4 and plotted in Figure 4.2.

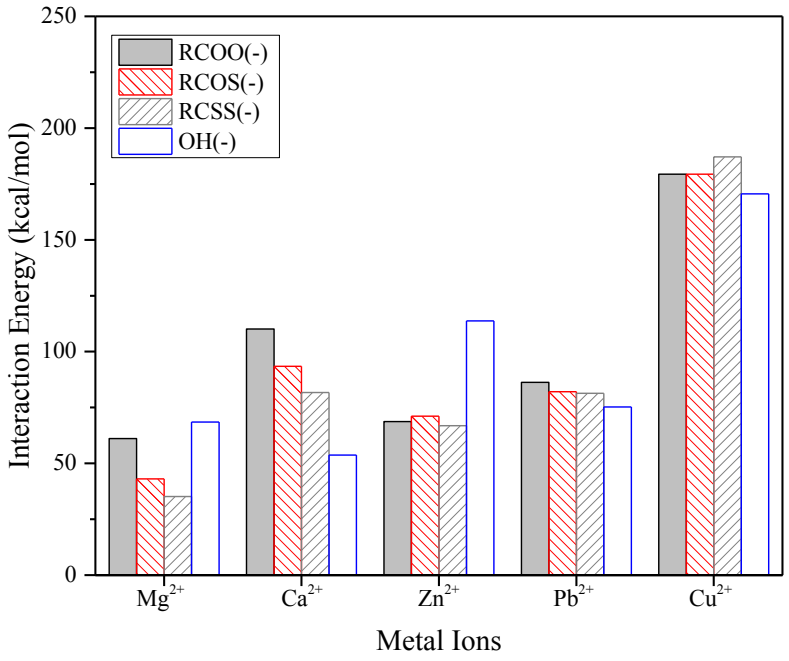

Figure 4.2. Interaction energies of alkyl carboxylate, alkyl monothiocarboxylate, alkyl dithiocarboxylate, and hydroxide ions with different metal ions in solution (R: ethyl).

Among the heavy metal ions studied as shown in Figure 4.2, all three reagents bind much more strongly to Cu than to any other divalent cations. Such finding is in excellent agreement with the fact that these reagents are good collectors for selective flotation of copper sulfide minerals (D. W. Fuerstenau, 1982). This selectivity of binding is also critical if the valuable copper ions in the waste water are to be recovered as a value-added product. Furthermore such selective binding will reduce the consumption of the reagents as they are preferentially consumed by binding with the valuable copper ions. Also evident from Figure 4.2 is that thio substitution in carboxylate head group has a minimal effect on its binding capability with heavy metal ions, as binding energy does not change with the thio substitution. However, for Mg and Ca ions, binding strength decreases with increasing degree of thio substitution in the carboxylate head group. The binding strength of dithiocarboxylate head group towards Ca ion was found to

be slightly higher than Pb and Zn. The stability constants for these complexes could not be found in literature for comparison. However, decrease in galena recovery using xanthate collector in the presence of Ca ions around neutral pH was reported earlier in an experimental study (Ikumapayi et al., 2012), and was attributed to adsorption of calcium xanthate species formed in the bulk solution on mineral surface.

Hydroxide ions present in the solution compete with these organic ligands to form metal complexes. A particular metal-ligand complex will be precipitated only if its solubility product is lower than the solubility product of the corresponding metal hydroxide precipitates. Therefore, the preferential precipitation of heavy metals cannot be predicted correctly without considering the formation of metal hydroxide complexes. To address this issue, metal hydroxide complexes of $M(OH)_2$ type were modeled and corresponding interaction energies are also plotted in Figure 4.2. As evident from the plot, only Ca, Pb and Cu ions can be removed from water using thiol type organic reagents at equal concentrations of organic ligands and hydroxide ions which are determined by pH. As reported in literature the order of the stability products of different metal hydroxides under consideration is as follows: Cu < Zn < Pb < Mg < Ca, which is opposite to the order of their calculated interaction energies (Euler, 2006; D. W. Fuerstenau, 1982).

4.3.2.2. Effect of side groups

To investigate the effect of the side group linked directly to the dithiocarboxylate head group ($-CS_2^-$) on its reactivity and binding affinity towards Pb, Cu and Zn metal ions, ethyl chain (E-) in ethyl dithiocarboxylate ($E-CS_2^-$) was replaced by EO-, ES-, ENH- and E_2N-. Collectively these four side groups represent the most commonly used reagents of $-CS_2^-$ head group, namely, xanthates, trithiocarbonates, alkyl dithiocarbamates and dialkyl dithiocarbamates. In addition, dithiophosphates ($EHO_2-PS_2^-$) were also included in the study as they represent another

important class of reagents and their binding properties closely resemble the reagents of the $-CS_2^-$ moiety. To ensure that the calculated reactivity indices and interaction energies are not influenced by the length and conformation of the alkyl tail, same alkyl chain (ethyl) was persisted with all the reagents. The calculated values of D, HOMO and LUMO energies, μ, η, and ω for different ligand ions are given in Table 4.4. The calculated values of dipole moment suggest that dithiocarbamate would be the first to interact with metal ions in solution due to their strong intermolecular forces, whereas dithiophosphate would be the last. Values of η suggest that alkyldithiophosphate is chemically the most stable, followed by dithiocarbamates, xanthate, trithiocarbonate and dithiocarboxylate.

Table 4.4. Dipole moment, energy of frontier molecular orbitals and global chemical reactivity indices for different ligand ions under consideration.

Ligand ion	D	HOMO (a.u)	LUMO (a.u)	μ (a.u)	η (a.u)	ω (a.u)
Ethylcarboxylate ($E–CS_2^-$)	6.30	-0.1936	-0.0532	-0.1234	0.0702	0.1084
Ethylxanthate ($EO–CS_2^-$)	9.44	-0.1943	-0.0353	-0.1148	0.0795	0.0829
Ethyltrithiocarbonate ($ES–CS_2^-$)	9.95	-0.1996	-0.0541	-0.1269	0.0727	0.1106
Ethyldithiocarbamate ($ENH–CS_2^-$)	10.83	-0.1893	-0.0230	-0.1062	0.0832	0.0678
Diethyldithiocarbamate ($E_2N–CS_2^-$)	12.83	-0.1792	-0.0213	-0.1003	0.0789	0.0637
Ethyldithiophosphate ($EHO_2PS_2^-$)	6.03	-0.2091	-0.0087	-0.1089	0.1002	0.0592

The escaping tendency of electrons from the ligand ions as depicted by values of μ follows the following order: $E_2N\text{-}CS_2^-$ > $EHN\text{-}CS_2^-$ > $EHO_2\text{-}PS_2^-$ > $EO\text{-}CS_2^-$ > $E\text{-}CS_2^-$ > $ES\text{-}CS_2^-$. The electron escaping tendency from a conjugative system is in the reverse order of conjugation. The average bond length of the two C-S bonds (or P-S) is a helpful criterion to determine the degree of conjugation for ligand molecules. A larger deviation from standard single bond length indicates a superior conjugative effect and thus inferior electron escaping tendency. Interestingly the deviation in the average C-S bond length from the standard single C-S bond follows an

opposite order to μ values, i.e. $ES–CS_2^-$ > $E\text{-}CS_2^-$ > $EO–CS_2^-$ > $EHN–CS_2^-$ > $E_2N–CS_2^-$. Considering the standard P-S single bond length equal to 2.09 Å (Trahar, Senior, Heyes, & Creed, 1997), $EHO_2–PS_2^-$ falls between $EO–CS_2^-$ and $EHN–CS_2^-$. The nucleophilic strength of the anionic ligands as depicted by the calculated values of ω follows the following order: $EHO_2\text{-}PS_2^-$ > $E_2N\text{-}CS_2^-$ > $EHN\text{-}CS_2^-$ > $EO\text{-}CS_2^-$ > $E\text{-}CS_2^-$ > $ES\text{-}CS_2^-$.

The binding ability of a ligand towards a metal ion in solution cannot be accurately assessed by only considering the reactivity of the ligand. The final outcome of the reaction depends on several other factors as well, such as steric compatibility between reacting species, ring size, etc. Therefore, metal-ligand complexes were modeled and their interaction energies were calculated. Interaction energies of different metal-ligand complexes are plotted in Figure 4.3. As seen from the plot, all the ligand species under consideration are most reactive towards Cu followed by Pb. The predicted reactivity is in the same order of solubility product constants reported in literature for xanthate, dithiocarbamate and dithiophosphate complexes with these metals, i.e, Cu^{2+} < Pb^{2+} < Zn^{2+} [62,65-66]. Peters and Shem (1993) established the hierarchy for selective removal of heavy metals by xanthate as Cu > Pb > Zn. Ying and Fang (2006), in their study relating to the use of dipropyl dithiophosphate to remove heavy metals from waste waters, found that the complex formed by dithiophosphate reagent with Cu was more stable than with Pb. Moreover, the reactivity order presented in this study is further supported by the fact that the flotation of sphalerite using sulphydryl collectors is usually carried out through activation by Cu and/or Pb ions (Ravitz & Wall, 1993; Trahar et al., 1997).. For a particular metal, binding ability of reagent molecules follows the order: $E_2N\text{-}CS_2^-$ > $EHN\text{-}CS_2^-$ > $EO\text{-}CS_2^-$ ≥ $E\text{-}CS_2^-$ > $ES\text{-}CS_2^-$ > $EHO_2\text{-}PS_2^-$.

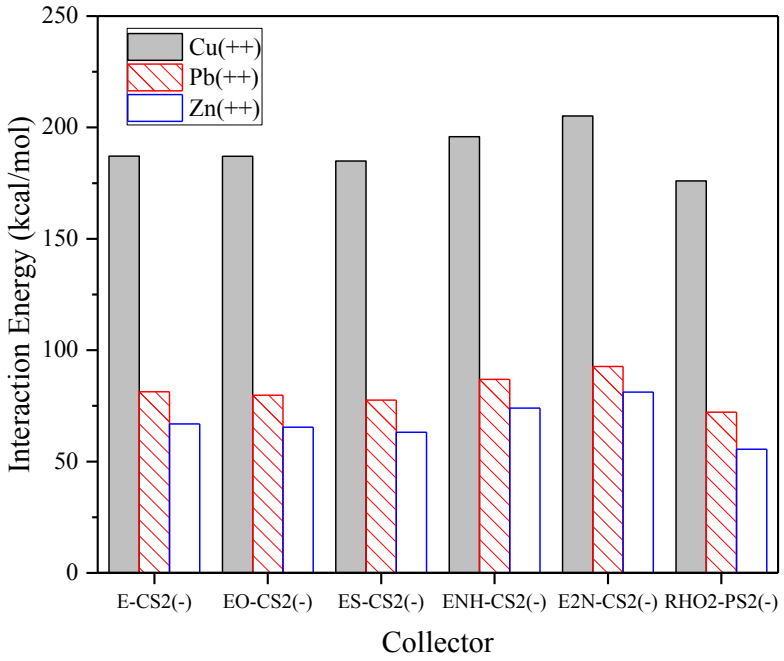

Figure 4.3. Interaction energy between different ligand anions and metal cations (R, E = ethyl).

Evidently, the interaction energy of different ligands toward heavy metal ions in solution follows the same trend as predicted by calculated values of ω, except for ethyldithiophosphate. The change in ∠Y-P-Y for ethyldithiophosphate ligand upon complex formation is larger than the change in ∠Y-C-Y for xanthate, trithiocarbonate and dithiocarbamate complexes for all three metals. Similarly, ∠O-P-O in dithiophosphate ligands also undergoes a change of about 2-3 degrees during the formation of different complexes. Due to this significant change in geometry, it could be concluded that the four-member ring(s) in ethyldithiophosphate complexes is under higher geometrical strain when compared to the remaining complexes. This could be one of the possible reasons for low binding energy values for ethyldithiophosphate complexes. For all three metals under consideration, stability product of their complexes with the reagents follows the

order: dithiocarbamate < xanthate < dithiophosphate, which is opposite to the order of their calculated interaction energies (M. C. Fuerstenau, 1982; D. W. Fuerstenau, 1982; Wing & Rayford, 1982). In a previous experimental investigation, the order of adsorption strength for a given sulfide mineral has been identified as: dithiocarbamates > xanthate > dithiophosphates (D. Nagaraj, 1988). The same order of reactivity was predicted in a previous theoretical study, when investigating binding of these ligand ions with Ag(I) ions (H. Yekeler & Yekeler, 2004). It is interesting to note that interaction energy of Pb and Zn dithiophosphate complexes is less than their hydroxide complexes. The solubility products of Zn and Pb dithiophosphate complex have been reported to be higher than their hydroxide complexes (D. W. Fuerstenau, 1982). The relative magnitude in binding energy of these metal ions with dithiophosphate or hydroxide ions also points to the enhanced selectivity of dithiophosphate reagents toward Cu ions in presence of Pb and Zn ions.

In order to investigate the metal selectivity offered by these reagents, relative interaction energies (with respect to Zn complexes) of different metal-ligand complexes are shown in Figure 4.4. It is evident from the plot that though the interaction between metal ions and dithiocarbamate reagents is strongest, they are least selective toward any particular metal. On the other hand dithiophosphates, which have weakest interaction energies, offer enhanced selectivity towards Cu ion. The enhanced selectivity offered by dithiophosphate toward Cu metal or Cu bearing minerals compared to xanthates and dithiocarbamates is well documented in literature (Adkins & Pearse, 1992; Somasundaran & Nagaraj, 1984).

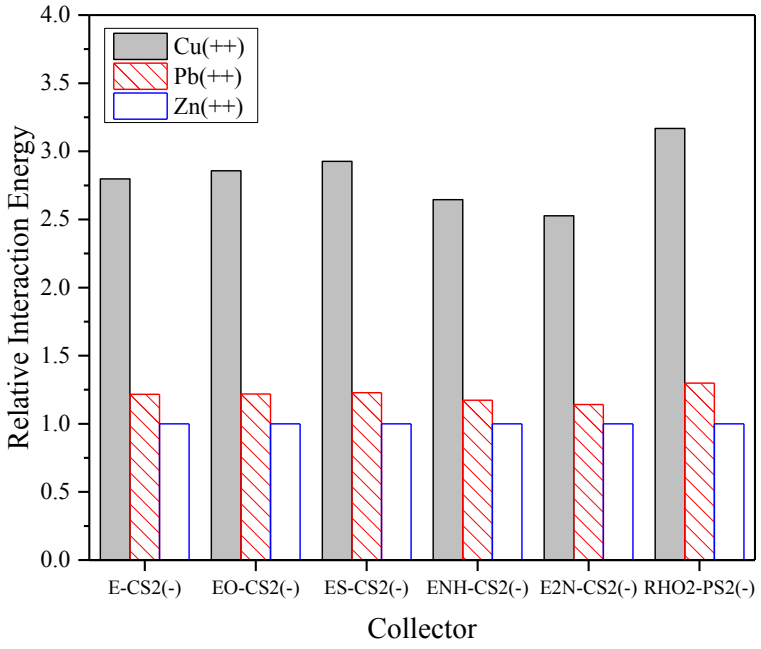

Figure 4.4. Relative interaction energies for different reagent ions and metal cations (R, E = ethyl).

DFT calculated interaction energies of some of the complexes are plotted against their experimentally derived pK_{sp} values in Figure 4.5. As evident from the plot the calculated interaction energies roughly follow the same order as pK_{sp} of these complexes. The data set has a poor determination coefficient as K_{sp} value of a metal-ligand complex is also influenced by the hydrophobicity of ligand reagent(s) along with its chelating capability towards a metal ion.

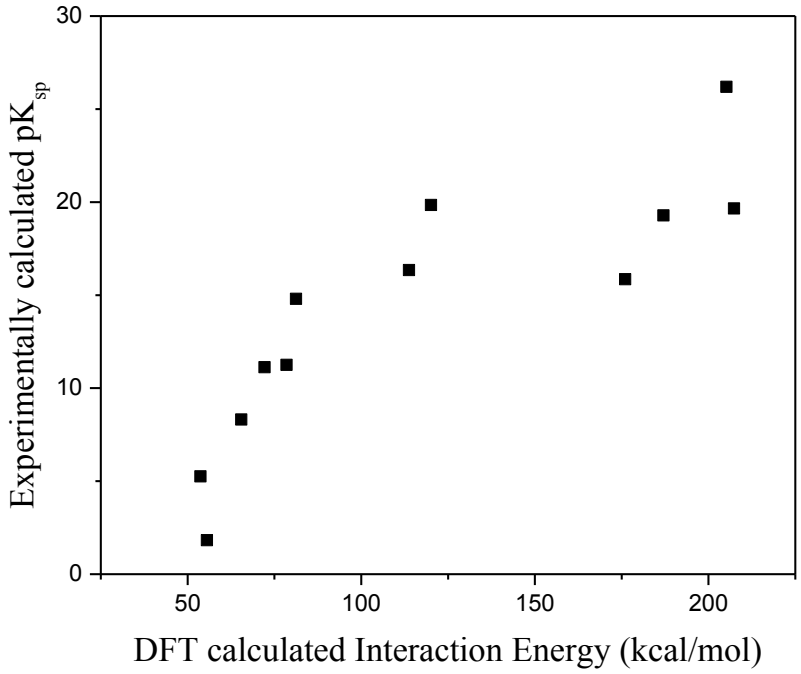

Figure 4.5. Correlation between DFT calculated interaction energies and experimentally derived pKsp for some of the complexes.

4.3.3. Vibrational Spectra

Vibrational frequencies were computed for all the molecules under consideration to validate the optimized geometries obtained using DFT methods. The calculated IR spectra of different complexes were compared with the experimental IR spectra reported in previous studies. Theoretically obtained IR spectra for dithiocarbamate and ethyl xanthate complexes of all three metals (Cu, Zn and Pb) are discussed in this section.

IR spectra for diethyl dithiocarbamate complexes are plotted in Figure 4.6. In diethyldithiocarbamate complexes, different vibrational modes corresponding to –CH stretching in $–CH_3$ and $–CH_2$ groups appeared between 3040-3135 cm^{-1} and are represented by four large bands with peaks around 3045 cm^{-1}, 3075 cm^{-1}, 3108 cm^{-1} and 3134 cm^{-1}. Previous studies

comprising vibrational analysis of Zn and Cu diethyldithiocarbamate complexes at B3LYP/6-311G (d, p) level have reported these vibrations to occur between 3036-3128 cm^{-1} while experimental values for these vibrations have been recorded between 2870-3000 cm^{-1} (Costa Jr. et al., 2013; Costa Jr., Ramos et al., 2013).

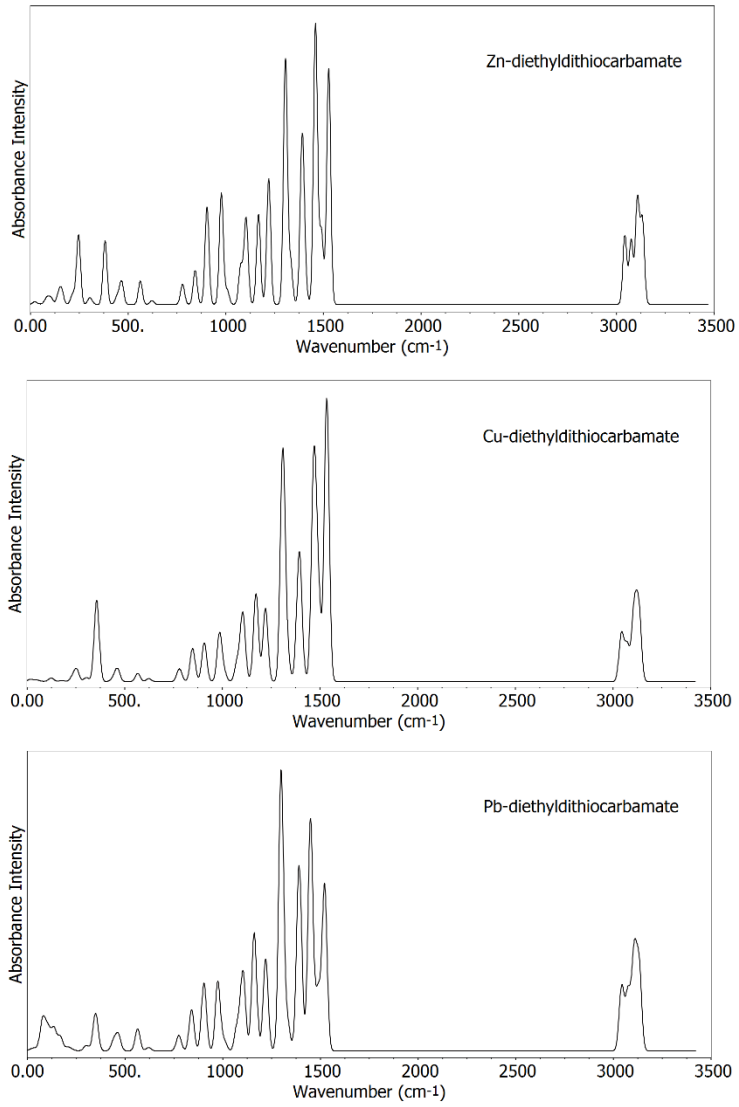

Figure 4.6. Calculated vibrational spectra for complexes of dialkyldithiocarbamate with Zn, Pb, and Cu ions.

The C-N double and C-S single bond stretching modes, the characteristic vibrations of dithiocarbamate complexes lie in the ranges 1450-1550 cm^{-1} (thioureide band) and 950-1050 cm^{-}

^{1} respectively (Sathiyaraj & Thirumaran, 2012). The C-N single bond stretching modes typically occur in the region 1250-1350 cm^{-1} (Sathiyaraj & Thirumaran, 2012), and is represented by the peaks at 1306 cm^{-1}, 1310 cm^{-1} and 1300 cm^{-1} for Zn, Cu and Pb diethyldithiocarbamate complexes respectively in the calculated infrared spectra. The thioureide band arising as a consequence of delocalization of lone pair electrons at N centre toward the $–CS_2$ moiety appears around 1528 cm^{-1} for Zn complex, 1536 cm^{-1} for Cu complex and 1522 cm^{-1} for Pb complex. This delocalization of electrons introduces double bond character in the C-N linkage and shifts the band toward the higher energy C-N double bond vibrational mode (1640-1690 cm^{-1}). Previous theoretical studies have reported the thiorueide band to occur around 1535 cm^{-1} for Zn complex and 1530 cm^{-1} for Cu complex (Costa Jr. et al., 2013; Sathiyaraj & Thirumaran, 2012). Experimental values for thioureide band for Zn and Cu diethyldithiocarbamate complexes have been reported to occur at 1507 cm^{-1} and 1503 cm^{-1}, and 1510 cm^{-1} and 1506 cm^{-1} respectively (Costa Jr. et al., 2013; Sathiyaraj & Thirumaran, 2012). The experimental value for thioureide band for Pb complex has been reported to occur at 1483 cm^{-1} (Rathore, Ishratullah, Varshney, Varshney, & Mojumdar, 2008).

A typical C-S single bond band appears in the region 570-710 cm^{-1} while the C-S double bond band generally occurs in between 1030-1275 cm^{-1}. In this study, stretching modes corresponding to the $–CS_2$ moiety in dithiocarbamate complexes appeared around 978 cm^{-1} for Zn complex, 981 cm^{-1} for Cu complex and 975 cm^{-1} for Pb complex. The occurrence of only one strong band and a value between the characteristic single and double C-S bond frequencies in all complexes suggests a bidentate coordination of the dithiocarbamate moiety. A previous experimental investigation reported this band to occur at 985 cm^{-1} for Zn complex, 993 cm^{-1} for Cu complex and 980 cm^{-1} for Pb complex (Rathore et al., 2008). However, theoretical studies in the past have

reported the occurrence of this band for Zn and Cu diethyldithiocarbamate complex at 916 cm^{-1} and 1003 cm^{-1} respectively (Costa Jr. et al., 2013; Costa Jr. et al., 2013). The experimental values reported in such studies are 864 cm^{-1} (Raman wavelength) and 917 cm^{-1} respectively. Different studies on other dithiocarbamates complexes indicated the occurrence of C-S band in the region 970-1015 cm^{-1} (Costa Júnior et al., 2012; Sathiyaraj & Thirumaran, 2012).

The identification of M-S stretching modes is often very complex as these vibrations are typically coupled with a number of vibrations corresponding to other internal coordinates (Costa Jr. et al., 2013; Costa Jr. et al., 2013; Costa Júnior et al., 2012). In all three metal dithiocarbamate complexes, four main contributions of the M-S stretching mode were observed. For Zn complex, Zn-S stretching occurs asymmetrically at 382 cm^{-1} and 371 cm^{-1} and symmetrically at 315 cm^{-1} and 247 cm^{-1}; experimental observations have been reported to lie at 396 cm^{-1}, 379 cm^{-1}, 335 cm^{-1} and 289 cm^{-1} (Costa Jr. et al., 2013). For Cu complex, asymmetrical stretching occurs at 357 cm^{-1} and 319 cm^{-1} while symmetrical stretching occurs at 304 cm^{-1} and 254 cm^{-1}; experimental frequencies for these vibrational modes have been reported to occur at 353 cm^{-1}, 287 cm^{-1}, 256 cm^{-1} and 241 cm^{-1} respectively (Costa Jr. et al., 2013). The far spectra (400-100 cm^{-1}) for Pb diethyldithiocarbamate complex appears to be very complex and different Pb-S bond stretching modes appear between 107-353 cm^{-1} with peaks at 353 cm^{-1}, 347 cm^{-1}, 311 cm^{-1}, 165 cm^{-1}, 134 cm^{-1} and 107 cm^{-1}. There exist no far spectra for Pb dithiocarbamate in literature; however, an experimental study in the past has mentioned the asymmetrical vibrations to occur at around 385 cm^{-1} and symmetrical vibrations at around 155 cm^{-1} (Kellner & St. Nikolov, 1981).

The calculated IR spectra of xanthates are shown in Figure 4.7. Consistent with dithiocarbamate complexes, the peaks corresponding to various –CH stretching modes in the $–CH_3$ and $–CH_2$ groups occurs in between 3040-3130 cm^{-1}. IR spectra of all three xanthate

complexes show three peaks of strong to moderate intensity in the region of 950-1300 cm^{-1} and correspond to the characteristic absorption peaks for xanthates. The peak occurring around 1020-1025 cm^{-1} for all three complexes is accompanied by a smaller peak with weaker intensity in the region of 1007-1009 cm^{-1}. Strong band lying around 1242 cm^{-1} for Zn complex, 1261 cm^{-1} for Cu complex and 1210 cm^{-1} for Pb complex is primarily the C-O stretching mode (C in $–CS_2$ moiety). Experimentally, this band appears around 1227 cm^{-1} and 1200/1207 cm^{-1} for Zn and Pb complexes respectively (Allison, Goold, Nicol, & Granville, 1972; Leppinen, Basilio, & Yoon, 1989). The three remaining peaks occurring around 1135 cm^{-1}, 1025 cm^{-1} and 1010 cm^{-1} are highly coupled with C-S stretching, C'-O-C stretching, C'-O stretching (where C': terminal carbon in alkyl chain) and C-C stretching vibrational modes as has been reported in the past (Agarwala, Lakshmi, & Rao, 1968). The moderately intense peak occurring at 1024 cm^{-1} for Zn complex, 1025 cm^{-1} for Cu complex and 1019 cm^{-1} for Pb complex is primarily dominated by C-S stretching mode as a single major contributor. The experimental values for C-S stretching in Zn and Pb xanthate complexes have been reported as 1024 cm^{-1} and 1016-1020 cm^{-1} respectively (Allison et al., 1972; Fredriksson & Holmgren, 2008). The absence of any strong bands in the region 570-710 cm^{-1} suggest a bidentate binding mode. The absorption peak occurring at 1135 cm^{-1} has major contributions from C'-O stretching mode as reported previously in an experimental study dealing with different transition metal xanthate complexes (Agarwala et al., 1968). The presence of two strong frequencies corresponding to carbon-oxygen bonds in the xanthate complexes suggests dissimilar nature of C-O and C'-O bonds. The C-O-C stretching modes in ethers generally occur in the range 1070-1150 cm^{-1} while C-O double bond stretching vibrations typically occur between 1670-1820 cm^{-1}. The shift of C-O vibrational mode (C in -CS_2 moiety) toward frequencies higher than typical ether range and closer to C-O double bond

frequency range suggest substantial double bond character. A difference of 80-160 cm^{-1} between two C-O frequencies in xanthate complexes has been reported previously depending on the central atom and alkyl chain length (Watt & McCormick, 1965). M-S vibrations for the xanthate complexes occur at frequencies lower than 300 cm^{-1}. However, all the M-S vibrational modes are highly coupled making it difficult to assign them explicitly by merely visualizing them.

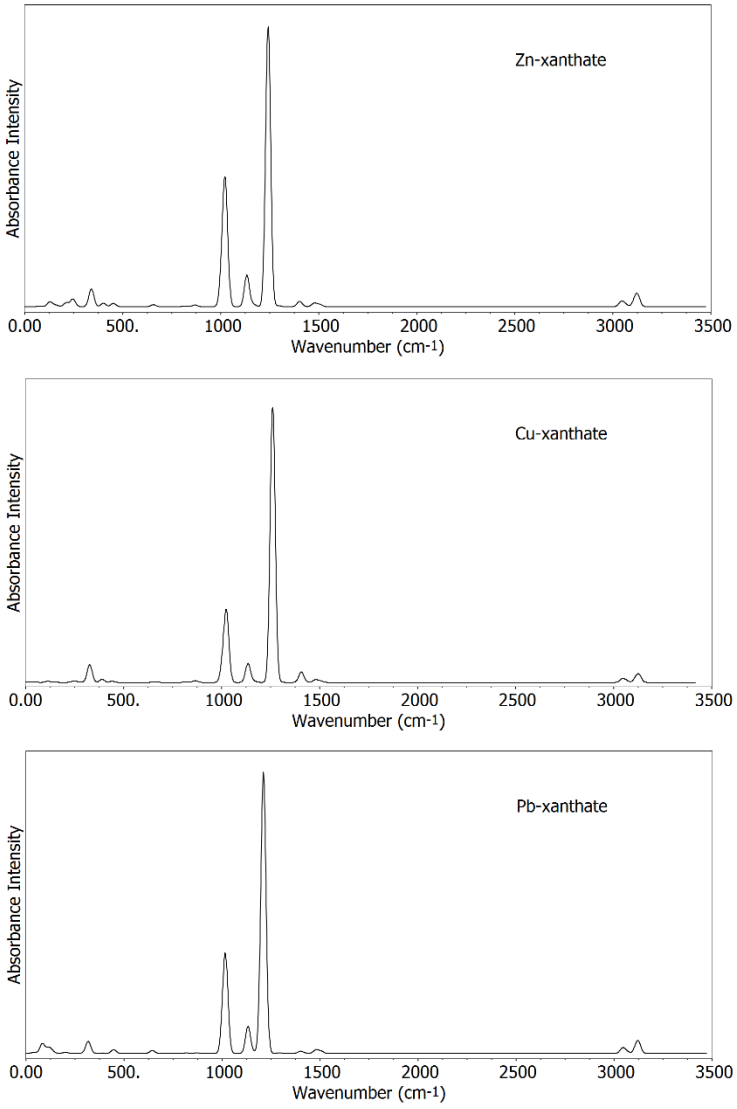

Figure 4.7. Calculated vibrational spectra for complexes of xanthate reagent with Zn, Pb, and Cu ions.

As evident from the above discussion, the calculated vibrational modes of xanthate and dithiocarbamate complexes of Zn, Cu and Pb ions in solution are in good agreement with the experimentally observed values as well as previous theoretical investigations. Consistent with numerous previous studies dealing with vibrational analysis of molecules using theoretical methods (Boddu et al., 2003; Chaitanya, Santhamma, Prasad, & Veeraiah, 2012; Costa Jr. et al., 2013; Costa Jr. et al., 2013; Costa Júnior et al., 2012; Hernández-Rivera & Castillo-Chará, 2010; Koca, Yildirim, Kirilmis, & Karaboga, 2012; Murali & Balachandranb, 2012), calculated frequencies in this study are slightly greater than the experimentally reported values. This could be attributed to the approximate nature of quantum mechanical methods as well as to the negligence of anharmonicity. Moreover, the calculated spectra were recorded for an isolated molecule in solution, whereas experimentally observed spectra are generally recorded for precipitated salts of these complexes. Previous authors have used scaling factors between 0.84-0.97 to compare the theoretically calculated vibrational modes with experimentally observed frequencies. A detailed analysis of the infrared spectrum via normal coordinate analysis and potential energy distribution to determine percent contribution of different normal modes to an observed frequency is not reported since it was considered out of scope for the present article.

4.4. Conclusion

In this study, the interaction of different thiol reagents with bivalent ions of Pb, Cu and Zn in solution was modeled using density functional theory methods. The use of the reactivity descriptors provided satisfactory description of the chemical activity of the reagents. All anionic ligands exhibited strong affinity towards Cu ion, followed by Pb and Zn ions. Based on the calculated interaction energies, dithiocarbamate reagents exhibit maximum chelating capability,

followed by xanthates and trithiocarbonates. Alkyldithiophosphate collectors were found to possess the weakest chelating power. However, they exhibited superior selectivity toward Cu ion. The interaction energies of reagents with the $–CO_2^-$ moiety towards heavy metal ions were similar or higher compared to those with the $–CS_2^-$ functional group. However, their weak selectivity against light non-toxic metals such as Ca and Mg works in favour of using thiol type precipitating reagents in the industry. The binding in all the complexes was found to be bi-dentate except in Zn-ethylmonothiocarboxylate complex. The structural data in monothiocarboxylates show much weaker interactions of central metal atom with O than with S. Structural data and theoretical IR spectra for different metal-ligand complexes matched closely with the experimental findings, demonstrating successful prediction of the chelating capability of reagents through DFT calculations.

4.5. References

Adkins, S. J., & Pearse, M. J. (1992). The influences of collector chemistry on kinetics and selectivity in base-metal sulphide flotation. *Minerals Engineering, 5*(3–5), 295-310.

Agarwala, U., Lakshmi, & Rao, P. B. (1968). Vibrational spectra of xanthate complexes. *Inorganica Chimica Acta, 2*, 337-339.

Allison, S. A., Goold, L. A., Nicol, M. J., & Granville, A. (1972). A determination of the products of reaction betweer various sulfide minerals and aqueous xanthate solution, and a correlation of the products with electrode rest potentials. *Metallurgical Transactions, 3*(10), 2613-2618.

Andrae, D., Haeussermann, U., Dolg, M., Stoll, H., & Preuss, H. (1990). Energy-adjusted ab initio pseudopotentials for the 2nd and 3rd row transition elements. *Theoretical Chemistry Accounts, 77*, 123-141.

Ayers, P., & Parr, R. (2008a). Beyond electronegativity and local hardness: Higher-order equilization criteria for determination of a ground-state electron density. *Journal of Chemical Physics, 129*(5), 054111-054117.

Ayers, P., & Parr, R. (2008b). Local hardness equilization: Exploiting the embiguity. *Journal of Chemical Physics, 128*(18), 184108-184115.

Babel, S., & Kurniawan, T. A. (2004). Cr(VI) removal from synthetic wastewater using coconut shell charcoal and commercial activated carbon modified with oxidizing agents and/or chitosan. *Chemosphere, 54*(7), 951-967.

Barakat, M. A. (2011). New trends in removing heavy metals from industrial wastewater. *Arabian Journal of Chemistry, 4*(4), 361-377.

Becke, A. D. (1988). Density-functional exchange-energy approximation with correct asymptotic behavior. *Physical Review A, 38*(6), 3098-3100.

Becke, A. D. (1993). Density-functional thermochemistry. III. the role of exact exchange. *The Journal of Chemical Physics, 98*(7), 5648-5652.

Billes, F., Holmgren, A., & Mikosch, H. (2010). A combined DFT and vibrational spectroscopy study of nickel and zinc O,O-diethyldithiophosphate complexes. *Vibrational Spectroscopy, 53*, 296-306.

Blue, L. Y., Jana, P., & Atwood, D. A. (2010). Aqueous mercury precipitation with the synthetic dithiolate, BDTH2. *Fuel, 89*(6), 1326-1330.

Boddu, V. M., Abburi, K., Talbott, J. L., & Smith, E. D. (2003). Removal of hexavalent chromium from wastewater using a new composite chitosan biosorbent. *Environmental Science & Technology, 37*(19), 4449-4456.

Breza, M., Bučinský, L., Šoralová, S., & Biskupič, S. (2010). On the origin of the hemidirected geometry of tetracoordinated lead(II) compounds. *Chemical Physics, 368*(1–2), 14-19.

Chaitanya, K., Santhamma, C., Prasad, K. V., & Veeraiah, V. (2012). Molecular structure, vibrational spectroscopic (FT-IR, FT-raman),first order hyperpolarizability, NBO analysis, HOMO and LUMO analysis, thermodynamic properties of 3,5-dimethylbenzophenone by ab inito HF and density functional method. *Journal of Atomic and Molecular Sciences, 3*(1), 1-22.

Chang, Q., & Wang, G. (2007). Study on the macromolecular coagulant PEX which traps heavy metals. *Chemical Engineering Science, 62*(17), 4636-4643.

Chang, Y., Chang, J., & Chiang, L. (2003). Leaching behavior and chemical stability of copper butyl xanthate complex under acidic conditions. *Chemosphere, 52*(6), 1089-1094.

Charerntanyarak, L. (1999). Heavy metals removal by chemical coagulation and precipitation. *Water Science and Technology, 39*(10–11), 135-138.

Cifuentes, L., García, I., Arriagada, P., & Casas, J. M. (2009). The use of electrodialysis for metal separation and water recovery from CuSO4–H2SO4–Fe solutions. *Separation and Purification Technology, 68*(1), 105-108.

Coetzer, G., du Preez, H. S., & Bredenhann, R. (2003). Influence of water resources and metal ions on galena flotation of rosh pinah ore. *The Journal of the South African Institute of Mining and Metallurgy,* (April), 193-208.

Costa Jr., A. C., Ondar, G. F., Versiane, O., Ramos, J. M., Santos, T. G., Martin, A. A., . . . Téllez Soto, C. A. (2013). DFT: B3LYP/6-311G (d, p) vibrational analysis of bis-(diethyldithiocarbamate)zinc (II) and natural bond orbitals. *Spectrochimica Acta Part A: Molecular and Biomolecular Spectroscopy, 105*(0), 251-258.

Costa Jr., A. C., Ramos, J. M., Téllez Soto, C. A., Martin, A. A., Raniero, L., Ondar, G. F., . . . Moraes, L. S. (2013). Fourier transform infrared and raman spectra, DFT: B3LYP/6-311G(d, p) calculations and structural properties of bis(diethyldithiocarbamate)copper(II). *Spectrochimica Acta Part A: Molecular and Biomolecular Spectroscopy, 105*(0), 259-266.

Costa Júnior, A. C., Versiane, O., Faget Ondar, G., Ramos, J. M., Ferreira, G. B., Martin, A. A., & Téllez Soto, C. A. (2012). An experimental and theoretical approach of spectroscopic and structural properties of the bis(diethyldithiocarbamate)–cobalt(II). *Journal of Molecular Structure, 1029*(0), 119-134.

Coucouvanis, D. (1970). The chemistry of the dithioacid and 1,1-dithiolate complexes. *Progress in Inorganic Chemistry, 11*, 233-371.

Dolg, M., Wedig, U., Stoll, H., & Preuss, H. (1987). Energy-adjusted ab initio pseudopotentials for the first row transition elements. *The Journal of Chemical Physics, 86*(2), 866-872.

Doula, M. K. (2009). Simultaneous removal of cu, mn and zn from drinking water with the use of clinoptilolite and its fe-modified form. *Water Research, 43*(15), 3659-3672.

Euler, B. (2006). Stability product constants near 25 degree celcius. Retrieved from http://bilbo.chm.uri.edu/CHM112/tables/KspTable.htm

Fredriksson, A., & Holmgren, A. (2008). An in situ ATR-FTIR investigation of adsorption and orientation of heptyl xanthate at the lead sulphide/aqueous solution interface. *Minerals Engineering, 21*(12–14), 1000-1004.

Frisch, M. J., Trucks, G. W., Schlegel, H. B., Scuseria, G. E., Robb, M. A., Cheeseman, J. R., . . . Fox, D. J. (2009). *Gaussian 09, revision A.1*. Wallingford CT: Gaussian, Inc.

Fu, F., Chen, R., & Xiong, Y. (2007). Comparative investigation of N,N′-bis-(dithiocarboxy)piperazine and diethyldithiocarbamate as precipitants for ni(II) in simulated wastewater. *Journal of Hazardous Materials, 142*(1–2), 437-442.

Fu, F., & Wang, Q. (2011). Removal of heavy metal ions from wastewaters: A review. *Journal of Environmental Management, 92*(3), 407-418.

Fu, F., Zeng, H., Cai, Q., Qiu, R., Yu, J., & Xiong, Y. (2007). Effective removal of coordinated copper from wastewater using a new dithiocarbamate-type supramolecular heavy metal precipitant. *Chemosphere, 69*(11), 1783-1789.

Fuerstenau, M. C. (1982). Chemistry of collectors in solution. In R. P. King (Ed.), *Principles of flotation* (1st ed., pp. 1-16). Johannesburg: South African Institute of Mining and Metallurgy.

Fuerstenau, D. W. (1982). Activation in the flotation of sulphide minerals. In R. P. King (Ed.), *Principles of flotation* (1st ed., pp. 183-198). Johannesburg: South African Institute of Mining and Metallurgy.

Fuerstenau, M. C., Clifford, K. L., & Kuhn, M. C. (1974). The role of zinc-xanthate precipitation in sphalerite flotation. *International Journal of Mineral Processing, 1*(4), 307-318.

Fuerstenau, M. C., & Han, K. N. (2002). Metal–Surfactant precipitation and adsorption in froth flotation. *Journal of Colloid and Interface Science, 256*(1), 175-182.

Ghosh, D., Bagchi, S., & Das, A. K. (2011). Theoretical study of electronic structure and complexation of PBII$(S_2COR)_2$ [R = me, et, ph] complexes. *Molecular Physics, 110*(1), 37-48.

Hellstrom, P., Oblatt, S., Fredriksson, A., & Holmgren, A. (2006). A theoretical and experimental study of vibrational properties of alkyl xanthates. *Spetrochim. Acta, 65A*, 887-895.

Henke, K. R. (1998). Chemistry of heavy metal precipitates resulting from reactions with thio-Red®. *Water Environment Research, 70*(6), 1178-1185.

Hernández-Rivera, S. P., & Castillo-Chará, J. (2010). Ab initio, DFT calculation and vibrational analysis of 2,4,6-trinitrotoluene. *Vibrational Spectroscopy, 53*(2), 248-259.

Ikeda, T., & Hagihara, H. (1966). The crystal structure of zinc ethylxanthate. *Acta Crystallographica, 21*, 919-927.

Ikumapayi, F., Makitalo, M., Johansson, B., & Rao, K. H. (2012). Recycling of process water in sulphide flotation: Effect of calcium and sulphate ions on flotation of galena. *Minerals Engineering, 39*(0), 77-88.

Ivanov, A., Bredyuk, O., Antzutkin, O., & Forsling, W. (2004). Copper(II) and nickel(II) alkylxanthate complexes (R = C_2H_5, i-C_3H_7, i-C_4H_9, s-C_4H_9, and C_5H_{11}): EPR and solid-state 13C CP/MAS NMR studies. *Russian Journal of Coordination Chemistry, 30*(7), 480-485.

Kang, K. C., Kim, S. S., Choi, J. W., & Kwon, S. H. (2008). Sorption of Cu^{2+} and Cd^{2+} onto acid- and base-pretreated granular activated carbon and activated carbon fiber samples. *Journal of Industrial and Engineering Chemistry, 14*, 131-135.

Kang, S., Lee, J., Moon, S., & Kim, K. (2004). Competitive adsorption characteristics of Co2+, Ni2+, and Cr3+ by IRN-77 cation exchange resin in synthesized wastewater. *Chemosphere, 56*(2), 141-147.

Kellner, R., & St. Nikolov, G. (1981). Far IR spectra of dithiocarbamate complexes correlations with structure parameters. *Journal of Inorganic and Nuclear Chemistry, 43*(6), 1183-1188.

Koca, M., Yildirim, G., Kirilmis, C., & Karaboga, F. (2012). Density functional theory study on the identification of pd(me-xanthate)$_2$. *Arabian Journal for Science and Engineering, 37*(5), 1283-1291.

Koopmans, T. (1934). Uber die zuordnung von wellenfunk-tionen und eigenwerten zu den einzelnen elektronen eines atoms. *Physica, 1*, 104.

Ku, Y., & Jung, I. (2001). Photocatalytic reduction of cr(VI) in aqueous solutions by UV irradiation with the presence of titanium dioxide. *Water Research, 35*(1), 135-142.

Kurniawan, T. A. (2002). *A research study on cr(VI) removal from electroplating wastewater using chemically modified low-cost adsorbents and commercial activated carbon* (Master).

Landaburu-Aguirre, J., García, V., Pongrácz, E., & Keiski, R. L. (2009). The removal of zinc from synthetic wastewaters by micellar-enhanced ultrafiltration: Statistical design of experiments. *Desalination, 240*(1–3), 262-269.

Lee, C., Yang, W., & Parr, R. G. (1988). Development of the colle-salvetti correlation-energy formula into a functional of the electron density. *Physical Review B, 37*(2), 785-789.

Leppinen, J. O. (1990). FTIR and flotation investigation of the adsorption of ethyl xanthate on activated and non-activated sulfide minerals. *International Journal of Mineral Processing, 30*(3–4), 245-263.

Leppinen, J. O., Basilio, C. I., & Yoon, R. H. (1989). In-situ FTIR study of ethyl xanthate adsorption on sulfide minerals under conditions of controlled potential. *International Journal of Mineral Processing, 26*(3–4), 259-274.

Li, Y., Liu, F., Xia, B., Du, Q., Zhang, P., Wang, D., Xia, Y. (2010). Removal of copper from aqueous solution by carbon nanotube/calcium alginate composites. *Journal of Hazardous Materials, 177*(1–3), 876-880.

Liang, S., Guo, X., Feng, N., & Tian, Q. (2010). Effective removal of heavy metals from aqueous solutions by orange peel xanthate. *Transactions of Nonferrous Metals Society of China, 20, Supplement 1*(0), s187-s191.

Liu, G., Zeng, H., Lu, Q., Zhong, H., Choi, P., & Xu, Z. (2012). Adsorption of mercaptobenzoheterocyclic compounds on sulfide mineral surfaces: A density functional theory study of structure–reactivity relations. *Colloids and Surfaces A: Physicochemical and Engineering Aspects, 409*(0), 1-9.

Marchioretto, M. M., Bruning, H., & Rulkens, W. H. (2002). OPTIMIZATION OF CHEMICAL DOSAGE IN HEAVY METALS PRECIPITATION IN ANAEROBICALLY DIGESTED SLUDGE. *Proceedings of XXVIII Congreso Interamericano De Sanataria Y Ambiental,* Cancun, Mexico. 1-7.

Matlock, M. M., Henke, K. R., & Atwood, D. A. (2002). Effectiveness of commercial reagents for heavy metal removal from water with new insights for future chelate designs. *Journal of Hazardous Materials, 92*(2), 129-142.

Matlock, M. M., Howerton, B. S., & Atwood, D. A. (2001). Irreversible precipitation of mercury and lead. *Journal of Hazardous Materials, 84*(1), 73-82.

Matlock, M. M., Howerton, B. S., Henke, K. R., & Atwood, D. A. (2001). A pyridine-thiol ligand with multiple bonding sites for heavy metal precipitation. *Journal of Hazardous Materials, 82*(1), 55-63.

Medina, B. Y., Torem, M. L., & de Mesquita, L. M. S. (2005). On the kinetics of precipitate flotation of cr III using sodium dodecylsulfate and ethanol. *Minerals Engineering, 18*(2), 225-231.

Miertus, S., Scrocco, E., & Tomasi, J. (1981). Electrostatic interaction of a solute with a continuum. A direct utilization of ab initio molecular potentials for the prevision of solvent effects. *Chemical Physics, 55*(1), 117-129.

Murali, M. K., & Balachandranb, V. (2012). FT-IR, FT-raman, DFT structure, vibrational frequency analysis and mulliken charges of 2-chlorophenylisothiocyanate. *Indian Journal of Pure & Applied Physics, 50*(January), 19-25.

Nagaraj, D. (1988). The chemistry and application of chelating or complexing agents in mineral separations. *Reagents in Mineral Technology,* New York, USA. 387-408.

Nataraj, S. K., Hosamani, K. M., & Aminabhavi, T. M. (2007). Potential application of an electrodialysis pilot plant containing ion-exchange membranes in chromium removal. *Desalination, 217*(1–3), 181-190.

Ngo, S. C., Banger, K. K., DelaRosa, M. J., Toscano, P. J., & Welch, J. T. (2003). Thermal and structural characterization of a series of homoleptic cu(II) dialkyldithiocarbamate complexes: Bigger is only marginally better for potential MOCVD performance. *Polyhedron, 22*(12), 1575-1583.

Parr, R., Donnelly, R., Levy, M., & Palke, W. (1978). Electronegativity-the density functional viewpoint. *Journal of Chemical Physics, 68*, 3801-3807.

Parr, R. G., & Pearson, R. G. (1983). Absolute hardness: Companion parameter to absolute electronegativity. *Journal of the American Chemical Society, 105*(26), 7512-7516.

Parr, R. G., Szentpaly, L. V., & Liu, S. (1999). Electrophilicity index. *Journal of the American Chemical Society, 121*(9), 1922-1924.

Pearson, R. G. (1988). Absolute electronegativity and hardness: Application to inorganic chemistry. *Inorganic Chemistry, 27*, 734-740.

Pearson, R. G. (1992). The electronic chemical potential and chemical hardness. *Molecular Structure (Theochem), 255*, 261-270.

Peters, R. W., & Shem, L. (1993). Separation of heavy metals: Removal from industrial wastewaters and contaminated soil. *Department of Energy - Office of Scientific and Technical Information, CONF-9303107--1*(08/10)

Porento, M., & Hirva, P. (2002). Theoretical studies on the interaction of anionic collectors with cu(+), cu(2+), zn(2+) and pb(2+) ions. *Theoretical Chemistry Accounts, 107*(4), 200-205.

Rathore, H. S., Ishratullah, K., Varshney, C., Varshney, G., & Mojumdar, S. C. (2008). Fungicidal and bacteridical activity of metal diethyldithiocarbamate fungicides: Synthesis and characteristics. *Journal of Thermal Analysis and Calorimetry, 94*(1), 75-81.

Ravitz, S. F., & Wall, W. A. (1993). The adsorption of copper sulfate by sphalerite and its RElation to flotation. *The Journal of Physical Chemistry, 38*(1), 13-18.

Roy, P. K., Rawat, A. S., Chaoudhary, V., & Rai, P. K. (2004). Removal of heavy metal ions using polydithiocarbamate resin supported on polystyrene. *Indian Journal of Chemical Technology, 11*(January), 51-58.

Rulisek, L., & Havlas, Z. (2000). Theoretical studies of metal ion selectivity. 1. DFT calculations of interaction energies of amino acid side chains with selected transition metal ions (Co^{2+}, Ni^{2+}, Cu^{2+}, Zn^{2+}, Cd^{2+}, and Hg^{2+}). *Journal of American Chemical Society, 122*, 10428-10439.

Samper, E., Rodríguez, M., De la Rubia, M. A., & Prats, D. (2009). Removal of metal ions at low concentration by micellar-enhanced ultrafiltration (MEUF) using sodium dodecyl sulfate (SDS) and linear alkylbenzene sulfonate (LAS). *Separation and Purification Technology, 65*(3), 337-342.

Sathiyaraj, E., & Thirumaran, S. (2012). Synthesis and spectral studies on pb(II) dithiocarbamate complexes containing benzyl and furfuryl groups and their use as precursors for PbS nanoparticles. *Spectrochimica Acta Part A: Molecular and Biomolecular Spectroscopy, 97*(0), 575-581.

Say, R., Birlik, E., Denizli, A., & Ersöz, A. (2006). Removal of heavy metal ions by dithiocarbamate-anchored polymer/organosmectite composites. *Applied Clay Science, 31*(3–4), 298-305.

Shaoyi, J., Dasgupta, S., Blanco, M., Frazier, R., Yamaguchi, E. S., Tang, Y., & Goddard, W. A. (1996). Structures, vibrations, and force fields of dithiophosphate wear inhibitors from ab initio quantum chemistry. *Journal of Physical Chemistry, 100*, 15760-15769.

Shimoni-Livny, L., Glusker, J., & Bock, C. (1998). Lone pair functinality in divalent lead compounds. *Inorganic Chemistry, 37*(8), 1853-1867.

Somasundaran, P., & Nagaraj, D. R. (1984). Chemistry and applications of chelating reagents in flotation and flocculation. In M. Jones, & R. Oblatt (Eds.), *Reagents in mineral industry* (pp. 209-219). London: Institution of Mining and Metallurgy.

Stephens, P. J., Devlin, F. J., Chabalowski, C. F., & Frisch, M. J. (1994). Ab initio calculation of vibrational absorption and circular dichroism spectra using density functional force fields. *The Journal of Physical Chemistry, 98*(45), 11623-11627.

Tare, V., & Chaudhari, S. (1987). Evaluation of soluble and insoluble xanthate process for the removal of heavy metals from wastewaters. *Water Research, 21*(9), 1109-1118.

Tiekink, E. R. D., & Winter, G. (2011). Inorganic xanthates : A structural perspective. *Reviews of Inorganic Chemistry, 12*(3-4), 183-302.

Tossell, J. A., & Vaughan, D. J. (1993). Theoretical studies of xanthates, dixanthogen, metal xanthates, and related compounds. *Journal of Colloid and Interface Science, 155*(1), 98-107.

Trahar, W. J., Senior, G. D., Heyes, G. W., & Creed, M. D. (1997). The activation of sphalerite by lead — a flotation perspective. *International Journal of Mineral Processing, 49*(3–4), 121-148.

Valero, D., & Ortiz, J. M. (2010). Electrochemical wastewater treatment directly powered by photovoltaic panels: Electrooxidation of a dye-containing wastewater. *Environ. Sci. Technol, 44*(13), 5182-5187.

Vosko, S. H., Wilk, L., & Nusair, M. (1980). Accurate spin-dependent electron liquid correlation energies for local spin density calculations: A critical analysis. *Canadian Journal of Physics, 58*(8), 1200-1211.

Wang, H., Zhou, A., Peng, F., Yu, H., & Yang, J. (2007). Mechanism study on adsorption of acidified multiwalled carbon nanotubes to pb(II). *Journal of Colloid and Interface Science, 316*(2), 277-283.

Waters, A. (1990). Dissolved air flotation used as primary separation for heavy metal removal. *Filtration & Separation, 27*(2), 70-73.

Watt, G. W., & McCormick, B. J. (1965). The infrared spectra and structure of transition metal xanthates. *Spectrochimica Acta, 21*(4), 753-761.

Whang, J. S., Young, D., & Pressman, M. (1982). Soluble-sulfide precipitation for heavy metals removal from wastewaters. engineering details of a treatment plant scheduled to be operational in september, 1981. *Environmental Progress, 1*(2), 110-113.

Wing, R. E., Doane, W. M., & Russell, C. R. (1975). Insoluble starch xanthate: Use in heavy metal removal. *Journal of Applied Polymer Science, 19*(3), 847-854.

Wing, R. E., & Rayford, W. E. (1982). Heavy metal removal using dithiocarbamates. *Plating and Surface Finishing, January*, 67-72.

Xu, Y., Xie, Z., & Xue, L. (2011). Chelation of heavy metals by potassium butyl dithiophosphate. *Journal of Environmental Sciences, 23*(5), 778-783.

Yekeler, H., & Yekeler, M. (2004). Reactivities of some thiol collectors and their interactions with ag (+1) ion by molecular modeling. *Applied Surface Science, 236*(1–4), 435-443.

Ying, X., & Fang, Z. (2006). Experimental research on heavy metal wastewater treatment with dipropyl dithiophosphate. *Journal of Hazardous Materials, 137*(3), 1636-1642.

Yuan, X. Z., Meng, Y. T., Zeng, G. M., Fang, Y. Y., & Shi, J. G. (2008). Evaluation of tea-derived biosurfactant on removing heavy metal ions from dilute wastewater by ion flotation. *Colloids and Surfaces A: Physicochemical and Engineering Aspects, 317*(1–3), 256-261.

Zhu, Y., Hu, J., & Wang, J. (2012). Competitive adsorption of pb(II), cu(II) and zn(II) onto xanthate-modified magnetic chitosan. *Journal of Hazardous Materials, 221–222*(0), 155-161.

Chapter – 5

Reactivity and Binding Ability of Heterocyclic Aromatic Collectors

5.1. Introduction

Mercaptoazole compounds and their derivatives have found important applications in different fields due to their ability to form metal complexes with various heavy metal ions (Liu et al., 2012). In particular, mercaptobenzoazole compounds such as 2-mercaptobenzothiazole (MBT), 2-mercaptobenzoxazole (MBO), and 2-mercaptobenzimidazole (MBI) and their derivatives have emerged as powerful flotation collectors for Pb, Cu, and Zn ores (Maier & Dobiáš, 1997; Marabini, Barbaro, & Alesse, 1991; Marabini, Ciriachi, Plescia, & Barbaro, 2007; Woods, Hope, & Watling, 2000).

Previous studies have shown that these reagents bind to metal ions primarily through exocyclic S and imine N atoms. Marbini et al. (2007) reported that substituent groups attached to benzene ring in mercaptobenzoazole reagents could have significant impact on their efficiency as flotation collectors. Maier and Dobias (1997) showed that at low dosage the collecting efficiency of MBT reagent for sulfide ores follows the order: chalcocite > galena > sphalerite. They also found that MBT has high affinity (and no selectivity) for mineral surfaces containing Pb or Cu. The selectivity towards galena over chalcocite can be improved by substituting pentyloxy group on the benzene ring. MBO and MBI were found to be weak collectors of galena due to their inability to chemisorb on mineral surface. However, reaction enthalpy during formation of

$Pb(MBO)_2$ in bulk was found to be higher than $Pb(MBT)_2$ (Maier & Dobiáš, 1997). Storvick (1986) reported that the efficiency of mercaptobenzoazole reagents as corrosion inhibitors of a 90/10 cupro-nickle alloy follows the order: MBT > MBI ≥ MBO. Same order of inhibition efficiency has also been reported for a stainless steel alloy (Ai-Mayouf, Al-Ameery, & Al-Suhybani, 2001). Foye and Lo (1972) studied binding abilities of some mercaptobenzoazole reagents toward Cu^{2+}, Fe^{3+} and Al^{3+} metal ions. They reported that binding ability of reagents for Cu^{2+} ion follows the order: 1-methyl-2-mercaptoimidazole > 2-mercaptobenzimidazole > 2-mercaptoimidazole, whereas for Fe^{3+} and Al^{3+} metal ions the order is: 1-methyl-2-mercaptoimidazole > 2-mercaptoimidazole > 2-mercaptobenzimidazole > 2-mercaptobenzothiazole.

In collector's molecule, the function of the head group is to bind selectively to the metal species on the mineral surfaces and the tail group is meant to impart hydrophobicity to the resultant metal-collector complexes. Flotation performance and inhibition efficiency when used as corrosion inhibitors are not direct parameters to assess the relative reactivity and chelating ability of azole reagents as measures of such parameters are shadowed by the hydrophobicity of the resultant modified surface. Moreover, these experimental techniques may not be the most suitable method to characterize the effect of each structural element in a reagent molecule on its reactivity and selectivity towards different metals in a quantitative manner. For a better understanding of the relationship between structure of mercaptoazole reagents and their reactivity and binding ability towards different metals, specific parameters that quantify reactivity are needed. As described in section 1.1, DFT methods are appropriate for such tasks.

Yekeler and Yekeler (2006; 2006) computed energies of frontier molecular orbitals (FMOs) and atomic charges for some MBT and MBO derivatives in vacuum and concluded that

methyloxy or methyl (both electron donating) substitution in benzene ring increases the reactivity of MBT and MBO molecule, and the effect is more prominent when substitution takes place at position 9 (refer to Figure 5.1). Liu et al. (2012) compared reactivity of MBT, MBI and MBO molecules utilizing DFT derived parameters and concluded that reactivity follows the order: MBT > MBI > MBO. However, the binding ability of reagents toward metal ions cannot be accurately assessed by only considering the reactivity of reagent molecules as it is influenced by other factors, such as steric compatibility between reacting species, chelate stability, ring size, etc.

In light of above discussion, present study makes an attempt to understand how an alteration in molecular structure influences the reactivity and binding affinity of azole reagents with Cu, Pb and Zn metal ions. Starting with simple mercaptoazole molecules, namely mercaptoimidazole, mercaptoxazole and mercaptothiazole, molecular structure of reagents was gradually modified to study the effect of type and position of different substituent groups on their chelating ability toward different heavy metal ions in water. Predicted orders of reactivity and interaction energies obtained through theoretical calculations were correlated to structural characteristics of the reagent molecules. This study provides an atomic level understanding of relationship between molecular structure of azole reagents and their reactivity and chelating ability towards different heavy metal ions.

5.2. Methodology

The methodology adopted for this study has been discussed in section 4.2.

5.3. Results and Discussion

Five membered aromatic heterocyclic systems containing two heteroatoms are shown in Figure 5.1A. NBO analysis shows strong delocalization of one lone pair of electrons belonging to heteroatom X over other ring atoms, thus confirming aromaticity and indicating weak coordinating ability of the delocalized lone pair orbital. NBO analysis also shows that the lone pair orbital of N_1 atom is ~ sp^2 hybridized ($sp^{1.6} - sp^{2.4}$), which indicates that the orbital lies in the molecular plane and does not participate in resonance. Therefore, the positions for mercaptan group (-SH) favoring chelate formation with metal atoms/mineral surfaces are 2 and 5 in imidazole, oxazole and thiazole and 2 in pyrazole, isoxazole and isothiazole (Figure 5.1B).

Mercapto derivatives of these reagents may exist as thione and/or thiol forms, and the thiol form can be further ionized in aqueous solutions (Figure 5.1C). As mentioned by Woods et al. (2000) for MBT at pH below their pK_a value (~7), the thione form of these reagents predominates the thiol form, while at pH above their pK_a value reagents exist mainly as thiol ion. Following the discussions from previous studies (Liu et al., 2012; M. Yekeler & Yekeler, 2006), it can be assumed that interaction between these reagents and metal ions or mineral surfaces proceeds through ionized thiol forms. Therefore, only ionized thiol forms were modeled, and their reactivity and interaction ability with metal ions are discussed.

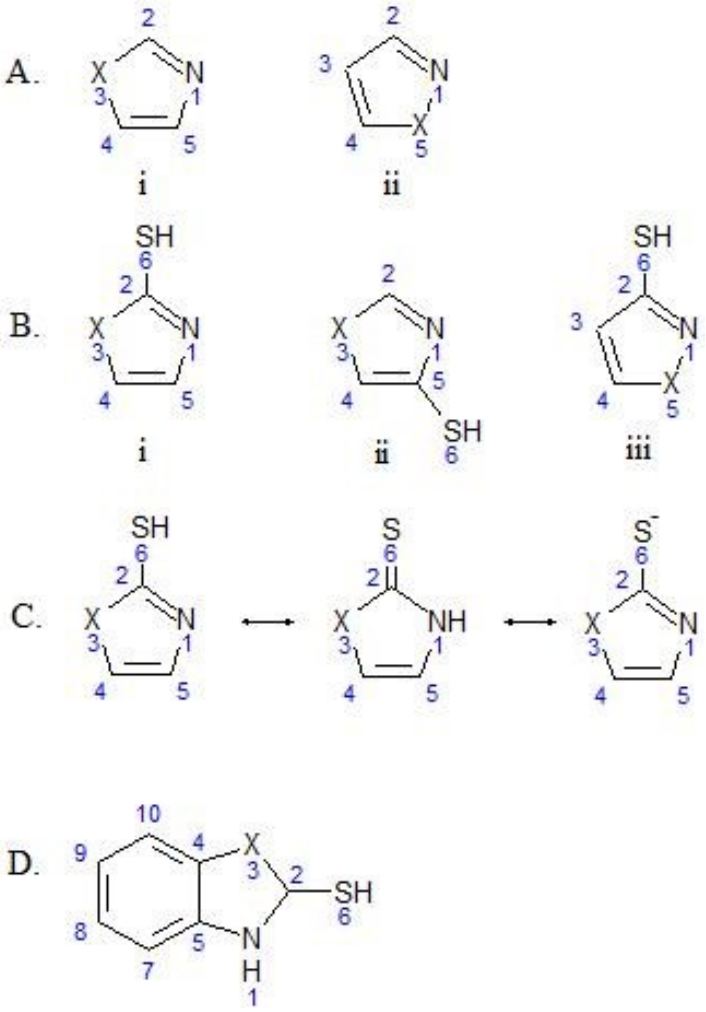

Figure 5.1. (A) Molecular structure of five-membered heterocyclic compounds with two heteroatoms in the aromatic ring (azoles), (i) X: NH in imidazole, O in oxazole and S in thiazole; (ii) X: NH in pyrazole, O in isoxazole and S in isothiazole. (B) Positions for mercaptan group that allow chelate formation with metal ions/mineral surfaces. (C) Schematic representation of thiol, keto and ionized thiol tautomerism in 2-mercaptoazoles. (D) Schematic representation of 2-mercaptobenzoazole compounds; X: NH in MBI, O in MBO and S in MBT.

5.3.1. Geometry and Hybridization of Collector Molecules

The optimized geometrical parameters for ionized form of 2-mercapto and 5-mercapto derivatives of imidazole, oxazole, and thiazole and 2-mercapto derivatives of pyrazole, isoxazole, and isothiazole are given in Table 5.1. The calculated values of different geometrical parameters for 2-mercapto derivatives of imidazole, oxazole, and thiazole are comparable to previously reported values for MBI, MBO and MBT molecules (Liu et al., 2012). For all reagents, the exocyclic S_6 atom and atoms constituting the ring lie in the same plane. This is also evident from the reported values of dihedral angle in Table 5.1.

Table 5.1. Optimized geometrical parameters for 2-mercapto and 5-mercapto derivatives of imidazole, oxazole and thiazole and 2-mercapto derivatives of pyrazole, isoxazole and isothiazole.

Reagent	$r(C_2\text{-}S_6)$[a]	$r(C_2\text{-}N_1)$	$r(C_2\text{-}X_3)$[b]	$r(X_3\text{-}C_4)$	$r(C_4\text{-}C_5)$	$r(N_1\text{-}C_5)$	$\angle(N_1\text{-}C_2\text{-}X_3)$	$\tau(N_1\text{-}S_6\text{-}C_2\text{-}X_3)$
2-mercapto imidazole	1.7395	1.3724	1.3341	1.3797	1.3639	1.3797	109.06	180.00
2-mercapto oxazole	1.7162	1.3143	1.3833	1.3730	1.3463	1.3874	111.13	179.99
2-mercapto thiazole	1.7241	1.3171	1.7764	1.7298	1.3578	1.3739	111.47	179.99
	$r(C_5\text{-}S_6)$	$r(C_5\text{-}N_1)$	$r(C_5\text{-}C_4)$[a]	$r(X_3\text{-}C_4)$	$r(C_2\text{-}X_3)$	$r(N_1\text{-}C_2)$	$\angle(N_1\text{-}C_5\text{-}C_4)$	$\tau(N_1\text{-}S_6\text{-}C_5\text{-}C_4)$
5-mercapto imidazole	1.7585	1.3933	1.3796	1.3815	1.3509	1.3180	108.25	-180.00
5-mercapto oxazole	1.7446	1.413	1.3617	1.3841	1.3442	1.2895	106.66	-180.00
5-mercapto thiazole	1.7512	1.3943	1.3769	1.7244	1.7234	1.2987	112.77	180.00
	$r(C_2\text{-}S_6)$	$r(C_2\text{-}N_1)$	$r(C_2\text{-}C_3)$[a]	$r(C_3\text{-}C_4)$	$r(C_4\text{-}X_5)$	$r(N_1\text{-}X_5)$	$\angle(N_1\text{-}C_2\text{-}C_3)$	$\tau(N_1\text{-}S_6\text{-}C_2\text{-}C_3)$
2-mercapto pyrazole	1.7551	1.3421	1.4261	1.3747	1.3484	1.3608	109.63	180.00
2-mercapto isoxazole	1.7385	1.3227	1.4406	1.3470	1.3406	1.4292	109.99	179.99
2-mercapto isothiazole	1.7451	1.7451	1.4423	1.3582	1.7132	1.6705	113.83	179.99

[a] Refer Figure 1 for numbering scheme; Bond distance (r) in angstrom (Å), bond angles (∠) and dihedral angles (τ) in degree (°).
[b] X atom: N in imidazole and pyrazole, O in oxazole and isoxazole, and S in thiazole and isothiazole.

For the five membered ring to be aromatic, one of the lone pair orbitals belonging to heteroatom X should be close to perpendicular to the molecular plane. NBO analysis shows 100% p-character in one of the lone pair orbitals of atom X for all nine reagent molecules. The

hybridization of the heteroatom X in these molecules is very different from their usual hybridization state (sp^3). For example, in 2-mercaptoimidazole and 2-mercaptoxazole, the hybridization of atoms N_3 and O_3 is close to sp^2. N_3 orbitals binding to C_2 and C_4 atoms through σ-bonds in 2-mercaptoimidazole are $sp^{1.78}$ and $sp^{1.88}$ hybridized, and O_3 orbitals binding to C_2 and C_4 atoms in 2-mercaptoxazole are $sp^{2.12}$ and $sp^{2.26}$ hybridized. The hybridization of two σ-binding orbitals of S_3 in 2-mercaptothiazole is $sp^{4.47}$ and $sp^{4.33}$. The higher p-character of S_3 orbitals binding to C_3 and C_4 atoms in 2-mercaptothiazole is also evident in $\angle C_2\text{-}S_3\text{-}C_4$ of ~ 90°. The lone pair of O_3 and S_3 atoms not participating in aromaticity is $sp^{1.66}$ and $sp^{0.57}$ hybridized in 2-mercaptoxazole and 2-mercaptothiazole, respectively.

The exocyclic S_6 atom binds to C atom through an orbital rich in p-character (hybridization ~ $sp^{4.4}$). Among the three lone pair orbitals of S_6, one has predominantly s-character (~ $sp^{0.2}$) and the remaining two have 100% p-character. Availability of a 100% p-character lone pair orbital perpendicular to the molecular plane indicates delocalization of S_6 lone pair electrons into the ring. This phenomenon is also evident in deviation of calculated C-S bond lengths (S: exocyclic S_6) from standard single C-S bond length of 1.82 Å. Resonance energies associated with delocalization of electrons from ring atoms to S_6 are negligible when compared to resonance energies linked to delocalization of lone pair electrons of S_6 into the ring. For example, in 2-mercapto derivatives of imidazole, oxazole and thiazole, the stabilization energy for delocalization of S_6 lone pair electrons into the ring is 61.56, 74.60 and 72.63 kcal/mol, respectively, while the energy associated with delocalization of electrons from ring atoms to C-S (S: exocyclic S_6) antibonding orbitals is 18.49, 17.74 and 16.57 kcal/mol, respectively.

The extent of delocalization of S_6 lone pair electrons into the aromatic ring should be inversely proportional to the delocalization among the five atoms of the ring. The extent of

resonance among ring atoms is mainly dependent on electronegativity and size of lone pair orbital of heteroatom X. Since O is the most electronegative, conjugation among ring atoms is least effective in molecules of oxazole series. Therefore, delocalization of electrons from S_6 into the ring is strongest in oxazole and isoxazole derivatives, resulting in the shortest C-S bonds. S in thiazole series is the least electronegative. However, size difference between 3p orbitals of S and 2p orbitals of C results in inferior conjugation compared to imidazole and pyrazole derivatives where both electronegativity and orbital size of N work in favour of a stronger conjugation among ring atoms. Thus, aromatic ring in imidazole and pyrazole derivatives is the most reluctant to accept electrons from S_6, resulting in the longest C-S bonds. This is further supported by the order of resonance stabilization energies associated with delocalization of electrons from S_6 into the ring. The C-S bond lengths in 2-mercapto derivatives of imidazole, oxazole and thiazole are significantly shorter than their 5-mercapto derivatives and 2-mercapto derivatives of pyrazole, isoxazole and isothiazole, as the C atom of C_2-S_6 bond in 2-mercapto derivatives of imidazole, oxazole and thiazole is attached directly to two highly electronegative centres (N and X) as compared to only one in other molecules.

5.3.2. Reactivity of Collector Molecules

Table 5.2 shows the calculated values of partial atomic charges, dipole moment, energy of FMOs, and reactivity descriptors (μ, η and ω) for different reagents. Partial charges at different atoms in a molecule are a good indicator of distribution of electron density and possible sites for nucleophilic/electrophilic attack. For all reagents, exocyclic S_6, imine N_1 and heteroatom X are found to be the electron rich centres and likely sites for electrophile attacks. Calculated values of dipole moment suggest that imidazole and pyrazole derivatives would have the strongest initial interactions with electrophilic species via van der Waals attractive forces.

Table 5.2. Calculated values of atomic charge at reactive sites, dipole moment, energy of HOMO and LUMO orbitals, global reactivity descriptors, and energy of molecular orbital containing lone pair of N_1 atom for different mercaptoazole reagents.

Reagent	Mulliken Charges			D (Debye)	HOMO (eV)	LUMO (eV)	μ (eV)	η (eV)	ω (eV)	HOMO-LP[a] (eV)	D′ (eV)
	S_6	N_1	X_3								
2-mercapto imidazole	-0.93	-0.98	-0.80	9.33	-4.851	-0.037	-2.444	2.407	1.241	-7.316	-12.167
2-mercapto oxazole	-0.83	-0.92	-0.57	8.12	-5.176	0.064	-2.556	2.620	1.247	-7.714	-12.890
2-mercapto thiazole	-0.86	-0.89	-0.30	8.85	-5.123	-0.524	-2.824	2.300	1.734	-7.222	-12.346
	S_6	N_1	X_3								
5-mercapto imidazole	-1.02	-0.96	-0.87	13.01	-4.651	-0.019	-2.335	2.316	1.177	-7.424	-12.076
5-mercapto oxazole	-0.96	-0.91	-0.57	9.26	-4.934	-0.182	-2.558	2.376	1.377	-7.953	-12.887
5-mercapto thiazole	-1.02	-0.87	-0.47	10.91	-4.925	-0.724	-2.824	2.101	1.899	-7.482	-12.407
	S_6	N_1	X_5								
2-mercapto pyrazole	-1.02	-0.74	-0.65	11.73	-4.886	0.000	-2.443	2.443	1.221	-7.785	-12.671
2-mercapto isoxazole	-0.92	-0.65	-0.54	8.80	-5.357	-0.376	-2.867	2.490	1.650	-8.291	-13.648
2-mercapto isothiazole	-1.03	-0.76	0.04	10.25	-5.155	-0.743	-2.949	2.206	1.971	-7.665	-12.820

[a] HOMO-LP: HOMO-4 in pyrazole, HOMO-2 in thiazole, and HOMO-3 in remaining reagents.

For all the reagents NBO analysis predicted $3p_z$ lone pair orbital of S_6 atom as the HOMO orbital. For 2-mercapto derivatives HOMO is primarily delocalized over C_2=N_1 antibonding orbital (stabilization energy ~ 30-40 kcal/mol), while for 5-mercapto derivatives it is primarily delocalized over C_5=C_4 antibonding orbital (stabilization energies ~ 25-30 kcal/mol). Mulliken population analysis also points toward similar conclusions. For example, HOMO in 2-mercaptoimidazole is composed of $3p_z$ orbital of S_6 (~ 56%) and $2p_z$ orbitals of N_1 (~ 9%), C_4 (~ 17%) and C_5 (~ 10%). Similarly, HOMO in 2-mercaptopyrazole is composed of $3p_z$ orbital of S_6 (~ 69%) and $2p_z$ orbitals of N_1 (~ 10%) and N_5 (~ 9%). HOMO in 5-mercaptoimidazole is composed of $3p_z$ orbital of S_6 (~ 62%) and $2p_z$ orbitals of C_5 (~ 8%), C_4 (~ 18%) and N_1 (~ 5%). Spatial distribution of HOMO for imidazole and pyrazole derivatives is shown in Figure 2.

Following the frontier molecular orbital theory, it can be concluded that it is primarily the exocyclic S_6 atom that coordinates with attacking electrophiles.

The LUMO in imidazole and pyrazole derivatives, as shown in Figure 5.2, is mainly composed of 2s orbital of H atom (~ 40-50%) in –NH, while remaining contribution comes equally from higher s orbitals of exocyclic S_6 and all atoms constituting the ring excluding atom N_1 and atom C of C-S_6. LUMO in other reagents is composed of higher s orbitals of exocyclic S_6 and all ring atoms except atom N_1 and atom C of C-S_6. The distribution of LUMO orbital over s orbitals of 3-4 atomic centres indicates minimal tendency of these reagents to form a back donation covalent bond with metal species.

Assuming negligible back donation and following the FMO theory, reactivity of these reagents towards heavy metal ions in solution can be described through escaping tendency of HOMO electrons (depicted by μ) and overall nucleophilicity (depicted by $1/\omega$), both of which follow the order: imidazole derivatives > oxazole derivatives > thiazole derivatives.

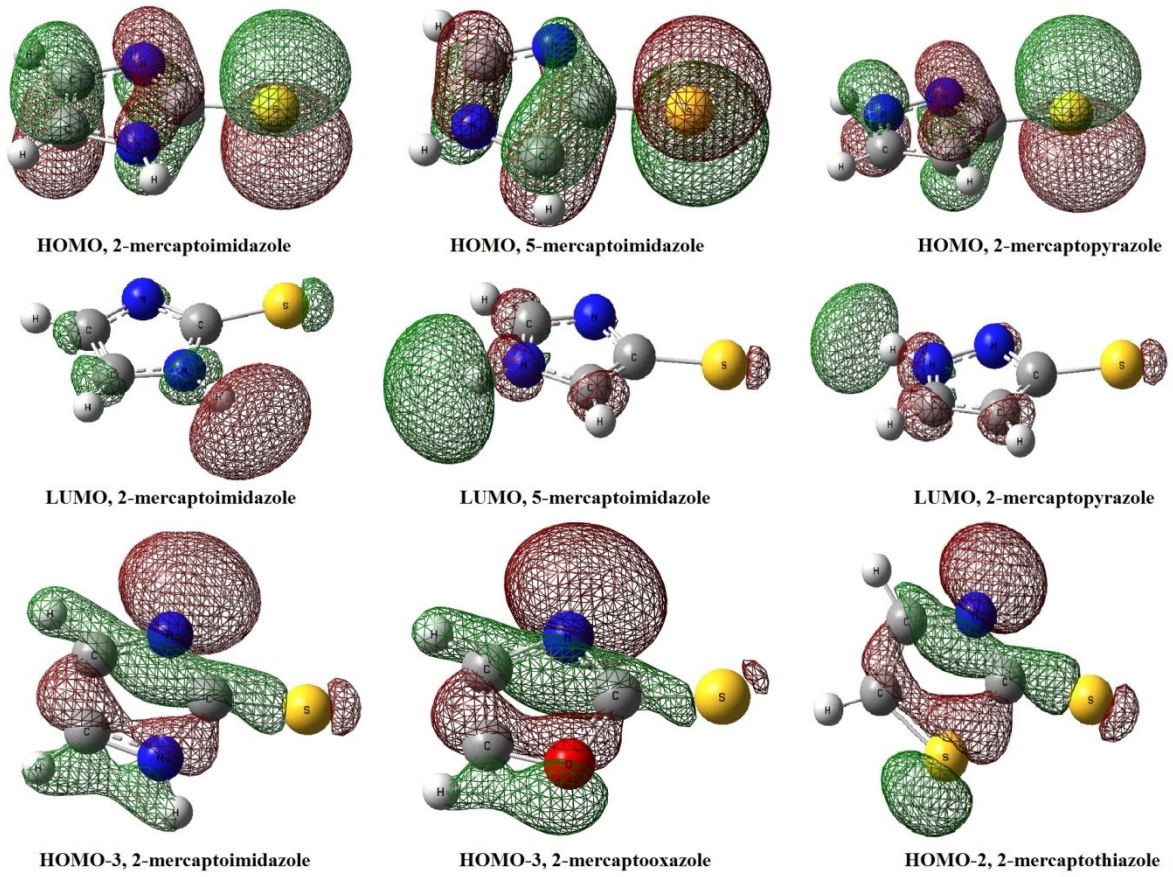

Figure 5.2. Spatial distribution of frontier molecular orbitals of ionised thiol forms of 2-mercaptoimidazole, 5-mercaptoimidazole and 2-mercaptopyrazole, and HOMO-LP orbital of 2-mercaptoimidazole, 2-mercaptoxazole and 2-mercaptothiazole.

The global reactivity descriptors (μ, η, and ω) are based on the energies of FMOs only. The above devised order of reactivity holds true if reactions between these reagents and metal ions (or minerals) are assumed to involve only interactions between their FMOs. However, it is widely known that in heterocyclic aromatic systems containing two heteroatoms, N_1 atom could also participate in bonding with metal ions (or mineral surfaces) via a dative bond due to availability of a non-conjugated lone pair orbital in molecular plane. However, this lone pair orbital is not part of HOMO orbital of these reagents. Instead it represents an occupied orbital lower in energy than the HOMO orbital (represented from hereby as HOMO-LP). The spatial

distribution of this orbital is shown for 2-mercapto derivatives of imidazole, oxazole and thiazole in Figure 5.2. Therefore to predict the correct order of reactivity of these reagents, a reactivity descriptor should also incorporate energy of HOMO-LP orbitals. Persuaded by unavailability of such a reactivity descriptor and considering a weak tendency to form back donation covalent bond, a new reactivity descriptor D′ defined below is considered.

$$D' = E_{HOMO} + E_{HOMO\text{-}LP} \tag{5.1}$$

where E_{HOMO} and $E_{HOMO\text{-}LP}$ are the energies of HOMO and HOMO-LP orbitals, respectively. Based on D′, the reactivity of reagents follows the following order: imidazole derivatives > thiazole derivatives > oxazole derivatives, which is the same as the observed trend for C-S_6 bond lengths. Even if it is assumed that reactivity of N_1 atom is equal among all reagents as lone pair of N_1 atom does not participate in resonance, reactivity order predicted by D′ appears to be correct. For example, reagents of imidazole series have the longest C-S bonds, and therefore it should be the easiest for S_6 atom in reagents of imidazole series to donate electrons. Similarly, the electron donation tendency of S_6 atom in reagents of oxazole series should be the least as they have the shortest C-S_6 bonds.

5.3.3. Complexes with Metal Ions

For the final assessment of chelating ability of different collector reagents shown in Table 5.2 towards Cu, Pb and Zn ions in aqueous solutions, metal-reagent complexes were modeled and their binding energies were calculated. In numerous previous studies, Pb^{2+} and Zn^{2+} ions have been reported to form ML_2 (M: metal, L: ligand) type complexes with these or similar ligands (Banerji, Byrne, & Livingstone, 1982; Buttrus & Mohamed, 2013; Castro et al., 1993; Khullar & Agarwala, 1975; Preti & Tosi, 1977; Szargan, Uhlig, Wittstock, & Roβbach, 1997). A quick

literature survey reveals an ambiguity around the type of complexes Cu forms with these ligands. Some authors suggested formation of CuL_2 type complexes (Basson & du Preez, 1974; Buckley, Goh, Lamb, Fan, & Yang, 2006; Buttrus & Mohamed, 2013; El-Shazly, Salem, El-Sayed, & Hedewy, 1978; Khullar & Agarwala, 1975; Yoshisa, Yamasaki, & Sawada, 1979; Zoete et al., 2000), while others pointed toward the formation of CuL type complexes (Banerji et al., 1982; Loeb, Crivelli, & Andrade, 1991; Preti & Tosi, 1977; Woods et al., 2000). However, it is believed that in all investigations initially CuL_2 type complexes were formed, which might got reduced to CuL type depending on the experimental conditions as mercaptide type ligands have tendency to reduce Cu^{2+} ion to Cu^{+} on complex formation (Loeb et al., 1991). Therefore, ML_2 type complexes were modeled for all three metals. The optimized structures of Cu^{2+}, Pb^{2+} and Zn^{2+} complexes of 2-mercaptoimidazole, 2-mercaptoxazole and 2-mercaptothiazole ligand ions are shown in Figure 5.3, along with Cu^{2+} complexes of 5-mercaptoimidazole and 2-mercaptopyrazole.

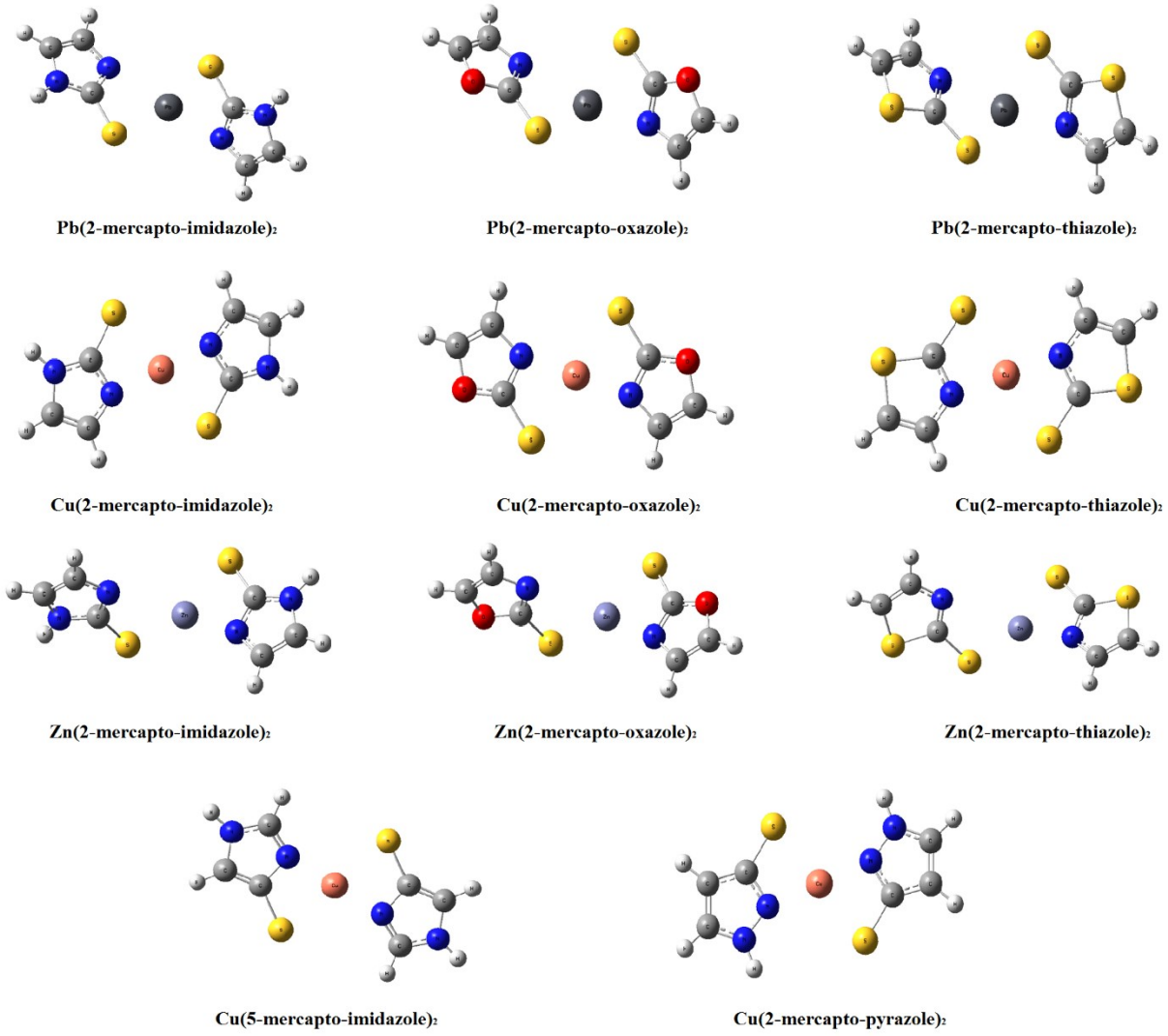

Figure 5.3. Optimized structures of Pb^{2+}, Cu^{2+} and Zn^{2+} complexes with 2-mercaptoimidazole, 2-mercaptoxazole and 2-mercaptothiazole ligands, and Cu^{2+} complexes with 2-mercaptoimidazole and 2-mercaptopyrazole ligands.

Selected optimized geometrical parameters of lead complexes are given in Table 5.3. In all Pb complexes, two ligand ions binds to Pb^{2+} ion to form a hemidirected or distorted square pyramid structure which suggests a gap or hole in the coordination sphere around the Pb^{2+} ion occupied by a stereo-chemically active lone pair of electrons ($6s^2$) on the Pb atom. The hemidirected

structure of Pb^{2+} complexes with anionic ligands and low coordination numbers (2-5) is well documented in literature. The ligand ions are placed symmetrically around the Pb atom as evident by two equal Pb-S and Pb-N distances. Imran et al. (2015) showed that Pb^{2+} bind to 2-mercapto-4-phenylthiazole forming a PbL_2 complex with a hemidirected structure. The reported Pb-S bond lengths (2.788 and 2.818 Å) and ∠S-Pb-N bond angles (58.2° and 57.8°) matches closely with the calculated values for Pb(2-mercaptothiazole)$_2$ complex (2.794 Å, 2.794 Å, 58.8° and 58.8° respectively). There is a scarcity of detailed structural analysis of Pb complexes with similar type of ligands in iterature. NBO analysis predicts covalent bond(s) between Pb and exocyclic S atom(s). It also shows that lone pair on imine nitrogen atom(s) is delocalised over empty lone pair orbital (100% p character) of Pb atom. The calculated stabilization energy for this delocalization for Pb complexes of 2-mercapto-imidazole, 2-mercapto-oxazole and 2-mercapto-thiazole ligands is 44.42, 41.43 and 43.18 kcal/mol respectively. NBO analysis also shows delocalization of 6s lone pair electrons of Pb atom over ring atoms representing backdonation. However, the stabilization energies associated with these delocalizations are very small. For example, the resonance stabilization energy associated with back donation in 2-mercapto-imidazole, 2-mercapto-oxazole and 2-mercapto-thiazole complexes is 1.26, 1.58 and 1.04 kcal/mol respectively. Therefore, the ligand ions bind to the Pb^{2+} ion or Pb atom on mineral surfaces in a bidentate fashion via a covalent bond through exocyclic sulphur (S_6) atom and a dative bond through nitrogen (N_1) atom which is consistent with previous findings. Also, it can be concluded that the extent of back-donation of electrons from Pb atom to ligand atoms is negligible.

Table 5.3. Selected optimized geometrical parameters for complexes of collectors ligands with Pb^{2+} metal ion.

Collector ion	r(Pb-S)	r(Pb-N)	r(C-S)	r(C-N)	∠S-Pb-N	∠S-C-N
2-mercapto-imidazole	2.7954, 2.7949	2.6341, 2.6364	1.7402, 1.7401	1.3296, 1.3297	59.6	122.7
5-mercapto-imidazole	2.7633, 2.7636	2.6583, 2.6580	1.7576, 1.7576	1.3848, 1.3848	60.0	118.8
2-mercapto-pyrazole	2.7566, 2.7567	2.6797, 2.6797	1.7550, 1.7550	1.3380, 1.3380	58.8	118.6
2-mercapto-oxazole	2.8013, 2.8013	2.6644, 2.6644	1.7221, 1.7222	1.3114, 1.3114	59.1	125.1
5-mercapto-oxazole	2.7633, 2.7633	2.7006, 2.6998	1.7481, 1.7481	1.4021, 1.4021	59.7	119.2
2-mercapto-isoxazole	2.7730, 2.7726	2.6946, 2.6993	1.7412, 1.7413	1.3185, 1.3185	57.7	118.5
2-mercapto-thiazole	2.7942, 2.7936	2.6504, 2.6490	1.7322, 1.7321	1.3180, 1.318	58.8	121.0
5-mercapto-thiazole	2.7590, 2.7588	2.6737, 2.6737	1.7564, 1.7564	1.3853, 1.3853	59.3	117.3
2-mercapto-isothiazole	2.7642, 2.7637	2.6691, 2.6688	1.7486, 1.7487	1.3289, 1.3289	58.5	118.7

The key optimized geometrical parameters for different Cu complexes are given in Table 5.4. Copper complexes of these ligands have distorted square planar structure with two chelate rings and five membered heterocyclic aromatic rings lying in same plane. The two ligand ions are placed symmetrically around the Cu atom as evident by two equal Cu-S and Cu-N distances. Some authors have suggested a distorted tetrahedral structures for Cu(II) complexes with similar ligands (Buttrus & Mohamed, 2013) while majority have reported a square planar geometry (Khullar & Agarwala, 1975; Zoete et al., 2000). DFT calculated energies show that a planar geometry is by far the most stable conformation. Furthermore, Cu^{2+} ion is known to form square planar complexes with ligands forming 4 membered chelate rings, e.g. dithiocarbamates (Ngo, Banger, DelaRosa, Toscano, & Welch, 2003) and xanthates (Ivanov, Bredyuk, Antzutkin, & Forsling, 2004). Trans complexes (two S atoms in trans position around Cu) are found to be more stable than cis complexes by 2-5 kcal/mol. NBO analysis shows a bidentate binding between Cu atom and ligand ions. The bond through exocyclic sulphur is predicted to have covalent nature (S ~75%, Cu ~25%). The binding through imine nitrogen is either predicted as a

highly polarized covalent bond (N ~87%, Cu ~13%) or via delocalization of imine nitrogen's lone pair electrons to Cu orbitals (resonance stabilization energy per imine nitrogen ~ 50 kcal/mol). The calculated values of C-N bond lengths in Cu(5-mercapto-imidazole)$_2$ correlates well with previously reported values of 1.961-1.984 Å for C-N bonds (N: heterocyclic imine nitrogen) in Copper(II)-(4-methyl-5-carboxyaldehyde-imidazole) complex (Dominguez-Vera, Rodriguez, Cuesta, Kivekas, & Colacio, 2002). The C-N bond lengths in Cu(2-mercapto-imidazole)$_2$ correlate well to C-N bond length (N: heterocyclic imine nitrogen) of 1.962 Å in Cu(II)-[(2-(benzimidazolyl)-5-(2'-pyridyl)-3-thiapentane] complex (Gilbert, Addison, Nazarenko, & Butcher, 2001a). The calculated values for Cu-S bond lengths couldn't be verified due to scarcity of literature data on copper complexes with four-membered S,N-chelating heterocyclic thionate ligands. However, as expected the calculated values are longer than reported Cu-S distances in copper thionate complexes with five-membered chelate rings (2.387 – 2.397 Å) to accommodate the additional strain (Akrivos, 2001). Similar observations for Cu-S bond lengths elongation (~0.05-0.12 Å) have been reported when the chelate ring size changes from six to five atoms (Akrivos, 2001). Resonance stabilization energies associated with backdonation covalent bonds or delocalization of electrons from Cu atom to ligand atoms or orbitals is negligible in all complexes. Therefore, it can be concluded that the ligand ions bind to copper ions in a bidentate fashion.

Table 5.4. Selected optimized geometrical parameters for complexes of collectors ligands with Cu^{2+} metal ion.

Collector ion	r(Cu-S)	r(Cu-N)	r(C-S)	r(C-N)	∠S-Cu-N	∠S-C-N
2-mercapto-imidazole	2.5027, 2.5059	1.9429, 1.943	1.7303, 1.7304	1.3318, 1.3318	70.9	117.2
5-mercapto-imidazole	2.4444, 2.4444	1.9652, 1.9652	1.7518, 1.7518	1.3827, 1.3827	71.8	112.5
2-mercapto-pyrazole	2.4450, 2.4450	1.9667, 1.9667	1.7513, 1.7513	1.335, 1.335	70.4	112.2
2-mercapto-oxazole	2.5113, 2.5118	1.9496, 1.9496	1.7103, 1.7103	1.3157, 1.3157	70.7	119.4
5-mercapto-oxazole	2.4132, 2.4132	1.9918, 1.9918	1.7432, 1.7432	1.3989, 1.3989	72.2	112.3
2-mercapto-isoxazole	2.4404, 2.4405	1.976, 1.976	1.7372, 1.7372	1.315, 1.315	69.4	112.0
2-mercapto-thiazole	2.4688, 2.4673	1.9594, 1.9595	1.7242, 1.7242	1.3249, 1.3249	70.9	116.4
5-mercapto-thiazole	2.3993, 2.399	1.9897, 1.9897	1.7516, 1.7516	1.3843, 1.3843	71.9	111.3
2-mercapto-isothiazole	2.4205, 2.4206	1.9819, 1.9818	1.740, 1.740	1.3312, 1.3312	70.6	113.0

In zinc complexes, the two ligand ions form a distorted tetrahedral geometry around the Zn atom. Distorted tetrahedral structure for zinc complexes with similar type ligands has been reported in many previous studies (Banerji et al., 1982; Khullar & Agarwala, 1975; Preti & Tosi, 1977). Selected optimized geometrical parameters for different zinc complexes are given in Table 5.5. Though widely used for pharmacological and rubber vulcanization purposes, detailed structural analysis of zinc complexes of these ligands or their benzo derivatives (MBT, MBI, MBO) is missing in literature and most of the related studies have only reported vibrational spectrum. The binding mode of these ligands with Zn^{2+} ion is still not completely understood. Previous studies have reported uni- (N or exocyclic S) and bi-dentate (N and exocyclic S) binding modes for Zn complexes with thiazole derivatives (Baggio, Garland, & Perec, 1993; McCleverty et al., 1980). Banerji et al. (1982) reported vibrational analysis of $Zn(MBT)_2$ and concluded that N atom doesn't participate in metal coordination. Buttrus and Mohamed (2013) and Preti and Tosi (1977) analyzed vibrational spectra of $Zn(MBO)_2$ and suggested bidentate binding through S and O atoms. The data in Table 5 shows that two C-S and C-N distances are different for complexes of imidazole, oxazole and thiazole while they are almost equal for

pyrazole, isoxazole and isothiazole complexes. NBO analysis predicts two Zn-S covalent bonds (S ~84-88%, Zn ~12-16%) for all the complexes. In addition, in imidazole, oxazole and thiazole complexes, lone pair electrons of exocyclic S atom (in shorter Zn-S bond) are delocalized in empty lone pair orbitals of Zn atom with stabilization energies of ~8-10 kcal/mol while the energy associated with this delocalization for other exocyclic S atom is ~2-3 kcal/mol. For pyrazole, isoxazole and isothiazole complexes the magnitude for this stabilization energy is ~8-12 kcal/mol for both exocyclic S atoms. The interaction between Zn and imine nitrogen atom is predicted in form of delocalization of nitrogen lone pair electrons in empty orbitals of Zn atom. The stabilization energy associated with this delocalization of electrons for N atom with shorter Zn-N distances in imidazole, oxazole and thiazole complexes is ~ 35-45 kcal/mol while for other N atom it is ~ 4 kcal/mol. The stabilization energy for nitrogen atom lone pair delocalization to Zn atom in pyrazole, isoxazole and isothiazole complexes for both N atoms is ~ 5kcal/mol. Therefore, from structural data and NBO analysis it can be concluded that in pyrazole, isoxazole and isothiazole complexes, ligand ions bind to Zn atom mainly through exocyclic S atom. In imidazole, oxazole and thiazole complexes, one of the ligand ions shows bidentate binding mode (imine N and exocyclic S) while the other binds to the Zn atom through exocyclic S atom only.

Table 5.5. Selected optimized geometrical parameters for complexes of collectors ligands with Zn^{2+} metal ion.

Collector ion	r(Zn-S)	r(Zn-N)	r(C-S)	r(C-N)	∠S-Zn-N	∠S-C-N
2-mercapto-imidazole*	2.2741, 2.4169	2.1089, 3.4287	1.7378, 1.7542	1.3213, 1.3341	57.1, 71.5	128.5, 119.1
5-mercapto-imidazole*	2.2564, 2.3450	2.2095, 3.252,	1.7661, 1.7561	1.3803, 1.3855	57.3, 71.5	124.0, 115.5
2-mercapto-pyrazole	2.2371, 2.2371	3.1178, 3.1178	1.7663, 1.7664	1.3328, 1.3329	58.8, 58.8	123.4, 123.4
2-mercapto-oxazole*	2.2773, 2.4079	2.1467, 3.2588	1.7214, 1.7395	1.3159, 1.3010	71.1, 56.9	121.4, 131.1
5-mercapto-oxazole*	2.2421, 2.3421	2.1928, 3.1902	1.7608, 1.7608	1.3987, 1.3987	55.1, 55.1	124.1, 124.1
2-mercapto-isoxazole	2.2565, 2.2565	3.2906, 3.2905	1.7532, 1.7532	1.3133, 1.3132	55.1, 55.1	124.9, 124.9
2-mercapto-thiazole*	2.2798, 2.3959	2.1792, 3.3472	1.7484, 1.7312	1.3047, 1.3233	54.8, 70.3	128.5, 118.9
5-mercapto-thiazole*	2.2468, 2.3556	2.2225, 3.0247	1.7657, 1.7552	1.3798, 1.3863	60.5, 70.5	121.0, 114.1
2-mercapto-isothiazole	2.2349, 2.2348	3.2107, 3.2109	1.7538, 1.7537	1.3027, 1.3027	56.7, 56.7	124.4, 124.4

*Zn-S longer for ligand with shorter Zn-N distance.

The Pb-S and Pb-N bonds in oxazole and isoxazole complexes are slightly longer than these bonds in complexes of their counterpart ligands in imidazole and thiazole series indicating a weaker metal-ligand binding in complexes of oxazole series ligands. This is consistent with smaller C-S bond lengths in oxazole series ligand ions. Similarly, the Pb-S bond lengths in complexes of 2-mercapto derivatives of imidazole, oxazole and thiazole are longer than in complexes of 5-mercapto derivatives of these compounds and 2-mercapto derivatives of pyrazole, isoxazole and isothiazole, which is consistent with smaller C-S bond lengths in these ligands in their anionic form. Similar trends are observed in copper and zinc complexes too.

The calculated interaction or binding energies of these complexes are plotted in Figure 5.4(A-C). As evident from the plot, all collector reagents have highest chelating ability towards Cu followed by Pb. For a particular metal, collectors of imidazole series have highest chelating capability followed by collectors of thiazole series. The binding energies for three series of collectors follow the same trend as predicted by D′ and C-S_6 bond lengths. Among the collectors of a particular series, 5-mercapto derivatives show highest binding capability.

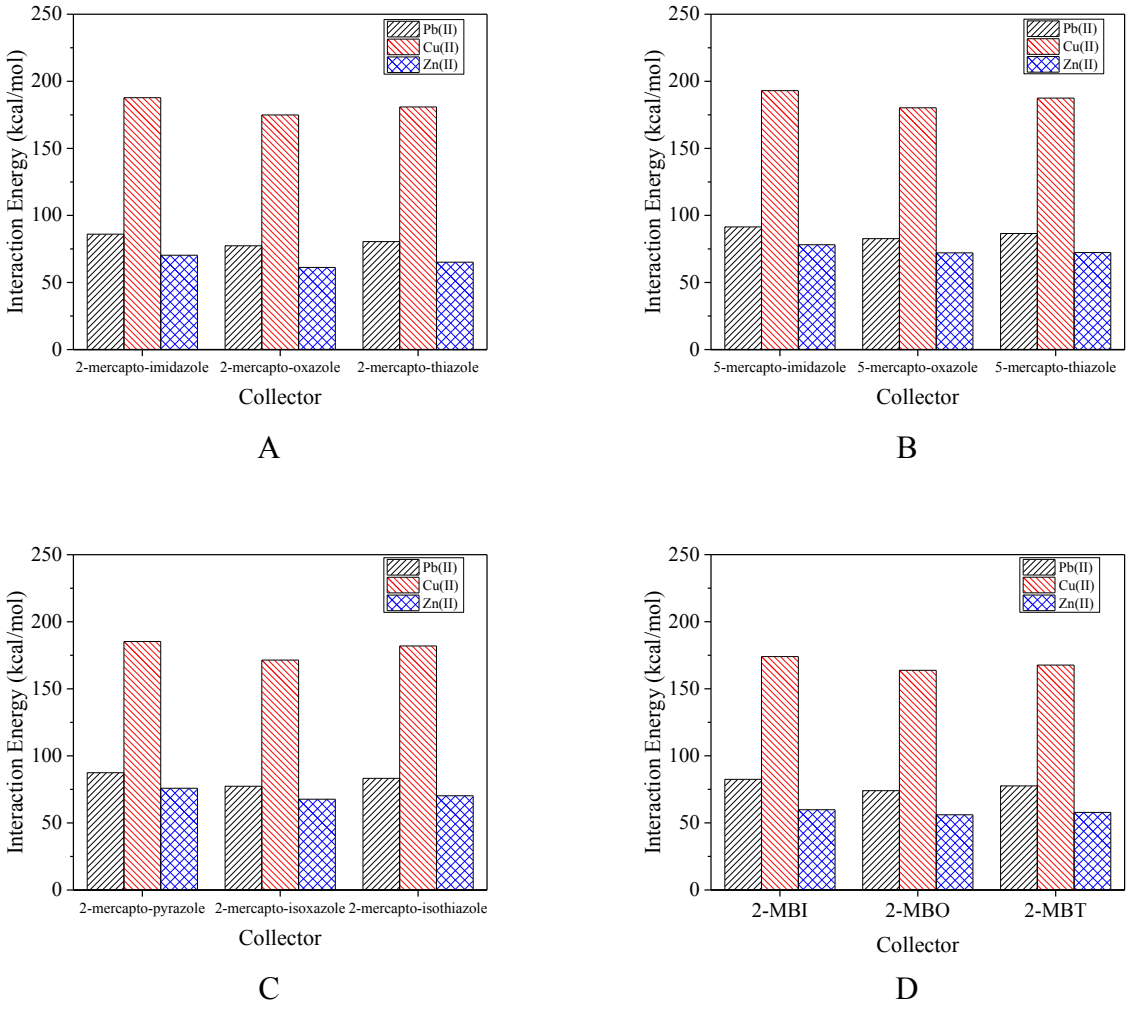

Figure 5.4. Interaction energy of ML_2 type complexes of Pb^{2+}, Cu^{2+} and Zn^{2+} metal ions with (A) 2-mercaptoimidazole, 2-mercaptoxazole and 2-mercaptothiazole; (B) 5-mercaptoimidazole, 5-mercaptoxazole and 5-mercaptothiazole; (C) 2-mercaptopyrazole, 2-mercaptoisoxazole and 2-mercaptoisothiazole; (D) MBI, MBO and MBT collector reagents.

5.3.4. Mercaptobenzoheterocyclic Collectors and their Complexes with Metal Ions

Benzoheterocyclic molecules are the most popular reagents of this class. To investigate the effect of addition of benzene ring on reactivity and chelating capability of basic mercaptoazole

molecules, MBI, MBO and MBT reagents and their complexes with Pb^{2+}, Cu^{2+} and Zn^{2+} ions were modeled. The optimized C_2-S_6 bond lengths, charges at reactive sites S_6 and N_1, and energy of HOMO and HOMO-LP orbitals of MBI, MBO and MBT reagents are given in Table 5.6.

Table 5.6. Optimized C_2-S_6 bond length, charges at binding sites, and energy of HOMO and HOMO-LP orbitals of MBI, MBO and MBT reagents.

Reagent	r(C_2-S_6)[a]	Mulliken Charges		HOMO (eV)	HOMO-LP (eV)
		S_6	N_1		
MBI	1.7244	-0.84	-0.99	-5.108	-6.985
MBO	1.7019	-0.76	-0.91	-5.350	-7.217
MBT	1.7129	-0.81	-0.85	-5.306	-6.376

[a] Previously reported values: 1.741 (MBI), 1.716 (MBO), and 1.728 (MBT) at B3LYP/6-31+G(d,p) level [11].

NBO analysis shows that fused benzene ring in imidazole, oxazole and thiazole molecules acts as a strong electron withdrawing group. Electron density from C_2-N_1 π-bonding orbital and X_3 lone pair orbital is delocalised over benzene atoms through C_4-C_5 π-bonding orbital. Consequently, the azole ring becomes electron deficient and delocalization of exocyclic S_6 lone pair electrons into the azole ring increases. This phenomenon is evident in the reduced bond lengths of C_2-S_6, which are shorter by 0.015, 0.014, and 0.011 Å in MBI, MBO and MBT, respectively than their parent molecules. The electron deficiency of heterocyclic ring is also evident in the decreased partial charge on S_6 and N_1 atoms as well as in decreased HOMO and HOMO-LP energies. Therefore, it can be concluded that mercaptobenzoazole molecules feature reduced nucleophilicity compared to their corresponding parent molecules.

Similar inference could be made from calculated binding energies of complexes of these reagents with Pb^{2+}, Cu^{2+} and Zn^{2+} ions which are plotted in Figure 5.4D. The decrease in binding energy of these reagents is the highest for Cu complexes, followed by Zn complexes. The binding affinity of collector reagents follows the same order as in parent molecules, i.e., MBI >

MBT > MBO. However, the difference in binding energies for any two types of reagents is smaller compared to parent molecules. The largest drop in interaction energies is observed for MBI reagent.

These observations are further supported by the structural data of molecules. The optimized M-S and M-N bond lengths of metal-collector complexes are given in Table 5.7. The structure of Pb and Zn complexes does not differ much from the complexes that these metal ions form with corresponding parent reagent molecules. The decreased electron donating capability of the S_6 atom is evident in increased M-S bond lengths for both Pb and Zn complexes. For Pb^{2+} complexes, the largest deviation in Pb-S bond length occurs in $Pb(MBI)_2$ complex, for which it is ~ 0.01 Å longer than the Pb-S bond in Pb(2-mercaptoimidazole)$_2$ complex, followed by $Pb(MBO)_2$ (~ 0.008 Å) and $Pb(MBT)_2$ (~ 0.006 Å). To accommodate this change while simultaneously avoiding any additional strain due to smaller S-Pb-N and S-C-N angles, the Pb-N bond in these complexes becomes slightly shorter than the Pb-N bond in Pb complexes of corresponding parent reagent molecules. The decrease in Pb-N bond length is the largest in $Pb(MBI)_2$ (~ 0.004 Å), followed by $Pb(MBO)_2$ (~ 0.003 Å) and $Pb(MBT)_2$ (~ 0.0 Å). For Zn^{2+} complexes, both Zn-S and Zn-N bond length are longer than what observed in corresponding complexes of Zn with parent reagent molecules. The largest deviation is observed in $Zn(MBI)_2$ where two Zn-S bonds are 0.056 and 0.005 Å longer and two Zn-N distances are 0.052 and 0.023 Å longer. In $Zn(MBO)_2$, the two Zn-S distances are 0.043 and 0.004 Å longer and two Zn-N distances are 0.019 and 0.042 Å longer whereas in $Zn(MBT)_2$, the two Zn-S distances are 0.048 and 0.004 Å longer and two Zn-N distances are 0.021 and 0.051 Å longer. The magnitude of deviation in M-S and M-N bond lengths in Pb and Zn complexes thus follows the observed trend of deceasing interaction energies.

The inclusion of benzene ring in these molecules results in a significant difference in the structure of Cu complexes. All three complexes are planar. NBO analysis shows strong interaction between Cu^{2+} and exocyclic S_6 atom, however, very weak interaction between Cu^{2+} and N_1 atom. This is supported by shorter Cu-S (~ 2.161-2.163 Å) and longer Cu-N (~ 3.175-3.218 Å) bond lengths in these complexes, compared to Cu-S and Cu-N bond lengths in complexes shown in Table 5.4. This observation suggests that the binding mode is primarily monodentate. This is the first report on the detailed structural analysis of $Cu(MBT)_2$, $Cu(MBI)_2$, and $Cu(MBO)_2$ complexes in molecular form. The change of binding mode from bidentate to mostly monodentate could be the reason for large differences in interaction energies of Cu^{2+} complexes of mercaptoazole and mercaptobenzoazole reagents. The bidentate or multidentate ligands have been verified experimentally to form more stable complexes than monodentate ligands (Schwarzenbach, 1952).

As mentioned earlier, previous experimental studies on flotation performance reported the order of reactivity of these reagents with Cu and Pb sulfides as: MBT > MBI > MBO. However, interaction energies, C-S_6 bond lengths, energy of HOMO and HOMO-LP orbitals and atomic charges calculated from DFT, all points toward the following decreasing order of reactivity for reagents' head groups: MBI > MBT > MBO. It is worth mentioning again that in addition to chelating ability of reagents' head group, flotation performance is also greatly influenced by the length and structure of the hydrocarbon tails. Due to lower electronegativity of heteroatom S, reagents (and resultant metal-complexes) of thiazole series including MBT would have lower solubility because of weaker hydrogen bonding with water molecules. Therefore, it may be concluded that though reactivity and chelating ability of reagents of thiazole series toward

different heavy metal ions is less than reagents of imidazole series, they could be better flotation collectors due to lower solubility of their metal complexes.

5.3.5. Effect of Substituent Groups on Reactivity and Chelating Ability of Collectors

The position and nature of substituent group(s) attached to the main functional group of a reagent could have great influence on its reactivity and chelating ability towards metal ions or mineral surfaces. To investigate this effect, different activating and deactivating groups were placed at positions 4 and 5 in 2-mercapto derivatives of imidazole, oxazole and thiazole, and at positions 8 and 9 in MBT. The reactivity parameters for modified collector molecules were calculated and their complexes with Pb^{2+} and Cu^{2+} ions were modeled.

Among the three substituent groups, ethyl features electron donating (inductive) effect; ethyl carbonyl, electron withdrawing (inductive and resonance) effect; and ethoxy group, either electron withdrawing or electron donating (inductive and/or resonance) effect. The C_2-S_6 bond lengths and HOMO energies of the substituted reagent molecules are given in Table 5.7.

Table 5.7. C_2-S_6 bond length and HOMO energy of substituted reagent molecules and change in C_2-S_6 bond length and HOMO energy compared to parent reagents.

Reagent	r(C_2-S_6)	Δ r(C_2-S_6)*	HOMO (eV)	Δ HOMO (eV)*
5-ethyl-2-mercaptoimidazole	1.7411	0.0016	-4.770	0.081
5-ethoxy-2-mercaptoimidazole	1.7375	-0.0020	-4.720	0.131
5-ethylcarbonyl-2-mercaptoimidazole	1.7315	-0.0080	-5.085	-0.233
4-ethyl-2-mercaptoimidazole	1.7419	0.0024	-4.729	0.122
4-ethoxy-2-mercaptoimidazole	1.7414	0.0019	-4.615	0.236
4- ethylcarbonyl-2-mercaptoimidazole	1.7205	-0.0190	-5.159	-0.308
5-ethyl-2-mercaptoxazole	1.7180	0.0018	-5.105	0.071
5-ethoxy-2-mercaptoxazole	1.7141	-0.0021	-5.079	0.097
5- ethylcarbonyl-2-mercaptoxazole	1.7112	-0.0050	-5.373	-0.198
4-ethyl-2-mercaptoxazole	1.7196	0.0034	-5.033	0.142
4-ethoxy-2-mercaptoxazole	1.7183	0.0021	-4.880	0.295
4- ethylcarbonyl-2-mercaptoxazole	1.6965	-0.0197	-5.485	-0.310
5-ethyl-2-mercaptothiazole	1.7259	0.0018	-5.051	0.072
5-ethoxy-2-mercaptothiazole	1.7215	-0.0026	-5.018	0.106
5- ethylcarbonyl-2-mercaptothiazole	1.7184	-0.0057	-5.298	-0.174
4-ethyl-2-mercaptothiazole	1.7264	0.0023	-5.024	0.100
4-ethoxy-2-mercaptothiazole	1.7275	0.0034	-4.892	0.232
4- ethylcarbonyl-2-mercaptothiazole	1.7034	-0.0207	-5.402	-0.279
9-ethyl-2-mercaptobenzothiazole	1.7148	0.0019	-5.230	0.078
9-ethoxy-2-mercaptobenzothiazole	1.7157	0.0028	-5.130	0.177
9- ethylcarbonyl-2-mercaptobenzothiazole	1.7042	-0.0087	-5.445	-0.137
8-ethyl-2-mercaptobenzothiazole	1.7141	0.0012	-5.260	0.048
8-ethoxy-2-mercaptobenzothiazole	1.7104	-0.0025	-5.248	0.059
8- ethylcarbonyl-2-mercaptobenzothiazole	1.7088	-0.0041	-5.401	-0.094

* Δ r(C_2-S_6) and Δ HOMO represent the change in C_2-S_6 bond length and HOMO energy of substituted reagents relative to parent reagents

Following inferences could be made from the data reported in Table 5.7:

- Ethylcarbonyl (COR) group decreases electron density of azole ring due to its deactivating nature, which results in the increased delocalization of S_6 lone pair electrons into the ring. This is evident in shorter C_2-S_6 bond lengths and lower HOMO energies of substituted molecules compared to parent molecules. COR group at position 4 has a greater influence on

the reactivity of the binding group as resonating structures shown in Figure 5C has a positive fractional charge on C_2 atom. When it is at position 5, resonance scheme of Figure 5.5D is followed wherein heteroatom X bears the positive charge.

- Ethoxy (OR) group decreases electron density of azole ring via inductive effect and act as an activing group via resonance (R). When OR group is at position 4, the inductive effect would create a δ^+ charge on atom 4 and delocalization of this charge follows the scheme shown in Figure 5.5D, whereas its substitution at position 5 would create a δ^+ charge on atom 5 as shown in Figure 5.5C. Therefore, the inductive effect of ethoxy group is stronger when it is placed at position 5. The excess negative charge due to resonance effect is delocalized over the ring atoms more effectively when OR group is placed at position 4 as shown in Figures 5.5A and 5.5B. When the OR group is at position 4, one of the resonating structures has negative charge on C_2 atom, which results in elongation of C_2-S_6 bond. Therefore, +R effect of OR group is stronger at position 4. For OR at position 4, strong resonance effect dominates weak inductive effect and results in longer C_2-S_6 bonds and increased HOMO energies. For substitution at position 5, strong inductive effect dominates weak resonance effect and results in shorter C_2-S_6 bonds.
- The inductive effect of ethyl group increases electron density of azole ring and results in longer C_2-S_6 bonds and increased HOMO energies. The increase in C_2-S_6 bond length and HOMO energy is more prominent when ethyl group is placed at position 4, as one of the resonating structures would have a δ^- charge on C_2 atom.
- For MBT, ethyl substitution at position 8 or 9 increases electron density of extended aromatic system and results in longer C-S bonds and increased HOMO energies. Ethyl group at position 9 causes a larger difference as the molecule would have a δ^- charge on position 5 due

to resonance, which could be delocalized over positions 1 and 2 as shown in Figure 5.5A. Placing ethyl group at position 8 would bring δ^- charge at position 4, which can not be delocalized further over the azole ring atoms (as shown in Figure 5B). Similarly, deactivating nature of COR group is more pronounced when it is at position 9, as such resonating structures would have a partial positive charge at atom 5. Following the above discussion, substitution of ethoxy group at position 9 (or 8) in MBT molecule would have a similar effect as substituting ethoxy group at position 4 (or 5) in 2-mercaptothiazole.

- Effect of substituent group(s) on collectors' reactivity is more prominent in 2-mercaptothiazole molecule than in MBT. This is because the influence of a substituent group on reactivity of reagent head group decreases with increasing its distance from the head group.

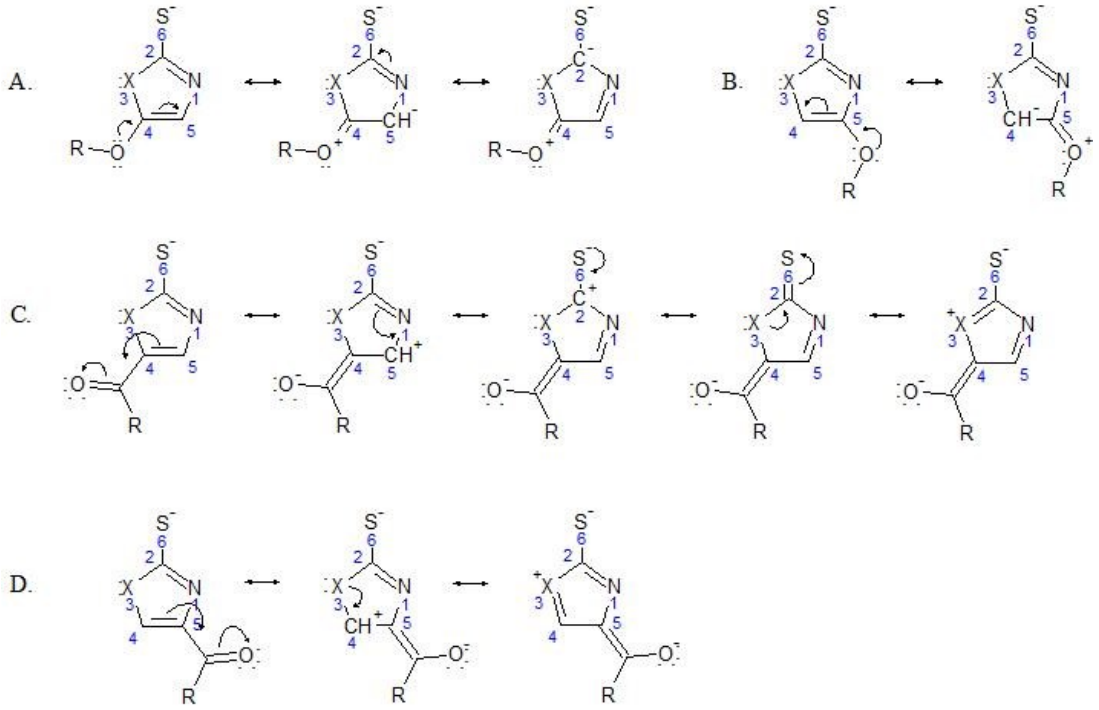

Figure 5.5. Resonance schemes demonstrating activating or deactivating effect of different types of substituent groups at position 4 or 5 in 2-mercaptoazole reagents.

DFT calculated interaction energies of Pb^{2+} and Cu^{2+} complexes of these reagents are plotted in Figure 5.6. As clearly seen, ethyl group at position 4 or 5 resulted in an increase in the interaction energies for both Pb and Cu complexes. Also evident is that the increase in the interaction energies is larger when ethyl group is at position 4 than at position 5. Deactivating influence of ethylcarbonyl group is also evident as shown by the decrease in the interaction energies for both Cu and Pb complexes, and the effect is more pronounced for Cu complexes than for Pb complexes. For Pb complexes, decrease in complexation or interaction energy is more pronounced when ethylcarbonyl group is at position 4 than at position 5, which is consistent with the observed trend of reactivity. However, for Cu complexes, ethylcarbonyl group at position 5 has a greater impact. This could be attributed to stearic effects of bulky ethylcarbonyl group at position 5 in square planar geometry, which reduces the accessibility of metal ions to N lone pair electrons. The impact of ethoxy group addition on collectors' chelating ability is consistent with the trend observed in reactivity of corresponding chelating molecules. At position 5, the presence of ethoxy group resulted in weaker binding with both Pb^{2+} and Cu^{2+} ions, whereas at position 4 it resulted in an increase in the interaction energies. It is also noteworthy to mention that the activating or deactivating effect of different substituent groups is more pronounced in the case of Cu complexes than Pb complexes.

The influence of substituent groups on reactivity and chelating capability of mercaptoazole reagents has never been explored before. Observations of present study correlate well with findings of the only previous study reported in this context (Foye & Lo, 1972). Observations for the effect of substituent groups on reactivity of MBT reagent correlate well with the findings reported in the past which showed that ethyl and alkoxy group at position 9 leads to increased

reactivity of the binding group and enhanced flotation performance (Marabini et al., 2007; M. Yekeler & Yekeler, 2006; H. Yekeler & Yekeler, 2006).

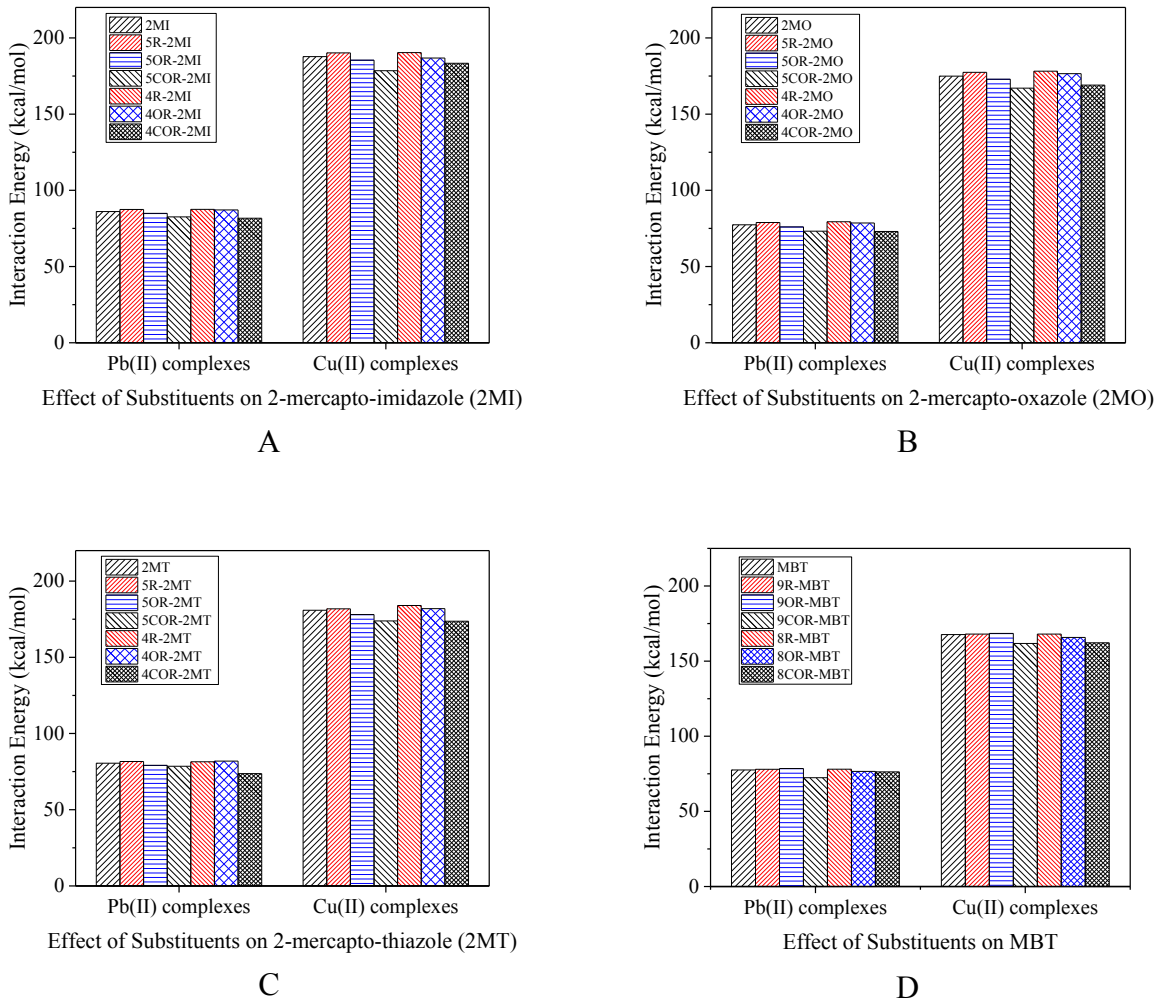

Figure 5.6. Effect of substituent groups' type and position on chelating abilities of collector molecules toward Pb^{2+} and Cu^{2+} ions; Parent collector molecule: (A) 2-mercaptoimidazole, (B) 2-mercaptooxazole, (C) 2-mercaptothiazole, and (D) MBT.

5.3.6. Effect of Chelate Ring Size

Reactivity and metal ion selectivity of a chelating reagent depend on many structural features of the reagent, including the size of the chelate ring it forms with the metal. Five or six membered

chelate rings are usually the most stable (Diehl, 1937; Sillen, Martell, & Bjerrum, 1984). To analyse the effect of chelate ring size on reactivity and chelating ability of heterocyclic aromatic reagents, mercaptan (–SH) group in 2-mercaptoimidazole was replaced by methylmercaptan (–CH_2SH) and ethenylmercaptan (–C_2H_2SH) groups as in 2-methylmercaptanimidazole (**I**) and 2-ethenylmercaptanimidazole (**II**) reagents, respectively. Geometry of anionic form of these reagents was optimized, and reactivity parameters were calculated. The molecular structure and spatial distribution of FMOs of **I** and **II** reagents are given in Figure 5.7.

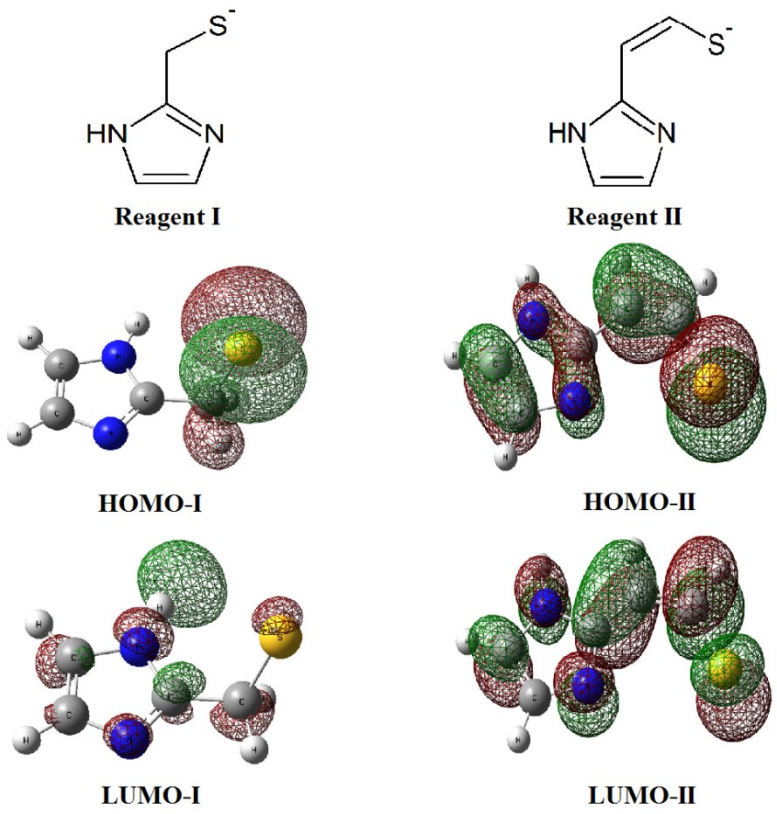

Figure 5.7. Molecular structure and spatial distribution of frontier molecular orbitals of reagents I and II.

In the most stable conformation, S atom in **I** lies outside the plane containing the ring atoms with $\tau(N_1\text{-}C_2\text{-}C_6\text{-}S_7) \sim 113°$ while S atom in **II** is coplanar with aromatic ring with $\tau(N_1\text{-}C_2\text{-}C_6\text{-}$

S_8) ~ 0°. The optimized C-S bond length is 1.856 Å in **I** and 1.733 Å in **II** (Table 5.8). A large deviation of C-S bond length from standard single C-S bond in **II** suggests a strong delocalization of S lone pair electrons over an extended conjugated system involving ring atoms and C_6–C_7 π-bond. This is also evident in a smaller atomic charge at S atom (-0.93) in **II** than in **I** (-1.04). Spatial distribution of HOMO orbital ($3p_z$ of S) shows that HOMO in **I** is concentrated mainly on S atom while in **II** it is delocalized throughout the molecule. A localized HOMO orbital with longer C-S bond and higher atomic charge at S suggests a higher nucleophilicity of **I**. The calculated values of ω for **I** and **II** are 1.363 and 1.627 eV, respectively, which are higher than corresponding 2-mercaptoimidazole.

Table 5.8. Calculated C-S bond length and energy of HOMO and LUMO of I and II reagents as well as M-S and M-N bond lengths in $Cu(I)_2$, $Cu(II)_2$, $Pb(I)_2$ and $Pb(II)_2$ complexes.

Reagent	r(C-S)	HOMO (eV)	LUMO (eV)	Pb Complex		Cu Complex	
				r(Pb-S)	r(Pb-N)	r(Cu-S)	r(Cu-N)
I	1.8553	-5.049	-0.130	2.718, 2.701	2.482	2.346	1.995
II	1.7326	-4.773	-0.500	2.753	2.620	2.332	1.992

Bond lengths (r) are in angstrom (Å)

ML_2 type complexes of **I** and **II** reagents with Cu^{2+} and Pb^{2+} ions were modeled. Optimized structures of these complexes are shown in Figure 5.8. In Cu complexes, ligand ions coordinate to metal ion in a bidentate manner through S and imine N atoms with two equal Cu-S and Cu-N bonds. Optimized Cu-S and Cu-N bond lengths are 2.346 and 1.995 Å, respectively, in $Cu(\mathbf{I})_2$ and 2.332 and 1.992 Å, respectively, in $Cu(\mathbf{II})_2$. The computed bond lengths compare well with the previously reported values (Cu-S ~ 2.33-2.37 Å, C-N ~1.96-2.01 Å) for S,N coordinated Cu^{2+} complexes of five and six membered chelate rings (Gilbert, Addison, Nazarenko, &

Butcher, 2001b; Vaidyanathan, Balamurugan, Sivagnanam, & Palaniandavar, 2001). Decreased strain due to the six-membered chelate ring in Cu(**II**)$_2$ is reflected in shortening of Cu-S bond by 0.014 Å. Cu(**I**)$_2$ complex is of distorted square planar geometry with two chelate rings and two imidazole rings lying in the same plane. Cu(**II**)$_2$ complex departs from planar structure and has a distorted tetrahedral geometry. Each individual chelate ring is coplanar with the imidazole ring being attached, and angle between the two chelate planes is ~ 40.15°. This structural difference seems to arise from very short distance between S atom of one ligand, and H atom and aromatic electron cloud of the other ligand in square planar geometry. Repulsion between lone pair electrons of S atom of one ligand, and H atom and aromatic electron cloud of the other ligand distorts the planar geometry of the complex. Thus, compared to 2-mercaptoimidazole, binding of Cu^{2+} with **I** and **II** is stronger through S atoms and slightly weaker through N atoms.

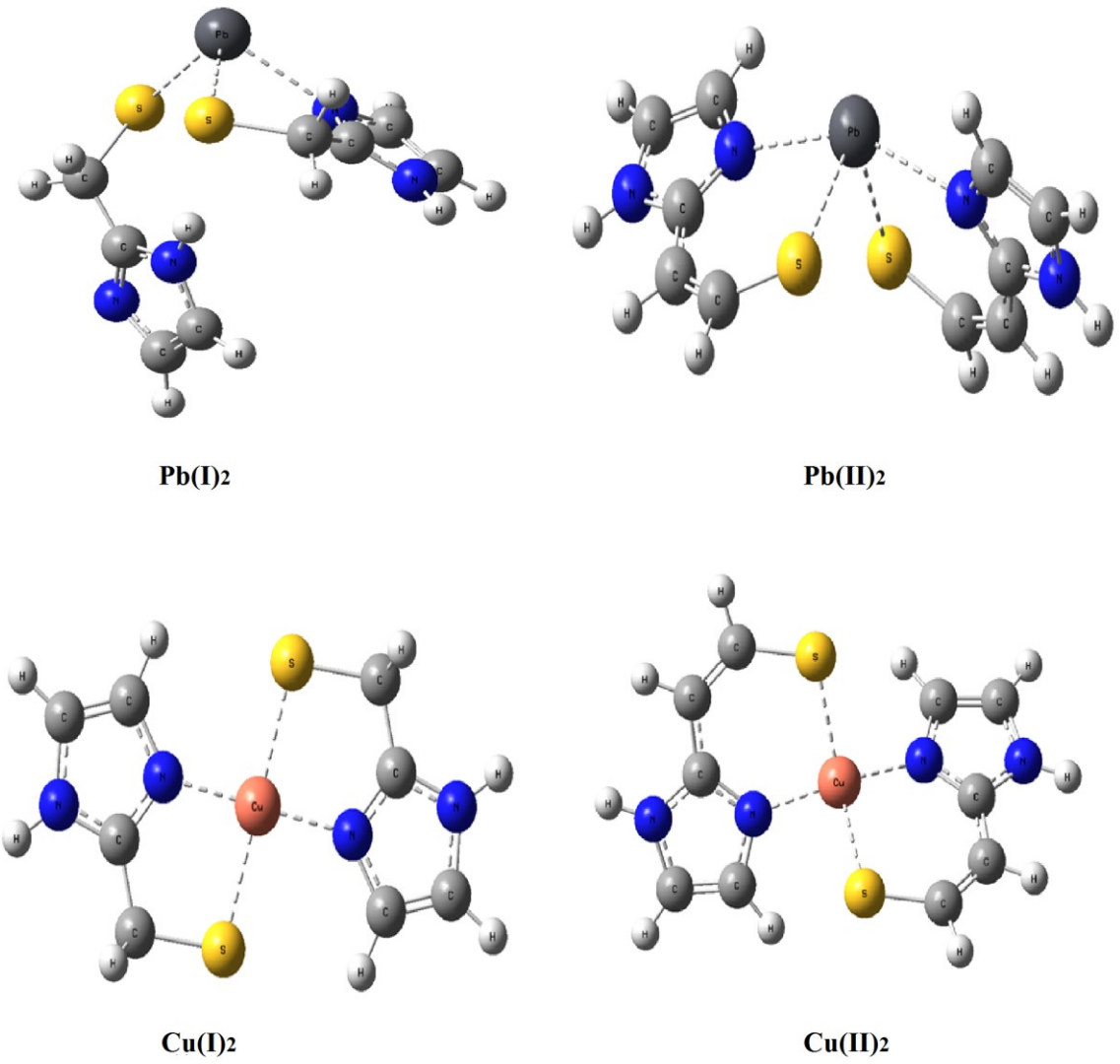

Figure 5.8. Optimized structures of Cu(I)$_2$, Cu(II)$_2$, Pb(I)$_2$ and Pb(II)$_2$ complexes.

Pb(**I**)$_2$ and Pb(**II**)$_2$ complexes have hemidirected trigonal pyramidal and distorted square pyramidal geometry, respectively. In Pb(**II**)$_2$ complex, ligand ions bind to Pb atom in a bidentate fashion with two equal Pb-S (2.753 Å) and Pb-N (2.620 Å) bonds. The Pb-S and Pb-N bond lengths correlate well with previous reported values in S,N coordinated Pb complexes of five-membered chelate rings (Casas et al., 2003; Pedrido et al., 2005; Labisbal et al., 2000; Sousa-Perdrares et al., 2005) . In Pb(**I**)$_2$ complexes, binding is bidentate through one ligand whereas other ligand binds to Pb atom through S only resulting in a three coordinated complex. Two Pb-S

bonds are slightly different (2.718 and 2.701 Å) from each other and both are slightly shorter than the corresponding bonds in Pb(**II**)$_2$. Pb-N bond (2.482 Å) is much shorter compared to Pb-N bonds in Pb(**II**)$_2$. Three coordinated Pb complexes are not unusual and complexes of Pb-S_3, Pb-S_2N binding modes (even though fourth electron rich centre was available for coordination) have been reported to exist (Magyar et al., 2005). We suggest that two ligands (**I**) are too close to each other for a distorted square pyramidal geometry around Pb atom, thus destabilizing the complex and resulting in three coordinated complex.

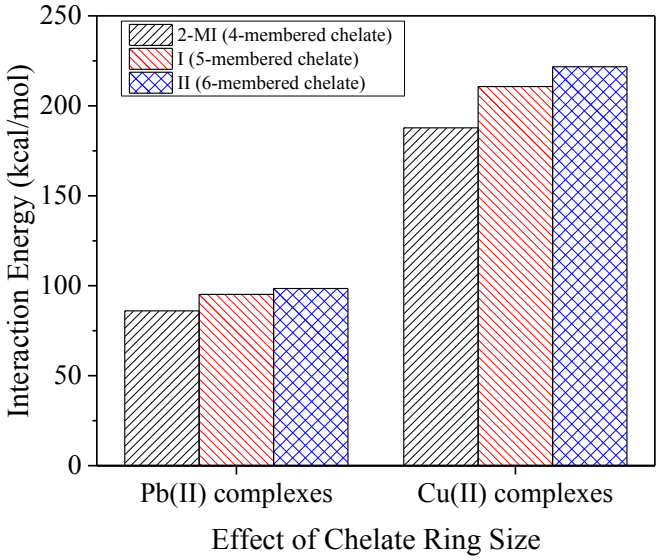

Figure 5.9. Comparison of DFT calculated interaction energies of Cu(I)$_2$, Cu(II)$_2$, Pb(I)$_2$, and Pb(II)$_2$ complexes with Cu(2-mercapto-imidazole)$_2$ and Pb(2-mercapto-imidazole)$_2$ complexes

DFT calculated binding energies for these Cu^{2+} and Pb^{2+} complexes are compared with Pb(2-mercapto-imidazole)$_2$ and Cu(2-mercapto-imidazole)$_2$ complexes in Figure 5.9. As clearly seen, five or six-membered chelate rings are more stable than four-membered chelates. Change in interaction energy on increasing chelate ring size from four-membered to five-membered is more

for Cu complex than for Pb complex. The relationship between the change in complex stability on increasing chelate ring size from five to six-membered is complex and often depends on the electronic feature and size of metal ions. An increase in chelate ring size from five-membered to six-membered is believed to favour the complex formation with smaller metal ions than larger metal ions (Cukrowski, Cukrowska, Hancock, & Anderegg, 1995). However, this rule has been devised by studying the chelating behavior of N-N, O-O and N-O chelating ligands (Cukrowski et al., 1995). For both Cu^{2+} and Pb^{2+} complexes under consideration, a slight increase in interaction energies with increasing chelate ring size from five-membered to six-membered is observed. However, the change in interaction energy is slightly higher for Cu complex than for Pb complex.

Observations reported in this and the earlier sections suggest that chelating reagents based on the imidazole molecules should be more powerful than the reagents based on thiazole or oxazole molecules. So, a detailed study on adsoption mechanism of 2-mercaptoimidazole reagent on mineral surfaces should be conducted. Also, designing the head group in a manner that it forms five or six membered chelate rings with metals instead of four membered chelate rings would increase the chelating ability.

5.4. Conclusion

In summary, reactivity and chelating ability of five membered heterocyclic aromatic reagents (azoles) toward Pb^{2+}, Cu^{2+}, and Zn^{2+} metal ions in aqueous solution is studied using density functional theory methods. A new reactivity descriptor (D′) that incorporates the role of lone pair orbital of imine N atom in determining the reactivity is established, as widely used global reactivity descriptors (μ, η, and ω) failed to predict the correct order of reactivity. Consistent

with experimental findings, reagents bind metal ions in a bidentate fashion through exocyclic S and endocyclic imine N atoms.

Reagents of imidazole series were found to possess the strongest chelating ability followed by reagents of thiazole and oxazole series. The extent of delocalization of lone pair electrons of exocyclic S atom over azole ring atoms plays a dominant role in determining reactivity of a reagent. All reagents showed the highest binding affinity toward Cu ions followed by Pb and Zn ions. It is observed that the reactivity and chelating capability of a reagent is influenced by both the type and position of substituent groups. Activating or deactivating effect of a substituent group was found to be more prominent at position 4 than at position 5. DFT calculation confirmed that widely used mercaptobenzoheterocyclic reagents were less reactive than their parent azole molecules. The predicted effect of substituted groups on reactivity of mercaptobenzoheterocyclic reagents is consistent with experimental results. The increase in chelate ring(s) size from four membered to five or six membered complexes showed a positive influence on the chelating ability of the reagent with heavy metal ions which had been verified experimentally in earlier studies. The observed order of reactivity among different collector molecules is successfully linked to the differences in molecular structure of the reagents.

Predicted order of reactivity and chelating ability of head groups of reagents are supported by the calculated values of multiple parameters, including C-S bond length, interaction energy of complex formation, HOMO energy and atomic charges. The deviation of predicted order of reactivity/chelating ability from the experimentally observed flotation performance is attributed to the influence of hydrophobicity of ligand molecules (linked to the structure of hydrocarbon chains) on these experimentally derived parameters as well as to the influence of mineral surface structure on the adsorption process.

5.3. References

Ai-Mayouf, A. M., Al-Ameery, A. K., & Al-Suhybani, A. A. (2001). Comparison of inhibition efficiency of some azoles on corrosion of type 304 stainless steel in acidic solutions. *British Corrosion Journal, 36*(2), 127-132.

Akrivos, P. D. (2001). Recent studies in the coordination chemistry of heterocyclic thiones and thionates. *Coordination Chemistry Reviews, 213*(1), 181-210.

Baggio, R., Garland, T., Maria, & Perec, M. (1993). Interaction of zinc and cadmium bis(benzothiazole-2-thiolates) with nitrogen bases. *Journal of Chemical Society, Dalton Transactions,* (1), 3367-3372.

Banerji, S., Byrne, R. E., & Livingstone, S. E. (1982). Metal complexes of 2-mercaptobenzothiazole. *Transition Metal Chemistry, 7*(1), 5-10.

Basson, W. D., & du Preez, A. L. (1974). Reactions of thiazolidine-2-thiones with copper(II). *Journal of the Chemical Society, Dalton Transactions,* (16), 1708-1711.

Buckley, A. N., Goh, S., Wei, Lamb, R., Fan, L., & Yang, Y. (2006). XPS, static SIMS and NEXAFS spectroscopic investigation of thiol adsorption on metals and metal sulfides. *ECS Transactions, 2*(3), 107-119.

Buttrus, N. H., & Mohamed, S. M. (2013). Synthesis and characterization of Ni^{+2}, Cu^{+2} and Zn^{+2} complexes with benzoxazole-2-thionate, diphenyl phosphinomethane and iodine. *Research Journal of Chemical Sciences, 3*(6), 54-59.

Casas, J. S., Castellano, E. E., Ellena, J., Garcia, T., Sanchez, A., Sordo, J. & Viddarate, M. J. (2003). Compositional and Structural Variety of Diphenyllead(IV) Complexes Obtained by Reaction of Diphenyllead Dichloride with Thiosemicarbazones. *Inorganic Chemistry*, *42*, 2584-2595.

Castro, R., Garcia-Vazquez, J. A., Romero, J., Sousa, A., McAuliffe, C. A., & Pritchard, R. (1993). Electrochemical synthesis of benzothiazole-2-thionato complexes of nickel(II), zinc(II) and cadmium(II): The crystal structure of 2,2′-bipyridine bis(benzothiazole-2-thionato)zinc(II). *Polyhedron, 12*(18), 2241-2247.

Cukrowski, I., Cukrowska, E., Hancock, R. D., & Anderegg, G. (1995). The effect of chelate ring size on metal ion size-based selectivity in polyamine ligands containing pyridyl and saturated nitrogen donor groups. *Analytica Chimica Acta, 312*(3), 307-321.

Diehl, H. (1937). The chelate rings. *Chemical Reviews, 21*(1), 39-111. doi:10.1021/cr60068a003

Dominguez-Vera, J. M., Rodriguez, A., Cuesta, R., Kivekas, R., & Colacio, E. (2002). A tris-imidazolecarboxyaldehyde copper(II) complex with unusual carbonyl co-ordination: Structure and reactivity. *Journal of the Chemical Society, Dalton Transactions,* (4), 561-565.

El-Shazly, M. F., Salem, T., El-Sayed, M. A., & Hedewy, S. (1978). Coordination chemistry of benzothiazole derivatives. 2-mercaptobenzothiazole and 2-(o-hydroxyphenyl)benzothiazole complexes with cu(II), ni(II) and co(II). *Inorganica Chimica Acta, 29*(0), 155-163.

Foye, W. O., & Lo, J. (1972). Metal-binding abilities of antibacterial heterocyclic thiones. *Journal of Pharmaceutical Sciences, 61*(8), 1209-1212.

Gilbert, J. G., Addison, A. W., Nazarenko, A. Y., & Butcher, R. J. (2001a). Copper(II) complexes of new unsymmetrical NSN thioether ligands. *Inorganica Chimica Acta, 324*(1-2), 123-130.

Gilbert, J. G., Addison, A. W., Nazarenko, A. Y., & Butcher, R. J. (2001b). Copper(II) complexes of new unsymmetrical NSN thioether ligands. *Inorganica Chimica Acta, 324*(1–2), 123-130.

Imran, M., Mix, A., Neumann, B., Stammler, H., Monkowius, U., Gründlinger, P., & Mitzel, N. W. (2015). Hemi- and holo-directed lead(II) complexes in a soft ligand environment. *Dalton Transactions,* (3), 924-937.

Ivanov, A., Bredyuk, O., Antzutkin, O., & Forsling, W. (2004). Copper(II) and nickel(II) alkylxanthate complexes (R = C_2H_5, i-C_3H_7, i-C_4H_9, s-C_4H_9, and C_5H_{11}): EPR and solid-state 13C CP/MAS NMR studies. *Russian Journal of Coordination Chemistry, 30*(7), 480-485.

Khullar, I. P., & Agarwala, U. (1975). Complexes of 2-mercaptobenzothiazole with cu(II), ni(II), co(II), cd(II), zn(II), pb(II), ag(I), and TI(I). *Canadian Journal of Chemistry, 53*(8), 1165-1171.

Labisbal, E., Sousa, A., Castiñeiras, A., García-Vázquez, J. A., Romero, J. & West, D. X. (2000). Spectral and structural studies of metal complexes of isatin 3-hexamethyleneiminylthiosemicarbazone prepared electrochemically. *Polyhedron, 19(10),* 1255-1262.

Liu, G., Zeng, H., Lu, Q., Zhong, H., Choi, P., & Xu, Z. (2012). Adsorption of mercaptobenzoheterocyclic compounds on sulfide mineral surfaces: A density functional theory study of structure–reactivity relations. *Colloids and Surfaces A: Physicochemical and Engineering Aspects, 409*(0), 1-9.

Loeb, B., Crivelli, I., & Andrade, C. (1991). The 2-mercaptobenzothiazole and copper(II) reaction. *Synthesis and Reactivity in Inorganic and Metal-Organic Chemistry, 21*(2), 331-342.

Magyar, J. S., Weng, T., Stern, C. M., Dye, D. F., Rous, B. W., Payne, J. C., . . . Godwin, H. A. (2005). Reexamination of lead(II) coordination preferences in sulfur-rich sites: Implications

for a critical mechanism of lead poisoning. *Journal of the American Chemical Society, 127*(26), 9495-9505.

Maier, G. S., & Dobiáš, B. (1997). 2-mercaptobenzothiazole and derivatives in the flotation of galena, chalcocite and sphalerite: A study of flotation, adsorption and microcalorimetry. *Minerals Engineering, 10*(12), 1375-1393.

Marabini, A. M., Barbaro, M., & Alesse, V. (1991). New reagents in sulphide mineral flotation. *International Journal of Mineral Processing, 33*(1–4), 291-306.

Marabini, A. M., Ciriachi, M., Plescia, P., & Barbaro, M. (2007). Chelating reagents for flotation. *Minerals Engineering, 20*(10), 1014-1025.

McCleverty, J. A., Morrison, N. J., Spencer, N., Ashworth, C. C., Bailey, N. A., Johnson, M. R., . . . Taylor, C. R. (1980). Aspects of the inorganic chemistry of rubber vulcanisation. part 2. anionic mixed-ligand zinc complexes derived from dialkyldithiocarbamates, 2-mercapto-benzothiazole, -benzoxazole, and -benzimidazole, and the crystal and molecular structures of $[NEt_4][zn(S_2CNMe_2)_3]$, $[NBun_4][zn(C_7H_4NS_2)_3(OH_2)]$, $[NBun_4][zn(S_2CNMe_2)_2(C_7H_4NS_2)]\cdot C_2H_5OH$, and $[NBun_4][zn(S_2CNMe_2)(C_7H_4NS_2)_2]$. *Journal of Chemical Society, Dalton Transactions,* (10), 1945-1957.

Ngo, S. C., Banger, K. K., DelaRosa, M. J., Toscano, P. J., & Welch, J. T. (2003). Thermal and structural characterization of a series of homoleptic cu(II) dialkyldithiocarbamate complexes: Bigger is only marginally better for potential MOCVD performance. *Polyhedron, 22*(12), 1575-1583.

Pedrido, R., Bermejo, M. R., Romero, J. M., Vazquez, M., Gonzalez-Noya, A. M., Manerio, M., Rodriguez, M. J. & Fernandez, M. I. (2005). Syntheses and X-ray characterization of metal complexes with the pentadentate thiosemicarbazone ligand bis(4-N-

methylthiosemicarbazone)-2,6-diacetylpyridine. The first pentacoordinate lead(II) complex with a pentagonal geometry. *Dalton Transactions, 2005*, 572-579.

Preti, C., & Tosi, G. (1977). Transition metal complexes of deprotonated 2-mercaptobenzoxazole. study of the thiol-thioketo form equilibrium. *Canadian Journal of Chemistry, 55*, 1409-1414.

Schwarzenbach, G. (1952). Der chelateffekt. *Helvetica Chimica Acta, 35*(7), 2344-2359.

Sillen, L. G., Martell, A. E., & Bjerrum, J. (1984). *Stability constants of metal-ion complexes, special publication (royal society of chemistry, great britain)* (2nd ed.). London: Chemical Society.

Sousa-Pedrares, A., Casanova, M. I., Garcia-Vazquez, J. A., M. L. Duran, M. L., J. Romero, J., Sousa, A., Silver, J. & Titler, P. J. (2003). Synthesis and X-ray Structures of Tin(IV) and Lead(II) Complexes with Heterocyclic Thiones. *European Journal of Inorganic Chemistry, vol. 2003*, 678-686.

Storvick, J. P. (1986). *A comparison of mercaptothiazoline, mercaptobenzothiazole, mercaptobenzimidazole, and mercaptobenzoxazole as inhibitors of 90/10 cupro-nickle alloy corrosion in searwater* (PhD).

Szargan, R., Uhlig, I., Wittstock, G., & Roβbach, P. (1997). New methods in flotation research—application of synchrotron radiation to investigation of adsorbates on modified galena surfaces. *International Journal of Mineral Processing, 51*(1–4), 151-161.

Vaidyanathan, M., Balamurugan, R., Sivagnanam, U., & Palaniandavar, M. (2001). Synthesis, structure, spectra and redox of cu(II) complexes of chelating bis(benzimidazole)-thioether ligands as models for electron transfer blue copper proteins. *Dalton Transactions,* (23), 3498-3506.

Woods, R., Hope, G. A., & Watling, K. (2000). **A SERS spectroelectrochemical investigation of the interaction of 2-mercaptobenzothiazole with copper, silver and gold surfaces**. *Journal of Applied Electrochemistry, 30*(11), 1209-1222.

Yekeler, M., & Yekeler, H. (2006). A density functional study on the efficiencies of 2-mercaptobenzoxazole and its derivatives as chelating agents in flotation processes. *Colloids and Surfaces A: Physicochemical and Engineering Aspects, 286*(1–3), 121-125.

Yekeler, H., & Yekeler, M. (2006). Predicting the efficiencies of 2-mercaptobenzothiazole collectors used as chelating agents in flotation processes: A density-functional study. *Journal of Molecular Modeling, 12*(6), 763-768.

Yoshisa, T., Yamasaki, K., & Sawada, S. (1979). An X-ray photoelectron spectroscopic study of 2-mercaptobenzothiazole metal complexes. *Bulletin of the Chemical Society of Japan, 52*(10), 2908-2912.

Zoete, V., Bailly, F., Vezin, H., Teissier, E., Duriez, P., Fruchart, J., . . . Bernier, J. (2000). 4-mercaptoimidazoles derived from the naturally occurring antioxidant ovothiols 1. antioxidant properties. *Free Radical Research, 32*(6), 515-524.

Chapter – 6

Reactivity and Binding Ability of Neutral Type Collectors

6.1. Introduction

Froth flotation is the single most commonly utilized separation process in the minerals industry for producing mineral concentrates and coal cleaning (Urbina, 2003). The choice of collector type to be used in flotation is of vital importance as these reagents induce differences in the hydrophobicity of the mineral surfaces to facilitate the attachment of target mineral particles to air bubbles. The most commonly used sulfide mineral collectors are xanthate derivatives. Xanthates are the most widely used collectors and they interact with majority of sulfide minerals. However, they suffer some practical disadvantages, including minimal selectivity among different sulfide minerals and ease of decomposition (Fairthorne, Fornasiero, & Ralston, 1997a). This poor selectivity often increases plant operating costs as additional reagents are employed to achieve the desired selectivity and efficiency.

Neutral collectors such as thionocarbamates, thioureas derivatives, and xanthogen formates are another important class of flotation reagents and have found extensive use in the industry especially in flotation of copper ores and copper activated zinc minerals. These collectors are generally less powerful than the xanthate family (Fairthorne, Fornasiero, & Ralston, 1996). However, they provide better selectivity against pyrite and are stable in acidic conditions (Ackerman, Harris, Klimpel, & Aplan, 2000; Fairthorne, Fornasiero, & Ralston, 1997b;

Fairthorne et al., 1996). Many previous studies have attempted to elucidate the interaction mechanisms of these collectors with base metal sulphides and/or metal ions. For dialkyl thionocarbamate and thiourea collectors a consensus on the interaction mechanism couldn't be reached from the literature. Some researchers have concluded these reagents binds to metal atoms mainly through sulphur atom (Brown, Hope, Schweinsberg, & Fredericks, 1995; Fairthorne et al., 1997b; Fairthorne et al., 1996; Woods, Hope, & Watling, 2000; Woods & Hope, 1999). Others have proposed chelate formation at the metal centre through binding with sulphur and nitrogen atoms (Ackerman, Harris, Klimpel, & Aplan, 1984; Ackerman, Harris, Klimpel, & Aplan, 1987a; Marabini, Barbaro, & Alesse, 1991). Leppinen, Basilio, & Yoon (1988) reported that a dialkyl thionocarbamate collector interact with Cu through its sulphur atom at pH < 6 and through sulphur and oxygen atoms at pH > 6. More recently developed derivatives having an alkoxy carbonyl group attached to nitrogen have been reported to form six membered rings with metal centre through sulphur and oxygen atom (of carbonyl) (Fairthorne et al., 1997a; Fairthorne et al., 1997b; Mielczarski & Yoon, 1989). Ackerman et al. (1987a; 2000) have reported formation of six membered rings through sulphur and oxygen atoms for xanthogen formate derivatives. Studies exploring the interaction of neutral S,N-dialkyl dithiocarbamate and dialkyl trithiocarbonate collectors can't be found in literature. However, their applications in mineral flotation have been reported (Coetzer & Davidtz, 1989; Kimble & Bresson, 1985).

The substituent groups in neutral collectors have a more profound effect than in xanthates where the alkyl group length/conformation primarily effects the reagent's solubility and hydrophobicity of the adsorbed species (Ackerman, Harris, Klimpel, & Aplan, 1987b). In addition to conferring hydrophobicity, the substituent groups in these molecules may also alter the electron density and thus modifies reactivity and binding mode of the functional group. Many

previous studies have explored the effect of substituent groups on performance of neutral collectors. Ackerman et al. (1984; 1987a) studied the effect of N- and O- substituents in thionocarbamates on flotation recovery. They concluded that a longer or branched alkyl chain linked to oxygen increases the collecting power of the reagent due to greater hydrophobicity. For nitrogen atom, an increase in recovery was reported for longer straight chains and accounted for lower solubility while for branched and unsaturated chains a decrease in recovery was observed which was attributed to stearic inaccessibility of the nitrogen centre and increased hydrophilicity. The increased recovery with introduction of an alkoxy carbonyl substituent on N-position has been explained through enhanced stability of the metal-reagent complex due to formation of six membered ring (Fairthorne et al., 1997b). For xanthate formate, Ackerman et al. (2000) concluded that a change in length and type of alkyl group to aralkyl for xanthogen substituent in xanthogen formate doesn't have a significant impact on recovery and flotation rate for copper sulphides. A slight decrease in recovery observed on increasing the chain length was attributed to decreased reagent solubility. Branched chain substituent were found to decrease selectivity against pyrite. For the formate substituent a decrease in recovery was observed on increasing the chain length and attributed to decreased solubility. The phenyl and benzyl groups were reported to increase and decrease the flotation recovery respectively as they change in the reactivity of the functional group due to their electron donating and withdrawing effects respectively. Coetzer et al. (1989) studied the effect of substituents on dialkyl dithiocarbamate and trithiocarbonate reagents and reported an increase in recovery with increase in chain length in both N- and S-positions. Substitution of benzyl/allyl group at S-position decreased recovery, while at N-position this resulted in an increase.

The selectivity of chelating reagents such as thionocarbamate and thiourea collectors arises due to metal ion specificity and is not eccentric to mineral surface structures as in the case of xanthate collectors (Ackerman et al., 1984; Basilio, 1989; Leppinen et al., 1988; D. Nagaraj, 1988; D. R. Nagaraj, Lewellyn, Wang, Mingione, & Scanlon, 1988; Seryakova, Vorobiova, Glembotsky, & Zolotov, 1975). The reactivity and degree of selectivity of such collectors towards a particular metal depends mainly on the nature of donor atoms in collector's functional group, attached substituent groups, and the resulting metal chelate stability (D. Nagaraj, 1988). However, as evident from the above discussion experimental techniques may not be the most suitable method to characterize the effect of each structural element in collector's molecular structure on its reactivity and selectivity towards different metals in a quantitative or qualitative manner. For example, increase and decrease in flotation recovery in case of thionocarbamates and xanthogen formates respectively, on increasing the alkyl chain length of substituent group has been explained through same logic of decreased solubility and increased hydrophobicity (Ackerman et al., 1984; Ackerman et al., 2000).

As discussed in chapter 1, effective and economical processing of future difficult-to-treat ores demands an urgent need to design and develop new performance chemicals with superior metal or mineral selectivity (Marabini et al., 1991; Urbina, 2003). In section 1.1, computational quantum chemistry methods were identified as powerful tools to establish the structural requirement of such reagents by exploring the reactivity and binding ability of existing collector classes theoretically. In the present chapter we use DFT to understand how the reactivity of neutral collectors and their interaction ability towards different metal ions is influenced by changes in the structure of collector molecules. Starting with a simple neutral collector, i.e., a mono-thio carbonate, the functional group of the collector molecules was gradually modified to

cover important neutral collector classes, namely, thionocarbamate, thiourea, dithiocarbamate, xanthogenformate and trithiocarbonate. The generic molecular structures of these collectors are given in section 2.3.2. Predicted orders of reactivity and interaction energies obtained through theoretical calculations were related to structural characteristics of the collector. Following that, the effect of different N and O-substituents in thionocarbamate and thiourea on their reactivity and interaction strength toward different metal ions is discussed

6.2. Methodology

The methodology specific to this part of the thesis is discussed in detail in section 4.2.

6.3. Results and Discussion

To analyse and understand the computed results in an efficient manner, this section is divided into two sub-sections. First the reactivity of basic functional group of various neutral collector classes and their binding affinities to different heavy metal ions is discussed. Followed by that the influence of substituent groups on a collector's reactivity and interaction capability with metal ions is discussed by considering different substituents groups attached to the main thionocarbamate and thiourea functional group.

6.3.1. Reactivity of Different Neutral Collectors

The basic functional group of the neutral collectors can be considered as $–X_1–(C_1=S_1)–X_2–$, where X_1 and X_2 are electronegative heteroatoms (O, N, and S). Various combinations of heteroatoms around the $–(C_1=S_1)–$ entity resulted in five neutral collector types, namely, thionocarbamate (TC), thiourea (TU), monothiocarbonate (MTC), dithiocarbamate (DTC), and

trithiocarbonate (TTC). Xanthogen formate (XF) represented by basic functional group $–O_1–(C_1=S_1)–S_2–(C_2=O_2)–O_3–$ is also considered in the analysis as it forms another important type of neutral collector. The substituent groups on all the molecules were kept fixed as 'ethyl' to eliminate the effect of substituent group(s) on the calculated parameters.

6.3.1.1. Geometry and Hybridization

Key geometric parameters involving different atoms comprising the functional group of these collector molecules are given in Table 1. The dihedral angle $\Omega(X_1\text{-}S_2\text{-}C_1\text{-}X_2)$ for TC, TU, MTC, DTC and TTC is close to 180 degrees which indicates that all four atoms in $–X_1–(C_1=S_1)–X_2–$ group lie in the same plane. The hybridization of carbon atom in these molecules is found to be very different from the usual sp^2 hybridization. As shown in Table 6.1, the three orbitals of carbon atom forming three sigma bonds (with S_1, X_1, and X_2) are hybridized differently in each of the molecules. For all the molecules, one lone pair at the two heteroatoms has 100% p-character and is in conjugation with π^*(C–S) orbital. The stabilization energies associated with these delocalization as predicted by NBO analysis are found to lie between 30-85 kcal/mol. This delocalization of electrons is also evident in the calculated values of $C_1–S_1$, $C_1–X_1$ and $C_1–X_2$ bond lengths. All the bond lengths in $–X_1–(C_1=S_1)–X_2–$ group lie between the values for the standard single and double bond lengths between the corresponding atoms.

Table 6.1. Key geometrical parameters and hybridization of carbon atom in basic functional group(s) of neutral collectors

Collector	Bond length (Å)			Dihedral angle	Hybridization of carbon atom		
	C_1-S_1	C_1X_1	C_1X_2	X_1-S_1-C_1-X_2	C_1-S_1	C_1X_1	C_1X_2
TC[a]	1.68[c]	1.34[c]	1.33[c]	-180.00	$sp^{1.61}$	$sp^{2.6}$	$sp^{1.94}$
TU	1.71[d]	1.35[d]	1.35[d]	-179.99	$sp^{1.82}$	$sp^{2.1}$	$sp^{2.1}$
DTC[b]	1.69	1.76	1.33	-178.65	$sp^{2.32}$	$sp^{2.34}$	$sp^{1.97}$
TTC	1.66	1.74	1.74	-180.00	$sp^{1.75}$	$sp^{2.15}$	$sp^{2.15}$
MTC	1.66	1.32	1.31	-179.99	$sp^{1.39}$	$sp^{2.44}$	$sp^{2.44}$
XF(I)	C_1-S_1: 1.65	C_1-O_1: 1.32	C_1-S_2: 1.77	S_2-S_1-C_1-O_1: -179.90	C_1-S_1: $sp^{1.45}$	C_1-O_1: $sp^{2.33}$	C_1-S_2: $sp^{2.32}$
	C_2-O_2: 1.20	C_2-S_2: 1.86	C_2-O_3: 1.31	O_3-O_2-C_2-S_2: 174.10	C_2-O_2: $sp^{1.67}$	C_2-S_2: $sp^{2.36}$	C_2-O_3: sp^{2}
XF(II)	C_1-S_1: 1.64	C_1-O_1: 1.32	C_1-S_2: 1.80	S_2-S_1-C_1-O_1: 174.88	C_1-S_1: $sp^{2.39}$	C_1-O_1: $sp^{2.43}$	C_1-S_2: $sp^{2.39}$
	C_2-O_2: 1.20	C_2-S_2: 1.80	C_2-O_3: 1.33	O_3-O_2-C_2-S_2: 175.86	C_2-O_2: $sp^{4.03}$	C_2-S_2: $sp^{2.22}$	C_2-O_3: $sp^{2.1}$

[a] X_1: oxygen, X_2: nitrogen; [b] X_1:sulphur, X_2: nitrogen

[c] Previously calculated values: 1.673 Å (C-S), 1.346 Å (C-N), and 1.337 Å (C-O) in O-isopropyl-N-ethyl thionocarbamate (Liu, Zhong, Dai, & Xia, 2008)

[d] Previously calculated values: 1.719 Å (C-S) and 1.35 Å (C-N) in N-propyl-N'-ethyl-thiourea(LIU, ZHONG, XIA, WANG, & DAI, 2010)

For xanthogen formate molecule, two optimized structures with an energy difference of 4.27 kcal/mol were obtained. For both the structures, atoms in O_1–(C_1=S_1)–S_2 and S_2–(C_2=O_2)–O_3 groups lie in two different planes. The two planes are perpendicular for the more stable structure XF(I) while they lie at an angle of 34 degrees for structure XF(II). For both structures, NBO analysis indicated strong delocalization stabilization energies (~30kcal/mol) for one of the lone pair of O_2 with antibonding orbitals of S_2-C_2 and C_2-O_3. This is also evident in the C_2-O_2 bond length which is less than standard C-O double bond indicating a partial triple bond. For structure XF(I), the lone pair at S_2 was found to be conjugation with C_1-S_1 with stabilization energy of 41 kcal/mol, whereas in XF(II) it was found to be conjugation with both C_1-S_1 and C_2-O_2 with stabilization energies of 13 kcal/mol and 9 kcal/mol. This phenomenon is evident in a longer C_1S_2 and a shorter C_2-S_2 bond length in XF(II).

6.3.1.2. Reactivity of Neutral Collectors

Partial charge at different atoms in a molecule is a good indicator of distribution of electron density and possible sites for nucleophilic or electrophilic attack. As evident from Table 6.2, both natural and mulliken population analysis schemes predicted the basic functional group in neutral collectors be electron rich and prone to be attacked by electrophiles. However, the trend observed through the schemes are different. Mulliken charges predicted atom S1 to be most electron rich for most of the collectors while natural scheme calculated excess electron density on heteroatoms X_1 and X_2 (three O atoms in XF). Thus, atomic charges, in alone shouldn't be used to compare the reactivity of two or more species or to locate the ultimate reactive site within a molecule.

Table 6.2. Partial atomic charges at the atoms comprising the basic functional groups

Collector	Mulliken charge			Natural charges		
	S_1	X_1	X_2	S_1	X_1	X_2
TC	-0.57	-0.57	-0.83	-0.36	-0.56	-0.61
TU	-0.86	-0.76	-0.76	-0.44	-0.61	-0.61
DTC	-0.75	-0.19	-0.63	-0.29	0.29	-0.58
TTC	-0.62	-0.37	-0.37	-0.11	0.37	0.37
MTC	-0.61	-0.54	-0.45	-0.29	-0.55	-0.55
XF(I)	S_1 = -0.52	O_1 = -0.43	S_2 = -0.47	S_1 = -0.14	O_1 = -0.54	S_2 = 0.24
	O_2 = -0.66	O_3 = -0.36		O_2 = -0.60	O_3 = -0.55	
XF(II)	S_1 = -0.54	O_1 = -0.45	S_2 = -0.14	S_1 = -0.07	O_1 = -0.54	S_2 = 0.19
	O_2 = -0.63	O_3 = -0.58		O_2 = -0.60	O_3 = -0.56	

The reactions between collectors and metal ions (or minerals) proceed through electrostatic interactions and formation of covalent and back donation covalent bonds (Liu et al., 2008). Calculated values for dipole moment (Table 3) suggest that TC, TU and XF(II) would have the strongest van der Waals interactions with metal ions and mineral surfaces in aqueous solutions. For all the collectors, natural bond order (NBO) analysis predicted one of the lone pairs of S_1

atom as the HOMO orbital. In $–X_1–(C_1=S_1)–X_2–$ functional group, this orbital is delocalised over C_1-X_1 and C_2-X_2 antibonding orbitals through small stabilization energies (~5-8 kcal/mol). Calculation of atomic percent contributions to HOMO through molecular orbitals coefficients for these collectors showed the major contribution (>80%) from p orbitals of S_1 atom, followed by smaller contributions from X_1 and X_2 atoms. For XF(I) and XF(II), the HOMO orbital lone pair electrons of S_1 is delocalised over antibonding orbitals of C_1-O_1 and C_1-S_2 with stabilization energies ~15-18 kcal/mol. For XF(II), the antibonding orbital of C_1-S_2 is further delocalised over C_2 and O_5 centres with stabilization energies ~10 kcal/mol. HOMO in XF(I) is mainly composed of p orbitals of S_1 (~76%) and S_2 (~14%), and in XF(II), major contributions come from S_1(~70%), S_2 (~11%) and C_2 (~11%).

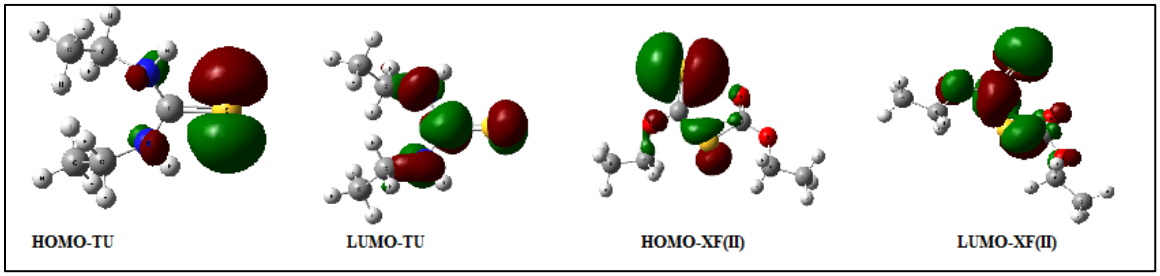

Figure 6.1. Spatial distribution of frontier orbitals for diethyl thiourea (TU) and diethyl xanthogen formate (XF(II))

The spatial distribution of HOMO and LUMO for TU and XF(II) collectors is shown in Figure 6.1. For $X_1–(C_1=S_1)–X_2–$ group collectors, LUMO is mainly composed of C_1 (~45%), with remaining contributions coming equally from S_1, X_1 and X_2 atoms. For XF(I), LUMO is composed of C_1 (~42%), S_1 (~20%), S_2 (~18%) and C_2 (~16%) with minor contributions from remaining atoms. In XF(II), LUMO comprises of C_1(~39%), S_1 (~26%), S_2 (~8%), C_2 (~11%) and O_7 (~11%). The spatial distribution and atomic composition of HOMOs indicate that the S atom in $C_1=S_1$ bond is the most reactive center of these collectors and could participate in covalent bond formation with a metal ion in pulp or metal center on mineral surface.

Table 6.3. Dipole moment, energy of frontier molecular orbitals, and global chemical reactivity indices for neutral collectors under consideration

Collector	D (Debye)	HOMO (eV)	LUMO (eV)	μ (eV)	η (eV)	ω (eV)
TC	9.18	-0.2321	-0.0241	-0.1281	0.1040	0.07887
TU	8.54	-0.2229	-0.0230	-0.1229	0.0999	0.07561
DTC	9.08	-0.2270	-0.0564	-0.1417	0.0853	0.11768
TTC	8.57	-0.2329	-0.0899	-0.1614	0.0715	0.18211
MTC	6.49	-0.2419	-0.0386	-0.1402	0.1016	0.09672
XF(I)	5.50	-0.2474	-0.0699	-0.1586	0.0887	0.14182
XF(II)	9.77	-0.2457	-0.0844	-0.1650	0.0807	0.16879

Calculated values of η suggest that TC and MTC collectors are chemically the most stable, followed by TU, XF(I), DTC, XF(II), and TTC. The escaping tendency of electrons from the collectors as depicted by values of μ follows the following order: TU > TC > MTC > DTC > XF (I) >TTC > XF(II). Interestingly, as evident from Table 1, the C_1-S_1 bond length is larger in TU and TC while it was shortest for XF(II). It can be concluded that the electron donating capacity of these collectors is directly proportional to extent of participation of X_1 and X_2 centers in conjugation with C_1-S_1 bond. Enhanced conjugation results in larger C_1-S_1 bond and thus makes it easier for S_1 atom to donate electrons. Nitrogen is less electronegative than oxygen, thus conjugation is more effective in TU followed by TC and MTC. In DTC and TTC, though sulphur atom is less electronegative, however, the size difference of 3p orbitals of sulphur and 2p orbital of carbon results in less effective conjugative effects. For XF(II), the lone pair of S_2 is delocalised over C_1-S_1 as well as C_2-O_2, thus resulting in smallest C_1-S_1 bond length and lowest electron donating capability. The nucleophilic strength (inverse of electrophilicity) of the collectors and thus, the order of reactivity towards metal atoms as depicted by the calculated values of ω follows the following order: TU > TC > MTC > DTC > XF(I) > XF(II) > TTC.

6.3.2. Binding Ability of Neutral Collectors

The binding ability of a collector towards a metal ion in solution cannot be accurately assessed by only considering the reactivity of the collector. The final outcome of the reaction depends on several other factors as well, such as steric compatibility between reacting species, ring size, etc. Therefore, metal-collector complexes were modeled and their binding energies were calculated. The complex formation for thiourea, thionocarbamate, and dithiocarbamate neutral collectors proceeds via dissociation of N-H bond releasing H^+ ions in solution (Mielczarski & Yoon, 1989; Woods & Hope, 1999). For these three collectors neutral metal-collector complexes of the type ML_2 (where, M: metal and L: collector ligand) were modeled and change in Gibbs free energy during the complex formation was calculated by treating H^+ ion(s) as a reaction product. For other collectors, positively charged complexes were modeled. Modeling of complexes of the type $[ML_2]Cl_2$ (where, M: metal and L: collector ligand) for these collectors and modeling of ML type collectors for cuprous ions is a subject of on-going work.

All the collectors belonging to the $–X_1–(C_1=S_1)–X_2–$ functional group bind to the metal ions through sulphur atom of $C_1=S_1$ bond. NBO analysis did not predict any interactions between the metal center and the heteroatoms X_1 and X_2. Due to the release of H^+ ion from the N-H bond in TU, TC and DTC complexes, the C_1-X_2 (X_2: N) bond length became closer to the standard C=N bond length. For example, in Cu-TU and Cu-TC complexes the resulting average C_1-N_2 bond length was found to be 1.272 and 1.251 Å, respectively. For xanthogen formate collectors, unidentate binding through S_1 atom was observed in XF(I) complexes. XF(II) collector binds with Pb and Cu ions in a bidentate fashion through S_1 and O_2 atoms. This finding is consistent with experimental observations (Ackerman et al., 1987a; Woods & Hope, 1999). The XF(II)-Zn complex could not be optimized successfully. Bidentate binding mode in XF(II) complexes

resulted in the formation of two six membered rings with the metal centers. Atoms S_1, C_1, S_2, C_4 and O_5 in the optimized XF(II) complexes were found to lie almost in a single plane, and the average dihedral angle $\Omega(O_2\text{-}C_2\text{-}S_2\text{-}C_1)$ was found to be 10 and 17 degrees for Cu and Pb complex, respectively. A detailed structural analysis of the optimised complexes will be reported separately.

The calculated interaction energies for different metal-collector complexes are plotted in Figure 6.2. As seen from the plot, all the collector species under consideration are most reactive towards copper, followed by lead. For a particular metal, binding ability of collector molecules follows the following order: TU > TC > XF(II) > MTC = DTC > XF(I) > TTC. The predicted order of binding ability for TU, TC, and XF is in agreement with previous experimental findings (Ackerman et al., 1987a; Fairthorne, Fornasiero, & Ralston, 1997c).

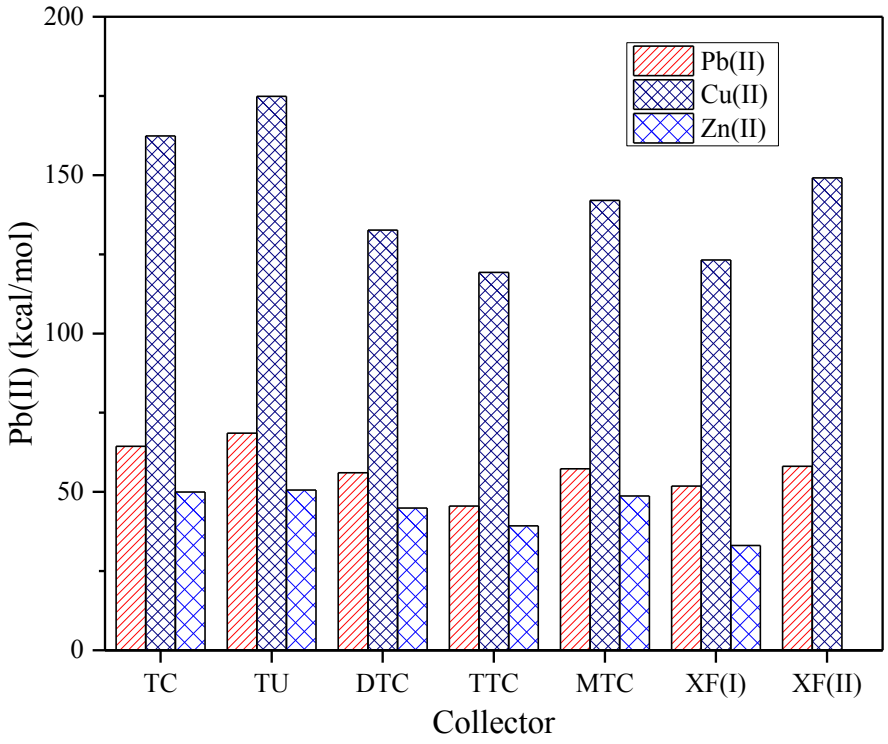

Figure 6.2. Interaction energies of different neutral collectors with divalent ions of Pb, Cu and Zn in solution.

Evidently, the binding ability of different collector ions toward heavy metal ions in solution follows the same trend as predicted by ω, except for XF(II) collector. Complex formation in case of XF(II) collector results in formation of six membered rings where the constituent atoms lie in a single plane. Six membered rings are widely recognised as a sign of enhanced stability. Ring formation also paved way for enhanced conjugate effect over S_1-C_1-S_2-C_4-O_5 group, resulting in higher delocalization stabilizing energies. Higher binding energy values for XF(II) over DTC and MTC collectors could be attributed to these two phenomena. NBO analysis of the complexes did not show any interactions through back donation covalent bond.

6.3.3. Effect of Substituent Groups on Collector's Reactivity and Binding Ability

To investigate the effect of substituent groups linked directly to the collector functional group on its reactivity and binding affinity towards Pb, Cu and Zn metal ions, ethyl group in TU and TC collectors was replaced by different electron withdrawing and donating substituent groups. Reactivity parameters were calculated for resulting collector molecules and their complexes with metal ions were modeled.

6.3.3.1. Effect of O-substituent in Thionocarbamate Collectors

Keeping ethyl group fixed at N-position, different substituent groups were placed on O-position in thionocarbamate collector. Table 4 tabulates the C_1-S_1 bond length, atomic charge on S_1 and calculated values of reactivity descriptors of the modified thionocarbamate collectors along with their interaction energies with Pb^{+2} and Cu^{+2} metal ions. A substituent group can modify the reactivity of the functional group through its electron donating or electron withdrawing nature. Butyl group being slightly more electron donating than ethyl increases the partial charge at the

binding site. Its superior inductive effect is also evident in a slightly longer C_1-S_1 bond and slightly improved electron donating capability and nucleophilicity. The calculated interaction energies are also slightly greater than interaction energies with ethyl substituent. The conjugation between vinyl group and lone pair electrons at oxygen atom results in a decrease in delocalization of oxygen lone pair electrons over C_1-S_1 bond, thus strengthening the C_1-S_1 bond as shown by a shorter C_1-S_1 bond length. The electron withdrawing nature of vinyl group thus decreases the electron donating capability and nucleophilicity of the binding site and result in a decrease in the interaction energies with metal ions.

Table 6.4. Effect of different O-substituent groups on reactivity and binding capability of thionocarbamate.

O-substituent	Partial charge on S_1	r(C_1-S_1) (Å)	μ (eV)	η (eV)	ω (eV)
ethyl	-0.5652	1.682	-0.1281	0.1040	0.0789
butyl	-0.6002	1.683	-0.1280	0.1040	0.0787
vinyl	-0.5313	1.670	-0.1393	0.0983	0.0987
allyl	-0.5710	1.681	-0.1293	0.1035	0.0807
acetyl	-0.4244	1.655	-0.1469	0.0960	0.1124
methylthionyl	-0.4638	1.651	-0.1580	0.0845	0.1477
phenyl	-0.6603	1.674	-0.1349	0.1012	0.0899

The deactivating resonance effect is more powerful in acetyl and methyl thionyl groups as the electronegativity of oxygen in carbonyl group and sulfur in thionyl group is more than carbon in vinyl group. Therefore, they have an enhanced negative effect on reactivity of collectors when compared to vinyl. Allyl group acts as a weak electron withdrawing group due to the presence of unsaturated carbon and results in a slight decrease in C_1-S_1 bond length, chemical potential and nucleophilicity. On a first look the phenyl group appears to be a strong deactivating substituent due to possibility of delocalizing oxygen lone pair electrons in the benzene ring. However, the

ring atoms in the optimized molecule do not lie in the same plane as the atoms in $–X_1–(C_1=S_1)–X_2–$ functional group. It acts as an electron withdrawing group through negative inductive effect only and thus does less damage than vinyl, acetyl and methyl thionyl groups.

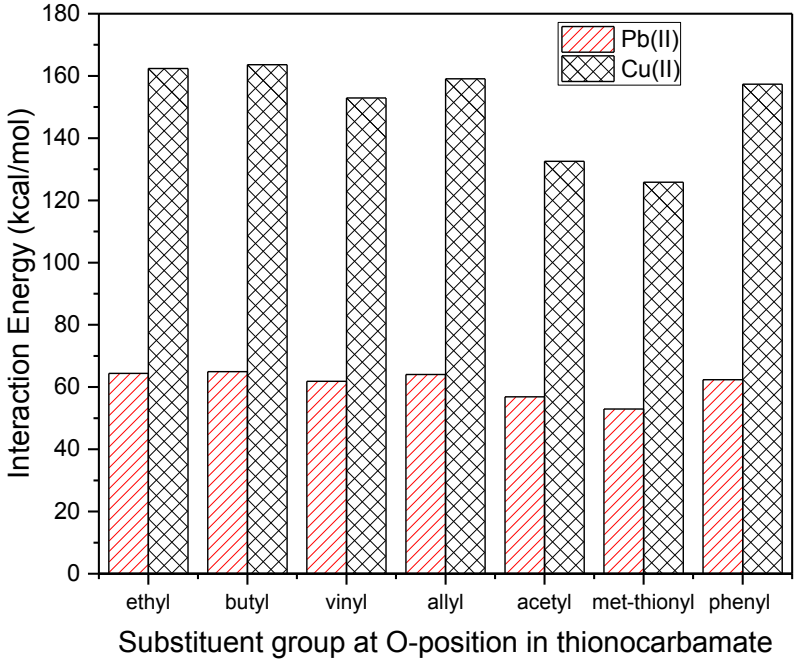

Figure 6.3. Interaction energies between Pb and Cu metal ions and thionocarbamate collectors with different O-substituents.

Unidentate binding is observed between metal ions and all the collectors. The interaction energies of these collectors with metal ions is plotted in Figure 6.3. Again, the binding energies followed the same trend as predicted by the calculated values of electrophilicity index, ω. Ackerman et al. (1984) suggested that O-substituents in thionocarbamate molecule do not have a major effect on the resulting reactivity of the collector. However, DFT calculations indicate that role of O-substituent in thionocarbamate collector is not merely to conform hydrophobicity, it also has significant effect on collector's reactivity too.

6.3.3.2. Effect of N-substituent in Thionocarbamate Collectors

Calculated values of different reactivity parameters for thionocarbamate collectors with different substituent groups at N-position and fixed substituent (ethyl) at O-position along with their interaction energies with metal ions are given in Table 6.5. A similar trend in reactivity and interaction energy data is observed as in the case of O-substituents, however the effect appears to be slightly more profound in case of N-substituents. Vinyl, acetyl, methylthionyl, and benzoyl groups resulted in significant decrease in collector's nucleophilicity and its interaction capability with metal ions as these groups decrease the electron density over binding site due to negative resonance effect with lone pair at nitrogen molecule. Butyl group resulted in better nucleophilicity and interaction energies due to positive inductive effect while allyl and phenyl groups does the opposite due to negative inductive effect. The interaction energies of these collectors with metal ions is plotted in Figure 6.4

Table 6.5. Effect of different N-substituent groups on reactivity and binding capability of thionocarbamate

N-substituent	Partial charge on S_1	$r(C_1\text{-}S_1)$ (Å)	μ (eV)	η (eV)	ω (eV)
ethyl	-0.5652	1.682	-0.1281	0.1040	0.0789
butyl	-0.5709	1.683	-0.1278	0.1040	0.0785
vinyl	-0.5453	1.675	-0.1436	0.0941	0.1096
allyl	-0.6026	1.683	-0.1312	0.1016	0.0847
acetyl	-0.4375	1.657	-0.1491	0.0839	0.1325
methylthionyl	-0.5293	1.650	-0.1547	0.0633	0.1891
phenyl	-0.6011	1.676	-0.1384	0.0930	0.1031
ethoxycarbonyl	-0.4914	1.653	-0.1503	0.0869	0.1299
benzoyl	-0.4276	1.655	-0.1600	0.0762	0.1680

The interaction energies of these collectors with metal ions is plotted in Figure 6.4

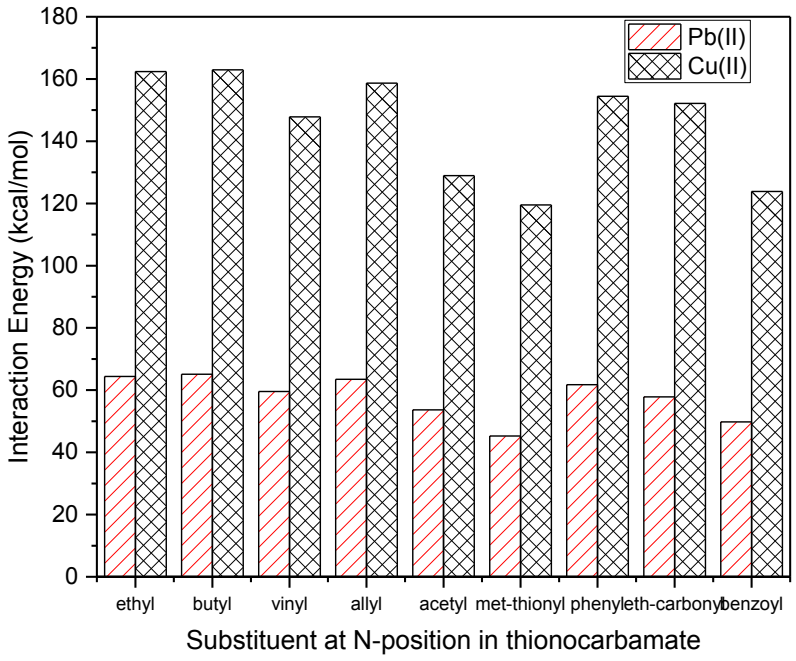

Figure 6.4. Interaction energies between Pb and Cu metal ions and thionocarbamate collectors with different N-substituents.

The reason behind higher ω and lower μ and interaction energy values for methyl thionyl substituted (for both O and N position) thionocarbamate collectors over acetyl substituted collectors remains unclear, as a reverse trend is expected based on the higher electronegativity of oxygen atom in acetyl group. A similar strong deactivating effect is expected from ethoxycarbonyl group and is evident from a much shorter C_1-S_1 bond and lower μ and higher ω values. However, the interaction energies for ethoxycarbonyl group were found to be much higher than acetyl, methylthionyl, and benzoyl. NBO analysis predicted delocalization of electron density from the carbonyl center in ethoxycarbonyl group over the metal atom thus indicating toward a bidentate binding resulting in formation of stable six membered rings at the metal center. This difference in reactivity and binding mode of ethoxycarbonyl could be attributed to increased electron density over carbonyl oxygen as lone pairs of ethoxy oxygen

were found to be delocalised over carbonyl group with stabilization energy ~50 kcal/mol and superior stability and delocalization with in the resulting six membered ring. Formation of six membered rings with ethoxycarbonyl substituted thionocarbamate and thiourea collectors has been observed in many previous experimental studies (Fairthorne et al., 1997c; Mielczarski & Yoon, 1989).

A trend similar to N-substituted thionocarbamate collectors was observed for thiourea collectors when the substituent groups at one N-position were changed while keeping the substituent group fixed at the second N-position. A formation of six membered ring is also observed with ethoxy carbonyl substituent group.

6.4. Conclusions

Use of DFT derived chemical reactivity descriptors provided satisfactory description of chemical activity of different neutral sulphide flotation collectors. The observed trends of reactivity order among different collector molecules were successfully linked to structural variations. The extent of delocalization of lone pair electrons belonging to two hetero atoms (linked directly to C=S bond) over the characteristic C=S center of neutral sulphide collectors was found to play a dominant role in determining the reactivity of collectors and their binding affinity to different heavy metal ions. Compared to other collectors, thiourea, thionocarbamate and dithiocarbamate collectors were found to possess superior nucleophilic character as lone pair electrons of nitrogen atom in these collectors could be easily delocalised over C=S bond as compared to oxygen and sulphur atoms. For thionocarbamate and thiourea collectors, substituent groups at both O and N-positions were found to have an effect on collector reactivity and binding affinities. Substituent groups capable of engaging the O and N centers in deactivating (with respect to C=S center) delocalization resulted in the weakest collectors. Substituent groups capable of donating or

withdrawing electrons through merely inductive effects were found to have less effect on reactivity of collectors. The binding in all the collector-metal complexes was found to be unidentate, except for the case of ethoxy carbonyl substituted (at N-position) thionocarbamate and thiourea collectors and xanthogen formate collectors. The trends of reactivity and binding abilities presented in this study matched closely with the experimental findings reported in literature, demonstrating successful application of DFT methods in linking the calculated structural and reactivity data to experimental observations.

A trend similar to N-substituted thionocarbamate collectors was observed for thiourea collectors when substituent groups at one N-position were changed while keeping the substituent group fixed at the second N-position. A formation of six membered ring is observed with ethoxy carbonyl substituent group.

6.5. References

Ackerman, P. K., Harris, G. H., Klimpel, R. R., & Aplan, F. F. (1984). Effect of alkyl substituents on performance of thionocarbamates as copper sulphide and pyrite collectors. In M. J. Jones, & R. Oblatt (Eds.), *Reagents in mineral industry* (pp. 69-78). London: IMM.

Ackerman, P. K., Harris, G. H., Klimpel, R. R., & Aplan, F. F. (1987a). Evaluation of flotation collectors for copper sulfides and pyrite, I. common sulfhydryl collectors. *International Journal of Mineral Processing, 21*(1–2), 105-127.

Ackerman, P. K., Harris, G. H., Klimpel, R. R., & Aplan, F. F. (1987b). Evaluation of flotation collectors for copper sulfides and pyrite, III. effect of xanthate chain length and branching. *International Journal of Mineral Processing, 21*(1–2), 141-156.

Ackerman, P. K., Harris, G. H., Klimpel, R. R., & Aplan, F. F. (2000). Use of xanthogen formates as collectors in the flotation of copper sulfides and pyrite. *International Journal of Mineral Processing, 58*(1–4), 1-13.

Basilio, C. I. (1989). *Fundamental studies of thionocarbamate interactions with sulfide minerals* (PhD).

Brown, G. M., Hope, G. A., Schweinsberg, D. P., & Fredericks, P. M. (1995). SERS study of the interaction of thiourea with a copper electrode in sulphuric acid solution. *Journal of Electroanalytical Chemistry, 380*(1–2), 161-166.

Coetzer, G., & Davidtz, J. C. (1989). Sulphydryl collectors in bulk and selective flotation. part 2. covalent dithiocarbamate derivatives. *Journal of the South African Institute of Mining and Metallurgy, 89*(11), 341-345.

Fairthorne, G., Fornasiero, D., & Ralston, J. (1997a). Formation of a copper-butyl ethoxycarbonyl thiourea complex. *Analytica Chimica Acta, 346*(2), 237-248.

Fairthorne, G., Fornasiero, D., & Ralston, J. (1997b). Interaction of thionocarbamate and thiourea collectors with sulphide minerals: A flotation and adsorption study. *International Journal of Mineral Processing, 50*(4), 227-242.

Fairthorne, G., Fornasiero, D., & Ralston, J. (1997c). Interaction of thionocarbamate and thiourea collectors with sulphide minerals: A flotation and adsorption study. *International Journal of Mineral Processing, 50*(4), 227-242.

Fairthorne, G., Fornasiero, D., & Ralston, J. (1996). Solution properties of thionocarbamate collectors. *International Journal of Mineral Processing, 46*(1–2), 137-153.

Kimble, K. B., & Bresson, C. R. (1985). *Ore flotation and flotation agents for use therein* (US4561971 A ed.). USA:

Leppinen, J. O., Basilio, C. I., & Yoon, R. H. (1988). FTIR study of thionocarbamate adsorption on sulfide minerals. *Colloids and Surfaces, 32*(C), 113-125.

Liu, G., Zhong, H., Dai, T., & Xia, L. (2008). Investigation of the effect of N-substituents on performance of thionocarbamates as selective collectors for copper sulfides by ab initio calculations. *Minerals Engineering, 21*(12–14), 1050-1054.

LIU, G., ZHONG, H., XIA, L., WANG, S., & DAI, T. (2010). Effect of N-substituents on performance of thiourea collectors by density functional theory calculations. *Transactions of Nonferrous Metals Society of China, 20*(4), 695-701.

Marabini, A. M., Barbaro, M., & Alesse, V. (1991). New reagents in sulphide mineral flotation. *International Journal of Mineral Processing, 33*(1–4), 291-306.

Mielczarski, J. A., & Yoon, R. H. (1989). Spectroscopic studies of the structure of the adsorption layer of thionocarbamate: I. on copper and activated zinc sulfide. *Journal of Colloid and Interface Science, 131*(2), 423-432.

Nagaraj, D. (1988). The chemistry and application of chelating or complexing agents in mineral separations. *Reagents in Mineral Technology,* New York, USA. 387-408.

Nagaraj, D. R., Lewellyn, M. E., Wang, S. S., Mingione, P. A., & Scanlon, M. J. (1988). New sulfide and precious metals collectors: For acid, neutral and mildly alkaline circuits. *Proceedings of XVIth International Mineral Processing Congress,* Stockholm. 1221-1232.

Seryakova, I. V., Vorobiova, G. A., Glembotsky, A. V., & Zolotov, Y. A. (1975). Extraction of metals by neutral sulfur-containing extractants. part I. o-isopropyl-n-ethylthiocarbamate. *Analytica Chimica Acta, 77*(C), 183-190.

Urbina, R. H. (2003). Recent developments and advances in formulations and applications of chemical reagents used in froth flotation. *Mineral Processing and Extractive Metallurgy Review, 24*(2), 139-182.

Woods, R., Hope, G. A., & Watling, K. (2000). Surface enhanced raman scattering spectroscopic studies of the adsorption of flotation collectors. *Minerals Engineering, 13*(4), 345-356.

Woods, R., & Hope, G. A. (1999). A SERS spectroelectrochemical investigation of the interaction of O-isopropyl-N-ethylthionocarbamate with copper surfaces. *Colloids and Surfaces A: Physicochemical and Engineering Aspects, 146*(1–3), 63-74.

Chapter – 7

Conclusions and Future Work

Among the various reagents used in flotation, the role of collectors is undoubtedly the most important, as they selectively render the desired mineral(s) hydrophobic while leaving the others hydrophilic. Sulfide ores generally have a complex mineralogy and typically contain more than one mineral (or metal) of interest. This has attracted a great interest from both the academia and industry to understand collector-mineral interactions, and to design and develop collectors with improved mineral selectivity. In particular, last three decades have witnessed introduction of a large number of new reagents promising enhanced performance. However, the industrial flotation practice is still majorly based on xanthates, dithiophosphates, thionocarbamates, and dithiophosphinate collectors (Nagaraj & Ravishankar, 2007).

Almost all the existing reagents interact with most of the sulfide minerals, and are rarely specific or sufficiently selective for most practical applications (Nagaraj & Ravishankar, 2007). Consequently, complex reagent and solution chemistry schemes have to be implemented, to achieve a minimum desired selectivity, and to ensure recovery of all valuable constituents from a mined ore. However, most often these schemes are not very robust, and have a narrow, unoptimized window of performance. These schemes are not easy to implement, given the significant routine variability in ore composition and other operating variables in a plant setting.

To ensure efficient processing of low grade and mineralogical complex sulfide ores, which are bound to become the source of our future material needs, strong mineral or metal specific collectors need to be developed. However, despite of massive research, till date no theory has

been developed that could guide us in selection of the functional group and molecular structure of a collector to achieve a desired separation efficiently (Rao, Kundu, & Parker, 2012). Collector-mineral interactions are generally interpreted and predicted using existing donor-acceptor relationships, such as Pearson's hard and soft acids and bases (HSAB) theory. However, these models are capable of providing only qualitative or generalist information. One of the other critical reasons, as cited by Nagaraj & Ravishankar (2007), has been the obsessiveness of the research community with only a handful of reagents.

Collector reagents generally interact with sulfide minerals via chemisorption, surface chemical reactions, and/or surface precipitation. The majority of sulfide collectors adsorb on minerals by forming a metal complex, either on the surface or in the bulk. Thus, the selectivity of a collector toward a particular mineral is mainly determined by its ability to form complexes with metal species (corresponding to that particular mineral) at mineral surface or in bulk. Thus, on a microscopic level, the interaction between sulfide minerals and collector molecules is actually the interaction between their molecular wave functions.

Moreover, the flotation efficiency and collector performance is generally determined by using experimentally driven parameters, such as flotation recovery, contact angle, and induction time, etc. The measure of these parameters is greatly influenced by the nature of hydrocarbon tail of collector molecule as well as other operational parameters, and does not provide direct information on the affinity of collector's head group toward a particular mineral. Without this kind of information it is hard to relate the molecular structure of a collector to its reactivity and binding affinity toward different metals or mineral surfaces.

Computational chemistry methods are powerful tools to understand chemical interactions at a microscopic scale. These techniques are suitable to relate the structural characteristics of

collector molecules to their reactivity, and binding affinity towards different mineral surfaces or metals. Last decade has seen an increase in number of publications exploring the reactivity, or the adsorption mechanism of collector molecules on mineral surfaces, by using computational chemistry techniques. However, majority of the studies that aimed to establish the relative reactivity of a set of collector molecules didn't include their binding with metal or mineral species, which is also influenced by factors other than collector's reactivity, such as stereo-compatibility and stability of resulting metal-collector complex. Moreover, these studies predicted the relative reactivity based on theoretically calculated parameters but didn't relate the value of these parameters to collectors' structures. On the other hand, the adsorption studies have been limited to a very few reagent-mineral combinations, and most of them were aimed to understand a detailed mechanism of adsorption, rather than relating collectors' structure to their adsorption abilities or establishing relative binding affinities of different reagents.

To establish a quantitative relationship between molecular structure of collector and its resultant reactivity toward different minerals, modeling of adsorption of a variety of collector molecules on surfaces of different minerals appears to be the best way. However, modeling of the adsorption process is time consuming and computationally intensive. Modeling the interaction of collector molecules with metal ions, on the other hand, could be achieved in a relatively short time. A robust relationship between collector's structure and its reactivity toward different metal/minerals can only be established by inclusion of a wide variety of complexing agents. Therefore, the latter approach is more suitable to establish the guidelines to design molecular structures of selective collectors. A few promising molecules can then be designed for a particular metal using these guidelines, and adsorption of these molecules can then be modeled on mineral surfaces containing that particular metal. The molecule(s) showing best adsorption

characteristics can then be synthesized and their collecting performance can be experimentally tested.

In this thesis, interaction of a variety of reagents, representing three important collector classes, namely, collectors based on CS_2^- head group (commonly referred as thiol type), thio-carbonyl head group (commonly referred as neutral type), and heterocyclic aromatic chelating reagents, were modeled with three different heavy metal ions, namely Cu, Pb, and Zn. Reactivity of individual collector molecules was expressed in a quantitative as well as qualitative manner through use of: (i) different theoretical calculated parameters, including partial atomic charges, spatial distribution and hybridization of frontier molecular orbitals, and geometrical parameters, and (ii) well-established reactivity descriptors, namely chemical potential, chemical hardness, and global electrophilicity. The predicted orders of reactivity were linked to structural differences in collectors' structure. Finally, metal-collector complexes were modeled and interaction energies for these complexes were calculated. The major conclusions, findings, and contributions of this work to the research community are summarized in the next section.

7.1. Major Conclusions and Contributions

The major conclusions of this study are summarized below:

(i) Our extensive computational results on three different classes of flotation collectors show that exploring their molecular reactivity through computational methods and modeling their interactions with metal ions is an efficient approach to relate molecular structure of collector reagents to their binding affinity toward different metals. Trends observed in the calculated interaction energies correlated well with the experimental findings cited in flotation literature. This implies that reactivity and selectivity of reagents towards metal

ions can be qualitatively extended to minerals. It is not practical to model surface adsorption for all collector-mineral combinations. However, a robust relationship between collectors' structure and their reactivity towards different minerals can only be formulated by inclusion of as many reagents as possible. Therefore, modeling metal-collector reactions is an appropriate approach to achieve this objective.

(ii) The calculated values of interaction energies show that all collector reagents considered have greater preference towards binding with Cu metal than Pb and Zn.

(iii) Reactivity of sulfhydryl collectors is mainly determined by the electron density around the reactive S center(s). The length of the C-S bond (where S is the reactive center) gives a fair approximation of collector's reactivity. Thus, the effect of remaining atoms or substituent groups that constitute the collector molecule on reactivity can be predicted by analyzing how they affect the C-S bond length.

(iv) Among the reagents studied, heterocyclic aromatic sulfhydryl reagents are the most powerful collectors, followed by aliphatic anionic (collectors with CS_2^- head group) and neutral sulfhydryl collectors (order based on calculated interaction energies with metal ions).

(v) The order of reactivity described in (iv) can be analyzed in terms of C-S bond lengths (where S is the binding center) as well. The C-S bond is the longest in heterocyclic aromatic reagents followed by aliphatic anionic and neutral type reagents, and so is the molecular reactivity.

(vi) The primary function of substituent groups in collector molecules is to impart hydrophobicity. However, these substituent groups may also alter the reactivity and binding capability of collectors' head groups if they are capable of increasing or

decreasing the C-S bond length (or electron density around reactive S atom) through inductive or resonance effect. Compared to groups which show only inductive effect, the groups that exhibit resonance with C-S bond have more significant effect on their reactivity of bonding to metal ions.

(vii) Anionic aliphatic sulfhydryl collectors (xanthate, dithiocarbamate, dithiophosphate, and trithiocarbonate) bind to metal atoms in a bidentate fashion.

(viii) The reactivity and binding ability (towards metal ions) of anionic aliphatic sulfhydryl collectors follows the order: dithiocarbamate > xanthate > dithiocarboxylate > trithiocarbonate > dithiophosphate. The reactivity order can be described in terms of C-S bond length of CS_2^- (PS_2^- in dithiophosphate) binding group. Resonance between lone pair electrons of O and N atoms, and pi-electrons of CS_2^- group in xanthate and dithiocarbamate, results in longer C-S bonds compared to C-S bonds in dithiocarboxylate. This makes xanthate and dithiocarbamate more reactive than dithiocarboxylate. In trithiocarbonate, the inductive effect of sulfur (heteroatom) is stronger than its resonance effect due to inefficient overlapping of π-orbitals of carbon (in CS_2^-) and sulfur (heteroatom) as lone pair orbital of sulphur is not perpendicular to molecular plane and the size of overlapping orbitals is not same. Thus, C-S bonds (in CS_2^-) in trithiocarbonate are shorter than corresponding bonds in dithiocarboxylate. Consequently, the reactivity of trithiocarbonate is less than dithiocarboxylate. The reactivity of dithiophosphate is the least, as there is no resonance between lone pair electrons of heteroatoms and P-S bonds in PS_2^-. Two hetero oxygen atoms exhibit strong negative inductive effect which decreases the P-S bond length and thus, the molecular reactivity of the reagent.

(ix) Among the anionic aliphatic sulfhydryl collectors, dithiophosphate exhibits superior selectivity for Cu.

(x) Alkyl groups, the most common substituent groups for anionic aliphatic sulfhydryl collectors, have negligible influence in determining the reactivity and binding ability of main functional group.

(xi) Neutral sulfhydryl collectors, namely dialkyl thiourea, dialkyl thionocarbamate, dialkyl dithiocarbamate, dialkyl monothiocarbonate and dialkyl trithiocarbonate, interact with metal centers mainly through S atom of the main thio-carbonyl functional group. The heteroatom(s) (O, N or S) next to the thio-carbonyl group does not participate in binding with the metal center.

(xii) In neutral sulfhydryl collectors, the presence of a substituent group containing an electron rich center capable of forming a dative bond with the metal center, e.g. carbonyl group of xanthate formate and O-ethyl-N-ethoxycarbonyl-thionocarbamate, may change the binding mode of the collector. For example, the carbonyl group in xanthate formate and O-ethyl-N-ethoxycarbonyl-thionocarbamate binds to the metal center along with the main thio-carbonyl functional group resulting in formation of chelate rings with the metal. The formation of six-membered chelate rings improves the binding ability of a neutral collector towards a particular metal ion due to increased stability of metal-collector complex.

(xiii) The reactivity and binding ability (towards metal ions) of neutral collectors follows the order: thiourea > thionocarbamate > monothiocarbonate > dithiocarbonate > trithiocarbonate, provided that both alkyl groups are same in all the reagents.

(xiv) For thionocarbamate, substituent groups present at N atom have more prominent effect on the reactivity and binding ability of collector head groups with metal ions.

(xv) 2-mercaptoazole reagents bind to the metal centers through exocyclic sulfur and endocyclic imine N atom, leading to the formation of chelate rings. The second heteroatom in the aromatic ring does not interact with metal ions.

(xvi) The reactivity of 2-mercaptoazole reagents follows the order: imidazole derivatives > thiazole derivative > oxazole derivative, provided that the aromatic ring contains the same substituent group. Reactivity order can be explained in terms of conjugative effects exhibited by the heteroatoms in the azole ring. Oxygen in oxazole, being the most electronegative, has the weakest conjugative effects. Conjugative effect for S in thiazole is inferior to N in imidazole due to inefficient overlapping of 2p carbon and 3p sulfur orbitals.

(xvii) Compared to substituent groups at the ortho position, substituent groups at meta position with respect to imine N has more influence on the reactivity of the head group in 2-mercaptoazole reagents.

(xviii) The reactivity and metal binding capability of 2-mercaptobenzoazole reagents are inferior to 2-mercaptoazole reagents. However, 2-mercaptobenzoazole reagents are more popular in industry.

(xix) Compared to a substituent group placed at other positions, a substituent group attached to benzene carbon that is para with respect to imine N in azole ring has a greater influence on reactivity and metal binding capability of the binding group in 2-mercaptobenzoazole reagents.

(xx) Chelating reagents that are capable of forming five or six membered chelate rings at the metal center are more powerful than those which form only four membered chelate rings.

(xxi) Numerous previous studies have used the energy and spatial distribution of frontier molecular orbitals as the ultimate parameter to determine relative reactivity and metal or mineral binding ability of a set of molecules. Our results of xanthogenformate, O-ethyl-N-ethoxycarbonyl-thionocarbamate and heterocyclic aromatic reagents show that it is not always just the frontier molecular orbitals that are important and participate in binding with metal. Special care should be taken for molecules which have tendency to coordinate metal atom via a dative bond through second reactive center.

The major contribution of this thesis is the successful correlation between structural differences among a variety of collector reagents to the observed trends in their reactivity toward different metal ions and mineral surfaces. By including a diverse set of reagents, it is probably shown for the first time that a robust framework to guide us in design of more powerful and metal/mineral selective reagents can also be formulated by considering just the interactions between metal and collector reagent. Our results could also be helpful in providing a better understanding of the mechanism through which some of these collectors bind to the metal species present on mineral surfaces in flotation environment. A detailed analysis of collectors' geometries and hybridization states that is presented in this study could be helpful in analyzing and comparing the flotation performance of these reagents from a structural point of view. Values of interaction energies could be helpful in predicting the relative reactivity and metal/mineral selectivity of the reagents covered in this study in a quantitative manner. The results obtained from this work could help in developing and enriching a framework that relates

the structural characteristics of reagent molecules to their reactivity towards different metals and mineral surfaces.

To summarize the observations of this study, sulfide collectors should be based on sulfur binding centers to ensure selectivity against gangue minerals. To ensure maximum chelating ability, the functional group of the collector should be designed in such a manner that five or six membered chelates could be formed with the metal atoms. Also, careful consideration should be given to the atoms attached to the main binding group as they are capable of increasing or decreasing the chelating ability of the binding group through inductive and/or mesomeric effects.

7.2. Limitation of the Present Study

In the present study, the interactions between collector molecules and heavy metal ions are modeled using theoretical computational techniques, as an approximation of the interactions between collector reagents and sulfide minerals surfaces in actual flotation environments. Results obtained from this work show that such a methodology may be helpful in determining the reactivity of different collector molecules in terms of theoretical parameters based on the molecular structure of the collector reagents. Thus, structural requirement of more powerful and/or metal specific collectors may be determined by utilizing the findings of such studies. However, it is important to mention here that the methodology used in this study suffers some limitations, the most significant of which are described here:

- In actual flotation, collector reagents interact primarily with mineral surfaces instead of metal ions. The nature and electronic properties of metal atoms embedded on mineral surfaces could be significantly different from the properties of metal ions in solution. Also, the effect of stearic accessibility between mineral surface and collector molecules cannot be

approximated in the present work. Thus, in some the cases, the observations from a study like the present may not be directly extendable to real flotation systems.

- In the present study, only the interactions between isolated collector molecules and metal ions were considered. In real flotation systems, these interactions (or collector-mineral interactions) are greatly influenced by the presence of other species, such as, numerous molecules of same or different reagents, mineral particles, other metal ions, and explicit solvent molecules, etc. The calculated trends in the interaction energy and molecular reactivity do not consider these effects.
- Theoretical modeling of interactions between collector molecules and metal ions do not take into account the solution conditions (pH, Eh, hydrodynamics, etc.) and other process variables (surface state of mineral particles, presence of competing species, etc.), which have significant influence on the flotation performance.
- The relative reactivity of a reagent X towards different metal ions could be obtained quantitatively from the calculated interaction energies. However, no specific criterion (e.g. required minimum difference in interaction energies) could be developed which could determine whether a reagent molecule would offer selectivity over a particular metal ion or whether it would be absolutely selective towards a specific metal ion. The development of such a criterion is very important if we aim to design and develop metal/mineral specific collectors by utilizing computational methods.
- Some of the collectors (e.g. xanthate and dithiocarbamate) exhibited a very small difference in interaction energies with a given metal ion and it is hard to explain or understand whether the observed difference in interaction energies is due to difference in structures of collector

molecules or is it the error associated with various approximations implemented in the computational methods.

7.3. Suggestions for Future Research

As this research work has shown, approximating the mineral-reagent interactions through modeling of reactions between metal ions and collector molecules is an efficient approach to formulate guidelines on required structural features that could make a reagent molecule very selective towards a particular metal or mineral. Based on our findings a number of conclusions were made regarding how structural differences in three major classes of flotation collectors can be correlated to their reactivity and binding abilities toward different metals. Based on the learnings and findings from this thesis, the following research works are suggested:

1. Explore the reactivity and binding capabilities of remaining collector classes, especially different types of chelating reagents, such as hydroxamates, aminothiophenol, hydroxyquinoline, cupferron, dialkylglyoxime, diphenylcarbazide, and salicylaldoxime. Examine what are the structural features that make them more or less reactive toward a particular metal ion. Examine how the nature and position of different types of substituent groups attached to these reagents may influence their reactivity or binding abilities toward different metals. As mentioned at many instances in this thesis, in order to build powerful criterion regarding structures of metal or mineral selective reagents, it is crucial that these guidelines be drafted based on the learnings and findings from investigations on a large number of complexing agents.
2. Synthesize and study the flotation performance of reagents of the type considered in section 5.3.6. Verify whether possibility of formation of five or six membered chelates at

the metal centres enhances the flotation performance of traditional reagents that generally form four membered chelates with metal centers.

3. Explore the option of using mercaptoazole compounds as flotation reagents, as the results from this study suggest that these reagents are more reactive than mercaptobenzoazole reagents. Mercaptobenzoazole reagents made their way to flotation industry from other areas such as pharmaceuticals industry. Not many structural variations of these reagents have been tried in the flotation industry yet.
4. Results from this study suggest that derivatives of imidazole should be more powerful reagents than their thiazole and oxazole counterparts; however, in flotation only mercaptobenzothiazole have gained attention.
5. Study adsorption of the collectors considered in this study on copper, lead, and zinc sulfide minerals using same computational method. Though the trends in reactivity and binding affinities of different collectors match well with observations reported in experimental flotation literature; it would be interesting to see if adsorption studies of these reagents also result in similar trends or not.

7.4. References

Nagaraj, D. R., & Ravishankar, S. A. (2007). Flotation reagents - A critical overview from an industry prospective. In M. C. Fuerstenau, G. Jameson & R. Yoon (Eds.), *Froth flotation: A century of innovation* . Littleton: SME.

Rao, H. K., Kundu, T., & Parker, S. (2012). Molecular modeling of mineral surface reactions in flotation. *Molecular modeling for the design of novel performance chemicals and materials* (pp. 65-105) CRC Press.

Bibliography

Ackerman, P. K., Harris, G. H., Klimpel, R. R., & Aplan, F. F. (1984). Effect of alkyl substituents on performance of thionocarbamates as copper sulphide and pyrite collectors. In M. J. Jones, & R. Oblatt (Eds.), *Reagents in mineral industry* (pp. 69-78). London: IMM.

Ackerman, P. K., Harris, G. H., Klimpel, R. R., & Aplan, F. F. (1987a). Evaluation of flotation collectors for copper sulfides and pyrite, I. common sulfhydryl collectors. *International Journal of Mineral Processing, 21*(1–2), 105-127.

Ackerman, P. K., Harris, G. H., Klimpel, R. R., & Aplan, F. F. (1987b). Evaluation of flotation collectors for copper sulfides and pyrite, III. effect of xanthate chain length and branching. *International Journal of Mineral Processing, 21*(1–2), 141-156.

Ackerman, P. K., Harris, G. H., Klimpel, R. R., & Aplan, F. F. (1999). Use of chelating agents as collectors in the flotation of copper sulfides and pyrite . *Miner. Met. Process, 16*(1), 27-35.

Ackerman, P. K., Harris, G. H., Klimpel, R. R., & Aplan, F. F. (2000). Use of xanthogen formates as collectors in the flotation of copper sulfides and pyrite. *International Journal of Mineral Processing, 58*(1–4), 1-13.

Adamo, C., & Barone,V. (1999). Toward reliable density functional methods without adjustable parameters: The PBE0 model. *The Journal of Chemical Physics, 110(13),* 6158-6170.

Adkins, S. J., & Pearse, M. J. (1992). The influences of collector chemistry on kinetics and selectivity in base-metal sulphide flotation. *Minerals Engineering, 5*(3–5), 295-310.

Agarwala, U., Lakshmi, & Rao, P. B. (1968). Vibrational spectra of xanthate complexes. *Inorganica Chimica Acta, 2*(0), 337-339.

Ahmed, N., & Jameson, G. J. (1985). The effect of bubble size on the rate of flotation of fine particles. *International Journal of Mineral Processing, 14*(3), 195-215.

Ahmed, S. M. (1978). Electrochemical studies of sulphides, II. measurement of the galvanic currents in galena and the general mechanism of oxygen reduction and xanthate adsorption on sulphides in relation to flotation. *International Journal of Mineral Processing, 5*(2), 175-182.

Ai-Mayouf, A. M., Al-Ameery, A. K., & Al-Suhybani, A. A. (2001). Comparison of inhibition efficiency of some azoles on corrosion of type 304 stainless steel in acidic solutions. *British Corrosion Journal, 36*(2), 127-132.

Allison, S. A., Goold, L. A., Nicol, M. J., & Granville, A. (1972). A determination of the products of reaction betweer various sulfide minerals and aqueous xanthate solution, and a correlation of the products with electrode rest potentials. *Metallurgical Transactions, 3*(10), 2613-2618.

Andrae, D., Haeussermann, U., Dolg, M., Stoll, H., & Preuss, H. (1990). Energy-adjusted ab initio pseudopotentials for the 2nd and 3rd row transition elements. *Theoretical Chemistry Accounts, 77*, 123-141.

Anthony, R. M., Kelsall, D. F., & Trahar, W. J. (1975). The effect of particle size on the activation and flotationof sphalerite. *Australian Institute of Mining and Metallurgy, 254* 47-58.

Armiento, R., & Mattsson, A. E. (2005). Functional designed to include surface effects in self-consistent density functional theory. *Phys. Rev. B, 72(8),* 0851081-0851085.

Assis, S. M., Montenegro, L. C. M., & Peres, A. E. C. (1996). Utilisation of hydroxamates in minerals froth flotation. *Minerals Engineering, 9*(1), 103-114.

Avotins, P. V., Wang, S. S., & Nagaraj, D. R. (1994). Recent advances in sulfide collector development . *Reagents for better metallurgy* SME.

Ayers, P., & Parr, R. (2008a). Beyond electronegativity and local hardness: Higher-order equilization criteria for determination of a ground-state electron density. *Journal of Chemical Physics, 129*(5), 054111-054117.

Ayers, P., & Parr, R. (2008b). Local hardness equalization: Exploiting the embiguity. *Journal of Chemical Physics, 128*(18), 184108-184115.

Babel, S., & Kurniawan, T. A. (2004). Cr(VI) removal from synthetic wastewater using coconut shell charcoal and commercial activated carbon modified with oxidizing agents and/or chitosan. *Chemosphere, 54*(7), 951-967.

Bag, B., Das, B., & Mishra, B. K. (2011). Geometrical optimization of xanthate collectors with copper ions and their response to flotation. *Minerals Engineering, 24*(8), 760-765.

Banerji, S., Byrne, R. E., & Livingstone, S. E. (1982). Metal complexes of 2-mercaptobenzothiazole. *Transition Metal Chemistry, 7*(1), 5-10.

Barakat, M. A. (2011). New trends in removing heavy metals from industrial wastewater. *Arabian Journal of Chemistry, 4*(4), 361-377.

Barbaro, M. (2000). Lead and zinc ores: Flotation. In C. Poola, & M. Cooke (Eds.), *Encyclopedia of separation science* (III ed., pp. 3215-3218) Academic Press, Elsevier.

Basilio, C. I. (1989). *Fundamental studies of thionocarbamate interactions with sulfide minerals* (PhD).

Basson, W. D., & du Preez, A. L. (1974). Reactions of thiazolidine-2-thiones with copper(II). *Journal of the Chemical Society, Dalton Transactions,* (16), 1708-1711.

Becke, A. D. (1988). Density-functional exchange-energy approximation with correct asymptotic behavior. *Physical Review A, 38*(6), 3098-3100.

Becke, A. D. (1993a). Density-functional thermochemistry. III. the role of exact exchange. *The Journal of Chemical Physics, 98*(7), 5648-5652.

Becke, A. D. (1993b). A new mixing of Hartree–Fock and local density-functional theories. *J. Chem. Phys, 98(2),* 1372-1377.

Bezuidenhout, J. (2011). *An investigation into the role of DTP as a co-collector in the flotation of a south african PGM ore.* (Unpublished MSc). University of Cape Town, Cape Town.

Billes, F., Holmgren, A., & Mikosch, H. (2010). A combined DFT and vibrational spectroscopy study of nickel and zinc O,O-diethyldithiophosphate complexes. *Vibrational Spectroscopy, 53*, 296-306.

Blue, L. Y., Jana, P., & Atwood, D. A. (2010). Aqueous mercury precipitation with the synthetic dithiolate, BDTH2. *Fuel, 89*(6), 1326-1330.

Boddu, V. M., Abburi, K., Talbott, J. L., & Smith, E. D. (2003). Removal of hexavalent chromium from wastewater using a new composite chitosan biosorbent. *Environmental Science & Technology, 37*(19), 4449-4456. Bodenant, B., & Fages, F. (1995). Synthesis, metal binding, and fluorescence studies of a pyrene-tethered hydroxamic acid ligand. *Tetrahedron Letters, 36*(9), 1451-1454.

Born, M., & Oppenheimer, R. (1927). Zur quantentheorie der molekeln. *Annalen Der Physik, 389*, 457-464.

Bradshaw, D. (1997). *Synergism between thiol collectors.* (Unpublished PhD). University of Cape Town, Cape Town.

Bradshaw, D. J., & O'Connor, C. T. (1997). The synergism of thiol collectors in a mixture used for the flotation of pyrite. *XX Mineral Processing Conference,* Aachen. 343-354.

Bradshaw, D. J., & O'Connor, C. T. (1994). The flotation of pyrite using mixtures of dithiocarbamates and other thiol collectors. *Minerals Engineering, 7*(5–6), 681-690.

Breza, M., Bučinský, L., Šoralová, S., & Biskupič, S. (2010). On the origin of the hemidirected geometry of tetracoordinated lead(II) compounds. *Chemical Physics, 368*(1–2), 14-19.

Brown, G. M., Hope, G. A., Schweinsberg, D. P., & Fredericks, P. M. (1995). SERS study of the interaction of thiourea with a copper electrode in sulphuric acid solution. *Journal of Electroanalytical Chemistry, 380*(1–2), 161-166.

Buckley, A. N., Goh, S., Wei, Lamb, R., Fan, L., & Yang, Y. (2006). XPS, static SIMS and NEXAFS spectroscopic investigation of thiol adsorption on metals and metal sulfides. *ECS Transactions, 2*(3), 107-119.

Buglyó, P., Nagy, E. M., Farkas, E., Sóvágó, I., Sanna, D., & Micera, G. (2007). New insights into the metal ion-peptide hydroxamate interactions: Metal complexes of primary hydroxamic acid derivatives of common dipeptides in aqueous solution. *Polyhedron, 26*(8), 1625-1633.

Bulatovic, S. (2007). Adsorption mechanism of flotation collectors . *Handbook of flotation reagents: Chemistry, theory and practice. volume 1: Flotation of sulfide ores* (1st ed., pp. 125-152) Elsevier Science.

Bulatovic, S. M. (2007a). In Bulatovic S. M. (Ed.), *Handbook of flotation reagents: Chemistry, theory and practice*. Amsterdam: Elsevier.

Bulatovic, S. M. (2007b). Collectors. *Handbook of flotation reagents: Chemistry, theory and practice. volume 1: Flotation of sulfide ores* (1st ed., pp. 5-42) Elsevier Science.

Buttrus, N. H., & Mohamed, S. M. (2013). Synthesis and characterization of Ni^{+2}, Cu^{+2} and Zn^{+2} complexes with benzoxazole-2-thionate, diphenyl phosphinomethane and iodine. *Research Journal of Chemical Sciences, 3*(6), 54-59.

Casas, J. S., Castellano, E. E., Ellena, J., Garcia, T., Sanchez, A., Sordo, J. & Viddarate, M. J. (2003). Compositional and Structural Variety of Diphenyllead(IV) Complexes Obtained by Reaction of Diphenyllead Dichloride with Thiosemicarbazones. *Inorganic Chemistry*, *42*, 2584-2595.

Castro, R., Garcia-Vazquez, J. A., Romero, J., Sousa, A., McAuliffe, C. A., & Pritchard, R. (1993). Electrochemical synthesis of benzothiazole-2-thionato complexes of nickel(II), zinc(II) and cadmium(II): The crystal structure of 2,2′-bipyridine bis(benzothiazole-2-thionato)zinc(II). *Polyhedron, 12*(18), 2241-2247.

Ceperley, D. M., & Alder, B. J. (1980). Ground state of the electron gas by a stochastic method. *Phys. Rev. Lett, 45(7),* 566-569.

Chaitanya, K., Santhamma, C., Prasad, K. V., & Veeraiah, V. (2012). Molecular structure, vibrational spectroscopic (FT-IR, FT-raman),first order hyperpolarizability, NBO analysis, HOMO and LUMO analysis, thermodynamic properties of 3,5-dimethylbenzophenone by ab inito HF and density functional method. *Journal of Atomic and Molecular Sciences, 3*(1), 1-22.

Chang, Q., & Wang, G. (2007). Study on the macromolecular coagulant PEX which traps heavy metals. *Chemical Engineering Science, 62*(17), 4636-4643.

Chang, Y., Chang, J., & Chiang, L. (2003). Leaching behavior and chemical stability of copper butyl xanthate complex under acidic conditions. *Chemosphere, 52*(6), 1089-1094.

Charerntanyarak, L. (1999). Heavy metals removal by chemical coagulation and precipitation. *Water Science and Technology, 39*(10–11), 135-138.

Chen, J., Lan, L., & Chen, L. (2013). Computational simulation of adsorption and thermodynamic study of xanthate, dithiophosphate and dithiocarbamate on galena and pyrite surfaces. *Minnerals Enginneering, 46-47*, 136-143.

Cifuentes, L., García, I., Arriagada, P., & Casas, J. M. (2009). The use of electrodialysis for metal separation and water recovery from CuSO4–H2SO4–Fe solutions. *Separation and Purification Technology, 68*(1), 105-108.

Clark, T. (1985). *A handbook of computational chemistry*. New York: John Wiley & Sons.

Coetzer, G., & Davidtz, J. C. (1989). Sulphydryl collectors in bulk and selective flotation. part 2. covalent dithiocarbamate derivatives. *Journal of the South African Institute of Mining and Metallurgy, 89*(11), 341-345.

Coetzer, G., du Preez, H. S., & Bredenhann, R. (2003). Influence of water resources and metal ions on galena flotation of rosh pinah ore. *The Journal of the South African Institute of Mining and Metallurgy,* (April), 193-208.

Costa Jr., A. C., Ondar, G. F., Versiane, O., Ramos, J. M., Santos, T. G., Martin, A. A., . . . Téllez Soto, C. A. (2013). DFT: B3LYP/6-311G (d, p) vibrational analysis of bis-(diethyldithiocarbamate)zinc (II) and natural bond orbitals. *Spectrochimica Acta Part A: Molecular and Biomolecular Spectroscopy, 105*(0), 251-258.

Costa Jr., A. C., Ramos, J. M., Téllez Soto, C. A., Martin, A. A., Raniero, L., Ondar, G. F., . . . Moraes, L. S. (2013). Fourier transform infrared and raman spectra, DFT: B3LYP/6-311G(d, p) calculations and structural properties of bis(diethyldithiocarbamate)copper(II). *Spectrochimica Acta Part A: Molecular and Biomolecular Spectroscopy, 105*(0), 259-266.

Costa Júnior, A. C., Versiane, O., Faget Ondar, G., Ramos, J. M., Ferreira, G. B., Martin, A. A., & Téllez Soto, C. A. (2012). An experimental and theoretical approach of spectroscopic and structural properties of the bis(diethyldithiocarbamate)–cobalt(II). *Journal of Molecular Structure, 1029*(0), 119-134.

Coucouvanis, D. (1970). The chemistry of the dithioacid and 1,1-dithiolate complexes. *Progress in Inorganic Chemistry, 11*, 233-371.

Cramer, C. J. (2004). *Essentials of computational chemistry* (2nd ed.) Wiley.

Cramer, C. J., & Truhlar, D. (1999). ChemInformAbstract:ImplicitSolvation models:Equilibria,structure,spectra,and dynamics. *Chemical Reviews, 99*, 2161-2200.

Crozier, R. (1992). *Flotation: Theory, reagents and ore testing.* New York: Pergamon Press.

Crozier, R. D. (1991). Sulphide collector mineral bonding and the mechanism of flotation. *Minerals Engineering, 4*(7–11), 839-858.

Cukrowski, I., Cukrowska, E., Hancock, R. D., & Anderegg, G. (1995). The effect of chelate ring size on metal ion size-based selectivity in polyamine ligands containing pyridyl and saturated nitrogen donor groups. *Analytica Chimica Acta, 312*(3), 307-321.

Damjanovic, A. (1969). In Bockris.J., Conway M. A. (Eds.), *Modern aspects of electrochemistry*

Davidson, E. R., & Felle, D. (1986). Basis set selection for molecular calculations. . *Chem. Rev, 86*(4), 681-696.

Desjonqueres, M. C., & Spanjaard, D. (1996). *Concepts in suface physics* (Second ed.) Springer.

Dewar, M. J. S., Zoebisch, E. G., & Healy, E. F. (1985). Development and use of quantum mechanical molecular models. AM1: A new general purpose quantum mechanical molecular model. *J. Am. Chem. Soc., 107*, 3902-3909.

Diehl, H. (1937). The chelate rings. *Chemical Reviews, 21*(1), 39-111.

Dixon, S. L., & Merz, K. M. (1996). Semiempirical molecular orbital calculations with linear system size scaling. *J. Chem. Phys, 104(17)*, 6643-6649.

Dolg, M., Wedig, U., Stoll, H., & Preuss, H. (1987). Energy-adjusted ab initio pseudopotentials for the first row transition elements. *The Journal of Chemical Physics, 86*(2), 866-872.

Doula, M. K. (2009). Simultaneous removal of cu, mn and zn from drinking water with the use of clinoptilolite and its fe-modified form. *Water Research, 43*(15), 3659-3672.

Dupuis, M., & King, H. F. (1978). Molecular symmetry. II. gradient of electronic energy with respect to nuclear coordinates. *Journal of Chemical Physics, 68*, 3998.

Dupuis, M., & King, H. F. (1977). Molecular symmetry and closed-shell SCF calculations. I. *International Journal of Quantum Chemistry, 11*(4), 613-625.

Elgiillani, D. A., & Fuerstenau, M. C. (1968). Mechanisms involved in cyanide depression of pyrite. *Transactions AIME, 241*, 437.

El-Shazly, M. F., Salem, T., El-Sayed, M. A., & Hedewy, S. (1978). Coordination chemistry of benzothiazole derivatives. 2-mercaptobenzothiazole and 2-(o-hydroxyphenyl)benzothiazole complexes with cu(II), ni(II) and co(II). *Inorganica Chimica Acta, 29*(0), 155-163.

Engel, E., & Dreizler, R. M. (2011). *Density functional theory* Springer.

Euler, B. (2006). Stability product constants near 25 degree celcius. Retrieved from

Fairthorne, G., Fornasiero, D., & Ralston, J. (1997a). Formation of a copper-butyl ethoxycarbonyl thiourea complex. *Analytica Chimica Acta, 346*(2), 237-248.

Fairthorne, G., Fornasiero, D., & Ralston, J. (1997b). Interaction of thionocarbamate and thiourea collectors with sulphide minerals: A flotation and adsorption study. *International Journal of Mineral Processing, 50*(4), 227-242.

Fairthorne, G., Fornasiero, D., & Ralston, J. (1997c). Interaction of thionocarbamate and thiourea collectors with sulphide minerals: A flotation and adsorption study. *International Journal of Mineral Processing, 50*(4), 227-242.

Fairthorne, G., Fornasiero, D., & Ralston, J. (1996). Solution properties of thionocarbamate collectors. *International Journal of Mineral Processing, 46*(1–2), 137-153.

Feng, D., & Aldrich, C. (1999). Effect of particle size on flotation performance of complex sulphide ores. *Minerals Engineering, 12*(7), 721-731.

Finch, J. A., Xiao, J., Hardie, C., & Gomez, C. O. (2000). Gas dispersion properties: Bubble surface area flux and gas holdup. *Minerals Engineering, 13*(4), 365-372.

Finch, J. A., Nesset, J. E., & Acuña, C. (2008). Role of frother on bubble production and behaviour in flotation. *Minerals Engineering, 21*(12–14), 949-957.

Finkelstein, N. P., & Allison, S. A. (1976). Natural and induced hydrophobicity in sulphide mineral systems. *AICLHE Symposium Series, 71*(150), 165-175.

Finkelstein, N. P., & Poling, G. W. (1977). The role of dithiolates in the flotation of sulfide minerals. *Mineral Science and Engineering, 9*, 177.

Fox, S. J. (2012). *Protein-ligand binding affinities from large-scale quantum mechanical simulations.* (Unpublished PhD). University of Southampton, Southampton.

Foye, W. O., & Lo, J. (1972). Metal-binding abilities of antibacterial heterocyclic thiones. *Journal of Pharmaceutical Sciences, 61*(8), 1209-1212.

Frauenheim, T., Seifert, G., Estner, M., Hajnal, Z., Jungnickel, G., & Porezag, D. (2000). *Phys. Stat. Sol (B), 217*, 41.

Fredriksson, A., & Holmgren, A. (2008). An in situ ATR-FTIR investigation of adsorption and orientation of heptyl xanthate at the lead sulphide/aqueous solution interface. *Minerals Engineering, 21*(12–14), 1000-1004.

Frisch, M. J., Trucks, G. W., Schlegel, H. B., Scuseria, G. E., Robb, M. A., Cheeseman, J. R., . . . Fox, D. J. (2009). *Gaussian 09, revision A.1*. Wallingford CT: Gaussian, Inc.

Fu, F., Chen, R., & Xiong, Y. (2007). Comparative investigation of N,N′-bis-(dithiocarboxy)piperazine and diethyldithiocarbamate as precipitants for ni(II) in simulated wastewater. *Journal of Hazardous Materials, 142*(1–2), 437-442.

Fu, F., & Wang, Q. (2011). Removal of heavy metal ions from wastewaters: A review. *Journal of Environmental Management, 92*(3), 407-418.

Fu, F., Zeng, H., Cai, Q., Qiu, R., Yu, J., & Xiong, Y. (2007). Effective removal of coordinated copper from wastewater using a new dithiocarbamate-type supramolecular heavy metal precipitant. *Chemosphere, 69*(11), 1783-1789.

Fuerstenau, M., Chander, S., & Woods, R. (2007). Sulphide mineral flotation. In M. Fuerstenau, G. Jameson & R. Yoon (Eds.), *Froth flotation – A century of innovation* (pp. 445-453). Littleton, Colorado: Society for Mining, Metallurgy and Exploration (SME).

Fuerstenau, M. C. (1982a). Chemistry of collectors in solution. In R. P. King (Ed.), *Principles of flotation* (1st ed., pp. 1-16). Johannesburg: South African Institute of Mining and Metallurgy.

Fuerstenau, M. C. (1982b). Sulphide mineral flotation. In R. P. King (Ed.), *Principles of flotation* (pp. 159-182) South African Institute of Mining and Metallurgy.

Fuerstenau, M. C., Huiatt, J. L., & and Kuhn, M. C. (1971). Dithiophosphate vs xanthate flotation of chalcocite and pyrite. *Transactions AIME, 250*, 227.

Fuerstenau, M. C., Kuhn, M. C., & Elgiillani, D. A. (1968). The role of dixanthogen in xanthate flotation of pyrite. *Transactions AIME, 241*, 148.

Fuerstenau, D. W. (1982). Activation in the flotation of sulphide minerals. In R. P. King (Ed.), *Principles of flotation* (1st ed., pp. 183-198). Johannesburg: South African Institute of Mining and Metallurgy.

Fuerstenau, D. W., Herrera-Urbina, R., & McGlashan, D. W. (2000). Studies on the applicability of chelating agents as universal collectors for copper minerals. *International Journal of Mineral Processing, 58*(1–4), 15-33.

Fuerstenau, D. W., & Urbina, R. H. (1990). Adsorption of cationic surfactants and the flotation of minerals. In D. N. Rubingh, & P. M. Holland (Eds.), *Cationic surfactants: Physical chemistry*. CRC Press.

Fuerstenau, M. C., Clifford, K. L., & Kuhn, M. C. (1974). The role of zinc-xanthate precipitation in sphalerite flotation. *International Journal of Mineral Processing, 1*(4), 307-318.

Fuerstenau, M. C., & Han, K. N. (2002). Metal–Surfactant precipitation and adsorption in froth flotation. *Journal of Colloid and Interface Science, 256*(1), 175-182.

Fuerstenau, M. C., Natalie, C. A., & Rowe, R. M. (1990). Xanthate adsorption on selected sulfides in the virtual absence and presence of oxygen, part 1. *International Journal of Mineral Processing, 29*(1–2), 89-98.

Gell-Mann, M., & Brueckner, K. A. (1957). Correlation energy of an electron gas at high density. *Phys. Rev., 106(2),* 364-368.

Ghosh, D., Bagchi, S., & Das, A. K. (2011). Theoretical study of electronic structure and complexation of PBII$(S_2COR)_2$ [R = me, et, ph] complexes. *Molecular Physics, 110*(1), 37-48.

Gilbert, J. G., Addison, A. W., Nazarenko, A. Y., & Butcher, R. J. (2001). Copper(II) complexes of new unsymmetrical NSN thioether ligands. *Inorganica Chimica Acta, 324*(1–2), 123-130.

Glendening, E. D., Badenhoop, J. K., Reed, A. E., Carpenter, J. E., Bohmann, J. A., Morales, C. M., & Weinhold, F. (2001). *NBO 5.0* Theoretical Chemistry Institute, University of Wisconsin, Madison.

Gontijo, C., Forenasiero, D., & Ralston, J. (2007). The limits of fine and coarse particle flotation . *Canadian Journal of Chemical Engineering, 85*, 739-747.

Goold, L. A. (1972). *The reaction of sulphide minerals with thiol compounds.* (No. 1439). Johannesburg, South Africa: National Institute of Metallurgy.

Griffith, D. M., Szocs, B., Keogh, T., Suponitsky, K. Y., Farkas, E., Buglyó, P., & Marmion, C. J. (2011). Suberoylanilide hydroxamic acid, a potent histone deacetylase inhibitor; its X-ray crystal structure and solid state and solution studies of its zn(II), ni(II), cu(II) and fe(III) complexes. *Journal of Inorganic Biochemistry, 105*(6), 763-769.

Hammer, B., Hansen, L. B., & Nørskov, J. K. (1999). Improved adsorption energetics within density-functional theory using revised perdew-burke-ernzerhof functionals. *Phys. Rev. B, 59(11),* 7413-7421.

Hanson, J. S., & Fuerstenau, D. W. (1987). An electrochemical investigation of the adsorption of octyl hydroxamate on chalcocite. *Colloids and Surfaces, 26*(C), 133-140.

Haung, H. H., & Miller, J. D. (1978). Kinetics and thermochemistry of amyl xanthate adsorption by pyrite and marcasite. *International Journal of Mineral Processing, 5*(3), 241-266.

Heisenburg, W. (1927). Uber den anschaulichen inhalt der quantentheoretischen kinematik und mechanik. *Zeitschrift Fur Physik, 43*, 172-198.

Hellstrom, P. (2007). *Ab initio modelling of xanthates adsorbed on ge and ZnS surfaces.* (Unpublished PhD). Luleå University of Technology, Sweden.

Hellstrom, P., Holmgren, A., & Oberg, S. (2007). An ab-initio study of ethyl xanthate adsorbed on ge (111) surface. *Journal of Physical Chemistry, 111*(45), 16920-16926.

Hellstrom, P., Oblatt, S., Fredriksson, A., & Holmgren, A. (2006). A theoretical and experimental study of vibrational properties of alkyl xanthates. *Spetrochim. Acta, 65A*, 887-895.

Henke, K. R. (1998). Chemistry of heavy metal precipitates resulting from reactions with thio-Red®. *Water Environment Research, 70*(6), 1178-1185.

Hernández-Rivera, S. P., & Castillo-Chará, J. (2010). Ab initio, DFT calculation and vibrational analysis of 2,4,6-trinitrotoluene. *Vibrational Spectroscopy, 53*(2), 248-259.

Ho, J., Coote, M. L., & Truhlar, D. G. (1999). Theoretical calculation of reduction potentials. In O. Hammerich, & B. Speiser (Eds.), *Organic electrochemistry* (5th ed., pp. 229-262). Florida: CRC Press.

Hodgson, M., & Agar, G. E. (1989). Eilectrochemical investigations into the flotation chemistry of pentlandite and pyrrhotite: Process water and xanthate interactions. *Canadian Metallurgical Quarterly, 28*(3), 189-198.

Hohenberg, P., & Kohn, W. (1964). Inhomogeneous electron gas. *Phys. Rev., 136(3B),* B864-B871.

Hope, G. A., Numprasanthai, A., Buckley, A. N., Parker, G. K., & Sheldon, G. (2012). Bench-scale flotation of chrysocolla with n-octanohydroxamate. *Minerals Engineering, 36–38*(0), 12-20.

Houot, R., & Duhamet, D. (1993). Floatability of chalcopyrite in the presence of dialkyl-thionocarbamate and sodium sulfite. *International Journal of Mineral Processing, 37*(3–4), 273-282.

Hung, A., Yarovsky, I., & Russo, S. (2003). Density-functional theory studies of xanthate adsorption on the pyrite FeS2 (110) and (111) surfaces. *Journal of Chemical Physics, 118*(13), 6022-6029.

Ikeda, T., & Hagihara, H. (1966). The crystal structure of zinc ethylxanthate. *Acta Crystallographica, 21*, 919-927.

Ikumapayi, F., Makitalo, M., Johansson, B., & Rao, K. H. (2012). Recycling of process water in sulphide flotation: Effect of calcium and sulphate ions on flotation of galena. *Minerals Engineering, 39*(0), 77-88.

Ivanov, A., Bredyuk, O., Antzutkin, O., & Forsling, W. (2004). Copper(II) and nickel(II) alkylxanthate complexes (R = C_2H_5, i-C_3H_7, i-C_4H_9, s-C_4H_9, and C_5H_{11}): EPR and solid-state 13C CP/MAS NMR studies. *Russian Journal of Coordination Chemistry, 30*(7), 480-485.

Jensen, F. (Ed.). (1998). *Introduction to computational chemistry*. Chichester, UK: John Wiley and Sons Ltd.

Jiwu, M., Longling, Y., & Kuoxiong, S. (1984). Novel frother-collector for flotation of sulphide minerals - CEED. *Reagents in the Minerals Industry,* London. 287-290.

Kakovsky, L. A. (1957). Physiochemical propreporties of some flotation reagents and their salts with ions of heavy iron-ferrous metals. *Int, Congry. Surface Activity,* London. *, 4* 225-237.

Kang, K. C., Kim, S. S., Choi, J. W., & Kwon, S. H. (2008). Sorption of Cu^{2+} and Cd^{2+} onto acid- and base-pretreated granular activated carbon and activated carbon fiber samples. *Journal of Industrial and Engineering Chemistry, 14*, 131-135.

Kang, S., Lee, J., Moon, S., & Kim, K. (2004). Competitive adsorption characteristics of Co2+, Ni2+, and Cr3+ by IRN-77 cation exchange resin in synthesized wastewater. *Chemosphere, 56*(2), 141-147.

Kellner, R., & St. Nikolov, G. (1981). Far IR spectra of dithiocarbamate complexes correlations with structure parameters. *Journal of Inorganic and Nuclear Chemistry, 43*(6), 1183-1188.

Khullar, I. P., & Agarwala, U. (1975). Complexes of 2-mercaptobenzothiazole with Cu(II), Ni(II), Co(II), Cd(II), Zn(II), Pb(II), Ag(I), and Ti(I). *Canadian Journal of Chemistry, 53*(8), 1165-1171.

Kimble, K. B., & Bresson, C. R. (1985). *Ore flotation and flotation agents for use therein* (US4561971 A ed.). USA:

Kitchener, J. A. (1984). The froth flotation process: Past, present and future-in brief. in the scientific bases of flotation. In K. J. Ives (Ed.), *Scientific bases of flotation*. The Hague: Martinus Nijhoff Publishers.

Kitchener, J. A., & Laskowski, J. S. (1968). The Hydrophylic–Hydrophobic transition on silica. *Journal of Colloid and Interface Science,* 165-175.

Klimpel, R. (1984). Froth flotation: The kinetic approach. *Mintek 50,* Johannesburg, South Africa.

Klimpel, R. R. (1999). A review of sulfide mineral collector practice. In B. K. Parekh, & J. D. Miller (Eds.), *Advances in flotation technology* (pp. 115-128) Society for Mining, Metallurgy and Exploration, Inc.

Klimpel, R. R. (1988). The industrial practice of sulfide mineral collectors. Paper presented at the *Reagents in Mineral Technology,* New York*., 27* 663-682.

Koca, M., Yildirim, G., Kirilmis, C., & Karaboga, F. (2012). Density functional theory study on the identification of pd(me-xanthate)$_2$. *Arabian Journal for Science and Engineering, 37*(5), 1283-1291.

Kohn, W., & Sham, L. J. (1965). Self-consistent equations including exchange and correlation effects. *Phys. Rev., 140(4A),* A1133-A1138.

Koopmans, T. (1934). Uber die zuordnung von wellenfunk-tionen und eigenwerten zu den einzelnen elektronen eines atoms. *Physica, 1*, 104.

Ku, Y., & Jung, I. (2001). Photocatalytic reduction of cr(VI) in aqueous solutions by UV irradiation with the presence of titanium dioxide. *Water Research, 35*(1), 135-142.

Kurniawan, T. A. (2002). *A research study on Cr(VI) removal from electroplating wastewater using chemically modified low-cost adsorbents and commercial activated carbon* (Master thesis).

Labisbal, E., Sousa, A., Castiñeiras, A., García-Vázquez, J. A., Romero, J. & West, D. X. (2000). Spectral and structural studies of metal complexes of isatin 3-hexamethyleneiminylthiosemicarbazone prepared electrochemically. *Polyhedron, 19(10),* 1255-1262.

Landaburu-Aguirre, J., García, V., Pongrácz, E., & Keiski, R. L. (2009). The removal of zinc from synthetic wastewaters by micellar-enhanced ultrafiltration: Statistical design of experiments. *Desalination, 240*(1–3), 262-269.

Laskowski, J. (1993). Frothers and flotation froth. *Mineral Processing and Extractive Metallurgy Review, 12*, 61-89.

Leach, A. R. (2001). *Molecular modelling* (2nd ed.) Prentice Hall.

Lee, B., & Richards, F. M. (1971). The interpretation of protein structures: Estimation of static accessibility. *Journal of Molecular Biology, 55*(3), 379-IN4.

Lee, C., Yang, W., & Parr, R. G. (1988a). Development of the colle-salvetti correlation-energy formula into a functional of the electron density. *Physical Review B, 37*(2), 785-789.

Lee, C., Yang, W., & Parr, Y. G. (1988b). Development of the colle-salvetti conelation energy formula into a functional of the electron density. *Phys. Rev. B, 37(2),* 785-789.

Lee, K., Archibald, D., McLean, J., & Reuter, M. A. (2009). Flotation of mixed copper oxide and sulphide minerals with xanthate and hydroxamate collectors. *Minerals Engineering, 22*(4), 395-401.

Leppinen, J. O. (1990). FTIR and flotation investigation of the adsorption of ethyl xanthate on activated and non-activated sulfide minerals. *International Journal of Mineral Processing, 30*(3–4), 245-263.

Leppinen, J. O., Basilio, C. I., & Yoon, R. H. (1988). FTIR study of thionocarbamate adsorption on sulfide minerals. *Colloids and Surfaces, 32*(C), 113-125.

Leppinen, J. O., Basilio, C. I., & Yoon, R. H. (1989). In-situ FTIR study of ethyl xanthate adsorption on sulfide minerals under conditions of controlled potential. *International Journal of Mineral Processing, 26*(3–4), 259-274.

Levy, M. (1982). Electron densities in search of hamiltonians. *Physical Review A, 26*, 1200-1208.

Li, B. (2009). *Density-functional theory and quantum chemistry studies on "dry" and "wet" NaCl(001).* (Unpublished PhD). TU Berlin, Berlin.

Li, Y., Liu, F., Xia, B., Du, Q., Zhang, P., Wang, D. Xia, Y. (2010). Removal of copper from aqueous solution by carbon nanotube/calcium alginate composites. *Journal of Hazardous Materials, 177*(1–3), 876-880.

Liang, S., Guo, X., Feng, N., & Tian, Q. (2010). Effective removal of heavy metals from aqueous solutions by orange peel xanthate. *Transactions of Nonferrous Metals Society of China, 20, Supplement 1*(0), s187-s191.

Liu, G., Zhong, H., & Dai, T. (2008). Investigation of the selectivity of ethoxylcarbonyl thionocarbametes during the flotation of copper sulfides. *Minerals and Metallurgical Processing, 25*(1), 19-24.

Liu, G., Zeng, H., Lu, Q., Zhong, H., Choi, P., & Xu, Z. (2012). Adsorption of mercaptobenzoheterocyclic compounds on sulfide mineral surfaces: A density functional theory study of structure–reactivity relations. *Colloids and Surfaces A: Physicochemical and Engineering Aspects, 409*(0), 1-9.

Liu, G., Zhong, H., Dai, T., & Xia, L. (2008). Investigation of the effect of N-substituents on performance of thionocarbamates as selective collectors for copper sulfides by ab initio calculations. *Minerals Engineering, 21*(12–14), 1050-1054.

Liu, G., Zhong, H., Xia, L., Wang, S., & Dai, T. (2010). Effect of N-substituents on performance of thiourea collectors by density functional theory calculations. *Transactions of Nonferrous Metals Society of China, 20*(4), 695-701.

Livshits, A. K., & Dudenkov, S. V. (1965). Some factors in froth stability. *Int. Min. Proc. Congr, 7*, 367-371.

Loeb, B., Crivelli, I., & Andrade, C. (1991). The 2-mercaptobenzothiazole and copper(II) reaction. *Synthesis and Reactivity in Inorganic and Metal-Organic Chemistry, 21*(2), 331-342.

Lotter, N. O., & Bradshaw, D. J. (2010). The formulation and use of mixed collectors in sulphide flotation. *Minerals Engineering, 23*(11–13), 945-951.

Lovell, V. M. (1976). Froth characterstics in phosphate flotation. In M. C. Fuerstenau (Ed.), *Flotation, A. M. gaudin memorial edition* (pp. 597-621). New York: Am. Inst. of Min. Metall and Pet. Engr.

Lovell, V. M. (1982). Industrial flotation reagents . In R. P. King (Ed.), *Principles of flotation* (pp. 73-91) South African Institute of Mining and Metallurgy.

Lowdin, P. O. (1998). In Lowdin P. O. (Ed.), *Advances in density functional theory* Elsevier.

Lowdin, P. O. (1955). Quantum theory of many-particle systems. I. physical interpretations by means of density matrices, natural spin-orbitals, and convergence problems in the method of configurational interaction. *Phys. Rev., 97*, 1474-1479.

Maeder-Vigne, F., & Claverie, P. (1987). Theoretical conformational study of carotenoporphyrins related to photophysical properties. *Journal of American Chemical Society, 109*(1), 24-28.

Maginn, E. J., & Elliott, J. R. (2010). Historical perspective and current outlook for molecular dynamics as a chemical engineering tool. *Industrial & Engineering Chemistry Research, 49*, 3059-3078.

Magnasco, V. (2013). *Elementary molecular quantum mechanics: Mathematical methods and applications* (2nd ed.). USA: Elsevier.

Magyar, J. S., Weng, T., Stern, C. M., Dye, D. F., Rous, B. W., Payne, J. C., Godwin, H. A. (2005). Reexamination of lead(II) coordination preferences in sulfur-rich sites: Implications for a critical mechanism of lead poisoning. *Journal of the American Chemical Society, 127*(26), 9495-9505.

Maier, G. S., & Dobiáš, B. (1997). 2-mercaptobenzothiazole and derivatives in the flotation of galena, chalcocite and sphalerite: A study of flotation, adsorption and microcalorimetry. *Minerals Engineering, 10*(12), 1375-1393.

Majima, H., & Takeda, M. (1968). Electrochemical studies of the xanthate-dixanthogen system on pyrite. *Transactions AIME, 241*, 431.

Malhotra, D. (1994). Reagents in the mining industry: Commodities or speciality chemicals. *Reagents for better metallurgy* (pp. 75-80) SME-AIME.

Marabini, A., Cases, J., & Barbaro, M. (1989). Chelating reagents as collectors and their absorption mechanism. In K. V. Sastry (Ed.), *Chellenges in mineral processing* (). Littleton, United States of America: AIME.

Marabini, A. M., Barbaro, M., & Alesse, V. (1991). New reagents in sulphide mineral flotation. *International Journal of Mineral Processing, 33*(1–4), 291-306.

Marabini, A. M., Ciriachi, M., Plescia, P., & Barbaro, M. (2007). Chelating reagents for flotation. *Minerals Engineering, 20*(10), 1014-1025.

Marabini, A. M., & Rinelli, G. (1973). Flotation of pitchblend with a chelating agent and fuel oil. *Transactions of Institution of Mining and Metallurgy, 82*, C225-C228.

Marabini, A. M., & Rinelli, G. (1982). The development of a specific reagent for futile flotation. *AIME Annual Meeting,* Dallas.

Marchioretto, M. M., Bruning, H., & Rulkens, W. H. (2002). OPTIMIZATION OF CHEMICAL DOSAGE IN HEAVY METALS PRECIPITATION IN ANAEROBICALLY DIGESTED SLUDGE. *Proceedings of XXVIII Congreso Interamericano De Sanataria Y Ambiental,* Cancun, Mexico. 1-7.

Matlock, M. M., Henke, K. R., & Atwood, D. A. (2002). Effectiveness of commercial reagents for heavy metal removal from water with new insights for future chelate designs. *Journal of Hazardous Materials, 92*(2), 129-142.

Matlock, M. M., Howerton, B. S., & Atwood, D. A. (2001). Irreversible precipitation of mercury and lead. *Journal of Hazardous Materials, 84*(1), 73-82.

Matlock, M. M., Howerton, B. S., Henke, K. R., & Atwood, D. A. (2001). A pyridine-thiol ligand with multiple bonding sites for heavy metal precipitation. *Journal of Hazardous Materials, 82*(1), 55-63.

McQuarrie, D. A., & Simon, J. D. (1999). *Molecular thermodynamics* University Science Books.

Mebi, C. A. (2011). DFT study on structure, electronic properties, and reactivity of cis-isomers of $[(NC_5H_4\text{-}S)_2Fe(CO)_2]$. *Journal of Chemical Sciences, 123*(5), 727-731.

Medina, B. Y., Torem, M. L., & de Mesquita, L. M. S. (2005). On the kinetics of precipitate flotation of cr III using sodium dodecylsulfate and ethanol. *Minerals Engineering, 18*(2), 225-231.

Mendiratta, N. K. (2000). *Kinetic studies of sulfide mineral oxidation and xanthate adsorption.* (Unpublished PhD). Virginia Polytechnic Institute and State University, Virginia.

Mennucci, B., & Cammi, R. (Eds.). (2007). *Continuum solvation models in chemical physics: From theory to applications* Wiley.

Mennucci, B., Tomasi, J., Cammi, R., Cheeseman, J. R., Frisch, M. J., Devlin, F. J., . . . Stehpens, P. J. (2002). Polarizable continuum model (PCM) calculations of solvent effects on optical rotations of chiral molecules. *The Journal of Physical Chemistry, 106*(25), 6102-6113.

Mielczarski, J. A., & Yoon, R. H. (1989). Spectroscopic studies of the structure of the adsorption layer of thionocarbamate: I. on copper and activated zinc sulfide. *Journal of Colloid and Interface Science, 131*(2), 423-432.

Miertus, S., Scrocco, E., & Tomasi, J. (1981). Electrostatic interaction of a solute with a continuum. A direct utilization of ab initio molecular potentials for the prevision of solvent effects. *Chemical Physics, 55*(1), 117-129.

Miller, J. D. (1970). *Pyrite depression by reductoon of sultion oxidation potential.* (No. 12010).Environmental Protection Agency, USA.

Montalti, M., Fornasiero, D., & Ralston, J. (1991). Ultraviolet-visible spectroscopic study of the kinetics of adsorption of ethyl xanthate on pyrite. *Journal of Colloid and Interface Science, 143*(2), 440-450.

Moudgil, B. M., Rogers, J. J., & Vasudevan, T. V. (1988). Effect of fines on the flotation recovery of coarse phosphate particles. *Int. Min. Proc. Congr.* Stockholm.

Moudgil, B. M. (1992). *Enhanced recovery of coarse particles during phosphate flotation* . (No. 86-02-067). Gainesville, Florida.

Mulliken, R. S. (1955). Electronic population analysis on LCAO-MO molecular wave function - I. *The Journal of Chemical Physics, 23*(10), 1833-1840.

Murali, M. K., & Balachandranb, V. (2012). FT-IR, FT-raman, DFT structure, vibrational frequency analysis and mulliken charges of 2-chlorophenylisothiocyanate. *Indian Journal of Pure & Applied Physics, 50*(January), 19-25.

Murrell, R. S., & Harget, A. J. (1972). *Semi-empirical self-consistent-field molecular orbital theory of molecules*. London: Wiely-Interscience.

Nagaraj, D. (1988). The chemistry and application of chelating or complexing agents in mineral separations. *Reagents in Mineral Technology,* New York, USA. 387-408.

Nagaraj, D. R., & Somasundaran, P. (1981). Chelating agents as collectors in flotation: Oximes 0 copper minerals systems. *Transactions AIME,* , 270-1351.

Nagaraj, D. R. (1982). Chelating agents in mineral processing. *III AIME Annual Meeting,* Dallas.

Nagaraj, D. R. (1994). A critical assessment of flotation agents. *Reagents for Better Metallurgy,* Littleton, CO. 81-90.

Nagaraj, D. R., Day, A., & Gorken, A. (1999). Nonsulphide minerals flotation: An overview. In B. K. Parekh, & J. D. Miller (Eds.), *Advances in flotation technology* (pp. 245-256). Littleton: SME.

Nagaraj, D. R., Lewellyn, M. E., Wang, S. S., Mingione, P. A., & Scanlon, M. J. (1988). New sulfide and precious metals collectors: For acid, neutral and mildly alkaline circuits. *Proceedings of XVIth International Mineral Processing Congress,* Stockholm. 1221-1232.

Nagaraj, D. R., & Ravishankar, S. A. (2007). Flotation reagents - A critical overview from an industry prospective. In M. C. Fuerstenau, G. Jameson & R. Yoon (Eds.), *Froth flotation: A century of innovation* (). Littleton: SME.

Nagaraj, D. R., Wang, S. S., & Frattaroli, D. R. (1986). Flotation of copper sulfide minerals and pyrite with new and existing sulfur-containing collectors. *Proceedings of 13th CMMI Congress,* Singapore. 49-57.

Nasab, M. E. l. D.,A. (2014). Investigation of the effects of hydrodynamic parameters on the flotation recovery of coal particles. *International Journal of Coal Preparation and Utilization, 34*(5), 260-275.

Nataraj, S. K., Hosamani, K. M., & Aminabhavi, T. M. (2007). Potential application of an electrodialysis pilot plant containing ion-exchange membranes in chromium removal. *Desalination, 217*(1–3), 181-190.

Newell, R., & Grano, S. (2007). Hydrodynamics and scale up in rushton turbine flotation cells: Part 1 — cell hydrodynamics. *International Journal of Mineral Processing, 81*(4), 224-236.

Ngo, S. C., Banger, K. K., DelaRosa, M. J., Toscano, P. J., & Welch, J. T. (2003). Thermal and structural characterization of a series of homoleptic cu(II) dialkyldithiocarbamate complexes: Bigger is only marginally better for potential MOCVD performance. *Polyhedron, 22*(12), 1575-1583.

Ochterski, J. W. (2000). *Thermochemistry in gaussian*

Onsager, L. (1936). Electric moments of molecules in liquids. *Journal of American Chemical Society, 58*, 1486-1493.

Öteyaka, B., & Soto, H. (1995). Modelling of negative bias column for coarse particles flotation. *Minerals Engineering, 8*(1–2), 91-100.

Pan, B. (2013). *Flotation of halite and sylvite from carnallite with dodecyl morpholine*. (Unpublished MSc). University of Utah,

Parfitt, G. D. (1983). In Parfitt G. D., Rochester C. H. (Eds.), *Adsorption from solution at the solid/liquid interface* (. ed.) Academic Press.

Parker, G. K., Buckley, A. N., Woods, R., & Hope, G. A. (2012). The interaction of the flotation reagent, n-octanohydroxamate, with sulfide minerals. *Minerals Engineering, 36–38*(0), 81-90.

Parr, R., Donnelly, R., Levy, M., & Palke, W. (1978). Electronegativity-the density functional viewpoint. *Journal of Chemical Physics, 68*, 3801-3807.

Parr, R. G., & Pearson, R. G. (1983). Absolute hardness: Companion parameter to absolute electronegativity. *Journal of the American Chemical Society, 105*(26), 7512-7516.

Parr, R. G., Szentpaly, L. V., & Liu, S. (1999). Electrophilicity index. *Journal of the American Chemical Society, 121*(9), 1922-1924.

Parr, R. G., & Yang, W. (Eds.). (1989). *Density-functional theory of atoms and molecules,*. New York: Oxford University Press.

Pearse, M. (2006). An overview of the use of chemial reagents in mineral processing. *Minerals Engineeering, 18*, 139-149.

Pearson, R. G. (1988). Absolute electronegativity and hardness: Application to inorganic chemistry. *Inorganic Chemistry, 27*, 734-740.

Pearson, R. G. (1992). The electronic chemical potential and chemical hardness. *Molecular Structure (Theochem), 255*, 261-270.

Pease, J. D., Curry, D. C., & Young, M. F. (2006). Designing flotation circuits for high fines recovery. *Minerals Engineering, 19*(6–8), 831-840.

Pecina-Treviño, E. T., Uribe-Salas, A., Nava-Alonso, F., & Pérez-Garibay, R. (2003). On the sodium-diisobutyl dithiophosphinate (aerophine 3418A) interaction with activated and

unactivated galena and pyrite. *International Journal of Mineral Processing, 71*(1–4), 201-217.

Pedrido, R., Bermejo, M. R., Romero, J. M., Vazquez, M., Gonzalez-Noya, A. M., Manerio, M., Rodriguez, M. J. & Fernandez, M. I. (2005). Syntheses and X-ray characterization of metal complexes with the pentadentate thiosemicarbazone ligand bis(4-N-methylthiosemicarbazone)-2,6-diacetylpyridine. The first pentacoordinate lead(II) complex with a pentagonal geometry. *Dalton Transactions, 2005*, 572-579.

Perdew, J. P., Burke, K., & Ernzerhof, M. (1997). Generalized gradient approximation made simple . *Phys. Rev. Lett, 77(18),* 3865-3868.

Perdew, J. P., Ernzerhof, M., & Burke, K. (1996). Rationale for mixing exact exchange with density functional approximations. *The Journal of Chemical Physics, 105(22),* 9982-9985.

Perdew, J. P., Ruzsinszky, A., Csonka, I. G., Vydrov, O. A., Scuseria, G. E., Constantin, L. A., . . . Burke, K. (2008). Restoring the density-gradient expansion for exchange in solids and surfaces. *Phys. Rev. Lett, 100(13),* 1364061-1364064.

Perdew, J. P., & Wang, Y. (1992). Accurate and simple analytic representation of the electron-gas correlation energy. *Physical Review B, 45(23),* 13244-13249.

Perdew, J. P., & Zunger, A. (1981). Self-interaction correction to density-functional approximations for many-electron systems. *Physical Review B, 23,* 5048-5079.

Perdew, J. P., Burke, K., & Wang, Y. (1996). Generalized gradient approximation for the exchange-correlation hole of a many-electron system. *Phys. Rev. B, 54(23),* 16533-16539.

Persson, P., & Malmensten, B. (1991). Interactions between sulfide minerals and alkylxanthate ions 5. A vibration spectroscopic study of the interactions between chalcocite, synthetic

copper(I) sulfide, acanthite and synthetic silver(I) sulfide, and ethylxanthate ions in aqueous and acetone solutions. *Colloids and Surfaces, 59*(0), 279-292.

Peters, R. W., & Shem, L. (1993). Separation of heavy metals: Removal from industrial wastewaters and contaminated soil. *Department of Energy - Office of Scientific and Technical Information, CONF-9303107--1*(08/10)

Phillips, J. C. (1958). Energy-band interpolation scheme based on a pseudopotential. *Phys. Rev., 112*(3), 685-695.

Pierotti, R. A. (1976). A scaled particle theory of aqueous and nonaqueous solutions. *Chem. Rev,* (76), 717-726.

Pople, J. A., & Beveridge, D. L. (1970). *Approximate molecular orbital theory*. New York: McGraw-Hill.

Pople, J. A., Santry, D. P., & Sehgal, G. A. (1965). Appximate self-consistent molecular orbital theory: Invariant procedures. *J. Chem. Phys, 43,* S129.

Pople, J. A., & Segal, G. A. (1965). Approximate self-consistent molecular orbital theory. II. calculations with complete neglect of differential overlap. *J. Chem. Phys, 43,* S136.

Porento, M., & Hirva, P. (2002). Theoretical studies on the interaction of anionic collectors with cu(+), cu(2+), zn(2+) and pb(2+) ions. *Theoretical Chemistry Accounts, 107*(4), 200-205.

Pradip. (1988). Applications of chelates in mineral processing. *Minerals and Met. Proc, 5*

Pradip. (1994). Reagents design and molecular recognition at mineral surfaces. In P. Mulukutla (Ed.), *Reagents for better metallurgy* (pp. 245-252). Denver: SME-AIME.

Pradip. (2012). Rational design of selective industrial performance chemicals based on molecular modeling computations. (pp. 27-64) CRC Press.

Pradip, & Fuerstenau, D. W. (2013). Design and development of novel flotation reagents for the beneficiation of mountain pass rare-earth ore. *Minerals & Metallurgical Processing, 30*(1), 1-9.

Pradip, & Rai, B. (2003). Molecular modeling and rational design of flotation reagents. *International Journal of Mineral Processing, 72*(1–4), 95-110.

Pradip, Rai, B., Rao, T. K., Krishnamurthy, S., Vetrivel, R., Mielczarski, J., & Cases, J. M. (2002). Molecular modeling of interactions of alkyl hydroxamates with calcium minerals. *Journal of Colloid and Interface Science, 256*(1), 106-113.

Preti, C., & Tosi, G. (1977). Transition metal complexes of deprotonated 2-mercaptobenzoxazole. study of the thiol-thioketo form equilibrium. *Canadian Journal of Chemistry, 55*, 1409-1414.

Pugh, R. J. (1996). Foaming, foam films, antifoaming and defoaming. *Advances in Colloid and Interface Science, 64*, 67-142.

Rahman, R. M., Ata, S., & Jameson, G. J. (2012). The effect of flotation variables on the recovery of different particle size fractions in the froth and the pulp. *International Journal of Mineral Processing, 106–109*, 70-77.

Rai, B. (2012). Basic concepts in molecular modeling. In B. Rai (Ed.), *Molecular modeling for the design of novel performance chemicals and materials* (pp. 1-26) CRC Press.

Rai, B., & Pradip. (2008). Design of highly selective industrial performance chemicals: A molecular modeling approach. *Molecular Simulation, 34*, 1209-1214.

Raju, G. B., & Forsling, W. (1991). Adsorption mechanism of diethyldithiocarbamate on covellite, cuprite and tenorite. *Colloids and Surfaces, 60*, 53-69.

Rand, D. A. J., & Woods, R. (1984). Eh measurements in sulphide mineral slurries. *International Journal of Mineral Processing, 13*(1), 29-42.

Rao, S. R. (2004). *Surface chemistry of froth flotation* Springer US. doi:10.1007/978-1-4757-4302-9

Rao, H. K., Kundu, T., & Parker, S. (2012). Molecular modeling of mineral surface reactions in flotation. *Molecular modeling for the design of novel performance chemicals and materials* (pp. 65-105) CRC Press. doi:doi:10.1201/b11590-4

Rathore, H. S., Ishratullah, K., Varshney, C., Varshney, G., & Mojumdar, S. C. (2008). Fungicidal and bacteridical activity of metal diethyldithiocarbamate fungicides: Synthesis and characteristics. *Journal of Thermal Analysis and Calorimetry, 94*(1), 75-81.

Ravitz, S. F., & Wall, W. A. (1993). The adsorption of copper sulfate by sphalerite and its RElation to flotation. *The Journal of Physical Chemistry, 38*(1), 13-18.

Reichardt, C. (Ed.). (2005). *Solvents and solvent effects in organic chemistry* (3rd ed.). Germany: Wiley-VCH.

Roy, P. K., Rawat, A. S., Chaoudhary, V., & Rai, P. K. (2004). Removal of heavy metal ions using polydithiocarbamate resin supported on polystyrene. *Indian Journal of Chemical Technology, 11*(January), 51-58.

Rulisek, L., & Havlas, Z. (2000). Theoretical studies of metal ion selectivity. 1. DFT calculations of interaction energies of amino acid side chains with selected transition metal ions (Co^{2+}, Ni^{2+}, Cu^{2+}, Zn^{2+}, Cd^{2+}, and Hg^{2+}). *Journal of American Chemical Society, 122*, 10428-10439.

Samper, E., Rodríguez, M., De la Rubia, M. A., & Prats, D. (2009). Removal of metal ions at low concentration by micellar-enhanced ultrafiltration (MEUF) using sodium dodecyl

sulfate (SDS) and linear alkylbenzene sulfonate (LAS). *Separation and Purification Technology, 65*(3), 337-342.

Saracoglu, M. (2013). *Froth flotation performance enhancement by feed cavitation and magnetic particle addition* (PhD).

Sathiyaraj, E., & Thirumaran, S. (2012). Synthesis and spectral studies on pb(II) dithiocarbamate complexes containing benzyl and furfuryl groups and their use as precursors for PbS nanoparticles. *Spectrochimica Acta Part A: Molecular and Biomolecular Spectroscopy, 97*(0), 575-581.

Say, R., Birlik, E., Denizli, A., & Ersöz, A. (2006). Removal of heavy metal ions by dithiocarbamate-anchored polymer/organosmectite composites. *Applied Clay Science, 31*(3–4), 298-305.

Schulze, H. (1984). *Physicochemical elementary processes in flotation. elsevier publishing.* . Amsterdam: Elsevier Publishing.

Schwarz, S. (2004). *The relationship between froth recovery and froth structure.* (Unpublished PhD). Ian Wark Institute, Austrralia.

Schwarzenbach, G. (1952). Der chelateffekt. *Helvetica Chimica Acta, 35*(7), 2344-2359. doi:10.1002/hlca.19520350721

Seeger, R., & Pople, J. A. (1977). Self-consistent molecular orbital methods. XVIII. constraints and stability in Hartree–Fock theory. *The Journal of Chemical Physics, 66(7)*, 3045-3050.

Seryakova, I. V., Vorobiova, G. A., Glembotsky, A. V., & Zolotov, Y. A. (1975). Extraction of metals by neutral sulfur-containing extractants. part I. o-isopropyl-n-ethylthiocarbamate. *Analytica Chimica Acta, 77*(C), 183-190.

Shaoyi, J., Dasgupta, S., Blanco, M., Frazier, R., Yamaguchi, E. S., Tang, Y., & Goddard, W. A. (1996). Structures, vibrations, and force fields of dithiophosphate wear inhibitors from ab initio quantum chemistry. *Journal of Physical Chemistry, 100*, 15760-15769.

Shimoni-Livny, L., Glusker, J., & Bock, C. (1998). Lone pair functinality in divalent lead compounds. *Inorganic Chemistry, 37*(8), 1853-1867.

Sholl, D. S., & Steckel, J. A. (2009). *Density functional theory: A practical introduction* Wiley-Interscience.

Šille, J., Šramko, M., Garaj, V., & Remko, M. (2009). Gas phase and solution state stability of complexes L...M, where M = Cu2+, Ni2+, or Zn2+ and L = R-C({double bond, long}O)NHOH (R = H, NH2, CH3, CF3, or phenyl). *Journal of Molecular Structure: THEOCHEM, 911*(1-3), 137-143.

Sillen, L. G., Martell, A. E., & Bjerrum, J. (1984). *Stability constants of metal-ion complexes, special publication (royal society of chemistry, great britain)* (2nd ed.). London: Chemical Society.

Snor, W. (2009). *Molecular modelling on cyclodextrin inclusion complexes.* (Unpublished PhD). University of Vienna, Vienna.

Somasundaran, P., & Nagaraj, D. R. (1984). Chemistry and applications of chelating reagents in flotation and flocculation. In M. Jones, & R. Oblatt (Eds.), *Reagents in mineral industry* (pp. 209-219). London: Institution of Mining and Metallurgy.

Somasundaran, P., & Wang, D. (2006a). Application of flotation agents and their structure–property . *Solution chemistry: Minerals and reagents* (1st ed.,) Elsevier Science.

Somasundaran, P., & Wang, D. (2006b). Chapter 4 mineral–flotation reagent equilibria. *Developments in Mineral Processing, 17*, 73-141.

Sousa-Pedrares, A., Casanova, M. I., Garcia-Vazquez, J. A., M. L. Duran, M. L., J. Romero, J., Sousa, A., Silver, J. & Titler, P. J. (2003). Synthesis and X-ray Structures of Tin(IV) and Lead(II) Complexes with Heterocyclic Thiones. *European Journal of Inorganic Chemistry, vol. 2003*, 678-686.

Stelle, H., Wright, K., & Hillier, I. (2003). A quantum-mechanical study of the (110) surface of sphalerite (ZnS) and its interaction with pb(2+) species. *Physics and Chemistry of Minerals, 30*, 69-75.

Stephens, P. J., Devlin, F. J., Chabalowski, C. F., & Frisch, M. J. (1994). Ab initio calculation of vibrational absorption and circular dichroism spectra using density functional force fields. *The Journal of Physical Chemistry, 98*(45), 11623-11627.

Stewart, J. J. P. (1989). Optimization of parameters for semi-empirical methods I - method. *J. Comput. Chem., 10(2)*, 209-220.

Stewart, J. J. P., & Stewart, A. C. (1999). Developing a semiempirical method. *Crystal engineering: The design and applicatiion of functional solids*. NATO ASI Ser.

Storvick, J. P. (1986). *A comparison of mercaptothiazoline, mercaptobenzothiazole, mercaptobenzimidazole, and mercaptobenzoxazole as inhibitors of 90/10 cupro-nickle alloy corrosion in searwater* (PhD).

Struebing, H. (2011). *Identifying optimal solvents for reactions using quantum mechanics and computer-aided molecular design.* (Unpublished PhD). Imperial College, London.

Sun, W., Hu, Y., & Qin, Q. (2004). DFT research on activation of sphalerite. *Transactions of Nonferrous Metals Society of China, 14*(2), 376-382.

Szarecka, A., Rychlewski, J., & Rychlewska, U. (1998). Theoretical solvation models: Ab initio study of molecular aggregation. *Computation Methods in Science and Technology, 4*(1), 25-33.

Szargan, R., Uhlig, I., Wittstock, G., & Roβbach, P. (1997). New methods in flotation research—application of synchrotron radiation to investigation of adsorbates on modified galena surfaces. *International Journal of Mineral Processing, 51*(1–4), 151-161.

Szatkowski, M., & Freyburger, W. (1985). Kinetics of flotation with fine bubble. *Transactions of the Institute of Mining and Metallurgy (Section C), 94*, 61-70.

Takada, T., Dupuis, M., & King, H. F. (1981). Molecular symmetry. III. second derivatives of electronic energy with respect to nuclear coordinates. *The Journal of Chemical Physics, 75(1)*, 332-336.

Tao, D. (2005). Role of bubble size in flotation of coarse and fine particles - A review. *Separation Science and Technology, 39*(4)

Tao, J., Perdew, J. P., Staroverov, V. N., & Scuseria, G. E. (2003). J. tao, J.P. perdew, V.N. staroverov, and G.E. scuseria, climbing the density functional ladder: Non-empirical meta-generalized gradient approximation designed for molecules and solids, *Phys. Rev. Lett, 91(14),* 1464011-1464014.

Tare, V., & Chaudhari, S. (1987). Evaluation of soluble and insoluble xanthate process for the removal of heavy metals from wastewaters. *Water Research, 21*(9), 1109-1118.

Theil, W. (1996). Perspectives on semiempirical molecular orbital theory. *Adv. Chem. Phys., 93*, 703-757.

Tiekink, E. R. D., & Winter, G. (2011). Inorganic xanthates : A structural perspective. *Reviews of Inorganic Chemistry, 12*(3-4), 183-302.

Tomasi, J., Mennucci, B., & Cancès, E. (1999). The IEF version of the PCM solvation method: An overview of a new method addressed to study molecular solutes at the QM ab initio level. *Journal of Molecular Structure: THEOCHEM, 464*(1–3), 211-226.

Tossell, J. A., & Vaughan, D. J. (1993). Theoretical studies of xanthates, dixanthogen, metal xanthates, and related compounds. *Journal of Colloid and Interface Science, 155*(1), 98-107.

Trahar, W. J. (1976). The selective flotation of galena from sphalerite with special reference to the effects of particle size. *International Journal of Mineral Processing, 3*(2), 151-166.

Trahar, W. J., Senior, G. D., Heyes, G. W., & Creed, M. D. (1997). The activation of sphalerite by lead — a flotation perspective. *International Journal of Mineral Processing, 49*(3–4), 121-148.

Ulig, H. H. (1937). The solubilities of gases and surface tension. *Journal of Physical Chemistry, 41*(9), 1215-1226.

Urbina, R. H. (2003). Recent developments and advances in formulations and applications of chemical reagents used in froth flotation. *Mineral Processing and Extractive Metallurgy Review, 24*(2), 139-182.

Vaidyanathan, M., Balamurugan, R., Sivagnanam, U., & Palaniandavar, M. (2001). Synthesis, structure, spectra and redox of Cu(II) complexes of chelating bis(benzimidazole)-thioether ligands as models for electron transfer blue copper proteins. *Dalton Transactions,* (23), 3498-3506.

Valero, D., & Ortiz, J. M. (2010). Electrochemical wastewater treatment directly powered by photovoltaic panels: Electrooxidation of a dye-containing wastewater. *Environ. Sci. Technol, 44*(13), 5182-5187.

Vanangamudi, M., Kumar, S. S., & Rao, T. C. (1989). Effect of fines content on the froth flotation of coal. *Powder Technology, 58*(2), 99-105.

Verdolino, V. (2009). *New computational methods and developments for molecular response properties in condensed matter.* (Unpublished PhD). University of Parma, Parma, Italy.

Veszpremi, T., & Feher, M. (1999). *Quantum chemistry* Springer US.

Vosko, S. H., Wilk, L., & Nusair, M. (1980a). Accurate spin-dependent electron liquid correlation energies for local spin density calculations: A critical analysis. *Canadian Journal of Physics, 58*(8), 1200-1211.

Wang, H., Zhou, A., Peng, F., Yu, H., & Yang, J. (2007). Mechanism study on adsorption of acidified multiwalled carbon nanotubes to pb(II). *Journal of Colloid and Interface Science, 316*(2), 277-283.

Waters, A. (1990). Dissolved air flotation used as primary separation for heavy metal removal. *Filtration & Separation, 27*(2), 70-73.

Watt, G. W., & McCormick, B. J. (1965). The infrared spectra and structure of transition metal xanthates. *Spectrochimica Acta, 21*(4), 753-761.

Whang, J. S., Young, D., & Pressman, M. (1982). Soluble-sulfide precipitation for heavy metals removal from wastewaters. engineering details of a treatment plant scheduled to be operational in september, 1981. *Environmental Progress, 1*(2), 110-113.

Whitfield, J. D. (2011). *At the intersection of quantum computing and quantum chemistry.* (Unpublished PhD). Harvard University, Cambridge, Massacchsetss.

Wills, B., & Napier-Munn, T. (2006). *Will's mineral processing technology* (7th ed.). Oxford, UK: Butterworth-Heinemann.

Wing, R. E., Doane, W. M., & Russell, C. R. (1975). Insoluble starch xanthate: Use in heavy metal removal. *Journal of Applied Polymer Science, 19*(3), 847-854.

Wing, R. E., & Rayford, W. E. (1982). Heavy metal removal using dithiocarbamates. *Plating and Surface Finishing, January*, 67-72.

Woods, R., Hope, G. A., & Watling, K. (2000a). A SERS spectroelectrochemical investigation of the interaction of 2-mercaptobenzothiazole with copper, silver and gold surfaces. *Journal of Applied Electrochemistry, 30*(11), 1209-1222.

Woods, R., Hope, G. A., & Watling, K. (2000b). Surface enhanced raman scattering spectroscopic studies of the adsorption of flotation collectors. *Minerals Engineering, 13*(4), 345-356.

Woods, R., & Hope, G. A. (1999). A SERS spectroelectrochemical investigation of the interaction of O-isopropyl-N-ethylthionocarbamate with copper surfaces. *Colloids and Surfaces A: Physicochemical and Engineering Aspects, 146*(1–3), 63-74.

Wu, Z., & Cohen, R. E. (2006). More accurate generalized gradient approximation for solids. *Phys. Rev., 73,* 2351161-2351166.

Xu, Y., Xie, Z., & Xue, L. (2011). Chelation of heavy metals by potassium butyl dithiophosphate. *Journal of Environmental Sciences, 23*(5), 778-783.

Yamasaki, T., & Usiu, S. (1965). Infrared spectroscopic studies of xanthate adsorbed on zinc sulfide. *Transactions AIME, 232*, 36.

Yekeler, M., & Yekeler, H. (2006). A density functional study on the efficiencies of 2-mercaptobenzoxazole and its derivatives as chelating agents in flotation processes. *Colloids and Surfaces A: Physicochemical and Engineering Aspects, 286*(1–3), 121-125.

Yekeler, H., & Yekeler, M. (2004). Reactivities of some thiol collectors and their interactions with ag (+1) ion by molecular modeling. *Applied Surface Science, 236*(1–4), 435-443.

Yekeler, H., & Yekeler, M. (2006). Predicting the efficiencies of 2-mercaptobenzothiazole collectors used as chelating agents in flotation processes: A density-functional study. *Journal of Molecular Modeling, 12*(6), 763-768.

Ying, X., & Fang, Z. (2006). Experimental research on heavy metal wastewater treatment with dipropyl dithiophosphate. *Journal of Hazardous Materials, 137*(3), 1636-1642.

Yoon, R., & Luttrell, G. H. (1989). The effect of bubble size on fine particle flotation *Mineral Processing and Extractive Metallurgy Review: An International Journal, 5*(1-4), 101-122.

Yoshisa, T., Yamasaki, K., & Sawada, S. (1979). An X-ray photoelectron spectroscopic study of 2-mercaptobenzothiazole metal complexes. *Bulletin of the Chemical Society of Japan, 52*(10), 2908-2912.

Yuan, X. Z., Meng, Y. T., Zeng, G. M., Fang, Y. Y., & Shi, J. G. (2008). Evaluation of tea-derived biosurfactant on removing heavy metal ions from dilute wastewater by ion flotation. *Colloids and Surfaces A: Physicochemical and Engineering Aspects, 317*(1–3), 256-261.

Zhu, Y., Hu, J., & Wang, J. (2012). Competitive adsorption of Pb(II), Cu(II) and Zn(II) onto xanthate-modified magnetic chitosan. *Journal of Hazardous Materials, 221–222*(0), 155-161.

Zoete, V., Bailly, F., Vezin, H., Teissier, E., Duriez, P., Fruchart, J., Bernier, J. (2000). 4-mercaptoimidazoles derived from the naturally occurring antioxidant ovothiols 1. antioxidant properties. *Free Radical Research, 32*(6), 515-524.